Identification of the modulators of and the molecular pathways involved in the BIN1-Tau interaction

Tiago Mendes

Identification of the Modulators of and the Molecular Pathways Involved in the BIN1-Tau Interaction

Thesis submitted in fulfilment of the requirements for the degree of PhD in Neurosciences

École Doctorale BIOLOGIE SANTÉ de Lille
Université de Lille

Presented by

Tiago Mendes

December 13th, 2018

Jury composed by

Peter Heutink, PhD	Rapporteur, president du Jury
Marie-Claude Potier, PhD	Rapportrice
Sylvie Claeysen, PhD	Examinatrice
Laurent Pradier, PhD	Examinateur

Under the supervision of

Jean-Charles Lambert, PhD

INSERM - U1167
Risk factors and molecular determinants of aging-related diseases
Institut Pasteur de Lille
France

Contents

Summary

Résumé en Français

Identification des modulateurs et des voies moléculaires impliqués dans l'interaction BIN1-Tau

Les principales caractéristiques neuropathologiques de la maladie d'Alzheimer (MA) sont les plaques séniles extracellulaires composées de peptide amyloïde β (Aβ) et les enchevêtrements neurofibrillaires intracellulaires composés de Tau hyperphosphorylé. Les mécanismes conduisant à la formation de ces lésions sont encore peu connus et le laboratoire a récemment caractériser le gène "bridging integrator 1" (BIN1), deuxième facteur de risque génétique le plus associé au risque de MA, comme facteur de risque potentiellement associé à la pathologie Tau. Une interaction entre les deux protéines a été décrite in vitro et in vivo suggérant que BIN1 pourrait être impliqué dans le développement de la pathologie associée à Tau dans le cadre de la MA. Cependant, ce rôle de l'interaction BIN1-Tau dans le processus pathophysiologique de la MA n'est pas connu et il reste ainsi à déterminer si cette interaction constitue une cible thérapeutique potentielle. Ce projet a visé alors à mieux comprendre les acteurs de cette interaction en identifiant les modulateurs et les voies moléculaires impliquées dans le contrôle de l'interaction BIN1-Tau, puis de déterminer comment cette interaction est modulée dans le contexte de la MA. Nous avons utilisé pour cela des approches complémentaires de biochimie, de résonance magnétique nucléaire et de microscopie confocale. Comme modèle cellulaire, des cultures primaires de neurones de rat ont été utilisées, et la méthode "proximity ligation assay" (PLA) a été développée comme approche principale pour observer l'interaction BIN1-Tau dans ces cellules. Nous avons déterminé que l'interaction se produit entre les domaines SH3 de BIN1 et le PRD de Tau et nous avons démontré que l'interaction est modulée par la phosphorylation de Tau et BIN1: la phosphorylation de la Thréonine 231 de Tau diminue son interaction avec BIN1, tandis que la phosphorylation de BIN1 à la Thréonine 348 (T348) augmente son interaction avec Tau. Nous avons mis au point une approche de criblage d'haut contenu semi-automatisée et basé sur une bibliothèque de composés commerciaux. Ce criblage s'est basé sur des cultures primaires de neurones comme modèle cellulaire et le

PLA pour détecter l'interaction BIN1-Tau. Nous avons identifié plusieurs composés capables de moduler l'interaction BIN1-Tau, notamment U0126, un inhibiteur de MEK-1/2, qui diminue cette interaction, et la cyclosporine A, un inhibiteur de la calcineurine, qui au contraire augmente celle-ci en augmentant la phosphorylation de T348 de BIN1. Par ailleurs les “Cyclin-dependent kinases” (CDK) ont été montré comme contrôlant aussi ce site de phosphorylation. Nous avons donc mis en évidence le couple Calcineurine/CDK comme contrôlant la phosphorylation T348 de Bin1 et donc l’interaction BIN1-Tau. Nous avons également développé un modèle murin de tauopathie dans lequel nous avons surexprimé BIN1 humain. Nous avons observé que la surexpression de BIN1 résorbait les déficits de mémoire à long terme et réduisait la présence d'inclusions intracellulaires de Tau phosphorylée, provoquées par la surexpression de Tau, ce qui était associé à une augmentation de l'interaction BIN1-Tau. En utilisant des échantillons de cerveau humain post-mortem, nous avons observé que les niveaux de l’isoforme BIN1 neuronal étaient diminués dans les cerveaux d’AD, alors que les niveaux relatifs de BIN1 phosphorylé à T348 étaient augmentés, suggérant un mécanisme compensatoire. Cette étude a démontré la complexité et la dynamique de l’interaction BIN1-Tau dans les neurones, a révélé des modulateurs et des voies moléculaires potentiellement impliquées dans cette interaction, et a montré que les variations de l’expression ou de l’activité de BIN1 ont des effets directs sur l’apprentissage et la mémoire, possiblement liés à la régulation de son interaction avec Tau.

Abstract in English

Identification of the modulators of and the molecular pathways involved in the BIN1-Tau interaction

The main neuropathological hallmarks of Alzheimer's disease (AD) are the extracellular senile plaques composed of amyloid-β peptide (Aβ) and the intracellular neurofibrillary tangles composed of hyperphosphorylated Tau. The mechanisms leading to the formation of these lesions is not well understood and our lab has recently characterized the bridging integrator 1 (BIN1) gene, the second most associated genetic risk factor of AD and the first genetic risk factor to have a potential link to Tau pathology. The interaction between BIN1 and Tau proteins has been described in vitro and in vivo, which suggests that BIN1 might help us to understand Tau pathology in the context of AD. However, the role of BIN1-Tau interaction in the pathophysiological process of AD is not known, and whether this interaction is a potential therapeutic target remains to be determined. The aim of this project is to better understand the actors of BIN1-Tau interaction through the identification of the modulators and the molecular pathways involved therein, as well as to understand how BIN1-Tau interaction is modulated in the context of AD. We employed biochemistry, nuclear magnetic resonance, and confocal microscopy. We used rat primary neuronal cultures (PNC) as the cellular model and developed the proximity ligation assay (PLA) as the main readout of the BIN1-Tau interaction in cultured neurons. We determined that the interaction occurs between BIN1's SH3 domain and Tau's PRD domain, and demonstrated that it is modulated by Tau and BIN1 phosphorylation: phosphorylation of Tau at Threonine 231 decreases its interaction with BIN1, while phosphorylation of BIN1 at Threonine 348 (T348) increases its interaction with Tau. We developed a novel, semi-automated high content screening (HCS) assay based on a commercial compound library, also using PNC as the cellular model and PLA as the readout of BIN1-Tau interaction. We identified several compounds that are able to modulate the BIN1-Tau interaction, most notably U0126, an inhibitor of MEK-1/2, which reduced the interaction, and Cyclosporin A, an inhibitor of Calcineurin, which increased the interaction through increasing the BIN1 phosphorylation at T348. Furthermore, Cyclin-dependent kinases (CDK) were also shown as regulator of this phosphorylation site. These results suggest that the couple Calcineurin/CDK regulates BIN1

phosphorylation at T348 and consequently the BIN1-Tau interaction. We also developed a mouse model of tauopathy in which we overexpressed human BIN1. We observed that the overexpression of BIN1 rescued the long-term memory deficits and reduced the presence of intracellular inclusions of phosphorylated Tau, caused by Tau overexpression, and this was associated with an increase of BIN1-Tau interaction. Also, using post-mortem human brain samples, we observed that the levels of the neuronal BIN1 isoform were decreased in AD brains, whereas the relative levels of BIN1 phosphorylated at T348 were increased, suggesting a compensatory mechanism. Altogether, this study demonstrated the complexity and the dynamics of BIN1-Tau interaction in neurons, revealed modulators of and molecular pathways potentially involved in this interaction, and showed that variations in BIN1 expression or activity have direct effects on learning and memory, possibly linked to the regulation of its interaction with Tau.

Acknowledgements

It is with great pleasure that I write a few words of gratitude towards those who somehow took part on the path that drove me to this moment.

First and foremost, I want to express my sincere and enormous gratitude to Jean-Charles Lambert for bringing me to his team and giving me this opportunity to do my PhD under his supervision. I also want to thank him for his almost unwearying patience and understanding during these almost 4 years, full of ups and even more downs. His support, encouragement and mentorship throughout my thesis have been invaluable, and I will try to make the best of the lessons learned under his wings.

On a similar note, I want to thank Devrim Kilinc for his scepticism, guidance and friendship. Since the moment he arrived in Lille that he tries to push and challenge me in order to make me a better researcher.

I also want to thank all the people that are or were members of U1167, and most particularly of Team 3, for the way I was received when arrived in Lille and for their help and support during these years, both inside and out of the lab; and to Philippe Amouyel, who leads a research unit full of high-quality researchers and allowed me to be part of it. I want to thank Pierre, Nicolas, Anne-Marie and Julien, for their fantastic support, scientific and personal (when needed), and for sharing their experience and knowledge. I must also thank to Anaïs-Camille for unburdening me when the necessity so required (otherwise I would still be running WB…). I want to give a special thanks to Amandine, Fanny (and Quentin), Florent and Ludovic, for their fantastic integration work and their ability to make me feel at home, their friendship will be cherished; and to Shruti, Ale, Maxime and Florie, for the weird sibling-like relationship we had, the jokes, the complaints, the annoyances and support. I am also very grateful to Adrien Herledan, from U1177, without whom I would never be able to develop and perform the HCS experiments.

I want to express my gratitude to Laurent Pradier, Philippe Bertrand and Stephanie Eyquem, from Sanofi, for their collaboration in this project and for their scientific output. I also need to thank Patricia Senneville for her help with all the bureaucracy and organizing all the scientific meetings held with and at Sanofi.

I want to thank the jury members, Peter Heutink, Marie-Claude Potier, Sylvie Claeysen and Laurent Pradier, for taking time from their busy schedules to read, criticise and discuss this work, manuscript and presentation, with me.

To all my friends in Lille, in and out of the lab, French nationals and foreigners like me, I express my gratitude for their friendship over all these years, and I apologise for not being able to be with them as often as they desired. I am also grateful to my friends from University time, they inspired me to embark on this 2-side adventure, do a PhD and live abroad.

My family, especially my parents and siblings which I miss and miss me most, are the cornerstone of the person I became and those to whom I owe everything. Without their support and encouragement, I would never be who I am and here I am now. I also need to thank my parents for giving me the microscopes and dissection kits, they became very helpful.

At last, but not least, there is someone who deserves my gratitude and love above anyone else, for her strength, support, serenity, challenging mind, and for being able to push me far more than I thought possible. She encouraged me to take this challenge and suffered with my struggles and our distance, she decided to leave her family behind and embark in my adventure. Therefore, I thank to Patricia, who I love from the bottom of my heart, one of the strongest persons I know and one of the major driving forces of my life.

List of abbreviations

3xTg-AD	-	Triple transgenic AD
5-HT	-	Serotonin
ABCA7	-	ATP-binding cassette sub-family A member 7
AD	-	Alzheimer's disease
ADAM10	-	Disintegrin and metalloproteinase domain-containing protein 10
AICD	-	APP intracellular domain
Amph	-	Amphiphysin
AMPK	-	AMP-activated protein kinase
APH-1	-	Anterior pharynx-defective 1
APOE	-	Apolipoprotein E
APP	-	Amyloid precursor protein
Aβ	-	Amyloid-beta peptide
BACE1	-	Beta-site APP cleaving enzyme 1
BiFC	-	Bimolecular fluorescence complementation
BIN1	-	Bridging integrator 1
BIN1 MBD	-	Myc-binding domain of BIN1
BIN1iso1	-	BIN1 isoform 1
Ca2+	-	Calcium ion
CaMKII	-	Ca2+/calmodulin-dependent protein kinase II
CD2AP	-	CD2-associated protein
CD33	-	CD33 molecule
Cdk	-	Cyclin-dependent kinase
Cdk5	-	Cyclin-dependent kinase 5
CLAP	-	Clathrin and AP2 binding domain
CLU	-	Clusterin
CR1	-	Complement receptor 1
CsA	-	Cyclosporin A
CTFα	-	C-terminal fragment alpha
CTFβ	-	C-terminal fragment beta
DRC	-	Dose-response curve

DsRed	-	Discosoma sp. Red fluorescent protein
ELISA	-	Enzyme-linked immunosorbent assay
EOAD	-	Early onset AD
ERK2	-	Mitogen-activated protein kinase 1
FAD	-	Familial AD
FERMT2	-	Fermitin family homolog 2
FRET	-	Förster resonance energy transfer
FTD	-	Frontotemporal dementia
FTDP-17	-	FTD with Parkinsonism linked to chromosome 17
GFP	-	Green fluorescent protein
GPCR	-	G protein-coupled receptor
GSK-3β	-	Glycogen-synthase kinase 3 beta
GWAS	-	Genome-wide association studies
HCS	-	High-content screening
hTau	-	Human Tau
HTS	-	High-throughput screening
IF	-	Immunofluorescence
LOAD	-	Late onset AD
MAP	-	Microtubule associated protein
MAPK	-	Mitogen-activated protein kinase
MEK1/2	-	Mitogen-activated protein kinase kinase 1/2
NADPH	-	Nicotinamide adenine dinucleotide phosphate
N-BAR	-	N-terminal BIN-Amphiphysin/Rvs domain
NFT	-	Neurofibrillary tangles
NOS	-	Nitric oxide synthase
PEN-2	-	Presenilin enhancer 2
PHF	-	Paired-helical filaments
PI	-	Phosphoinositide binding motif
PICALM	-	Phosphatidylinositol binding clathrin assembly protein
PKA	-	Protein kinase A
PLA	-	Proximity ligation assay
PNC	-	Primary neuronal culture

PP2A	-	Protein phosphatase 2 A
PRD	-	Proline-rich domain
PSEN1	-	Presenilin 1
PSEN2	-	Presenilin 2
PTK2B	-	Protein tyrosine kinase 2 beta
PTM	-	Post-translational modification
q-PCR	-	Quantitative polymerase chain reaction
SAD	-	Sporadic AD
sAPPα	-	Soluble APP extracellular fragment alpha
sAPPβ	-	Soluble APP extracellular fragment beta
SH3	-	Src-homology 3 domain
SORL1	-	Sortilin-related receptor 1
Tau	-	Microtubule associated protein Tau
Tau MBD	-	Microtubule binding domain of Tau
TREM2	-	Triggering receptor expressed on myeloid cells 2
WB	-	Western blot / Immunoblot

Introduction

La Maladie d'Alzheimer

En 1906, Alois Alzheimer décrit plusieurs caractéristiques anatamo-cliniques d'une forme de démence qui finira par porter son nom. La maladie d'Alzheimer est la principale forme de maladie neurodégénérative, représentant de l'ordre de 50 à 70% de ces maladies regroupées sous un continuum de syndromes apparentés tels que les démences vasculaires, la maladie à corps de Lewy, les dégénérescences fronto-temporales ou bien encore la paralysie supra-nucléaire progressive. Les frontières entre ces différentes formes de démence ne sont pas toujours clairement définies et les formes mixtes ne sont pas rares, ce qui peut poser un problème de diagnostic.

D'ailleurs, dans le cadre de la maladie d'Alzheimer (qui est encore à ce jour un diagnostic différentiel donc basé sur l'exclusion d'autres causes susceptibles d'expliquer les symptômes cliniques observés,), on parlera de formes possibles, probables (du vivant du patient) et certaines. Ce diagnostic de certitude est basé sur un examen anatomo-pathologique du cerveau et la mise en évidence de lésions cérébrales de types plaques amyloïdes et dégénérescence neurofibrillaires en quantité et localisation significatives.

Le diagnostic du vivant du patient s'est appuyé durant longtemps principalement sur des examens neuropsychologiques permettant d'objectiver les symptômes hétérogènes cliniques résultant de la détérioration des fonctions cognitives et mnésiques associée à la maladie. Cependant, un certain nombre de marqueurs biologiques se sont développés au cours de ces vingt dernières années. L'imagerie médicale par résonance magnétique a permis de mettre en évidence une atrophie plus marquées de l'hippocampe chez les patients puis le développement de marqueurs utilisant la tomographie par émission de positron a récemment permis de pouvoir observer et quantifier les lésions amyloïdes et la dégénérescence neurofibrillaire du vivant du patient. En parallèle, des marqueurs protéiques quantifiables dans le liquide céphalo-rachidien ont montré leurs intérêts pour l'aide au diagnostic. Il s'agit dans ce cas de mesurer les quantités de peptides amyloïdes, de protéines Tau total et phosphorylés. Récemment se sont ajoutées les quantifications des neurofilaments et potentiellement des formes solubles de Trem2. L'utilisation de ces

marqueurs pour le diagnostic est pour l'instant encore restreinte aux centres de référence en France mais il se généralise d'ores et déjà dans les pays d'Europe du nord. Finalement, il est par ailleurs probable que dans les années à venir des marqueurs plasmatiques soient disponibles, là encore les peptides amyloïdes étant une piste prometteuse.

La conséquence du développement de ces marqueurs biologiques conduit à une redéfinition du diagnostic de MA et à la possibilité de détecter de plus en plus tôt une problématique pathologique avant même les premiers signes cliniques (avec la définition de l'entité «mild cognitive impairment»). Si cette redéfinition du diagnostic clinique de MA n'aura probablement que peu d'impact sur les projections des cas de démences dans les années à venir, cette redéfinition risque cependant de modifier la catégorisation des types de démences au sein de ces projections (avec la possibilité de redéfinir de nouvelles catégories pathologiques comme nous commençons à le voir avec la «primary age-related tauopathy» même si la réalité de cette nouvelle entité pathologique est fortement discuté).

Au niveau épidémiologique, il a été estimé en 2015 par l'organisation mondiale de la santé que la démence touchait 47 millions de personnes dans le monde (avec une incidence de, 9 millions de personnes chaque année). Selon les prédictions, le nombre de malades devrait atteindre 75 millions en 2030 et 132 millions d'ici à 2050. Cette augmentation s'explique par le fait que le premier facteur de risque de la démence (et principalement de la MA) est l'âge avec 5 % des plus de 65 ans touchés, et plus de 20% des plus de 80 ans et que l'espérance de vie progresse le plus vite dans les pays en voie de développement. En effet, près de 60 % des personnes atteintes de démence vivent dans un pays à revenu faible ou intermédiaire et on estime que la majeure partie des nouveaux cas (71 %) survient dans ces pays.

Ces chiffres alarmants ne sont cependant qu'une estimation basée sur des observations réalisée essentiellement à partir de cohortes en population générale. Ainsi ce type d'information n'est pas forcement disponible dans de nombreux pays en voie de développement et particulièrement africains. Par ailleurs, un certain nombre de facteurs pourraient amener à une modification notable de ces projections dans un sens ou l'autre. En effet, concernant la MA, il s'agit d'une maladie multifactorielle résultant de l'interaction de facteurs génétiques et environnementaux. Même si la part des facteurs non modifiables

apparaît très élevée dans le cadre de cette pathologie (de l'ordre de 60 à 80%), la part des facteurs modifiables n'est évidemment pas négligeable. Ceci est d'autant plus important qu'il a été estimé que retarder de 5 ans l'apparition des premiers signes cliniques de la maladie pourrait réduire par deux le nombre de cas prévalent de la MA ceci par mortalité compétitive. En l'absence de traitements pharmaceutiques, connaître ces facteurs modifiables pourraient donc être un premier levier pour mieux endiguer le problème majeur de santé publique qu'est la MA et ses syndromes apparentés.

Alzheimer's disease

Alzheimer's disease (AD) was identified more than 100 year ago and is the most common form of dementia, accounting for more than 50% of the cases. This disease predominantly affects elderly people, older than 65 years, and it was estimated in 2015 that about 30 million people worldwide were affected by this disease, and because of the increase in life expectancy and population ageing this number is expected to triple until 2050. The healthcare cost, and the socio-economic burden, associated with AD (and dementia in general) is very high and increases with disease's progression: AD is commonly associated to initial symptoms such as memory decline and cognitive impairment, followed by loss of motor functions and communication skills, all of which are progressive in severity until death (Alzheimer's Association 2015; Winblad et al. 2016).

AD is a complex, multifactorial and progressive neurodegenerative disorder, characterized by two main neuropathological hallmarks (H. Braak and Braak 1991): the formation of Amyloid-β peptide (Aβ) extracellular senile plaques and the development of intracellular neurofibrillary tangles (NFT), composed of abnormally hyperphosphorylated Tau, Figure 1; associated with progressive loss of synapse (Tackenberg et al. 2013; Eckermann et al. 2007) and leading to neuronal degeneration (Wenk 2003; Herrup 2015); with massive atrophy of the brain observed in severe AD patients, showing an extreme reduction on the hippocampus and cerebral cortex and an enlargement of the ventricles (Teipel et al. 2005; Van De Pol et al. 2006; Herrup 2015), Figure 2.

The identification of mutations in the *APP* gene (Amyloid precursor protein) that promoted increased levels of Aβ forms, as well as the duplication of APP gene in Down syndrome, lead to the initial formulation of the Amyloid cascade hypothesis in 1992 (J. Hardy and Higgins 1992), which postulates that "the deposition of Aβ is the causative agent of Alzheimer's pathology and that the neurofibrillary tangles, cell loss, vascular damage and dementia follow as direct result from this deposition". Later on, the identification of mutations on the genes *PSEN1* and *PSEN2*, coding the catalytic subunits of γ-secretase complex, Presenilin 1 and 2 (PSEN1 and PSEN2), responsible for cleavage of APP into Aβ, gave strength to this hypothesis (John Hardy and Selkoe 2002). The amyloid cascade

hypothesis played an influential role in the explanation of AD's pathogenesis, prompting the research towards APP metabolism and Aβ toxicity.

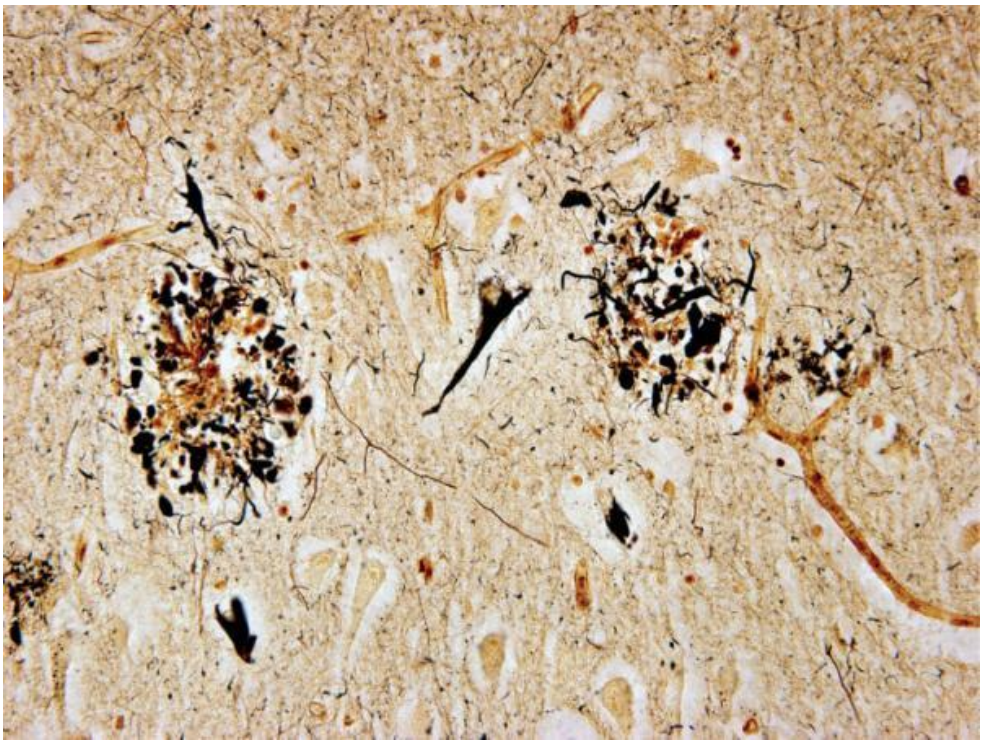

Figure 1 Photomicrograph of the temporal cortex of a patient with Alzheimer's disease (modified Bielschowski stain; magnification, 400×), showing two senile plaques with a neurofibrillary tangle between them (Perl 2010).

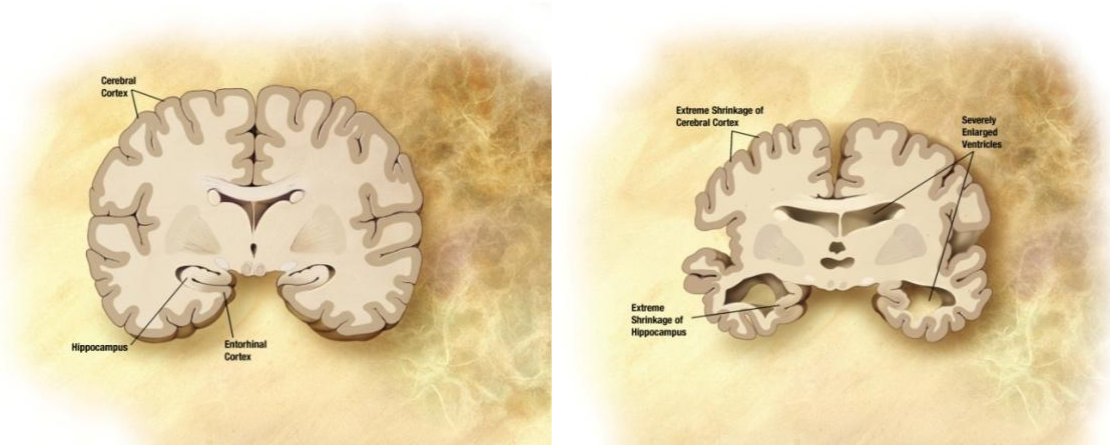

Figure 2 Schematic representation of transversal cut of preclinical and severe AD brain, depicting the regions with severe alterations. Adapted from ADEAR (Alzheimer's Disease Education and Referral Center, a service of the National Institute of Aging, National Institute of Health, USA; source http://www.nia.nih.gov/Alzheimers/Resources/MediaRoom.htm).

APP metabolism and Amyloid-β peptides

Amyloid-β (Aβ) peptides derive from the cleavage of Amyloid precursor protein (APP), coded by a gene with the same name (*APP*) located on chromosome 21 in humans. APP has about 10 different isoforms, from 639 to 770 amino acids, generated by alternative splicing. APP is ubiquitously expressed in all human tissues, mostly isoforms APP751 and APP770, with higher expression in the central nervous system (CNS), due to the predominant expression of isoform APP695 in neurons, and all these three isoforms can generate Aβ (X. Wang et al. 2017).

In neurons, APP has been associated with cell adhesion, cell-to-cell and cell-to-substratum interactions (Reinhard, Hébert, and De Strooper 2005), the modulation of cell survival, growth, motility, and neurite outgrowth (O'Brien and Wong 2011), and the regulation of synapse formation (Hick et al. 2015). APP is cleaved by two main pathways during maturation and processing, the amyloidogenic and the non-amyloidogenic pathways. During the non-amyloidogenic pathway, in the plasma membrane of the cell surface, APP is cleaved by a α-secretase (e.g. ADAM10), creating a soluble extracellular fragment termed sAPPα that is released, and a transmembranar C-terminal fragment α, known as CTFα, that is subsequently cleaved by a γ-secretase (i.e. enzyme complex composed by nicastrin, APH-1, PEN-2, and PSEN1 or 2), creating a fragment corresponding to APP intracellular domain (AICD) and a 3 kDa peptide corresponding to the amino acids between α- and γ-secretases cleavage (p3). The amyloidogenic pathway occurs in endosomes, where APP is cleaved by the β-secretase BACE1, creating and releasing to the endosome lumen the sAPPβ, a soluble fragment slightly shorter than sAPPα, and the transmembranar CTFβ, which is further cleaved by a γ-secretase to produce the same AICD and a 4 kDa peptide resulting from the cleavage by β- and γ-secretases called Aβ (Nhan, Chiang, and Koo 2015; van der Kant and Goldstein 2015), Figure 3.

Aβ can have several amino acids in length, due to N- or C-terminal truncation (Dunys, Valverde, and Checler 2018). Differences in the N-terminal are most commonly achieved by BACE1 cleavage of APP at two different sites: between Methionine 596 and Aspartate 597, giving origin to Aβ1-X, and between Tyrosine 606 and Glutamate 607, giving origin to Aβ11-X (Zhang and Song 2013). The production of Aβ11-X or truncation of Aβ1-X' N-terminal can

expose glutamate residues, located at positions 3 and 11, to cyclization by glutaminyl cyclase, and transform these residues into pyroglutamate (Gunn et al. 2016). The C-terminal of Aβ also varies in residue length, mostly due to γ-secretase differential endoproteolysis of the CTFβ: (i) γ-secretase cleavage starts at the endproteolytic ε sites, (between Leucine 49 and Valine 50 or Threonine 48 and Leucine 49) to generate Aβ49 or Aβ48, (ii) followed by trimming of the C-terminal mostly every three amino acids called ζ sites, and (iii) finishing at the γ sites (following the sequences Aβ49-46-43-40 and Aβ48-45-42-38) to produce Aβ forms with 43 to 38 residues long; but how the ε sites are recognized by γ-secretase to start the endoproteolysis process is still poorly understood (De Strooper 2010; Fernandez et al. 2016).

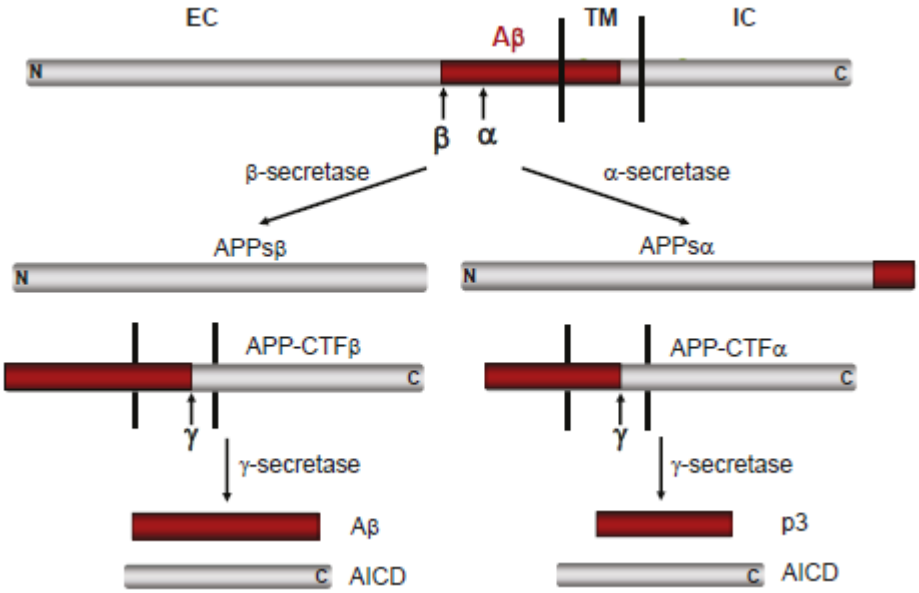

Figure 3 Schematic representation of APP canonical processing pathways (Hui Zheng and Koo 2011), showing the intermediate C-terminal fragments (APP-CTF) resulting from α- and β-cleavage and prior to γ-cleavage. EC extracellular, TM transmembrane, IC intracellular, Aβ domain is identified in red.

Aβ40 and Aβ42 are the most common forms in human brain, existing in a proportion of 9:1, and it was reported that small changes in this ratio towards Aβ42 promote the formation of oligomers, synaptic toxicity and lead to cell death (Kuperstein et al. 2010). Other studies also showed that Aβ42 are the Aβ forms more prone to oligomerize (Dahlgren et al. 2002; Resende et al. 2008), and that Aβ42 oligomers are more toxic than monomers, fibrils, and other Aβ forms (Deshpande et al. 2006; Ferreira et al. 2012; T. L. Spires-Jones and Hyman 2014), thus it was proposed that Aβ42 oligomers are the main promoters of amyloid

plaques, existing in dynamic equilibrium with its monomeric species, toxic oligomeric species and fibrils (Benilova, Karran, and De Strooper 2012). However, in recent years, it has been demonstrated that pyroglutamate-Aβ peptides are more hydrophobic, form oligomers at lower concentrations, aggregate more quickly and enhance the aggregation and neurotoxiciy of Aβ42 (Pagano et al. 2018; Dammers et al. 2017; Dunys, Valverde, and Checler 2018; Gunn et al. 2016).

Aβ oligomers have been reported to play a wide variety of roles in various culture and animal models of AD pathology such as synaptic degradation and plasticity dysfunction, Tau aberrant phosphorylation and axonal transport disruption, membrane receptor redistribution and insulin resistance, Ca2+ homeostasis, oxidative and endoplasmic reticulum stress, neuroinflammation, cell cycle re-entry and selective neuronal death (Cline et al. 2018). However, the multitude of experimental procedures used to produce or extract and characterize these oligomers makes it difficult to interpret and compare studies (Benilova, Karran, and De Strooper 2012).

While genetic studies have strongly implicate amyloid as the initiating factor in AD, the correlation of tangles with neuronal loss in AD brain, together with the lack of neuronal loss and tangle formation in APP transgenic models contributed to the idea that Tau pathology is the major contributor to dementia (T. Spires-Jones and Knafo 2012).

Microtubule associated protein Tau

Tau is part of the microtubule associated proteins (MAP) family, highly conserved in the animal kingdom, which have the canonical function of microtubule assembly regulation and stabilization, through direct binding of tubulin (Himmler et al. 1989; Al-Bassam et al. 2002). Tau is almost exclusively expressed in neurons, especially in the axons, and Tau proteins are expressed in the human brain in 6 functional isoforms, resulting from the alternative splicing of the gene *MAPT* (microtubule associated protein Tau) (Buée et al. 2000; G. Lee and Leugers 2012). These isoforms differ between them by the presence or absence of one or two inserts in the N-terminal part of the protein (0N, 1N, 2N), responsible for the interaction with other proteins of the cytoskeleton and plasma membrane, and the presence of three or four peptide repeats before the C-terminal part of Tau (3R, 4R), mainly responsible for the interaction with tubulin and identified as the microtubule binding domain (MBD). Linking the N-terminal region and the MDB, Tau has a proline-rich domain (PRD) between amino acids 151 and 244 (using as reference the longest isoform, 2N4R, with 441 amino acids) and after the MDB, from amino acid 369 to 441, Tau has a conserved C-terminal region, both of which are present in all Tau isoforms, Figure 4. The expression levels of Tau isoforms differ during neuronal development, brain region and between physiological and pathological conditions (Y. Wang and Mandelkow 2016; Guo, Noble, and Hanger 2017).

The PRD of Tau contains 7 sequences of amino acids comprised by a Proline, any two amino acids and another Proline, known as PxxP motifs, which are commonly recognized by, and are the binding sites of, Src-homology 3 domain (SH3)-containing proteins (Reynolds et al. 2008; Morris et al. 2011).

In neurons, Tau is predominantly axonal and plays a role in the stability and regulation of microtubule dynamics, regulation of axonal transport, and regulation of actin cytoskeleton; and has a plethora of partners and interactors, from microtubules and cytoskeleton proteins (tubulin and actin), passing by transport motor complexes (e.g. kinesin, p150), and protein kinases and phosphatases (e.g. Cdk5, Gsk-3β, PP2A, Calcineurin), to signal transduction proteins (e.g. 14-3-3) (G. Lee and Leugers 2012; Noble et al. 2013; Elie et al. 2015; Biswas and Kalil 2017). Tau is tightly regulated by phosphorylation: having about

eighty putative phosphorylation sites, it is targeted by several protein kinases and phosphatases; in combination with the isoform type, Tau phosphorylation modulate its sub-cellular localization; Tau phosphorylation status changes during development, with shifts in the activity ratio of kinases and phosphatases, which modulate its properties and affinity towards its partners (Buée et al. 2000; G. Lee and Leugers 2012; Y. Wang and Mandelkow 2016; Guo, Noble, and Hanger 2017).

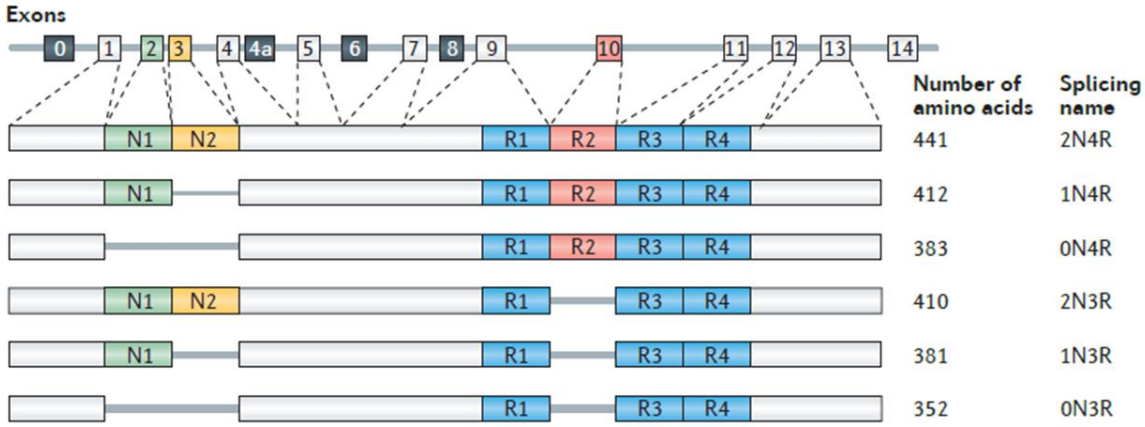

Figure 4 The human *MAPT* gene and splicing isoforms of Tau in the human brain, (Y. Wang and Mandelkow 2016). Exon 1 (E1), E4, E5, E7, E9, E11, E12 and E13 are constitutively expressed; whereas E2, E3 and E10 are subject to alternative splicing and generate the six human brain isoforms; and E4a, E6 and A8 are transcribed only in the peripheral tissue. The six brain isoforms differ according to the presence of 0,1 or 2 inserts in the N-terminal region of the protein, coded by E2 and E3 (0N, 1N, 2N), and the absence or presence of repeat R2, coded by E10, in the C-terminal region (3R, 4R) of the protein. The proline-rich domain (PRD) is coded by E5, E7 and part of E9, and connects the N-terminal to the C-terminal regions of Tau proteins.

Besides phosphorylation, Tau is target of a wide range of post-translational modifications (PTM), including isomerisation, glycation, nitration, O-GlcNAcylation, acetylation, oxidation, polyamination, sumoylation, and ubiquitynation, Figure 5; that may regulate Tau interaction with other proteins, e.g. microtubules, and even with its own modulators, e.g. protein kinases and phosphatases, possibly exacerbating or reducing Tau phosphorylated state (Iqbal, Liu, and Gong 2016; Guo, Noble, and Hanger 2017).

Tau, especially hyperphosphorylated Tau, is a hallmark of several neurodegenerative diseases including AD, commonly called tauopathies (G. Lee and Leugers 2012; Iqbal, Liu, and Gong 2016). For many years, the *MAPT* gene was a genetic risk factor of other tauopathies than AD, such as frontotemporal dementia (FTD) and FTD with parkinsonism

linked to chromosome 17 (FTDP-17) (Hutton et al. 1998) or progressive supranuclear palsy (Baker et al. 1999). However, it has been recently identified a possible association between a polymorphism in the *MAPT* region and AD (Jun et al. 2016).

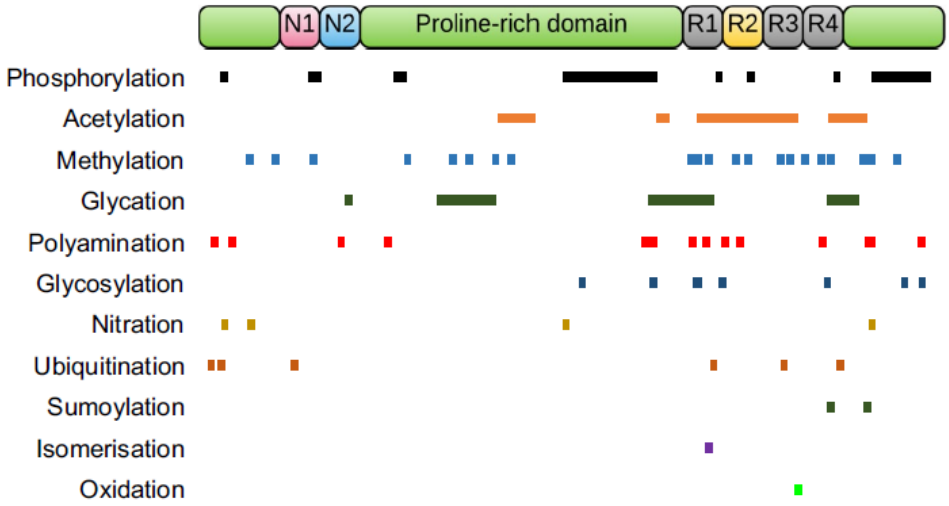

Figure 5 Distribution of known post-translational modification sites of Tau, throughout the largest human isoform, 2N4R with 441 amino acids (Guo, Noble, and Hanger 2017)

NFTs, the intracellular inclusions observed, and hallmark, in AD, are predominantly composed by paired-helical filaments (PHF) of hyperphosphorylated Tau protein (Grundke-Iqbal et al. 1986). The mechanisms underlying Tau pathology in AD are not well understood, but it is currently accepted that at least two processes contribute to the development of Tau hyperphosphorylation and aggregation, neuronal toxicity and degeneration: an imbalance on Tau phosphorylation status and the detachment of Tau from the microtubules (Ballatore, Lee, and Trojanowski 2007; Iqbal, Liu, and Gong 2016). Tau abnormal phosphorylation is enough to induce Tau aggregation, without any other aggregation promoter (Despres et al. 2017). On the other hand, Tau dissociation from the microtubules is by itself a destabilising event, prompting axonal transport dysregulation, Tau mislocalization, microtubule disassembly and synaptic dysfunction (Decker et al. 2015). Besides, it was shown that free Tau is more prone to phosphorylation at Threonine 231 than microtubule-bound Tau, and that phosphorylation at this site promotes the detachment of Tau from the microtubules (Sengupta et al. 2006).

These two processes could occur consecutively, simultaneously, and/or in parallel, and several Tau PTM have been associated with their development: changes in the activity of certain protein kinases and phosphatases (e.g. PKA, CaMKII, GSK-3β, Cdk5, PP2A, calcineurin) was shown to promote Tau abnormal phosphorylation and reduce the interaction between Tau and microtubules; wile O-glycosylation reduces Tau phosphorylation, N-glycosylation, nitration and acetylation reduce Tau microtubule binding ability and prime Tau for phosphorylation; sumoylation and acetylation promote Tau aggregation; both abnormally phosphorylated and aggregated Tau fail to be degraded by the proteasome (Buée et al. 2000; J. Z. Wang et al. 2012; Iqbal, Liu, and Gong 2016; Guo, Noble, and Hanger 2017).

Taken together, the wide variety of Tau partners (such as microtubules, actin, kinases, phosphatases, transport motor complexes) in combination with the wide variety of Tau PTMs present in physiological and/or pathological conditions (G. Lee and Leugers 2012; Guo, Noble, and Hanger 2017) makes it difficult to identify the most important pathways that lead to Tau modification and how they might be affected in pathology.

Interplay between Tau and Aβ

One of the major questions of debate in AD research is regarding which of the pathologies, Tau or Aβ, appears first and/or is more important in AD pathology (Nisbet et al. 2015; Selkoe and Hardy 2016).

It is proposed that the development and progression of the two hallmarks have distinct and independent spatiotemporal progression (Brettschneider et al. 2015), with Aβ-plaques accumulation starting several years prior to clinical symptoms in the neocortical region and progressing towards limbic regions, while NFT appears in association with neurodegeneration and develops initially in the locus coeruleus and entorhinal cortex (Iaccarino et al. 2018). Thus, it is accepted that AD starts much earlier than the detection of the first symptoms, which makes it very difficult to clinically identify and understand the biological mechanisms that lead to it (Heiko Braak and Del Tredici 2012; Villemagne et al. 2013).

Adding complexity to this question, Amyloid plaques were observed in the brains of "healthy" people, upon autopsy, and Tau is also hallmark of other neurodegenerative diseases. Tau was shown to be essential for Aβ-induced toxicity (Rapoport et al. 2002), either through interaction with Src kinase Fyn in the postsynaptic compartment of neurons (Ittner et al. 2010), and through CaMKII-AMPK pathway and Tau phosphorylation (Mairet-Coello et al. 2013). Conversely, Aβ was shown to induce mislocalization of Tau and destabilization of synapses and microtubules (Zempel et al. 2013), and reported to induce and enhance the formation of NFT (J. Götz et al. 2001; Hurtado et al. 2010; Bennett et al. 2017).

Taken together, this information suggest that although the progression processes of AD hallmarks might be independent, the physiological mechanisms underlying them might cross paths at some point, and have synergistic effects that trigger AD pathology and progression (Armstrong 2011; Jack et al. 2013; Gulisano et al. 2018). However, neither these mechanisms nor their interplay are well understood, and further investigation aimed to decipher them is warranted.

Genetics of Alzheimer's disease

AD can be arbitrarily divided into two major categories, according to the age at which patients develop the first symptoms: the early onset forms of AD (EOAD), before 65 years old, and the late onset forms of AD (LOAD), after the age of 65. Both types of AD can be further subdivided into autosomal dominant forms of AD, familial forms (FAD) and sporadic forms (SAD) (J. C. Lambert and Amouyel 2011), depending on the prevalence and hereditability of mutations in known genes, family history context and/or lack of both, Figure 6.

The genes *APP*, *PSEN1*, *PSEN2* are responsible for the rare monogenic forms of AD with autosomal dominant heritability, and the characterization of the mechanism that lead to these forms supported the amyloid cascade hypothesis. However, monogenic forms of AD only correspond to less than 1% of all clinically diagnosed AD cases (Piaceri et al. 2013).

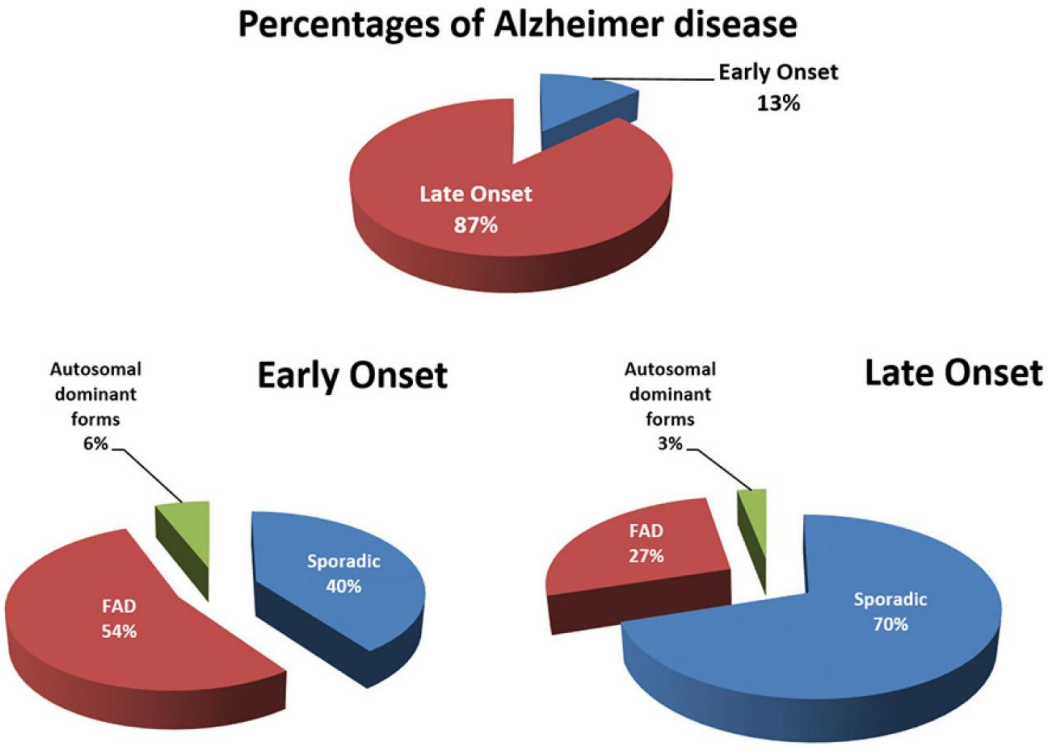

Figure 6 Percentages of early and late onset forms of AD (EOAD and LOAD, respectively), subdivided in familial (FAD), sporadic (SAD) and autosomal dominant forms of AD (Gentier and van Leeuwen 2015).

The aetiology of the remaining forms of AD cases is far more complex, resulting from the combination of environmental and genetic risk factors, such as lifestyle, mental and physical health, cognitive and physical activity, vascular and metabolic factors, aging, and several gene polymorphisms, but the way these determinants interact is unknown (Alzheimer's Association 2015; Winblad et al. 2016; Reitz and Mayeux 2014). FAD is predominantly of early onset and characterized by the knowledge of diagnosed AD in first degree relatives, indicating a very strong genetic component. Most of the LOAD forms are considered SAD because there is not an obvious familial association, either due to the lack of known genetic transmission model or insufficient family history information (Piaceri et al. 2013; Gentier and van Leeuwen 2015; J. C. Lambert and Amouyel 2011). Although the weight of the genetic component in these sporadic forms is still debatable, with genetic studies in twins showing that AD has an estimated heritability between 50 and 80 % (Gatz et al. 2006), it is currently accepted that that they involve a strong genetic predisposition and that the genetic component is complex and heterogeneous, with no simple model of disease transmission and with possible crosstalk between genetic risk factors and between genetic and environmental factors (J. C. Lambert and Amouyel 2011; Tanzi 2012).

The apolipoprotein E (*APOE*) gene was the first identified and validated gene for which different polymorphisms modulated the risk of developing AD (W. J. Strittmatter et al. 1993; Corder et al. 1993). APOE is a plasma protein involved in cholesterol transport and was shown to bind Aβ peptides (Warren J Strittmatter et al. 1993; W. J. Strittmatter et al. 1993). *APOE* gene has 3 common alleles (ε2, ε3 and ε4), with different frequencies in the Caucasian population: the most common allele of APOE is ε3 with an averaged frequency of 75%, followed by ε4 with an averaged frequency of 15%, and finally ε2 with a frequency of about 8%; that correspond to 6 different phenotypes. Genetic association studies of APOE alleles in AD and control cases reported that ε4 allele was significantly associated with AD, which means that persons carrying the APOE allele ε4 had higher risk of developing Alzheimer's disease, independent of sex but with some differences according to the ethnic group, and that this risk is considerably increased with homozygosity and age (Farrer et al. 1997; Genin et al. 2011). Interestingly, these studies also suggested that the presence of allele ε2, in homozygosity or heterozygosity with ε3, could decrease the risk of developing AD.

For years *APOE* was the sole genetic susceptibility or risk marker of LOAD, but the fact that this gene only accounted for about 20 % of LOAD's estimated heritability, indicated that additional genetic factors should be involved in the risk of LOAD, and efforts were focused in the identification of these genes (Rosenthal and Kamboh 2014). Several genes have been proposed as contributors to the susceptibility or risk of LOAD through genetic association studies, in which allele frequencies for polymorphisms in loci (regions of interest in the genome) are compared between cases and controls: when frequencies differ significantly between the groups, the gene closest to that locus is identified as susceptibility gene for the disease. However, these genetic association studies only tested small number of genes at a time and employed modest populations in the evaluation. Advances in key technological and analytical areas, in the early 2000s, made possible to evaluate practically all the genome in a single experiment, and gave rise to a methodology called genome-wide association studies (GWAS) (Schellenberg and Montine 2012). With the advent of this methodology, more than 25 loci have already been identified and associated with AD, and the closest genes identified as genetic risk factors of AD (J.-C. Lambert et al. 2013; Sims et al. 2017; J.-C. Lambert et al. 2009; Seshadri et al. 2010; Coon et al. 2007).

Because the genetic association studies identify loci, more than one gene and/or more than one polymorphism could contribute to the detection of those loci. Hence it is of the utmost importance to identify the functional polymorphism(s) in each locus, identify the causal gene(s) in each locus, and understand the contribution of these genes to AD pathogenesis (Pierre Dourlen, Chapuis, and Lambert 2018). In recent years, several studies have been performed, in order to characterize the function of the polymorphism(s) identified through GWAS, and understand the relationship between (i) AD's genetic risk factors, (ii) AD's neuropathological hallmarks, and (iii) the pathophysiological processes leading to AD. These studies tried to identify the function of the polymorphism(s) identified (Nicolas et al. 2016; Bettens et al. 2012; Brouwers et al. 2012; Malik et al. 2013), employed diverse models to characterize or validate the gene(s), from cell lines to full organisms (J Chapuis et al. 2013; Tian et al. 2013; Y. Zhou et al. 2014), and some even involved cell-based and whole-organism screening strategies to assess the function of the gene(s) of interest in AD pathological process (Julien Chapuis et al. 2017; P. Dourlen et al. 2017).

In silico approaches have been invaluable, both in the identification of genes as risk factors of AD and their possible association with AD's pathophysiological process. Taking advantage of the current knowledge of each gene function/pathway/process, researchers elaborated maps of these networks and developed bioinformatics tools, to cross-reference data obtained from high-throughput technologies with these network maps, known as pathway and network analysis approaches. The main objectives of these approaches are the (i) identification of relevant groups of related genes that are associated with specific signalling pathways, cellular processes or diseases; (ii) generation of new branches or gene clusters in these pathways and networks; and (iii) evaluation of the relationship between the various components in the same pathway or network. Altogether, these approaches have helped researchers to identify protein interactions, characterize cellular mechanisms, and propose biological roles for newly disease-associated genes, facilitating the generation of new research hypothesis (García-Campos, Espinal-Enríquez, and Hernández-Lemus 2015; Creixell et al. 2015). In the context of AD, network and pathway analysis have been useful to understand the relationship between genes associated with AD (Hu et al. 2017), identify cellular and molecular mechanisms that might be deregulated in the disease (McKenzie et al. 2017) or may be susceptible to the modulation of GWAS-defined genes (Krasemann et al. 2017), and suggest genes that may be implicated in specific disease-related pathways (Camargo et al. 2015; Julien Chapuis et al. 2017).

Although the mechanisms, by which most of the genetic risk factors of AD might be involved in AD pathological process, have not yet been unveiled, these genes can be grouped into three categories, according to their principal functions, all of which have been suggested to play some role in AD. Between the genes that regulate lipid metabolism we can find *APOE*, associated to binding and clearance of Aβ; *ABCA7*, associated with APP processing and Aβ deposition; and *CLU*, associated with Aβ clearance and fibril formation, and its protein was shown to interact with BIN1 and Tau (Y. Zhou et al. 2014). Regulating cell membrane processes (e.g. endocytosis and cell adhesion) we can find *SORL1*, associated with Aβ production; *PICALM*, shown to regulate γ-secretase endocytosis and CTF degradation, and was associated with Aβ clearance and loads; *PTK2B*, was shown to modulate Tau toxicity and co-localized with neurofibrillary degeneration markers (P. Dourlen et al. 2017); *CD2AP*, associated with APP endocytosis and blood-brain barrier

integrity; *BIN1*, associated with Aβ production and Tau oligomerization and toxicity, and also shown to interact with Tau (J Chapuis et al. 2013); and FERMT2, associated with APP metabolism and Aβ loads (Julien Chapuis et al. 2017), and possibly with Tau toxicity (Shulman et al. 2014). In the category of genes expressed in microglia and involved in immune response we have *CR1*, associated with the regulation of the complement system, the mechanism responsible for microglia phagocytosis of synapses; *CD33*, associated with the degradation of Aβ through microglia phagocytosis; and *TREM2*, responsible for the recognition of apoptotic neurons and APOE and CLU containing lipoprotein particles (shown to form complexes with Aβ) to undergo phagocytosis by the microglia, and is associated with Aβ deposition and microglia viability. These and other genetic risk factors of AD, Table 1, may have more than one physiological role and share pathophysiological processes, hence it is still necessary to further map their pathological functions, for the better understanding of AD development at cellular and molecular level (Piaceri et al. 2013; Rosenthal and Kamboh 2014; Kanatsu and Tomita 2017; Pimenova, Raj, and Goate 2018).

Table 1 Known AD genetic risk factors and their possible association with AD pathophysiological process. Adapted from Pimenova, Raj, and Goate 2018.

Gene Name	Cell Type - Specific Expression	Biological Processes	Possible Association with AD	Reference(s)
ABCA7	Ubiquitous	Lipid metabolism and phagocytosis	APP processing and Aβ deposition	(J.-C. Lambert et al. 2013; Guennec et al. 2016; Steinberg et al. 2015; Satoh et al. 2015)
ABI3	Microglia	Cell growth	—	(Sims et al. 2017)
ADAM10	Ubiquitous	Protein processing	APP processing to Aβ	(Kim et al. 2009; Saftig and Lichtenthaler 2015; Yuan et al. 2017)
AKAP9	Ubiquitous	Kinase signalling	—	(Logue et al. 2014)
APOE	Ubiquitous, major in astrocytes and microglia	Lipid metabolism and phagocytosis	Aβ binding and clearance	(Corder et al. 1993; W. J. Strittmatter et al. 1993)
APP	Ubiquitous	—	APP processing to Aβ	(Jonsson et al. 2012)
BIN1	Ubiquitous	Endocytosis	Aβ production, Tau oligomerization and toxicity, also shown to interact with Tau	(J.-C. Lambert et al. 2013; J Chapuis et al. 2013; Ubelmann et al. 2017; Calafate et al. 2016)
CD2AP	—	Endocytosis	APP endocytosis and blood-brain barrier integrity	(J.-C. Lambert et al. 2013; Ubelmann et al. 2017; Cochran et al. 2015)
CD33	Microglia	Immune response and phagocytosis	Aβ degradation	(J.-C. Lambert et al. 2013; Raj et al. 2014; Griciuc et al. 2013; Bradshaw et al. 2013)
CLU	Astrocytes	Lipid metabolism	Aβ clearance and fibril formation, also interacts with BIN1 and Tau	(J.-C. Lambert et al. 2013; Bettens et al. 2012; Y. Zhou et al. 2014)
CR1	Microglia	Immune response and phagocytosis	Synapse phagocytosis by microglia	(J.-C. Lambert et al. 2013; Brouwers et al. 2012; S. Hong et al. 2016; Crehan, Hardy, and Pocock 2013)

Table 2 (continued)

Gene Name	Cell Type - Specific Expression	Biological Processes	Possible Association with AD	Reference(s)
FERMT2	—	—	APP metabolism and Aβ loads, and possibly with Tau toxicity	(J.-C. Lambert et al. 2013; Julien Chapuis et al. 2017; Shulman et al. 2014)
MAPT	Neurons	Microtubule stability	Tau oligomerization, toxicity and NFT formation	(Jun et al. 2016; G. Lee and Leugers 2012; Iqbal, Liu, and Gong 2016)
MEF2C	—	Cell differentiation and synaptic regulation	—	(J.-C. Lambert et al. 2013; Harrington et al. 2016)
MS4A6A	Microglia	Chemosensory receptors	—	Lambert et al. 2013; Huang et al. 2017)
PICALM	—	Endocytosis and sorting	γ-secretase endocytosis and CTF degradation, also associated with Aβ clearance and loads	(J.-C. Lambert et al. 2013; Tian et al. 2013; Kanatsu et al. 2014)
PLCG2	Microglia	Phospholipase signalling	—	(Sims et al. 2017)
PLD3	Ubiquitous	—	—	(Cruchaga et al. 2014)
PTK2B	—	Cell adhesion and hippocampal long-term depression	Modulate Tau toxicity and co-localize with NFT markers	(J.-C. Lambert et al. 2013; P. Dourlen et al. 2017; Hsin et al. 2010)
SORL1	Ubiquitous	Endocytosis and sorting	Aβ production	(J.-C. Lambert et al. 2013; Nicolas et al. 2016; Kitago et al. 2015)
TREM2	Microglia	Immune response and phagocytosis	Aβ deposition and microglia viability	(Jonsson et al. 2013; Guerreiro et al. 2013; Yeh et al. 2016; Jay et al. 2017)
TREML2	Microglia	Immune response	—	(Benitez et al. 2014; Honghua Zheng et al. 2016; de Freitas et al. 2012)
UNC5C	Neurons	Response to neurotoxic stimuli, cell death	—	(Wetzel-Smith et al. 2014)

Bridging integrator 1

Genetic risk factors play a critical role in AD susceptibility, thus the comprehension of the mechanisms underlying LOAD associated genes has broaden researchers understanding of the pathways associated to AD progression, and shifted research attention from Aβ metabolism to other cellular pathways (Pimenova, Raj, and Goate 2018). One of the genetic risk factors identified through GWAS is the gene coding the protein bridging integrator 1 (BIN1) (Seshadri et al. 2010), which was described as the second most associated genetic risk factor of AD, just after APOE (J.-C. Lambert et al. 2013).

BIN1, which is also known as Amphiphysin II, is highly conserved, having high protein and DNA sequence homology between humans and other mammalian (https://www.uniprot.com/; https://www.ncbi.nlm.nih.gov/UniGene/), and has orthologs in several non-mammalian models (Prokic, Cowling, and Laporte 2014). BIN1 was initially described as Myc-binding protein able to suppress tumour growth present in (Sakamuro et al. 1996), followed by the characterization of a neuronal isoform (A. R. Ramjaun et al. 1997), and the identification of neuronal- and muscle-specific protein isoforms coded by the same gene (Butler et al. 1997).

The *BIN1* gene is ubiquitously expressed and BIN1 protein has 10 known tissue-specific isoforms, , with tissue-specific expression levels and profiles due to alternative splicing (Tan, Yu, and Tan 2013; Prokic, Cowling, and Laporte 2014). All the isoforms are composed by a N-terminal BIN-Amphiphysin/Rvs domain (N-BAR) responsible for the curvature recognition and binding of plasma membrane (Peter et al. 2004), a Myc-binding domain (MBD) responsible for the interaction with Myc boxes and inhibition of c-Myc (Pyndiah et al. 2011), and a Src-homology 3 domain (SH3) in the C-terminal of the protein, responsible for the recognition and interaction with motifs rich in proline on target proteins (Leprince et al. 1997). Isoforms 1 to 7 have an extra exon 7 in the N-BAR domain, are the only ones that express alternative splicing products of the exons 13 to 16, encoding the Clathrin and AP2 binding domain (CLAP) (Antoine R. Ramjaun and McPherson 2002) associated to vesicle formation (Slepnev et al. 1998), and are exclusively expressed in the brain. Isoform 8 has a phosphoinositide binding motif (PI) coded in exon 11, is highly expressed in the muscle, predominantly in the T-tubules (E. Lee et al. 2002). The last two

isoforms, 9 and 10, do not possess PI motif or CLAP domain, differ in the splicing of exon 17 coding MBD, and have ubiquitous expression (Wechsler-Reya, Sakamuro, et al. 1997), Figure 7.

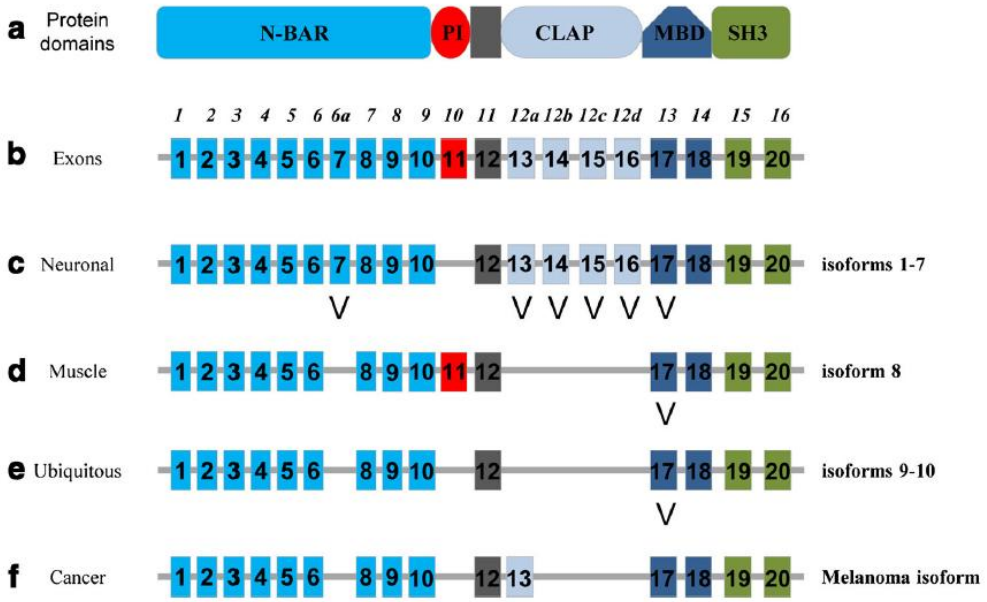

Figure 7 BIN1 protein domains, gene organization and isoforms (Prokic, Cowling, and Laporte 2014). **a**) Protein domains: N-BAR domain; PI motif; CLAP preceded by a Proline-Serine rich region; MBD; and SH3 domain. **b**) Gene organization of *BIN1*, with exons identification using the main nomenclature from NCBI and with the initial nomenclature above, in italic (Wechsler-Reya, Sakamuro, et al. 1997). Transcript isoforms found in **c**) brain, **d**) skeletal muscle, **e**) ubiquitously, and **f**) in melanoma. Alternative exons are indicated with "V".

BIN1 has been described to be involved in the most diverse functions, such as (i) cell cycle, DNA repair and apoptosis (Sakamuro et al. 1996; Wechsler-Reya, Elliott, et al. 1997; Pyndiah et al. 2011); (ii) membrane remodelling, endocytosis and recycling endosome regulation (Itoh and De Camilli 2006; Leprince et al. 1997; Pant et al. 2009); and (iii) cytoskeleton network remodelling (Meunier et al. 2009; Butler et al. 1997; Dräger et al. 2017).

Several studies have already shown that the reduction, alterations in expression or mutations on BIN1 are crucial for the development and/or progression of certain types of cancer and muscle related diseases. The underexpression or inhibition of BIN1 ubiquitous isoforms was shown to induce chemotreatment resistance in cancer cell lines through direct interaction with DNA repair proteins (Pyndiah et al. 2011); besides, the reduction of isoform 9 and the presence of a similar isoform which possessed the amino acid sequence coded by

exon 12a (BIN1+12a+13) were identified in several types of cancer (Ge et al. 1999; Pineda-Lucena et al. 2005), suggesting that the addition of this brain-specific sequence causes loss of Myc-binding function of ubiquitous BIN1 isoform. Aberrant splicing of BIN1 and mutations on BIN1 N-BAR domain were also identified in myopathies and were associated to T-tubule structural and location defects (Fugier et al. 2011; Toussaint et al. 2011; Böhm et al. 2013); whereas the decrease of BIN1's muscle isoform (BIN1+10+13) expression was associated with arrhythmia and cardiomyopathies, knockout of BIN1 in mice lead to perinatal lethal cardiomyopathy (Prendergast et al. 2009; T. Hong et al. 2014; K. Zhou and Hong 2017).

BIN1 loci was first associated with AD in GWAS through the polymorphism signal rs744373 (Seshadri et al. 2010), located 28kb upstream of BIN1 coding region. Fine mapping of this risk locus identified several single nucleotide polymorphisms and insertion/deletions, one of which, an insertion of three C bases (rs59335482), was associated with a higher risk of AD through the increase of BIN1 transcript levels, either experimentally and in the brains of AD patients (J Chapuis et al. 2013), and this polymorphism was also associated with a later age of onset and shorter disease duration (Karch et al. 2012).

Following these observations, other studies reported that in AD brains the protein levels of BIN1 neuronal isoform are decreased (Glennon et al. 2013; Holler et al. 2014; De Rossi et al. 2016), while the levels of the ubiquitous isoform are increased (Holler et al. 2014; De Rossi et al. 2016), which have higher expression in the white matter as compared to the grey matter (De Rossi et al. 2016). Consistently with this last report, immunohistochemistry of AD patient brains showed a decrease of BIN1 immunoreactivity in the neuropil region, with an increase in the neuronal soma (Adams et al. 2016), and a predominant immunoreactivity of oligodendrocytes and white matter (De Rossi et al. 2016).

Although *BIN1* loci polymorphisms had been associated with Tau loads (J Chapuis et al. 2013) and with Tau and phosphorylated Tau levels in cerebrospinal fluid (H.-F. Wang et al. 2016), there has been conflicting reports on BIN1 association with NFT and Tau pathology: some studies present no association (Adams et al. 2016) or co-staining between BIN1 and NFT (J Chapuis et al. 2013; De Rossi et al. 2017), and no correlation between BIN1 protein levels and Tau pathology (Glennon et al. 2013); while other studies show a positive

correlation between the increase of BIN1 ubiquitous isoform levels and the number of NTF in AD brains (Holler et al. 2014), or a co-localization of the neuronal isoform of BIN1 and phosphorylated Tau in the cytoskeleton/insoluble fraction of AD brain lysates (Y. Zhou et al. 2014). However, none of these studies identified any association between BIN1 and Aβ peptides or amyloid plaques.

Similar to other GWAS-associated genes, the role of BIN1 in AD is not well understood and, based on previously described functions of BIN1, it was proposed that BIN1 could modulate Tau pathology, endocytosis and recycling pathway, calcium homeostasis or inflammation (Tan, Yu, and Tan 2013), Figure 8.

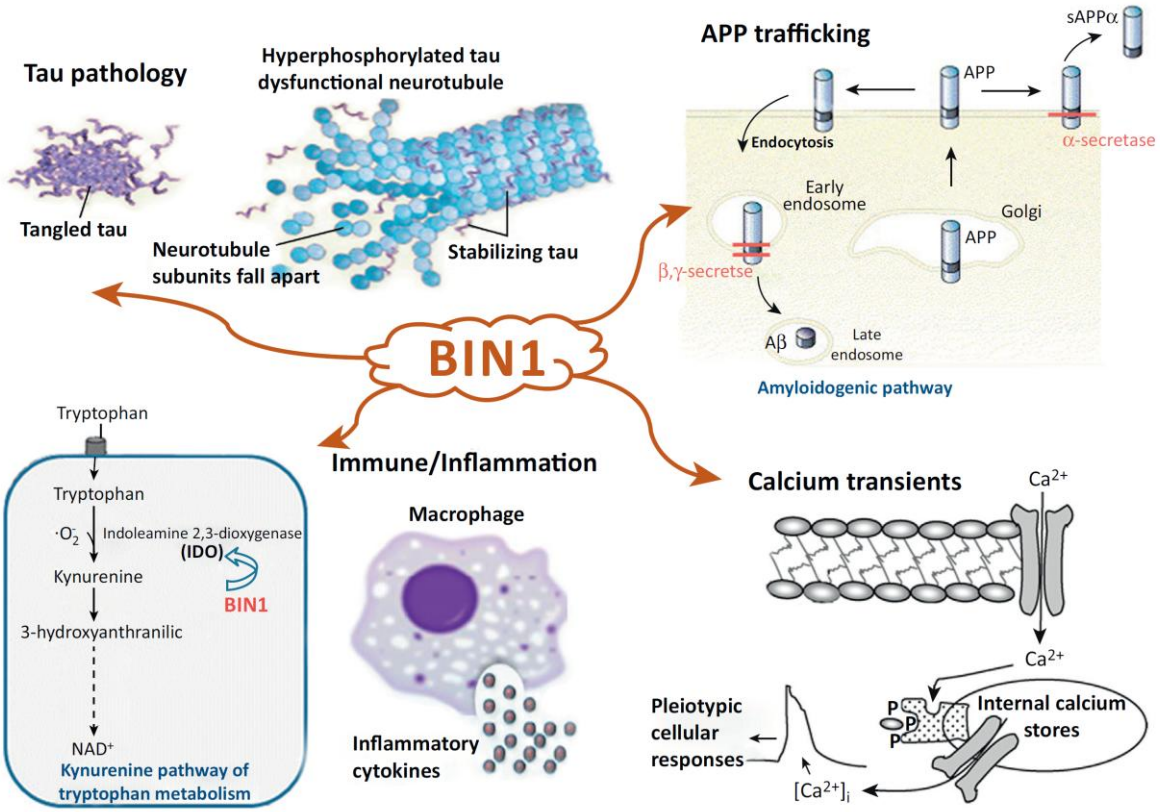

Figure 8 Summary of proposed roles for BIN1 in AD (Tan, Yu, and Tan 2013).

Previous studies have shown that the lack of BIN1 increases endocytosis (Muller et al. 2003) and disrupts recycling trafficking (Pant et al. 2009), suggesting that BIN1 regulates Clathrin-mediated endocytosis and the formation and/or transport of endocytic recycling vesicles. More recently, and in the context of AD, it was shown that the reduction of BIN1

isoform 1 protein levels is linked with the increase of Aβ production via disruption of BACE1 recycling (Miyagawa et al. 2016; Ubelmann et al. 2017) and with increase on Tau endocytosis and cell-to-cell propagation (Calafate et al. 2016).

Other studies focussed on the association of BIN1 with Tau pathology and reported that BIN1 was able to directly interact with Tau, in vitro and in vivo, and that the silencing of *BIN1* fly ortholog *Amph* was able to rescue Tau rough eye phenotype (J Chapuis et al. 2013; P. Dourlen et al. 2017), indicating that BIN1 is able to directly modulate Tau neurotoxicity. It has also been shown that BIN1 interacts with Tau through BIN1 SH3 domain, present in all BIN1 isoforms, and Tau PRD, also present in all Tau isoform, and that this interaction is modulated by Tau phosphorylation (Sottejeau et al. 2015). Additionally, it was shown that SH3 domain of BIN1 isoform 1 is naturally engaged in intramolecular interaction with its CLAP domain, due to the presence of a proline-rich motif in between residues 336 and 342, and that this domain is in competition with Tau-PRD for BIN1-SH3 binding site (Malki et al. 2017).

BIN1 has not been associated with any other neurodegenerative disease and was until recently the only genetic risk factor of AD directly associated with Tau pathology, therefore BIN1 could be the missing link between Tau pathology and LOAD development. Despite the research on BIN1 function in AD, the role of BIN1-Tau interaction in physiology or the pathophysiological process of AD it is not known, neither if it could be a potential therapeutic target for AD.

Animal models of Alzheimer's disease

Currently, there is no effective treatment for AD and part of the reduced therapeutic effectiveness lies in the difficulty to translate models of disease from one species to another and, as consequence, potential therapies that work in rodents often do not translate to humans (De Felice and Munoz 2016). One of the problems in the majority of the animal models of AD is the fact that these models are created based on the mutations or duplication of genes responsible for neurodegenerative diseases other than AD (e.g. Tau mutations responsible for FTD), or responsible for the rare monogenic forms of AD (i.e. *APP*, *PSEN1* and *PSEN2*). Moreover, to replicate some of the events associated with AD, such as the development and distribution of AD's neuropathological hallmarks, two or more of these mutated genes need to be expressed together (Jürgen Götz and Ittner 2008).

Nevertheless, animal models are indispensable tools in biomedical research, not only being invaluable in the evaluation of novel therapeutic approaches, but also of the utmost importance in the identification and characterization of critical disease-related mechanisms. Thus, the development of models, animal and/or cellular, that better recapitulate the mechanisms that lead to the development or progression of human diseases, notably AD, has been the goal of many researchers (LaFerla and Green 2012).

Such is the case of the 3xTg-AD mouse model, that was generated through the combined expression of APP^{SWE} and Tau^{P301L} on a $PSEN1^{M146V/-}$ background mouse model, and closely recapitulates human AD pathology: development and distribution of senile plaques and NFT, synaptic transmission and long-term potentiation deficits, and learning and memory impairment (Oddo et al. 2003). Other models use non-mutated human genes, such as *MAPT*, to assess the development of hyperphosphorylated Tau, PHF and NFTs in mouse brains (Andorfer et al. 2003; Polydoro et al. 2009), or to evaluate the modulation of Tau toxic phenotype *in vivo* in fruit fly (J Chapuis et al. 2013). Although it could be argued that these models are more tauopathy models than AD's, they allow the dissection of the pathways that lead to the development of NFTs and the associated toxicity, which is less known than the metabolism of APP.

Although several mouse models have been developed to study the mechanisms underlying APOE role in AD (Knouff et al. 1999; Sun et al. 1998; Youmans et al. 2012), and more recently TREM2 and ABCA7 (https://www.alzforum.org/research-models/alzheimers-disease), the contribution of other GWAS-defined genes in the progression of AD has not yet been validated in mouse models. Only recently it was reported the development of a mouse model based on the overexpression of the human gene of BIN1 (Daudin et al. 2018).

Another advantage of animal model is the wide range of studies that can be performed, such as behaviour, lifespan and viability studies, live imaging, cellular and molecular analysis. Although mouse models are the usually the models of choice for most researchers, the roundworm *Caenorhabditis elegans* and the fruit fly *Drosophila melanogaster* also have their advantages in translational research, notably of AD: both are easy to produce and maintain, have short lifespans and reproduce in large numbers, both possess orthologs of human genes associated with AD, little gene redundancy, and genetic mutations can easily be performed, to generate several transgenic lines simultaneously. While *C. elegans* is a perfect model to perform whole-organism screenings in microtiter plates, it is nearly impossible to perform behavioural studies. On the other hand, *Drosophila* has shown its potential as a model for a wide range of studies, and a powerful tool in the screening of modifiers that either enhance or suppress AD-associated pathology (Jürgen Götz and Ittner 2008; Jürgen Götz and Götz 2009).

Currently, screening approaches are some of the most powerful tools to identify and study potential pathophysiological functions of GWAS-defined risk genes of AD (Pierre Dourlen, Chapuis, and Lambert 2018). Our lab possesses the knowhow and the tools to develop and perform cell-based and whole-organism (i.e. *Drosophila*) functional screenings. For instance, two studies have recently been published by our lab: one employed a high content screening (HCS) approach with siRNA, and associated FRMT2 to the metabolism of APP (Julien Chapuis et al. 2017); another used *Drosophila* to perform *in vivo* functional screening of AD risk loci, and identified PTK2B as a modulator and marker of Tau pathology (P. Dourlen et al. 2017).

High Content Screening

High throughput screening (HTS) is a method commonly used in pharmaceutical research that allow the evaluation of large amounts of reagents to identify potential biological targets and/or biologically active compounds that can be used as drugs. Since the 1970s, HTS has been used to biochemically characterize compounds against purified molecular targets, but the fact that these targets were isolated from their biological environment lead to the characterization of millions of compounds that had very little or no effect when tested in complex biological models. In the 1990s, cell-based assays started to be introduced in HTS in order to overcome the lack of physiological significance of basic biochemical assays. The introductions of cells in HTS pipelines introduced other levels of complexity to these assays: now researchers could (i) test not only thousands of compounds in parallel but also genes and/or their respective proteins, and (ii) analyse a wide range of cellular responses. To address these challenges, several readout techniques were developed and implemented to HTC, such as microscopy, leading to the development of high content screening (HCS) (Xia and Wong 2012). In recent years, both HTS and HCS techniques took advantage of the development and miniaturization of biochemical and cellular assays, liquid handling automation, and the development of automated quantitative readouts and analysis software (Varma, Lo, and Stockwell 2011; Jain and Heutink 2010).

HCS can be considered as a cell-based multi-metric HTS, resulting from the merge of large cellular screening automated assays and multiple readout analysis, obtained from the development of microscopy techniques, equipment and resolution. HCS is a technology that does not require any prior knowledge of the molecular targets, being particularly useful in the characterization of unknown cellular mechanisms and molecular pathways, and is a huge advantage when compared to traditional cellular assays in which only few numbers of genes can be modulated, or compounds tested, at each experiment (Xia and Wong 2012; Mattiazzi Usaj et al. 2016).

HCS is gaining its space in pharmaceutical industry and academia, applied and basic research, but it is still not frequently used as the major primary screening assay. Possibly this is due to the long development time, the high throughput microscopy and computational hardware and analysis software required, and the specialized expertise needed to carry it

out. Another reason for the reduced use of HCS as principal screening assay is the stiff statistical requirement to validate the assay's quality in both HCS and HTS, normally using readouts that employ only one variable (e.g. Z'-factor or β-score (Bray and Carpenter 2013)), that not only can limit or arrest the development of a HCS assay, often due to the readout variability, but also weight in favour of a simpler and/or cell-based HTS instead of a HCS (Singh, Carpenter, and Genovesio 2014; Mattiazzi Usaj et al. 2016).

HCS allows the identification, and possibly the characterization, of regulators and molecular pathways of biological, physiological and pathophysiological processes in an unbiased manner, using cellular models and microscopy imaging, in automated fashion.

Most HCS studies are performed with immortalized cell lines, which are easier to maintain, manipulate and transfect, usually producing more homogenous cellular responses (Daub, Sharma, and Finkbeiner 2009), but in recent years there was an increase in the number of studies developed using more physiologically relevant cellular models, most notably primary neurons (Evans et al. 2008; Hattori et al. 2010; Charoenkwan et al. 2013; McDonough et al. 2017; van Deijk et al. 2017) and induced pluripotent stem cells (Sherman and Bang 2018; Ryan et al. 2016). Despite the multiple phenotypic measurements available, and sometimes analysed (such as cell number and categorization, neurite length, synaptic puncta, etc...), most of the HTS/HCS studies in the field of neurobiology tend to analyse almost exclusively cellular development, toxicity and degeneration, and pay little attention to the underlying cellular and molecular mechanisms (Cooper et al. 2017).

To challenge the cellular models and develop any phenotypic modifications, HCS rely in three major types of libraries: (i) complementary DNA (cDNA) libraries for the study of gene overexpression, (ii) short hairpin and small interfering RNA (shRNA and siRNA) libraries to study gene loss-of-function, and (iii) chemical compound libraries that have been used since the initial development of HTS. The use of compound libraries enables the direct and fast identification of pharmacologically active molecules and new biological targets of known compounds, not only leading to the characterization of molecular pathways but also to a practical result translation in drug-discovery research. Another advantage of compound libraries is that they are fairly easy to automatize and deliver into the cells. On the other hand, the compounds active concentrations tend to vary across the library and experimental

model, and drugs with higher efficacies usually have multiple targets, potentially compensating for pathway redundancies, especially in the nervous system (Cooper et al. 2017).

Finally, in order to identify and evaluate those phenotypic changes two major approaches can be employed, in association with microscopy. Reporter peptides, such as fluorescent proteins (e.g. GFP, DsRed), can be used in live imaging to follow the dynamics of target proteins over-time, and even assess protein-protein interaction dynamics through techniques such as Förster resonance energy transfer (FRET); however, this approach requires the overexpression of modified target proteins. On the other hand, the endogenous protein levels and their location can be assessed with the use of antibodies; however, immunofluorescence (IF) is not compatible with the study of live cells and simple IF does not allow the detection of protein-protein interactions. In the last 15 years, a new technique, *in situ* proximity ligation assay (PLA), has been developed to study protein-protein interactions at their endogenous levels through microscopy and shown to be a powerful tool to analyse protein interactions in physiological levels, in the presence or absence of genes and/or compounds of interest (Weibrecht et al. 2010). In fact, *in situ* PLA was even reported to be the major readout in a small-scale screening, using 96-well plate format, for the identification of compounds that inhibited the platelet-derived growth factor receptor (K.-J. Leuchowius et al. 2010).

Proximity Ligation Assay

Since the development of microscopy several approaches were developed for the identification of cell types, detection of subcellular structures, their localization and even interaction. Traditional histochemistry and cytochemistry techniques have commonly been used to target a heterogeneity of biomolecules, detect cell populations and subcellular structures, while the application of antibodies allowed the detection of specific proteins in these structures. With the development of fluorescent microscopy, thanks to discovery of fluorescent molecules such as the green fluorescent protein (GFP), IF became very popular to detect endogenous proteins, identify of their subcellular localization and co-localization. This last one can be accomplished by superimposing images of fluorescent channels from different targets, but the microscopic resolution does not allow the differentiation of proteins co-localization from protein-protein interaction. The possibility to fuse these fluorescent molecules to target proteins allowed the development of several assays for the *in vivo* detection of proteins and their subcellular localization, and protein-protein interactions, e.g. FRET and bimolecular fluorescence complementation (BiFC). However, these techniques rely on the overexpression of proteins and cannot be used to study proteins interaction at their endogenous levels. On the other hand, proximity ligation assay (PLA) was specifically developed to allow the detection of protein interactions and protein PTM at endogenous levels (Weibrecht et al. 2010).

Since it was first described in 2002, PLA has been used in association with techniques as diverse as western blot (WB), ELISA, q-PCR, flow cytometry and IF, to detect (or improve the detection of) proteins, PTMs and protein interactions, at endogenous levels. This methodologies have been applied in a range of biological systems, such as cell lines and primary cultures, tissue section and samples, purified *in vitro* protein suspensions and plasma, in the most diverse fields, including cancer research, immunology, virology, neurobiology, drug discovery, and PLA proved to be a useful tool in research and clinical diagnose (Blokzijl et al. 2014; K. J. Leuchowius, Weibrecht, and Söderberg 2011).

In situ PLA is a development of the proximity ligation strategy that allows the detection of protein-protein interactions and protein post-translational modifications through microscopy with high selectivity and sensitivity, so long as the distance between the

target epitopes is inferior to 40 nm (Söderberg et al. 2006; Jarvius et al. 2007; Bagchi, Fredriksson, and Wallén-Mackenzie 2015).

This technique combines the use of (i) specific antibodies targeting the protein(s) of interest, with the methods of (ii) proximity ligation, in which DNA strands attached to antibodies that bind the target molecule(s) are connected by enzymatic ligation, if the targeted molecule(s) are in close proximity, and (iii) rolling-circle amplification, in which a single strand of DNA is amplified with fluorescent-labelled oligonucleotides, using the ligation product as template, and generates a randomly coiled fluorescent product (Gustafsdottir et al. 2005; Weibrecht et al. 2010), Figure 9. Like an IF, *in situ* PLA can be performed using only antibodies targeting the protein(s) of interest or in association with secondary antibodies targeting the primary antibodies, and although the use of secondary antibodies requires extra steps of incubation and washing, it allows a broader choice of primary antibodies. As stated before, the use of antibodies allows the detection of proteins at endogenous levels, however this detection is highly dependent of the antibodies affinity, sensitivity and selectivity towards the target protein, as well as sample and/or tissue processing (fixation, permeabilization, saturation, storage and preservative, and section thickness). Another aspect of endogenous protein detection with antibodies is the fact that samples need to be fixed, producing only endpoint images of the biological processes of interest and not the temporal study of it (Stadler et al. 2013).

From here on, *in situ* PLA will be simply referred to as PLA, Figure 10.

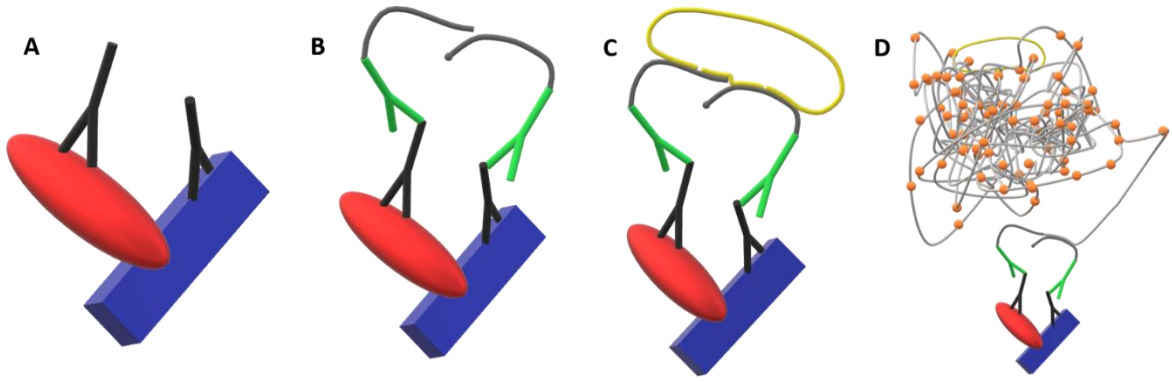

Figure 9 Proximity Ligation Assay (PLA) steps. **A**) The two proteins of interest are targeted by specific primary antibodies, produced in different hosts. **B**) The two primary antibodies are targeted by secondary antibodies with strands of DNA covalently attached, called PLA probes. **C**) The DNA strands form a template for the ligation of additional oligonucleotides. **D**) The resulting DNA strand is used as template in a rolling circle amplification (RCA) reaction using fluorophores-labelled oligonucleotides, which can be visualized by microscopy as intense fluorescent spot.

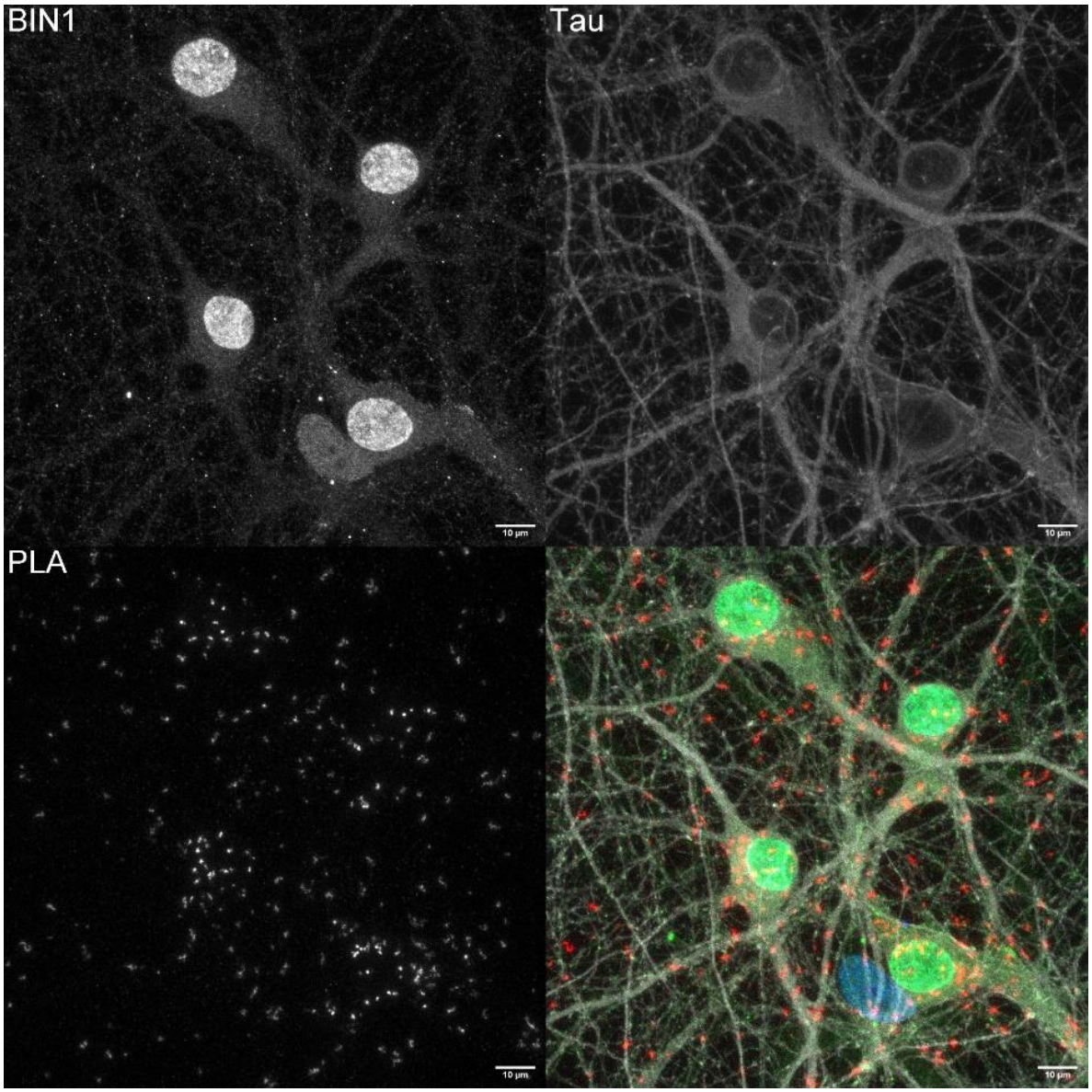

Figure 10 Representative image of BIN1, Tau and BIN1-Tau interaction through PLA, in 14 DIV mixed PNC. Maximum intensity projection of images acquired using confocal microscope Zeiss LSM710, with 63x glycerol objective. Scale bar correspond to 10 µm.

Objectives

BIN1 is AD's second most associated genetic risk factor, and is the first to be directly associated with Tau. Our team has previously shown that (i) *BIN1* risk allele was not only associated with higher *BIN1* expression levels but also with Tau loads in AD patient brains (rs59335482), (ii) variation in the expression of *BIN1* fly ortholog, *Amph*, modulated Tau toxic phenotype, and that (iii) BIN1 and Tau interacted *in vitro* and *in vivo* (J Chapuis et al. 2013).

Although some studies have explored BIN1's physiological function in neurons and its possible role in AD pathophysiological process (Calafate et al. 2016; Ubelmann et al. 2017; Miyagawa et al. 2016), these studies do not take into account the fact that BIN1 and Tau interact. In addition, the function of BIN1-Tau interaction it is not known, nor its role in the pathophysiological process of AD, which could be a potential therapeutic target.

In order to better understand BIN1-Tau interaction, this project was developed with three major objectives: (i) identify the interaction sites between BIN1 and Tau, (ii) identify how the interaction could be modulated, (iii) highlight molecular pathways that could be involved in the modulation of BIN1-Tau interaction, and (iv) understand how BIN1-Tau interaction is involved in AD pathological process.

Results

Tau phosphorylation regulates the interaction between BIN1's SH3 domain and Tau's proline-rich domain

Tau is the main component of one of AD's neuropathological hallmarks, associated with neurodegeneration, and BIN1 is a genetic risk factor of AD. Previous work carried out in our lab showed that (i) BIN1 risk allele rs59335482 was associated with higher BIN1 expression levels and with Tau loads in AD patient brains, (ii) Tau toxic phenotype was modulated by variation in the expression of BIN1 fly ortholog, *Amph*, and that (iii) BIN1 and Tau interacted *in vitro* and *in vivo* (J Chapuis et al. 2013). Tau, besides being a microtubule associated protein, is also involved in cell signalling pathways via the recruitment of kinases and signalling adaptors through its PRD. Moreover, Tau is strongly regulated by phosphorylation, which is deregulated in AD (Guo, Noble, and Hanger 2017). BIN1 is a protein with roles in the regulation of the cytoskeleton, membrane remodelling and recycling, and endocytosis, mediated by its N-BAR, CLAP and SH3 domains, which bind to proline-rich motifs (Prokic, Cowling, and Laporte 2014).

Therefore, we started by hypothesising that BIN1 and Tau interact through BIN1-SH3 domain and Tau-PRD, and that Tau phosphorylation could regulate this interaction. Then we question if BIN1-Tau interaction is involved in the neuropathological process of a mouse model of tauopathy, and searched for the cellular processes and molecular pathways that are potentially involved in the modulation of BIN1-Tau interaction.

Firstly, not only we demonstrated that the interaction between BIN1 and Tau occurs through the SH3 domain and the PRD but we also determined that the sequence of amino acids from T212 to T231, within the PRD, is involved in this interaction. Furthermore, our data indicate that BIN1-Tau interaction is modulated in vitro by Tau phosphorylation of PRD, particularly at T231. Upon the confirmation of this data in situ through proximity ligation assay (PLA) in primary neuronal cultures (PNC), it was observed a huge decrease of BIN1-Tau interaction when targeting Tau phosphorylation at T231, but not when targeting Tau phosphorylation at S396/404. This data is consistent with other studies that identified the PRD as the interaction site between Tau and its partners, notably those of Src family or that

possess SH3 domain, and that demonstrated that T231, but not S396/404, is important in the regulation of Tau interaction with Fyn-SH3 domain (Reynolds et al. 2008; Bhaskar, Yen, and Lee 2005). Tau is hyperphosphorylated in AD and the phosphorylation of T231 occurs in the earlier stages of the disease, before tangle formation (Augustinack et al. 2002).

Then, we decided to further characterize BIN1-Tau interaction by looking at the subcellular localization of this interaction relative to markers of cellular compartments, essential to neuronal functions. Using PNC, we saw no co-localization between PLA and a marker of the endocytosis pathway, Clathrin, neither with pre- or post-synaptic markers, suggesting that BIN1-Tau interaction is not involved in the pathogenic pathways involving BIN1 in endocytosis and Tau at the synapse. Conversely, we found a considerable co-localization between PLA and actin cytoskeleton, leading to the postulation that BIN1-Tau interaction might have a role at the interface between actin cytoskeleton and microtubule networks. Interestingly, it has been demonstrated that BIN1 and Tau, independently, regulate actin dynamics (Elie et al. 2015; Dräger et al. 2017). Furthermore, Tau was shown to interact with actin at the post-synaptic densities (Frandemiche et al. 2014) and at the axonal growth cone (Biswas and Kalil 2017), and to promote the development of actin bundles, when Tau is abnormally phosphorylated (Fulga et al. 2007), suggesting a possible interplay between actin cytoskeleton and BIN1-Tau interaction dynamics.

Our results suggest a link between BIN1, Tau phosphorylation and AD-related pathways, and highlight the need for further researched aimed to understand the connection between BIN1, Tau, actin cytoskeleton and AD.

This work was published in Acta Neuropathologica Communications in September 2015, being presented here in its published form, and with the supplementary data (except “Additional file 11: A movie showing 3D images processed with IMARIS software”).

Sottejeau *et al. Acta Neuropathologica Communications* (2015) 3:58
DOI 10.1186/s40478-015-0237-8

ACTA NEUROPATHOLOGICA COMMUNICATIONS

RESEARCH Open Access

Tau phosphorylation regulates the interaction between BIN1's SH3 domain and Tau's proline-rich domain

Yoann Sottejeau[1,2,3†], Alexis Bretteville[1,2,3†], François-Xavier Cantrelle[3,4,5], Nicolas Malmanche[1,2,3], Florie Demiaute[1,2,3], Tiago Mendes[1,2,3], Charlotte Delay[1,2,3], Harmony Alves Dos Alves[1,2,3], Amandine Flaig[1,2,3], Peter Davies[6,9], Pierre Dourlen[1,2,3], Bart Dermaut[1,2,3,8], Jocelyn Laporte[7], Philippe Amouyel[1,2,3], Guy Lippens[3,4,5], Julien Chapuis[1,2,3], Isabelle Landrieu[3,4,5*†] and Jean-Charles Lambert[1,2,3*†]

Abstract

Introduction: The application of high-throughput genomic approaches has revealed 24 novel risk loci for Alzheimer's disease (AD). We recently reported that the bridging integrator 1 (BIN1) risk gene is linked to Tau pathology.

Results: We used glutathione S-transferase pull-down assays and nuclear magnetic resonance (NMR) experiments to demonstrate that BIN1 and Tau proteins interact directly and then map the interaction between BIN1's SH3 domain and Tau's proline-rich domain (PRD) . Our NMR data showed that Tau phosphorylation at Thr231 weakens the SH3-PRD interaction. Using primary neurons, we found that BIN1-Tau complexes partly co-localize with the actin cytoskeleton; however, these complexes were not observed with Thr231-phosphorylated Tau species.

Conclusion: Our results show that (i) BIN1 and Tau bind through an SH3-PRD interaction and (ii) the interaction is downregulated by phosphorylation of Tau Thr231 (and potentially other residues). Our study sheds new light on regulation of the BIN1/Tau interaction and opens up new avenues for exploring its complex's role in the pathogenesis of AD.

Introduction

Alzheimer's disease (AD) is a progressive, neurodegenerative disorder characterized by (i) the massive loss of neurons in several regions of the brain. There are two distinct types of lesion: intraneuronal neurofibrillary tangles (NFTs, composed of abnormally phosphorylated Tau proteins) and extracellular amyloid deposits (composed of amyloid-β peptide (Aβ)). Mutations in the genes for amyloid precursor protein (APP), presenilin-1 and presenilin-2 are responsible for rare, autosomal-dominant forms of AD. The discovery of these mutations prompted the amyloid cascade hypothesis, which has radically changed our understanding of AD; APP metabolism and Aβ peptide production/degradation are thought to have a key role in the pathogenesis of AD (or at least the rare, familial forms of AD) [1]. However, the validity of this hypothesis in the vast majority of cases of AD (the so-called sporadic form) is subject to debate. Since 2009, the application of high-throughput genomic approaches has led to the characterization of 24 additional genetic risk factors for sporadic AD (following on from the apolipoprotein E (APOE) gene, which was characterized as a major genetic risk factor in 1993) [2]. We recently reported that the bridging integrator 1 (BIN1) gene is the first of these new genetic determinants for sporadic AD with a clear link to Tau pathology and (potentially) neurofibrillary degeneration [3]. We found that BIN1 was upregulated in the brains of AD cases and that a functional variant modulating BIN1 expression was associated with NFT loads. We were also able to show that BIN1 and Tau were directly interacting together *in vitro* and that human Tau toxicity observed in *Drosophila melanogaster* was partly suppressed by the silencing of the *Drosophila* BIN1 ortholog [3]. Taken as a whole, these data

* Correspondence: isabelle.landrieu@univ-lille1.fr; jean-charles.lambert@pasteur-lille.fr
†Equal contributors
[3]Université de Lille, Lille, France
[1]INSERM, UMR 1167, Lille, France
Full list of author information is available at the end of the article

suggest that BIN1 interacts with Tau and is involved in Tau pathology. We therefore decided to characterize the BIN1-Tau interaction and the latter's putative regulatory mechanisms in more detail. In the present work, we used glutathione S-transferase (GST) pull-down and nuclear magnetic resonance (NMR) experiments to show that BIN1's SH3 domain interacts with Tau's proline-rich domain (PRD). We found that amino acids [212–231] in Tau are essential for this interaction, and that phosphorylation within this sequence weakens the binding. Lastly, we used a proximity ligation assay (PLA) in primary neuron cultures to show that BIN1-Tau complexes co-localize with the actin cytoskeleton. However BIN1-Tau complexes were not observed in neurons when Tau Thr231 is phosphorylated. Taken as a whole, our results provide a detailed view of the molecular interplay between Tau and BIN1 and show for the first time that Tau phosphorylation weakens the interaction between these two proteins.

Materials and methods

cDNA and plasmids

Tau full-length (FL) 2N4R cDNA in pcDNA four was a kind gift from Luc Buée (INSERM U837, Lille, France). The BIN1 isoform used in the present study corresponds to the longest neuronal isoform 1 and will be denoted as BIN1 FL. For GST pull-down experiments, both Tau FL and Tau sub-fragment cDNA sequences were obtained by PCR with the primers described in Additional file 1, and subcloned into the pGEX-4 T2 vector (General Electric Healthcare Bio-Sciences, Piscataway, NJ, USA) to produce GST-Tau constructs. GST BIN1 FL and GST-BIN1/SH3 were obtained as previously described [4]. BIN1/ΔSH3 cDNA sequence was obtained by PCR from BIN1 FL cDNA (NM_139343.1) in PCMV6-XL5 (Origene, Rockville, MD, USA). For NMR experiments, the BIN1/SH3 domain cDNA was synthesized with optimized codons for recombinant expression in *E. coli* (Genecust, Dudelange, Luxembourg). The cDNA was subcloned between the *NdeI* and *XhoI* restriction sites in pET15b (Novagen, EMD Millipore, Darmstadt, Germany), thus allowing its expression with an N-terminal HisTag under the control of a T7 promoter. Recombinant Tau-F5[165-245] and TauFL were prepared for NMR experiments without a N-terminal tag with a pET15B vector. All cDNAs were checked by sequencing.

Cell cultures and transfection

Human embryonic kidney 293 (HEK293) cells (CRL-1573 from LGC Standards/American Type Culture Collection, Molsheim, France) were cultured in Dulbecco's modified Eagle's medium (DMEM)/F12 (1:1) supplemented with 10 % fetal bovine serum, 2 mM glutamine, 20 units/ml penicillin and 20 μg/ml streptomycin (Gibco, LifeTechnologies, Carlsbad, CA, USA) in 5 % CO_2 atmosphere and at 37 °C. Transient transfections were performed using Fugene-HD (Promega, Madison, WI, USA) according to the manufacturer's instructions. Forty-eight hours later, cells were harvested in Tris-buffered saline (100 mM NaCl, 1 mM EDTA, 50 mM Tris–HCl) and centrifuged at 1000 g for 10 min at room temperature. Cell pellets were stored at−80 °C until processing for GST pull-down.

The GST pull-down assay

The GST fusion proteins were expressed in *Escherichia coli* BL21(DE3) after induction with isopropyl 1-thio-β-D-galactopyranoside. Proteins were extracted from bacterial inclusion bodies by incubation with lysosyme for 1 h, overnight incubation with N-sarkosyl (0.001 %) and Triton X-100 (0.5 %), sonication and then centrifugation at 12,500 g for 30 min. All steps were performed at 4 °C. The GST fusion proteins were immobilized on glutathione-Sepharose beads (Pierce, ThermoFisher Scientific, Rockford, IL USA) according to the manufacturer's instructions, and then incubated with HEK293 cell lysates for 1 h at room temperature. Beads were washed in Tris buffered saline, centrifuged at 10,500 g for 1 min and processed for SDS-PAGE analysis.

Isotopic labelling and protein purification

Isotopic labelling of Tau and Tau-F5 was performed by growing recombinant BL21 (DE3) in minimal growth medium supplemented with ^{15}N NH_4Cl. The first purification step was performed by heating the bacterial protein extract for 15 min at 75 °C. The ^{15}N Tau protein and ^{15}N Tau[165–245] were recovered in the soluble fraction after centrifugation at 15,000 g for 30 min. The ^{15}N Tau protein and ^{15}N Tau-F5 were purified by cation exchange chromatography in 50 mM phosphate buffer pH 6.3, 1 mM EDTA (5 ml Hitrap SP Sepharose FF, General Electric Healthcare, Little Chalfont, United Kingdom). The pooled fractions from the chromatography purification step were transferred to ammonium bicarbonate by desalting on a 15/60 Hiprep desalting column (G25 resin, General Electric Healthcare) and lyophilized. The His-SH3 protein was purified on Ni-NTA resin, according to the manufacturer's protocol.

Acquisition and analysis of NMR spectra

1 mM d_4-TMSP (3-(trimethylsilyl) propionate was used as an internal reference for proton chemical shifts (CSs) (0 ppm). The NMR buffer was 25 mM Tris-d11 pH 6.6, 30 mM NaCl, 2.5 mM EDTA and 1 mM DTT and 5 % D_2O. Two-dimensional [^1H, ^{15}N] heteronuclear single quantum coherence (HSQC) spectra were recorded at 298 K on a Bruker 900 spectrometer equipped with a triple-resonance cryogenic probe (Bruker, Karlsruhe, Germany). Spectra were processed using Bruker TopSpin software (version 2.1, Bruker, Karlsruhe, Germany),

and peaks were picked using Sparky software (version 3, T. D. Goddard and D. G. Kneller, University of California, San Francisco, CA, USA). The delta (δ) CSs of individual amide resonances of Tau-F5 and Tau FL were calculated with the following equation, while taking account of the relative dispersion of the proton and nitrogen CSs: $\delta(CS) = [((CS^{1}H_{bound} - CS^{1}H_{free}) + 0.2 (CS^{15}N_{bound} - CS^{15}N_{free}))^{2}]^{1/2}$. The "bound" and "free" subscripts in the equation correspond to the CSs in the SH3-bound protein or the free protein, respectively.

Phosphorylation of Tau protein

The CDK2/CycA3 protein was prepared and Tau was phosphorylated *in vitro* as previously described [5]. Enzymatic reactions were terminated by heating for 15 min at 75 °C and then centrifuged. The phosphorylation mixture was buffer-exchanged for NMR buffer using centrifugal desalting columns (Zeba Desalting Columns, with a 0.5 ml bed of G25 resin and a 7 kDa cut-off (Thermofisher Scientific, Waltham, MA USA)).

Electrophoresis and Western blots

Samples were resuspended in Lithium Dodecyl Sulfate buffer supplemented with Nupage antioxidant, heated for 10 min at 95 °C, loaded and separated on a 4–12 % acrylamide gel (Nupage, Novex, Life Technologies, Carlsbad, CA, USA) and blotted on nitrocellulose membranes using a BioRad Trans-Blot transfer system kit (BioRad, Hercules, CA, USA) according to the manufacturer's instructions. Membranes were blocked and probed with antibodies diluted at the concentration indicated in Additional file 2. All antibodies were purchased directly from the provider (described in Additional file 2), except for CP13 [6], RZ3 [7] and PHF1 [8]. Membranes were incubated with a horseradish-peroxidase-conjugated secondary antibody (Jackson Immunoresearch Laboratories, West Grove, PA, USA), and revealed by chemiluminescence (Luminata Classico^{TM}, EMD Millipore) in a BioRad Chemidoc XRS system (BioRad). Immunoblot data were quantified with ImageLab software (BioRad). Coomassie staining was performed with 0.05 % Brilliant Blue G (mass/volume) in 50 % methanol (vol/vol) and 10 % acetic acid (v/v). Destaining was performed with a 25 % methanol (v/v) and 7 % acetic acid (v/v) solution.

Immunofluorescence assays and PLAs

Cultured cells were fixed on glass coverslips with either 4 % paraformaldehyde (EMS, Hatfield, PA, USA) in Phosphate Buffered Saline (PBS) (Life Technologies). Fixed cells were washed and permeabilized for 10 min in PBS supplemented with 0.25 % Triton X-100, and then blocked in PBS supplemented with 2 % bovine serum albumin for 2 h at room temperature. Coverslips were incubated overnight at 4 °C with primary antibodies (as specified in Additional file 2), washed in PBS and incubated for 45 min with Alexa Fluor antibodies diluted at 1/400 from stock (Molecular Probes, Life Technologies). Alexa Fluor 647 phalloidin (Molecular Probes, Life Technologies)was used as per the manufacturer's instructions to stain the actin cytoskeleton. For PLAs, the initial steps (from fixation to primary antibody incubation) were the same as those described above for immunofluorescence assays. The following steps (i.e., secondary antibody incubation, ligation, amplification and probing) were performed according to the manufacturer's instructions (Olink Bioscience, Uppsala, Sweden). Images were acquired with a confocal microscope (LSM 710, Zeiss, Oberkochen, Germany) and processed using ZEN 2012 software (Zeiss). Three independent experiments were performed for each condition. The mean intensity per pixel in three different fields was measured using ImageJ software. Imaris software (Bitplane, Zurich, Switzerland) was used for three-dimensional (3D) image processing.

Primary neuron cultures

Mixed cortical and hippocampal primary cultures were obtained from P0 rats, according to previously described procedures [9]. Briefly, hippocampi and cortices were isolated from newborn rats, and neurons were dissociated by trypsin digestion. Neurons were plated on poly-L-lysine-coated coverslips or six-well plates, and were incubated with Minimal Essential Medium (MEM) supplemented with 10 % fetal bovine serum, Glutamax, MEM vitamins and penicillin/streptomycin (Life Technologies), according to the manufacturer's instructions. After 24 h, neurons were transferred into serum-free Neurobasal-A medium supplemented with B27 (Gibco, Life Technologies), Glutamax and uridine-deoxyfluorouridine for 14 days of in vitro culture. For Western blot analysis, primary neurons were directly harvested in LDS buffer supplemented with Nupage antioxidant (Life Technologies) and processed as described above in the "Electrophoresis and Western blots" section. For immunofluorescence assays, cells were fixed in 4 % paraformaldehyde (EMS) and processed as described above in the "Immunofluorescence assays and PLAs" section.

Results

BIN1's SH3 domain interacts with Tau's PRD

In previous work [3], we evidenced a direct interaction between full-length BIN1 and Tau *in vitro*. To further identify the protein domains involved in this interaction, we generated various constructs of Tau and BIN1 (Fig. 1a). We first incubated purified GST-Tau FL 1–441 or Tau domains (GST-Tau/N-terminal part (Nter), GST-Tau/PRD, GST-Tau/microtubule binding domain (MBD)) with HEK293 cell lysates overexpressing BIN1 FL. Only GST-Tau FL and GST-Tau/PRD pulled down BIN1

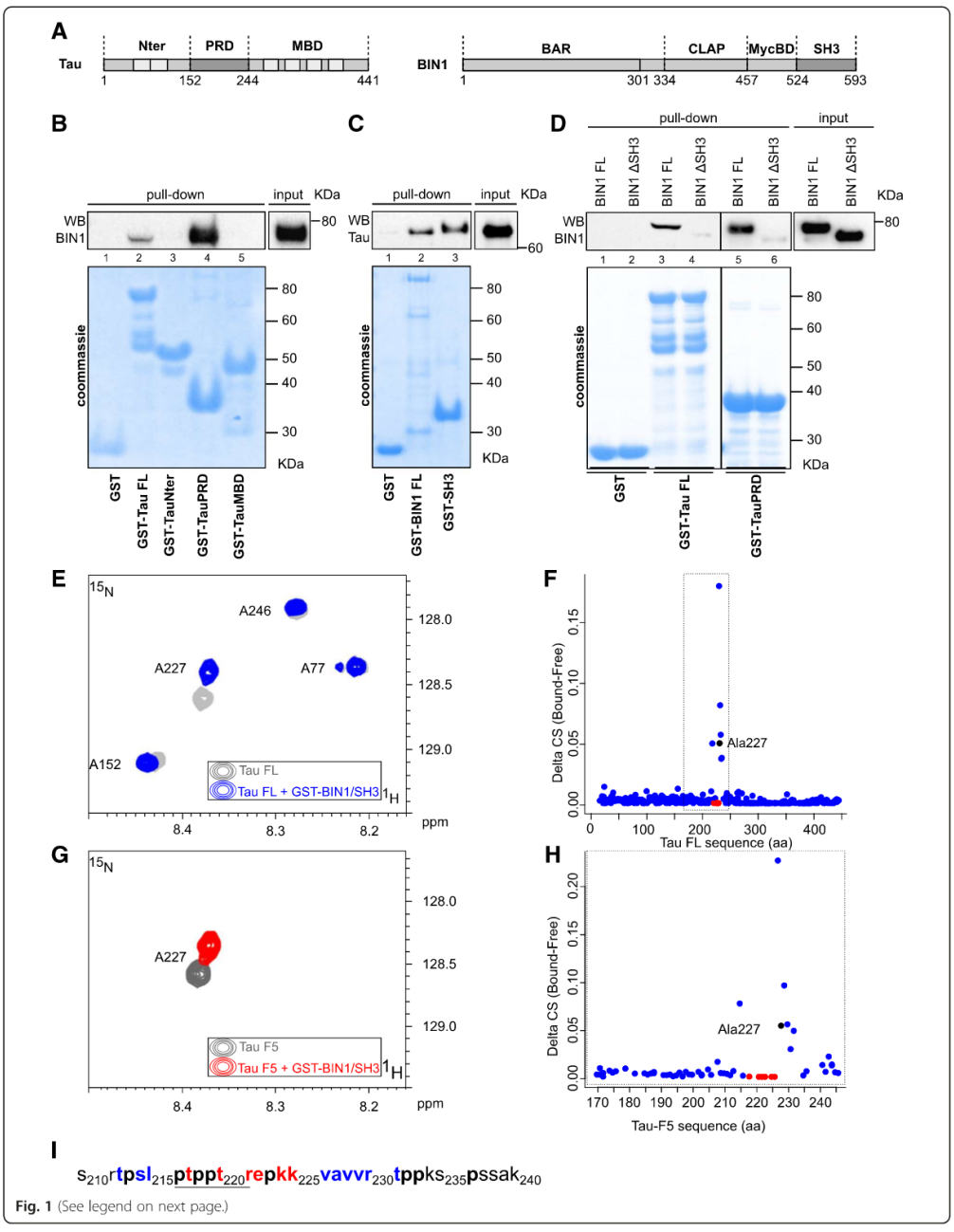

Fig. 1 (See legend on next page.)

(See figure on previous page.)
Fig. 1 The BIN1-Tau interaction is mediated by the Tau PRD and the BIN1 SH3 domain. **a**. A schematic linear representation of 2N4R Tau (Tau FL) and BIN1 isoform1 (BIN1 FL) sequences and their respective domains (as used in GST pull-down assays). MBD: microtubule-binding domain; PRD: proline-rich domain; Bar: BIN1-amphiphysin-Rvs167; CLAP: clathrin and AP-2 binding; MycBD: Myc-binding domain; SH3: Src homology 3. **b**. GST pull-down assays performed with various Tau constructs corresponding to specific Tau subdomains (Lane 2: GST-Tau FL 2N4R; lane3: GST-Tau/Nter[1–152]; lane 4: GST-Tau/PRD[153–244]; lane 5: GST-Tau/MBD[244–441]) incubated with homogenates from BIN1-overexpressing HEK293 cells ($n = 3$). Upper panel: A representative immunoblot of BIN1 pull-down, revealed with a 99D anti-BIN1 antibody. **c**. GST pull-down assays performed either with full length BIN1 (Lane 2: GST-BIN1 FL) or the BIN1 SH3 domain (lane 3: GST-BIN1/SH3) incubated with homogenates from Tau FL-overexpressing HEK293 cells ($n = 3$). Upper panel: A representative immunoblot of Tau pull-down, revealed with a Dako anti-Tau antibody. **d**. GST pull-down assays performed with GST-Tau FL (lanes 3 and 4) or GST-Tau/PRD (lanes 5 and 6) incubated with homogenates from HEK293 cells overexpressing either BIN1 FL (lanes 3 and 5) or a BIN1 construct lacking the SH3 domain (BIN1/ΔSH3, lanes 4 and 6) ($n = 3$). Upper panel: A representative immunoblot of BIN1 pull-down, revealed with a 99D anti-BIN1 antibody. Lower panels (B, C, D): the corresponding Coomassie blue gels, used as loading controls for the pull-down assays. **e**. Two-dimensional (2D) [^{1}H, ^{15}N] HSQC spectra of 100 μM ^{15}N 2N4R Tau, either free in solution (gray) or with a 1.6 molar amount of GST-BIN1/SH3 (blue, superimposed): Overlaid details of the full spectra presented in Additional file 3. **f**. Combined ^{1}H, ^{15}N CS perturbations (δ CS) in ppm, as defined in the Methods, in [^{1}H, ^{15}N] HSQC spectra of ^{15}N 2N4R Tau with a 1.6 molar ratio of GST-BIN1/SH3 versus the molecule free in solution for every resonance along the sequence. The dashed box indicates the position of the Tau-F5 fragment within the Tau FL sequence. **g**. 2D [^{1}H, ^{15}N] HSQC spectra of 100 μM ^{15}N Tau-F5 [165–245] free in solution (gray) or with a 1.2 molar amount of GST-BIN1/SH3 (red, superimposed): Overlaid details of full spectra presented in Additional file 4. **h**. Combined ^{1}H, ^{15}N CS perturbations (δ CS) in ppm, as defined in the Methods, in [^{1}H, ^{15}N] HSQC spectra of ^{15}N Tau-F5 [165–245] with a 1.6 molar ratio of GST-BIN1/SH3, versus the free molecule in solution and for every resonance along the sequence. **i**. The *a minima* SH3 binding sequence in Tau. Proline residues are shown in bold, residues with resonance broadenings upon interaction are shown in red and residues with CS deviation when comparing free and bound states are shown in blue. The underlined amino acid residues fit the consensus sequence for SH3 binding (PxxPx+, where x is any residue and + is a positively charged residue) [30]

(Fig. 1b, lanes 2 and 4). In contrast, no interaction was observed with GST-Tau/Nter or (GST-Tau/MBD) (Fig. 1b, lanes 3 and 5). Secondly, we performed the reciprocal experiments by incubating Tau-overexpressing HEK293 cell lysates with either GST-BIN1 FL or GST-BIN1/SH3. In both cases, we observed an interaction with Tau FL (Fig. 1c). Lastly, we incubated GST-Tau FL or GST-Tau/PRD with HEK293 lysates overexpressing BIN1 FL or BIN1 lacking its SH3 domain. Removal of the BIN1 SH3 domain markedly weakened the BIN1-Tau interaction (Fig. 1d, lanes 4 and 6 vs lanes 3 and 5).

We next used NMR spectroscopy to determine which *a minima* sequence in Tau interacts with BIN1. Briefly, comparison of the ^{1}H, ^{15}N HSQC spectrum of Tau441 (which we and others have fully assigned [10]) with that of the protein in the presence of GST-BIN1/SH3 domain revealed perturbations in the CS of several amino acids (Fig. 1e, f, and Additional file 3). Analysis of the δ CS ([Tau + BIN1/SH3] *versus* [Tau]) for each Tau amino acid clearly delimited a short interaction region within the aa 212–231 sequence (Fig. 2f, i). These results were validated by studying a Tau domain encompassing aa 165 to 245 (Tau-F5) (Fig. 1g, h, and Additional file 4).

In vitro, the BIN1-Tau interaction depends on Tau's phosphorylation status

As Tau phosphorylation has been previously shown to regulate Tau PRD-SH3 interactions [11, 12], we next looked at whether Tau phosphorylation could interfere with the BIN1-Tau interaction. We acquired NMR data after the *in vitro* phosphorylation of Tau FL or a Tau fragment (Tau-F5[165–245]) by recombinant kinases (Fig. 2). Firstly, following *in vitro* incubation with CDK2/CycA3 [5], we confirmed that phosphorylation levels increased at several major Tau phosphoepitopes such as pT181 (AT270), pS199, pT205, pS202-T205 (AT8, Tau-1) and pT231 (RZ3, AT180), as shown by immunoblots (Fig. 2a) and NMR analysis (see Additional file 5). A comparison of NMR spectra of CDK2/CycA3-phosphorylated Tau-FL and Tau-F5 in the presence or absence of BIN1/SH3 did not reveal any significant CS perturbations. These findings indicated a lack of interaction between BIN1/SH3 domain and *in vitro*-phosphorylated Tau-F5 fragment or Tau-FL (Fig. 2b, c and Additional file 6, Additional file 7). Additional experiments with either a recombinant ERK kinase (see Additional file 8) or rat brain extract kinases (see Additional file 9) confirmed these findings. Taken as a whole, our results demonstrate that Tau phosphorylation in and around the PRD weakens the BIN1-Tau interaction by precluding SH3-PRD binding.

BIN1-Tau complexes partly co-localized with the actin cytoskeleton network

In order to further investigate the significance of BIN1-Tau binding in a physiological context, we used both conventional immunofluorescence experiments (Fig. 3a) and PLAs (Fig. 3b) to assess the intracellular location(s) of BIN1 and Tau in rat primary neurons. As described in the literature, Tau was found in the soma and the neurites (Fig. 3a-c), whereas BIN1 was found in the nucleus, the soma and the neurites (Fig. 3a). Within the neurites, we observed several puncta corresponding to the putative co-localization of BIN1-Tau (Fig. 3a). To validate these results, we used PLAs to detect potentially interacting BIN1 and Tau molecules (within 28 nm of each other). In agreement with the immunofluorescence experiments, a PLA signal for the BIN1 and Tau pair was identified in both the neuronal soma and the dendrites (Fig. 3b). This

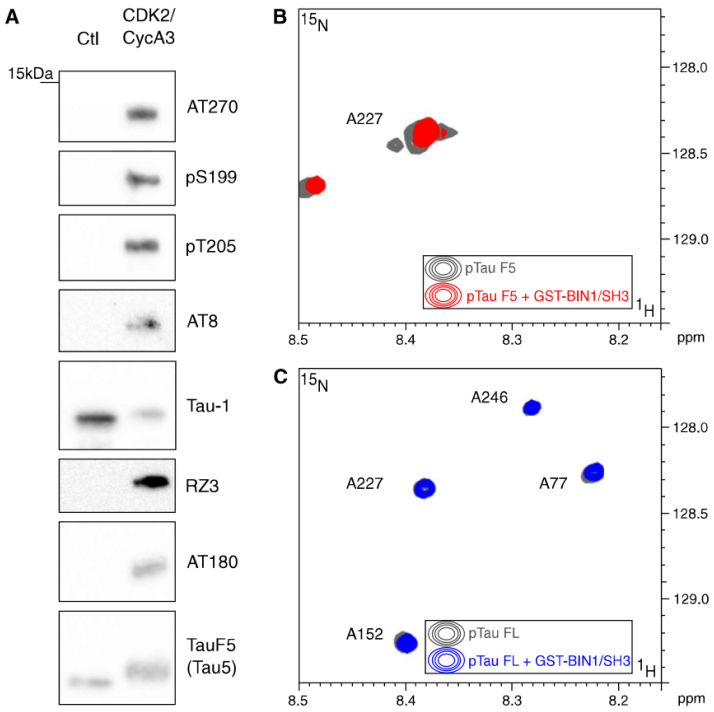

Fig. 2 Tau phosphorylation precludes the BIN1-Tau interaction *in vitro*. **a**. Tau-F5 fragment phosphorylation analysis after *in vitro* phosphorylation by CDK2/CycA3 kinase. Representative immunoblots using various antibodies against phosphorylation epitopes in Tau. The total amount of Tau-F5 was revealed by the phosphorylation-independent antibody Tau5. The significant shift in molecular weight observed in CDK2/CycA3-treated samples indicates Tau hyperphosphorylation. In contrast to other antibodies, the Tau-1 antibody binds to various non-phosphorylated Tau sites; the signal thus decreases when Tau is hyperphosphorylated [31]. **b**. 2D [^{1}H, ^{15}N] HSQC spectra of 125 μM ^{15}N CDK-phosphorylated Tau-F5[165–245] free in solution (gray) and with a 1 molar amount of GST-BIN1/SH3 (red, superimposed): Overlaid details of 2D [^{1}H, ^{15}N] HSQC spectra presented in Additional file 6. **c**. 2D [^{1}H, ^{15}N] HSQC spectra of 60 μM ^{15}N CDK-phosphorylated 2N4R Tau free in solution (gray) and with a 2 molar amount of GST-BIN1/SH3 (blue, superimposed): Overlaid details of full spectra presented in Additional file 7

staining pattern contrasted with both the homogeneous immunofluorescence pattern observed for total Tau (Fig. 3c) and the strong PLA signal for Tau and tubulin (a major Tau partner) (Fig. 3d). Lastly, the BIN1-Tau PLA staining partly co-localized (mean ± standard deviation (SD) co-localization coefficient: 0.399 ± 0.041) with the actin cytoskeleton (as revealed by phalloidin staining; Fig. 3e, f, Additional file 10 and Additional file 11). In additional experiments, we further characterized the subcellular location of BIN1-Tau complexes in primary neurons (Fig. 4). Firstly, on the basis of the previously described role of BIN1 in endocytosis, we co-stained BIN1-Tau complexes and the endocytosis marker clathrin; the co-localization was very weak (Fig. 4a and Additional file 10; mean ± SD co-localization coefficient: 0.054 ± 0.014). Likewise, specific pre- or post-synaptic markers of functional neuronal compartments (such as synaptophysin (Fig. 4b) and PSD95 (Fig. 4c)) did not co-localize with BIN1-Tau complexes (mean co-localization coefficient ~0; see Additional file 10).

In conclusion, these results showed that Tau/BIN1 complexes are found at specific locations in primary neurons (as suggested by the dot-like staining) and partly co-localize with the actin cytoskeleton.

Tau's phosphorylation status influences BIN1-Tau binding in primary neurons

Since we had observed that Tau phosphorylation within or close to the Tau/PRD was able to modulate the BIN1-Tau interaction *in vitro*, we next looked at whether phosphorylation might modulate the interaction in primary neurons. To this end, we used a PLA that combined a BIN1

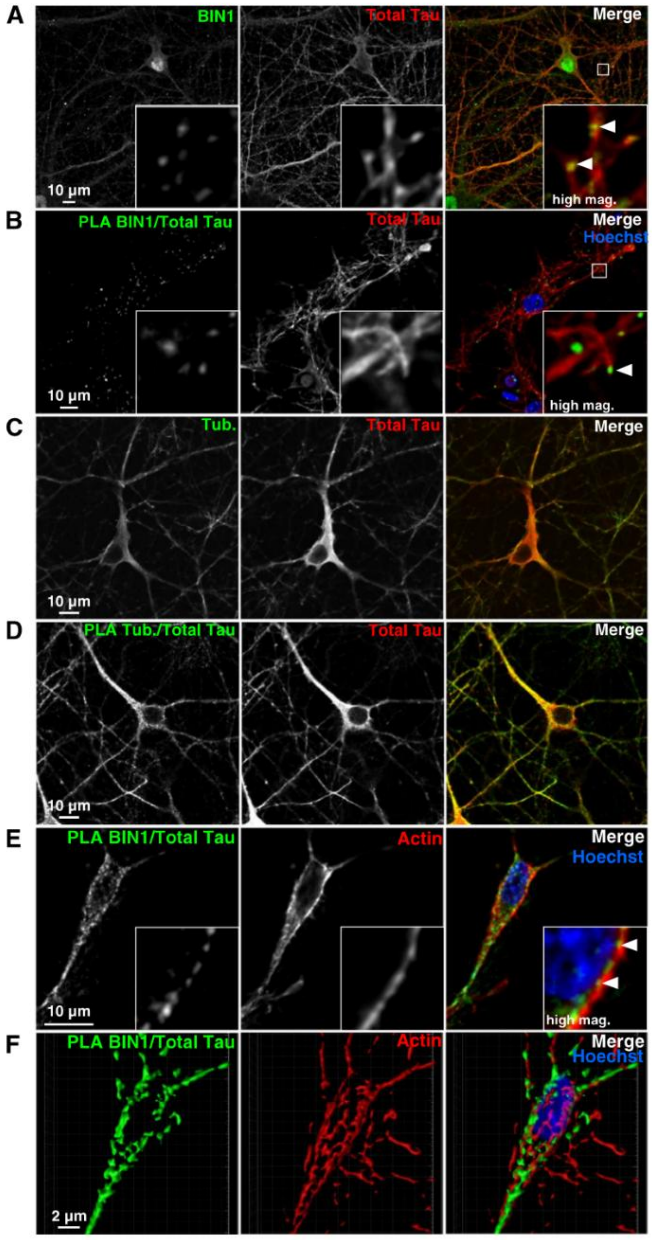

Fig. 3 (See legend on next page.)

(See figure on previous page.)
Fig. 3 BIN1-Tau complexes partly co-localize with the actin cytoskeleton network. **a**. Immunofluorescence staining of endogenous BIN1 (green) and total Tau (red) in primary neuron cultures. Arrows indicate the co-localization of BIN1 and total Tau staining. **b**. PLAs (green) were been used to visualize endogenous BIN1-Tau complexes. Co-staining for total Tau (red) was compared with the PLA (BIN1/total Tau) signal. The arrow indicates the PLA signal located at the end of microtubule structures. **c**. Immunofluorescent staining of endogenous tubulin (tub, in green) and total Tau (red) in primary neuron cultures. **d**. A PLA (green) for visualizing endogenous complexes between tubulin and total Tau, combined with immunofluorescent staining of total Tau (red). **e**. A PLA for BIN1/total Tau (green) was combined with actin staining (red) using Alexa-Fluor633 phalloidin. The arrow shows the location of the PLA signal, with actin staining . **f**. A 3D image showing the proximity of the green (BIN1/total Tau) signal to the actin staining. A 3D video is presented in Additional file 11. Mag: magnification

antibody with several specific, phosphorylation-dependent anti-Tau antibodies: an antibody against phosphorylation sites within Tau's C-terminal region (pSer396-pSer404) (Fig. 5a, b) and two antibodies against phosphorylation sites near to or within the PRD peptide sequence that interacts with the BIN1/SH3 domain, i.e. pS202 (Fig. 5c, d) and pT231 (Fig. 5e, f). A PLA signal was observed with pSer202 and pSer396-pSer404 antibodies but not with antibodies against pThr231 (RZ-3, Fig. 5e, and AT180, data not shown). It should be noted that this difference cannot be attributed to differences in Tau phosphorylation levels in the various primary neuron cultures, since conventional immunofluorescence experiments did not highlight any obvious differences between the staining levels obtained for all the epitopes studied (Fig. 5b, d, f, g). These PLA results are in full agreement with those of our NMR experiments. Hence, in primary neurons, the phosphorylation status of the Tau/PRD sequence modulates interaction with the BIN1/SH3 domain. Moreover, our results suggest that Thr231 is one of the phosphorylation sites that modulates this interaction.

Discussion

Progress in genetic analysis (notably in genome-wide association studies) has led to the identification of 24 validated risk loci for AD [13]. BIN1 is the first of these risk factors to have been linked to Tau pathology [3]. In the present study, we used biochemical and cellular approaches to further characterize the relationship between Tau and BIN1. Firstly, we found that BIN1's SH3 domain interacts directly with the Tau PRD. Secondly, we determined that the amino acid sequence [212–231] within the PRD is involved in this interaction. Thirdly, we showed that Tau phosphorylation weakens the Tau-BIN1 interaction both *in vitro* and in primary neurons. Fourthly, we found that BIN1-Tau complexes exhibit a co-localization with the actin cytoskeleton in primary neurons.

BIN1 belongs to the amphiphysin protein family, the best-known function of which is to sense and generate membrane curvature through its BAR domain. This protein is also a key regulator of biological functions such as endocytosis, membrane recycling and cytoskeleton regulation [14]. Accordingly, BIN1 recruits some partners (such as AP-2 and clathrin) through its CLAP domain and others (such as dynamin and synaptojanin) through its SH3 domain [14]. Tau proteins are microtubule-associated proteins whose main function is to promote the polymerization and stabilization of the cytoskeleton microtubule network [15]. Tau is also involved in cell signaling pathways via the recruitment of kinases (such as Lck, Fyn, Src [16, 17] and phosphatidylinositol 3-kinase) and signaling adaptors (such as Grb2 [11, 18]). These interactions are mediated by Tau's PRD. In the present work, we extended these results by showing that BIN1-Tau binding occurs through the SH3 domain and the PRD. Given that Tau phosphorylation (strong regulator of Tau function) is deregulated in AD, we sought to determine whether Tau phosphorylation was involved in regulation of the BIN1-Tau interaction. Our data indicate that Tau phosphorylation can indeed modulate the interaction between BIN1 and Tau *in vitro*. These results are consistent with previous reports of phosphorylation-dependent binding between Tau PRD and SH3 domains in proteins such as phosphatidylinositol 3-kinase, phospholipase C γ1, Grb2, and Src family kinases [11, 18]. Importantly, the results of our NMR and cell biology experiments suggest that phosphorylation at Thr231 (which is within the Tau PRD sequence that interacts with the BIN1 SH3 domain) weakens this interaction. These data are coherent with previous studies showing that Tau mutants mimicking phosphorylation at Thr231/Ser235 (T231D/S235D) bind 8 times less avidly (compared with native Tau) to the SH3 domain of Fyn [18], whereas a single mutation at Ser235 (S235E) does not affect the binding [11]. In contrast, mimicking phosphorylation at Ser396 and Ser404 (S396D/S404D) did not modify the affinity of 3-repeat Tau isoforms for Fyn/SH3. The latter literature data are consistent with (i) our PLA staining results for pS396-404 Tau and BIN1 and (ii) the fact that 3-repeat Tau isoforms are expressed in primary neuron cultures. Indeed, it has been well established that both 4-repeat and 3-repeat Tau isoforms are expressed in primary neurons after 14 days of in vitro culture [19]. Moreover, Tau proteins with different phosphorylation patterns (generated with various kinases) failed to interact with BIN1 *in vitro* (Fig. 3 and Additional file 8 and Additional file 9) but all were phosphorylated at Thr231. This strongly suggests that pThr231 is an important

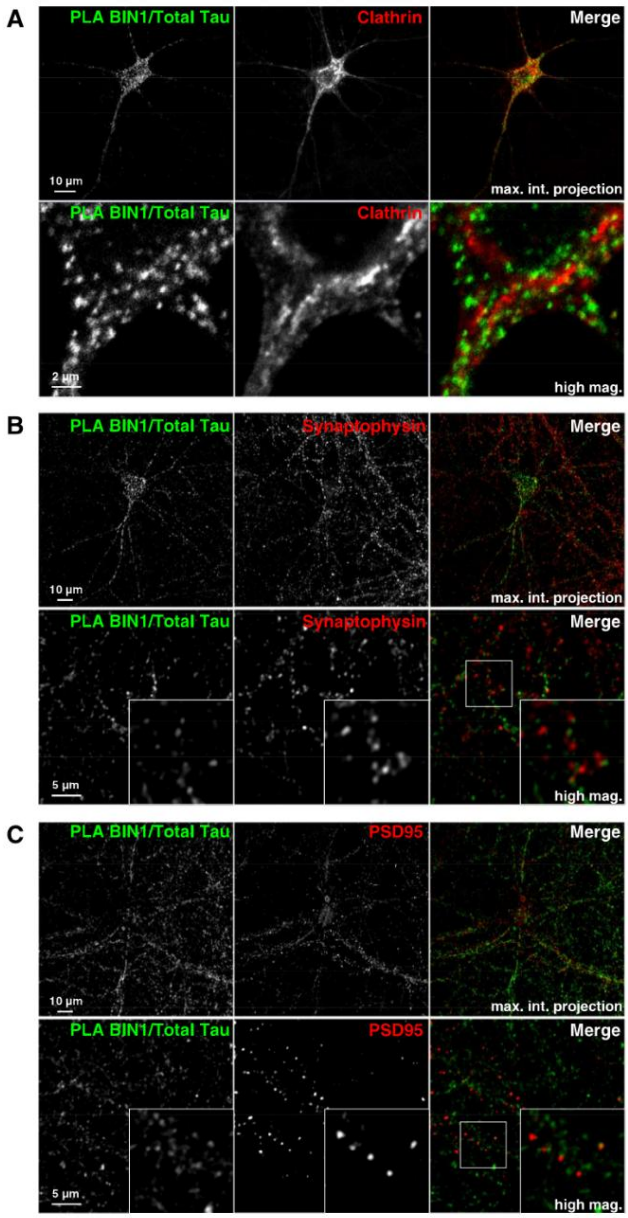

Fig. 4 (See legend on next page.)

(See figure on previous page.)
Fig. 4 BIN1-Tau complexes are rarely co-localized with clathrin-coated membranes and are not co-localized with synaptic markers. **a**. A PLA for Tau-BIN1 (green) and clathrin staining (red) in primary neuron cultures. **b**. A PLA for Tau-BIN1 (green) and the pre-synaptic marker synaptophysin (red) in primary neuron cultures. **c**. A PLA for Tau-BIN1 (green) and the post-synaptic marker PSD95 (red) in primary neuron cultures. Upper panels: maximum intensity projection. Lower panels: a single confocal Z-stack. Mag: magnification

regulator of the BIN1/Tau interaction. Indeed, these findings were confirmed by our PLAs, since no interaction was observed with Thr231-phosphorylated Tau species in primary neurons. However, since Tau phosphorylation patterns are known to be associated with different subcellular locations (e.g. low Thr231 phosphorylation at the neuron's cortical membrane [20]), one can argue that cell-sorting mechanisms might be responsible for the lack of interaction of BIN1 with pThr231 Tau in neurons. However, given that other sites in pThr231 Tau may also be phosphorylated, we cannot rule out the possibility that the latter also modify the BIN1/Tau interaction. Further experiments will be required to specify the possible contributions of other Tau phosphorylation sites and identify the mechanisms that underlie the regulation of the BIN1-Tau interaction by phosphorylation. Nevertheless, our finding that phosphorylation of Thr231 strongly influences the BIN1-Tau interaction highlights a putative link to the pathogenesis of AD. Indeed, Thr231 hyperphosphorylation occurs in the very early stages of neurofibrillary degeneration [21]. The enzymes that control this phosphorylation (such as Cdk5 [22], Gsk3-β [23], PP2A [24] and PIN1 [25]) are markedly deregulated during the AD process. These findings suggest that Tau hyperphosphorylation during AD (or at least phosphorylation at Thr231) can interfere with the physiological stoichiometry of BIN1-Tau complexes and may have a particular impact in the early stages of AD. We and others have shown that BIN1 expression is elevated in AD brains [3] and that BIN1 levels are correlated with the presence of neurofibrillary tangles [26]. Moreover, our previous work demonstrated that Tau toxicity in *Drosophila* models was suppressed by downregulating the *Drosophila* BIN1 ortholog [3]. Although our earlier results suggest that BIN1-Tau complexes have toxic effects, we cannot yet clearly define the roles of these complexes in AD or how Tau Thr231 phosphorylation contributes to this pathway during AD pathogenesis. In order to better understand the role of BIN1-Tau complexes, we performed experiments with markers of the various cell compartments involved in fundamental neuronal functions (such as synapses and endocytosis). Our results showed that BIN1-Tau complexes did not co-localize with either pre-synaptic or post-synaptic terminal markers. Moreover, clathrin (a marker of the endocytosis pathway) did not particularly co-localize with BIN1-Tau complexes. These results suggest that BIN1-Tau complexes exert their functions through cellular pathways other than the currently known pathogenic pathways involving Tau at the synapse [27] or involving BIN1 in endocytosis [14]. Nonetheless, we demonstrated substantial co-localization of BIN1-Tau complexes and the actin cytoskeleton. Therefore, one can postulate that BIN1 and microtubule-associated Tau have a role at the interface between actin and the microtubule network in neurons. Indeed, previous research has found that BIN1 interacts with the actin cytoskeleton [14] and serves as a membrane anchoring point for microtubules [28]. Further studies will be needed to fully understand the roles of BIN1-Tau complexes in neurons.

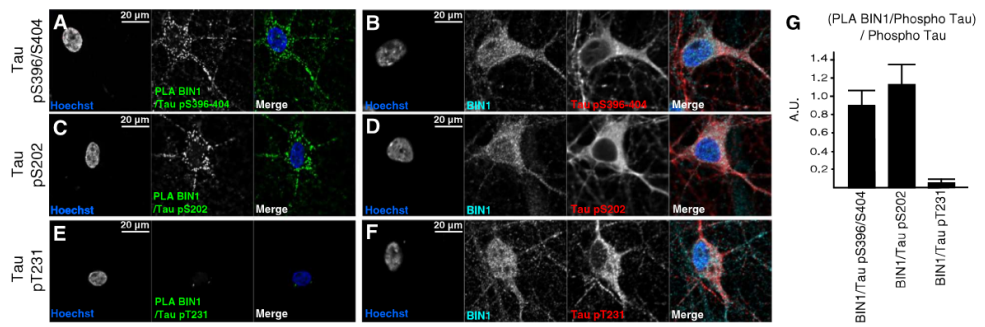

Fig. 5 Specific Tau phosphorylation patterns for endogenous BIN1-Tau complexes in primary neuron cultures. A PLA (green) combining anti-BIN1 with either anti-phospho Tau pS396-404 **a**, pS202 **c**. or pT231 **e** antibodies. There was no PLA signal when anti-Tau pT231 was combined with anti-BIN1. Conventional immunofluorescence staining for BIN1 (cyan) and phospho-Tau (red) obtained with the antibodies used in the PLAs (pS396-404 **b**, pS202 **d** or pT231 **f**). **g**. Quantification of PLA fluorescence intensity in three fields and three independent experiments. The graph shows the ratio between the PLA intensity for BIN1/phosphoTau and phosphoTau alone. ($n = 3$) AU: arbitrary units. The error bars correspond to the SD

Conclusions

Our results show that BIN1's SH3 domain interacts directly with the Tau PRD, and that Tau phosphorylation (notably at Thr231) weakens this interaction. Taken as a whole, our findings highlight the link between BIN1, regulation of Tau phosphorylation and AD-related cellular pathways. Better knowledge of the interactions between Tau, BIN1 and the cytoskeleton in neurons may open up some exciting avenues for further research.

Additional files

Additional file 1: Primer sequences used to amplify the constructs studied in the present work. (PDF 37 kb)

Additional file 2: Antibodies used and their respective dilutions. All dilutions refer to the stock solution provided by the manufacturer. (PDF 55 kb)

Additional file 3: BIN1-Tau interaction is mediated by the Tau sequence from aa 212 to aa 231. 2D [^{1}H, ^{15}N] HSQC spectra of 100 μM ^{15}N 2N4R Tau-FL free in solution (gray) or with a 1.6 molar amount of GST-BIN1/SH3 (blue, superimposed). The CS perturbations and peak broadening indicate the existence of an interaction. Annotated resonances correspond to the SH3 binding site, as defined in the sequence in Fig. 2e. (PDF 87 kb)

Additional file 4: BIN1-Tau interaction is mediated by the Tau sequence from aa 212 to aa 231. Overlaid detail of 2D [^{1}H, ^{15}N] HSQC spectra of 100 μM ^{15}N Tau-F5 [165–245] free in solution (gray) or with a 1.2 molar amount of GST-BIN1/SH3 (red, superimposed). Blue arrows link the corresponding resonances in the free (gray) and bound (red) states. (PDF 74 kb)

Additional file 5: Phosphorylation of Tau with the CDK2/CycA3 kinase. A. Details of 2D [^{1}H, ^{15}N] HSQC spectra of 125 μM ^{15}N Tau[165–245] (Tau-F5) phosphorylated with CDK2/CycA3 kinase. B. Details of 2D [^{1}H, ^{15}N] HSQC spectra of 100 μM ^{15}N Tau phosphorylated with CDK2/CycA3 kinase. Shifted resonances corresponding to phosphorylated Ser and Thr residues are labelled [29]. Resonances located within the SH3 binding site are annotated in red. (PDF 76 kb)

Additional file 6: Tau phosphorylation precludes the BIN1-Tau interaction in vitro. 2D [^{1}H, ^{15}N] HSQC spectra of 125 μM ^{15}N CDK-phosphorylated Tau-F5[165–245] free in solution (gray) and with a 1 molar amount of GST-BIN1/SH3 (red, superimposed). No CS perturbations or peak broadening were observed - indicating the absence of interaction between BIN1 and Tau-F5. (PDF 67 kb)

Additional file 7: Tau phosphorylation precludes the BIN1-Tau interaction in vitro. 2D [^{1}H, ^{15}N] HSQC spectra of 100 μM ^{15}N CDK-phosphorylated 2N4R Tau, free in solution (gray) or with a 1.6 molar amount of GST-BIN1/SH3 (blue, superimposed). No CS perturbations or peak broadening were observed – indicating the absence of interaction between BIN1 and Tau FL (PDF 82 kb)

Additional file 8: Interaction of GST-BIN1/SH3 with phospho-Tau. A. In vitro phosphorylation of Tau by ERK kinase. Details of 2D [^{1}H, ^{15}N] HSQC spectra of ^{15}N Tau-F5 [165–245] phosphorylated with ERK kinase. Shifted resonances corresponding to phosphorylated Ser and Thr residues are labelled [29]. Resonances of pT231 and pS235 are broader and less intense. Resonances located within the SH3 binding site are annotated in red. B. Interaction of GST BIN1/SH3 with phospho Tau-F5. HSQC spectra of 125 μM ^{15}N ERK-phosphorylated Tau-F5 [165–245] free in solution (gray) and with a 1 molar amount of GST-BIN1/SH3(red, superimposed) C. Overlaid detail of 2D [^{1}H, ^{15}N] HSQC spectra presented in B. For details of the methods, see Additional file 12. (PDF 123 kb)

Additional file 9: Interaction of GST-BIN1/SH3 with phospho-Tau. A. in vitro phosphorylation of Tau by rat brain extracts. Details of 2D [^{1}H, ^{15}N] HSQC spectra of ^{15}N Tau phosphorylated with rat brain extracts. Shifted resonances corresponding to phosphorylated Ser and Thr residues are labelled [29]. Resonances of pT231 and pS235 are broader and less intense. Resonances located within the SH3 binding site are annotated in red. B. Interaction of phosphorylated Tau FL with GST-BIN1/SH3. 2D [^{1}H, ^{15}N] HSQC spectra of 100 μM ^{15}N Tau phosphorylated with rat brain extract, free in solution (gray) or with a 1.6 molar amount of GST-BIN1/SH3 (blue, superimposed). C. Overlaid detail of 2D [^{1}H, ^{15}N] HSQC spectra presented in B. For details of the methods, see Additional file 12. (PDF 137 kb)

Additional file 10: Co-localization measurement of BIN1-Tau complexes with actin, clathrin-coated membranes and synapse terminal markers. PLA Tau-BIN1 staining (green) with (A) actin staining, (B) clathrin staining, (C) the pre-synaptic marker synaptophysin and (D) the post-synaptic marker PSD95 (red) in primary neuron cultures. The right-hand panels show the pixels with co-localization (in white) of PLA and the various markers. The co-localization coefficient was calculated according to Mander's method using ZEN 2012 software. The red channel was used as a reference. E. A graph showing the mean ± SD (error bar) coefficient for co-localization between PLA BIN1/Tau and the indicated markers ($n = 6$). For details of the methods, see Additional file 12. (PDF 3475 kb)

Additional file 11: A movie showing 3D images processed with Imaris software. The PLA (BIN1/total Tau) signal (green) was located in the vicinity of the actin staining (red) at the membrane. (ZIP 10MB)

Additional file 12: Supplementary methods. (PDF 89 kb)

Competing interests

All authors declare that they have no competing interests.

Authors' contributions

YS, JC, AB, GL, IL and JCL designed the experiments. YS, JC, AB, FXC, FD, TM, HAD and AF, performed the experiments. YS, JC, AB, IL and JCL wrote the manuscript. NM, CD, PiD, PeD, BD, PA and GL revised the manuscript. All authors read and approved the final manuscript.

Acknowledgments

We thank the BioImaging Center Lille-Nord de France (BICeL) facility (Lille, France) and the TGE RMN THC FR-3050 facility (Gif-sur-Yvette, France). We also thank the Albert Einstein College of Medicine of Yeshiva University (New York, USA) for the kind gift of Tau-phosphorylation-dependent antibodies. This work was funded by the French National Foundation on Alzheimer's disease and related disorders, the *Lille Métropole Communauté Urbaine* council, the French government's LABEX DISTALZ (development of innovative strategies for a transdisciplinary approach to Alzheimer's disease) and the US Alzheimer's association (IIRG-06-25487).

Author details

[1]INSERM, UMR 1167, Lille, France. [2]Institut Pasteur de Lille, Lille, France. [3]Université de Lille, Lille, France. [4]CNRS, UMR 8576, Lille, France. [5]FraBio IR 3688, Lille, France. [6]Litwin-Zucker Research Center, Feinstein Institute for Medical Research, North-Shore Long Island Jewish Health System, Manhasset, NY, USA. [7]Department of Translational Medicine and Neurogenetics, IGBMC, INSERM U964, CNRS UMR7104, Université de Strasbourg, Illkirch, France. [8]Center for Medical Genetics, Ghent University Hospital, Ghent, Belgium. [9]Albert Einstein College of Medicine of Yeshiva University, New York, NY, USA.

Received: 10 August 2015 Accepted: 7 September 2015
Published online: 23 September 2015

References

1. Hardy JA, Higgins GA (1992) Alzheimer's disease. the amyloid cascade hypothesis 256:184–185. doi:10.1126/science.1566067
2. Genin E, Hannequin D, Wallon D, Sleegers K, Hiltunen M, Combarros O, Bullido MJ, Engelborghs S, De Deyn P, Berr C, Pasquier F, Dubois B, Tognoni G, Fiévet N, Brouwers N, Bettens K, Arosio B, Coto E, Del Zompo M, Mateo I, Epelbaum J, Frank-Garcia A, Helisalmi S, Porcellini E, Pilotto A, Forti P, Ferri R, Scarpini E, Siciliano G, Solfrizzi V et al (2011) APOE and Alzheimer disease: a major gene with semi-dominant inheritance. Mol Psychiatry 16:903–907. doi:10.1038/mp.2011.52
3. Chapuis J, Hansmannel F, Gistelinck M, Mounier A, Van Cauwenberghe C, Kolen KV, Geller F, Sottejeau Y, Harold D, Dourlen P, Grenier-Boley B, Kamatani Y, Delepine B, Demiautte F, Zelenika D, Zommer N, Hamdane M, Bellenguez C, Dartigues J-F, Hauw J-J, Letronne F, Ayral A-M, Sleegers K, Schellens A, Broeck LV, Engelborghs S, De Deyn PP, Vandenberghe R,

O'Donovan M, Owen M et al (2013) Increased expression of BIN1 mediates Alzheimer genetic risk by modulating tau pathology. Mol Psychiatry 18:1225–1234. doi:10.1038/mp.2013.1
4. Nicot A-S, Toussaint A, Tosch V, Kretz C, Wallgren-Pettersson C, Iwarsson E, Kingston H, Garnier J-M, Biancalana V, Oldfors A, Mandel J-L, Laporte J (2007) Mutations in amphiphysin 2 (BIN1) disrupt interaction with dynamin 2 and cause autosomal recessive centronuclear myopathy. Nat Genet 39:1134–1139. doi:10.1038/ng2086
5. Amniai L, Barbier P, Sillen A, Wieruszeski J-M, Peyrot V, Lippens G, Landrieu I (2009) Alzheimer disease specific phosphoepitopes of Tau interfere with assembly of tubulin but not binding to microtubules. FASEB J 23:1146–1152. doi:10.1096/fj.08-121590
6. Weaver CL, Espinoza M, Kress Y, Davies P (2000) Conformational change as one of the earliest alterations of tau in Alzheimer's disease. Neurobiol Aging 21:719–727. doi:10.1016/S0197-4580(00)00157-3
7. Vingtdeux V, Davies P, Dickson DW, Marambaud P (2011) AMPK is abnormally activated in tangle-and pre-tangle-bearing neurons in Alzheimer's disease and other tauopathies. Acta Neuropathol 121:337–349. doi:10.1007/s00401-010-0759-x
8. Otvos L, Feiner L, Lang E, Szendrei GI, Goedert M, Lee VMY (1994) Monoclonal antibody PHF-1 recognizes tau protein phosphorylated at serine residues 396 and 404. J Neurosci Res 39:669–673. doi:10.1002/jnr.490390607
9. Morel E, Chamoun Z, Lasiecka ZM, Chan RB, Williamson RL, Vetanovetz C, Dall'Armi C, Simoes S, Point Du Jour KS, McCabe BD, Small SA, Di Paolo G (2013) Phosphatidylinositol-3-phosphate regulates sorting and processing of amyloid precursor protein through the endosomal system. Nat Commun 4:2250. doi:10.1038/ncomms3250
10. Lippens G, Sillen A, Smet C, Wieruszeski J-M, Leroy A, Buée L, Landrieu I (2006) Studying the natively unfolded neuronal Tau protein by solution NMR spectroscopy. Protein Pept Lett 13:235–246
11. Reynolds CH, Garwood CJ, Wray S, Price C, Kellie S, Perera T, Zvelebil M, Yang A, Sheppard PW, Varndell IM, Hanger DP, Anderton BH (2008) Phosphorylation regulates tau interactions with Src homology 3 domains of phosphatidylinositol 3-kinase, phospholipase Cgamma1, Grb2, and Src family kinases. J Biol Chem 283:18177–18186. doi:10.1074/jbc.M709715200
12. Pooler AM, Usardi A, Evans CJ, Philpott KL, Noble W, Hanger DP (2012) Dynamic association of tau with neuronal membranes is regulated by phosphorylation. Neurobiol Aging 431(33):e27–38. doi:10.1016/j.neurobiolaging.2011.01.005
13. Lambert JC, Ibrahim-Verbaas CA, Harold D, Naj AC, Sims R, Bellenguez C, DeStafano AL, Bis JC, Beecham GW, Granier-Boley B, Russo G, Thorton-Wells TA, Jones N, Smith AV, Chouraki V, Thomas C, Ikram MA, Zelenika D, Vardarajan BN, Kamatani Y, Lin CF, Gerrish A, Schmidt H, Kunkle B, Dunstan ML, Ruiz A, Bihoreau MT, Choi SH, Reitz C, Pasquier F et al (2013) Meta-analysis of 74,046 individuals identifies 11 new susceptibility loci for Alzheimer's disease. Nat Genet 45:1452–8. doi:10.1038/ng.2802
14. Prokic I, Cowling BS, Laporte J (2014) Amphiphysin 2 (BIN1) in physiology and diseases. J Mol Med 2:1–11. doi:10.1007/s00109-014-1138-1
15. Weingarten MD, Lockwood AH, Hwo SY, Kirschner MW (1975) A protein factor essential for microtubule assembly. Proc Natl Acad Sci U S A 72:1858–1862. doi:10.1073/pnas.72.5.1858
16. Lee G, Newman ST, Gard DL, Band H, Panchamoorthy G (1998) Tau interacts with src-family non-receptor tyrosine kinases. J Cell Sci 111(Pt 2):3167–3177
17. Lee G (2005) Tau and src family tyrosine kinases. Biochim Biophys Acta, Mol Basis Dis 1739:323–330. doi:10.1016/j.bbadis.2004.09.002
18. Bhaskar K, Yen SH, Lee G (2005) Disease-related modifications in tau affect the interaction between Fyn and tau. J Biol Chem 280:35119–35125. doi:10.1074/jbc.M505895200
19. Smith CJ, Anderton BH, Davis DR, Gallo JM (1995) Tau isoform expression and phosphorylation state during differentiation of cultured neuronal cells. FEBS Lett 375:243–248
20. Maas T, Eidenmuller J, Brandt R (2000) Interaction of tau with the neural membrane cortex is regulated by phosphorylation at sites that are modified in paired helical filaments. J Biol Chem 275:15733–15740. doi:10.1074/jbc.M000389200, M000389200 [pii]
21. Augustinack JC, Schneider A, Mandelkow EM, Hyman BT (2002) Specific tau phosphorylation sites correlate with severity of neuronal cytopathology in Alzheimer's disease. Acta Neuropathol 103:26–35. doi:10.1007/s0040101000423
22. Patrick GN, Zukerberg L, Nikolic M, de la Monte S, Dikkes P, Tsai LH (1999) Conversion of p35 to p25 deregulates Cdk5 activity and promotes neurodegeneration. Nature 402:615–622. doi:10.1038/45159
23. Leroy K, Boutajangout A, Authelet M, Woodgett JR, Anderton BH, Brion J-P (2002) The active form of glycogen synthase kinase-3beta is associated with granulovacuolar degeneration in neurons in Alzheimer's disease. Acta Neuropathol 103:91–99. doi:10.1007/s004010100435
24. Gong CX, Shaikh S, Wang JZ, Zaidi T, Grundke-Iqbal I, Iqbal K (1995) Phosphatase activity toward abnormally phosphorylated tau: decrease in Alzheimer disease brain. J Neurochem 65:732–738
25. Lu PJ, Wulf G, Zhou XZ, Davies P, Lu KP (1999) The prolyl isomerase Pin1 restores the function of Alzheimer-associated phosphorylated tau protein. Nature 399:784–788. doi:10.1038/21650
26. Holler CJ, Davis PR, Beckett TL, Platt TL, Webb RL, Head E, Murphy MP (2014) Bridging Integrator 1 (BIN1) Protein Expression Increases in the Alzheimer's Disease Brain and Correlates with Neurofibrillary Tangle Pathology - Journal of Alzheimer's Disease - IOS Press. J Alzheimers Dis 42:1221–7. doi:10.3233/JAD-132450
27. Ittner LM, Ke YD, Delerue F, Bi M, Gladbach A, van Eersel J, Wölfing H, Chieng BC, Christie MJ, Napier IA, Eckert A, Staufenbiel M, Hardeman E, Götz J (2010) Dendritic function of tau mediates amyloid-β toxicity in alzheimer's disease mouse models. Cell 142:387–397. doi:10.1016/j.cell.2010.06.036
28. Meunier B, Quaranta M, Daviet L, Hatzoglou A, Leprince C (2009) The membrane-tubulating potential of amphiphysin 2/BIN1 is dependent on the microtubule-binding cytoplasmic linker protein 170 (CLIP-170). Eur J Cell Biol 88:91–102. doi:10.1016/j.ejcb.2008.08.006
29. Landrieu I, Lacosse L, Leroy A, Wieruszeski J-M, Trivelli X, Sillen A, Sibille N, Schwalbe H, Saxena K, Langer T, Lippens G (2006) NMR analysis of a Tau phosphorylation pattern. J Am Chem Soc 128:3575–83. doi:10.1021/ja054656+
30. Lim WA, Richards FM, Fox RO (1994) Structural determinants of peptide-binding orientation and of sequence specificity in SH3 domains. Nature 372:375–379. doi:10.1038/372375a0
31. Binder LI, Frankfurter A, Rebhun LI (1985) The distribution of tau in the mammalian central nervous system. J Cell Biol 101:1371–1378. doi:10.1083/jcb.101.4.1371

Primer sequences used to amplify the various constructs used

Tau FL	ggatcc- ATGGCTGAGCCCCGCCAGGA **BamHI**	ctcgag- TCACAAACCCTGCTTGGCCA **XhoI**
Tau Nter	ggatcc- ATGGCTGAGCCCCGCCAGGA **BamHI**	ctcgag- TCAGGCGATCTTCGTTTTACCAT **XhoI**
Tau PRD	ggatcc- ACACCGCGGGGAGCAGCCCC **BamHI**	ctcgag- TCACAGGCGGCTCTTGGCGGAAG **XhoI**
Tau MBD	ggatcc- CAGACAGCCCCCGTGCCCAT **BamHI**	ctcgag- TCACAAACCCTGCTTGGCCA **XhoI**
BIN1deltaSH3	GGCTGGGAGCGCGGCGCGC	aagctt- TCATGGGGGCAGGTCCAAGCGCC **HindIII**

Antibodies used and their respective dilutions.

Antibody	epitope	Western Blot dilution	Immunofluorescence Dilution	Reference
AT270	pT181	1/1,000		Pierce antibodies MN1050
pS199	pS199	1/1,000		LifeTechnologies 44-734G
Tau-1	pS199-S208			Millipore MAB3420
CP13	pS202	1/1,000	1/200	Gift of Peter Davies
AT8	pS202/pT205	1/1,000		Pierce antibodies MN1020
AT180	pT231	1/1,000		Pierce antibodies MN1040
RZ3	pT231	1/1,000	1/200	Gift of Peter Davies
PHF-1	pS396/pS404	1/1,000	1/200	Gift of Peter Davies
Tau	Total tau		1/400	Dako Cytomation A0024
Tau-5		1/1,000		LifeTechnologies AHB0042
BIN1 99D	MycBD	1/1,000	1/200	Millipore 05-449
BIN1 Anti SH3	SH3	1/1,000	1/200	Abcam ab27796
α-tubulin		1/1,000		Abcam ab24622
PSD95			1/500	SYSY 124012
Synaptophysin			1/500	SYSY 101004
Clathrin			1/400	Santa-cruz sc-6579

Additional File 3

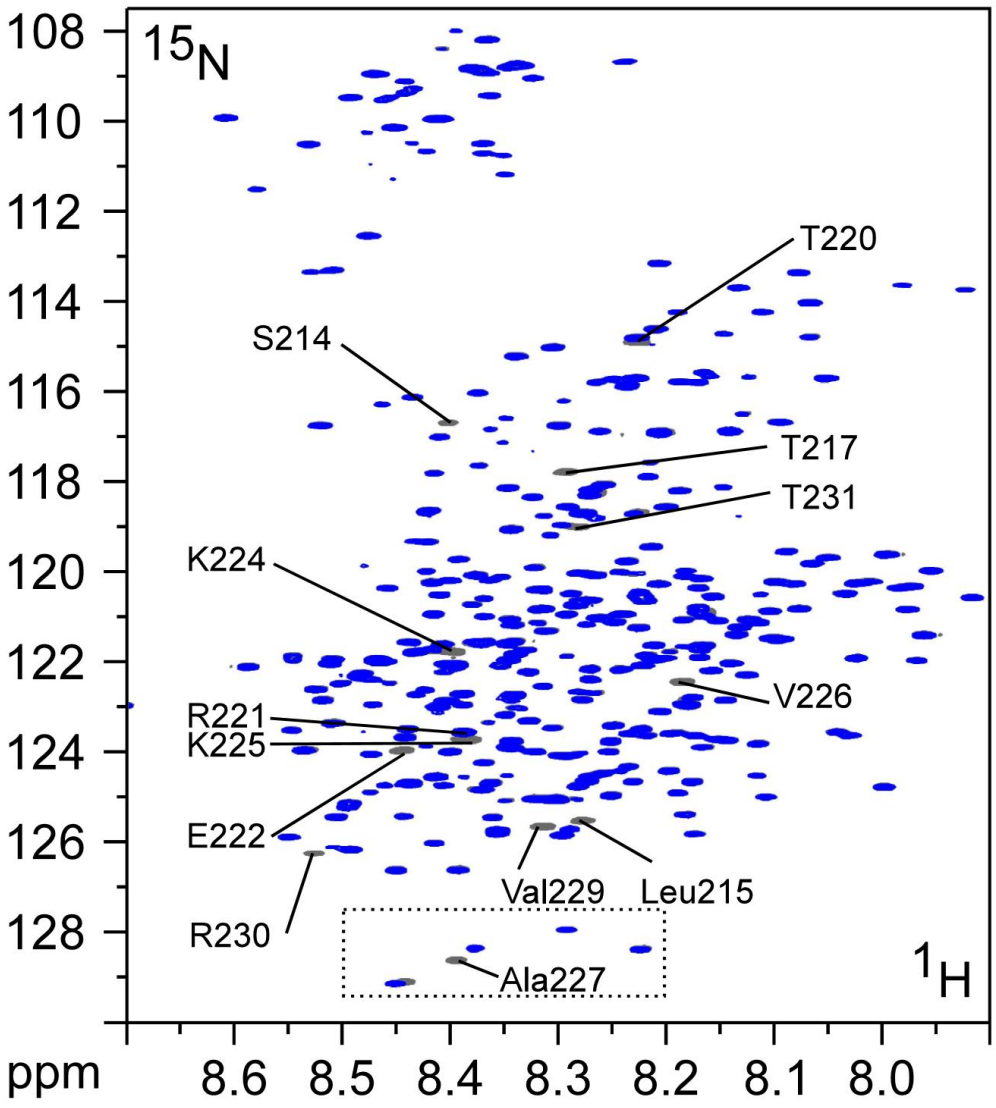

Additional File 4

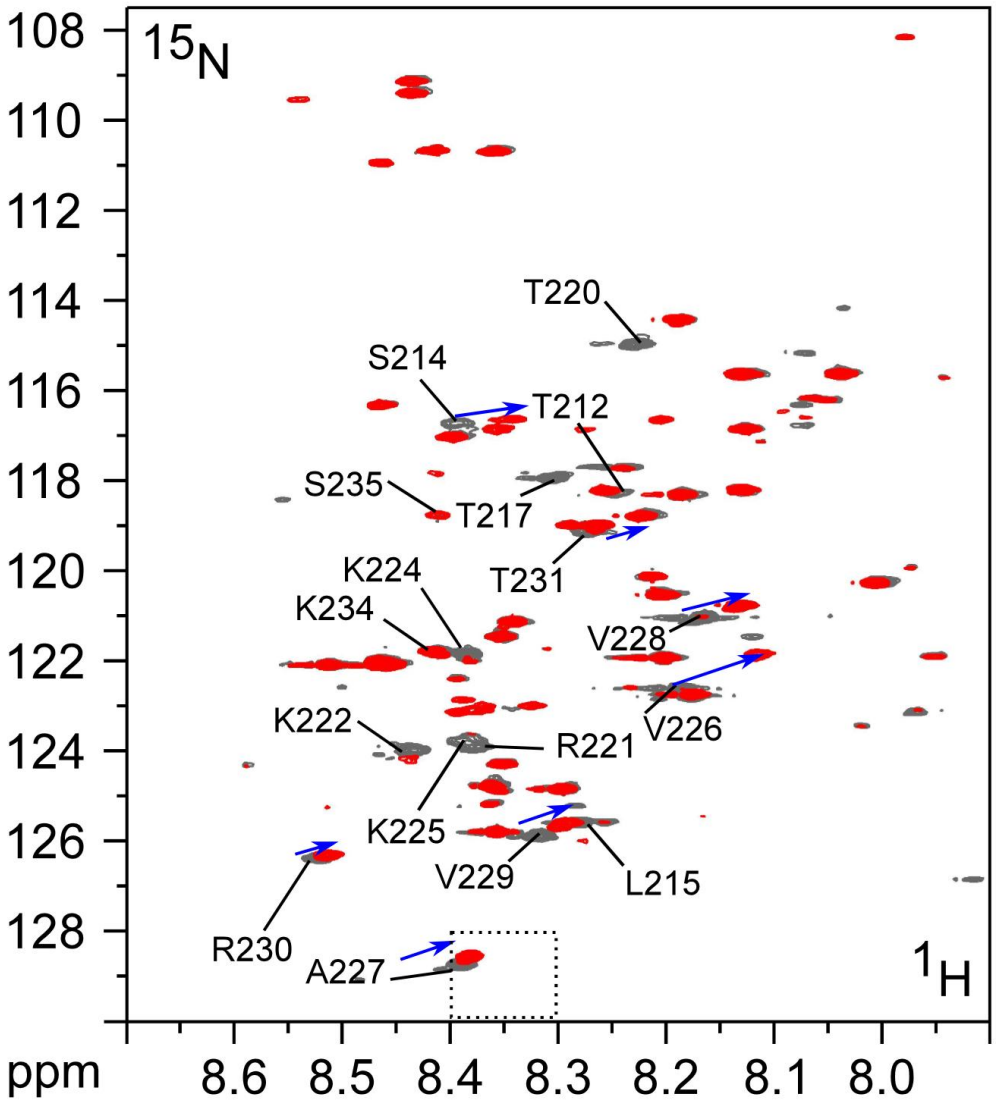

Additional File 5

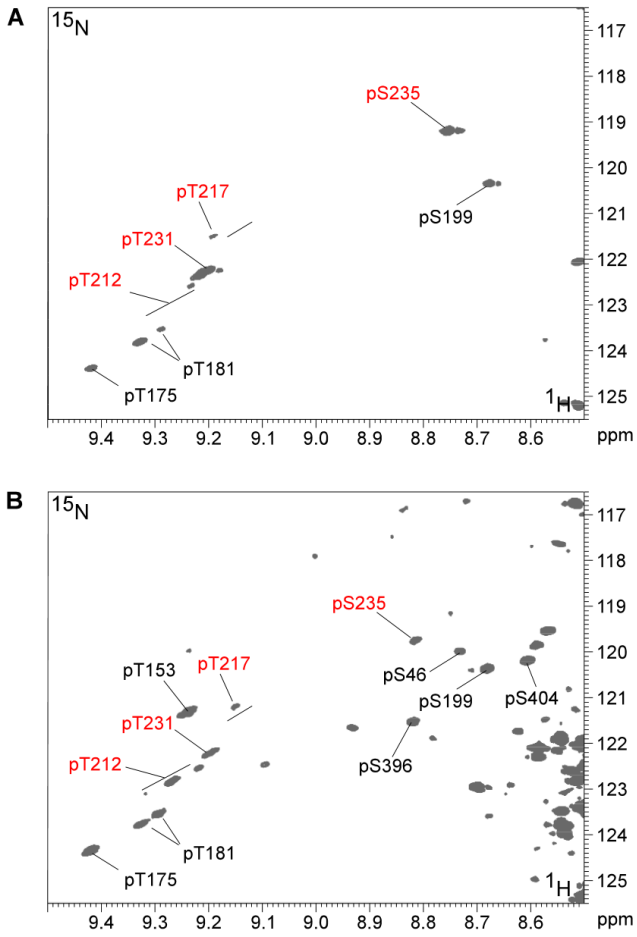

Additional File 6

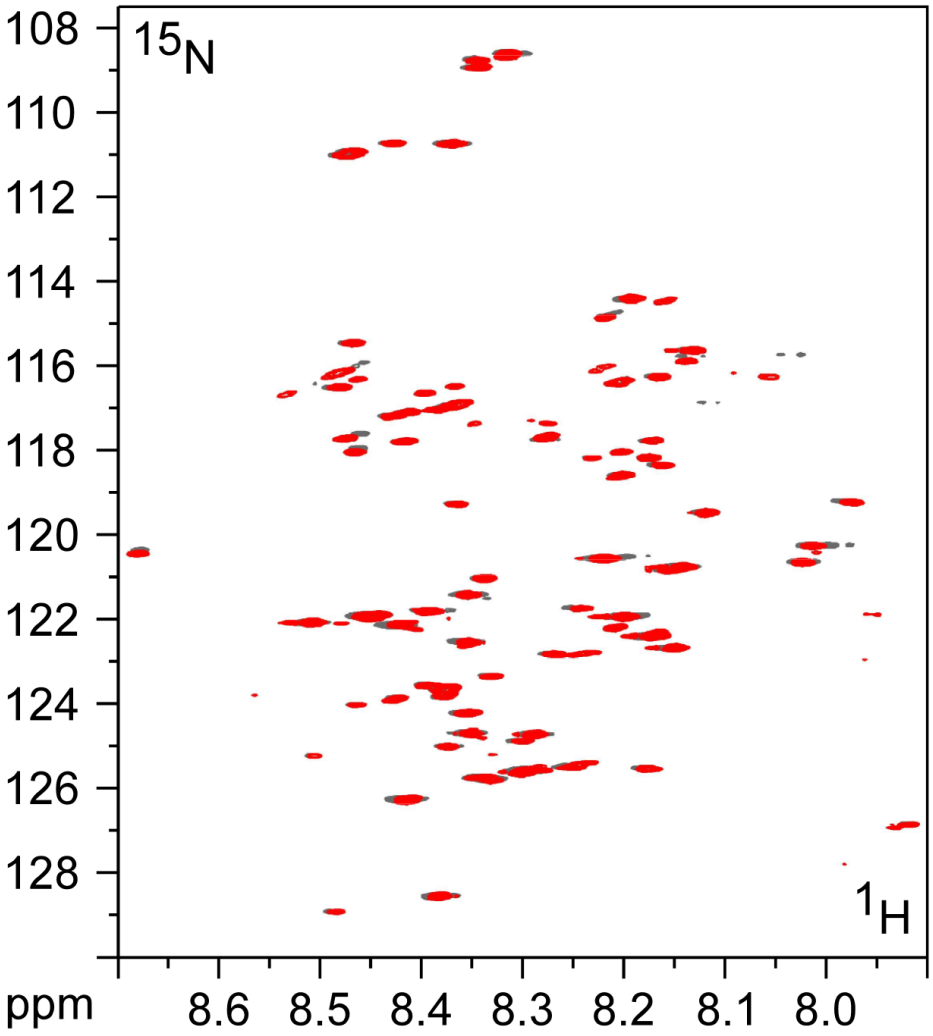

Additional File 7

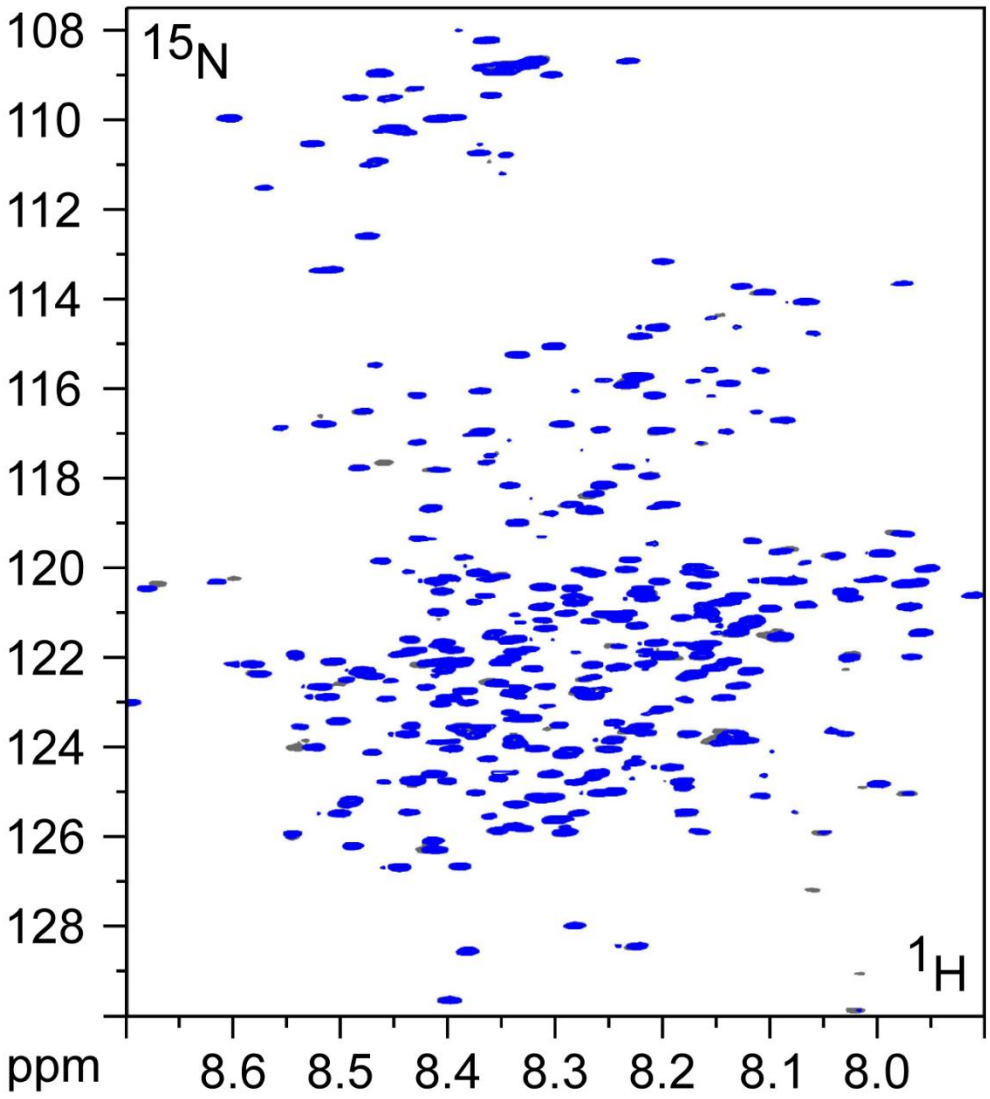

Additional File 8

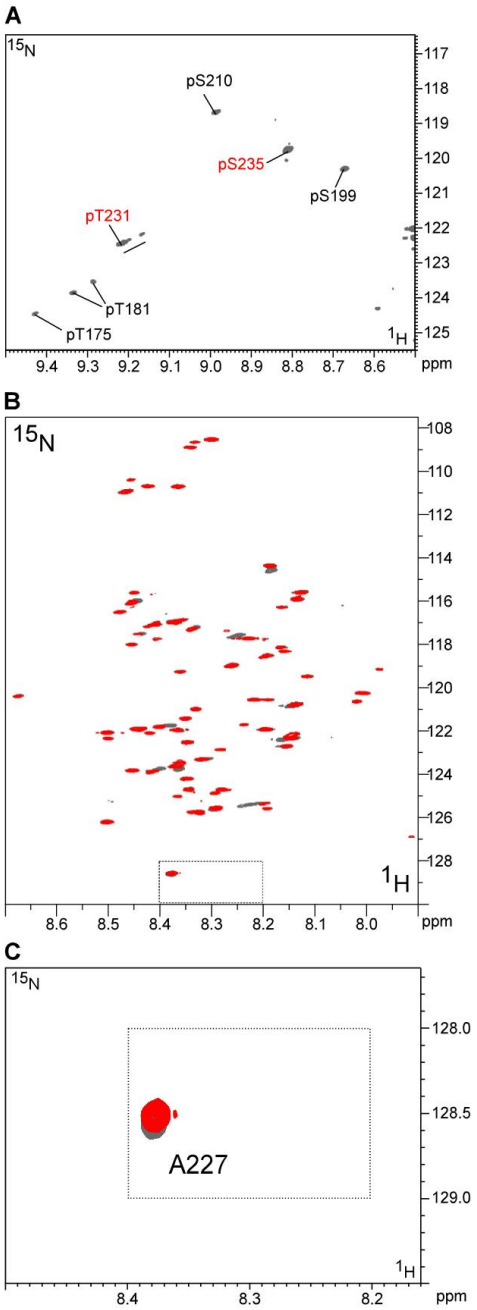

Additional File 9

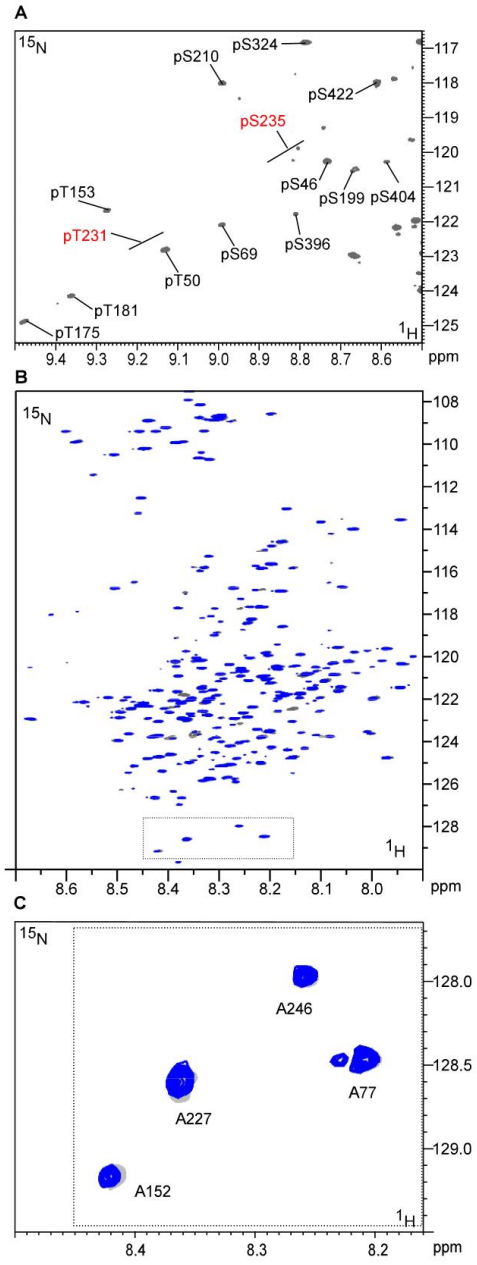

Addittional file 10

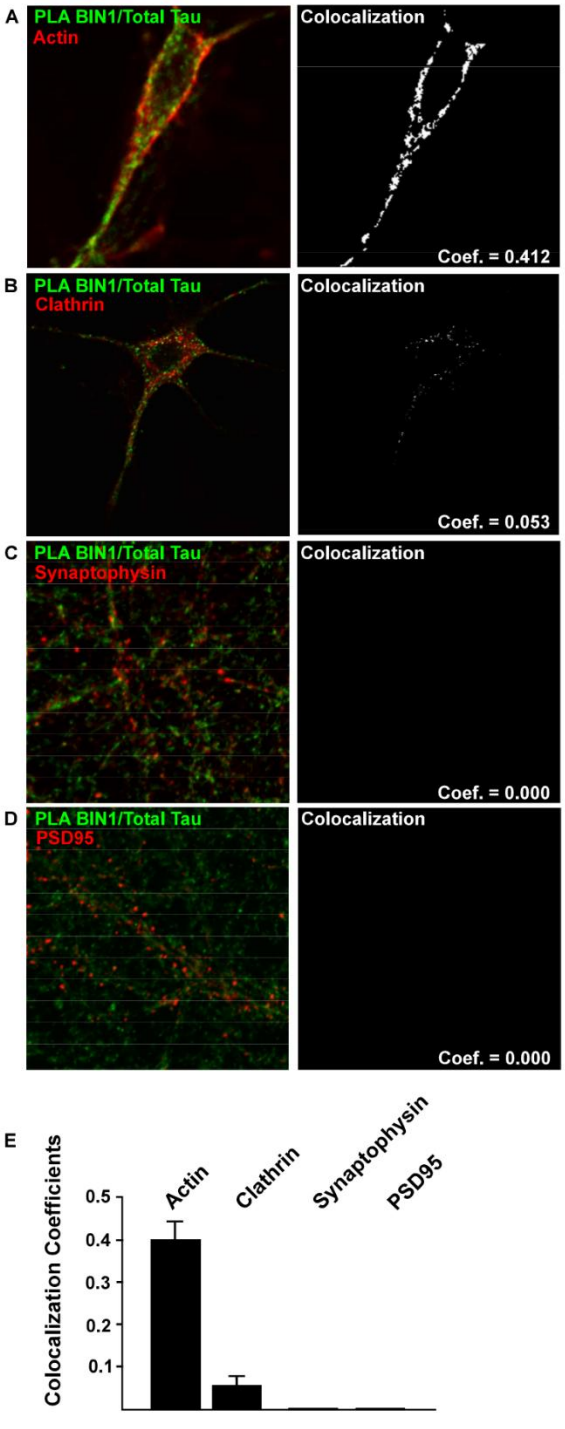

Supplemental experimental procedures

Phosphorylation of the Tau protein

The CDK2/CycA3 protein was prepared as primarily described in (1) and modified in (2). Phosphorylation of Tau by the CDK/CycA3 kinase is described in (2). The ERK kinase was prepared as described in (3). 100µM of ^{15}N-labelled recombinant Tau[165-245] was phosphorylated by incubation with 1 µM of activated ERK at 37°C during 3h in 200µL of phosphorylation buffer 50mM Hepes pH 8.0, 50 mM NaCl, 12.5 mM $MgCl_2$, 2.5mM ATP, 2mM DTT, 1 mM EDTA, 2mM EGTA and protease inhibitor cocktail (ROCHE, Complete Inhibitors without EDTA).

Rat brain extract was prepared by homogenizing rat brains (about 2g in 5 ml) in homogenizing buffer (10mM Tris.Cl pH 7.4, 5mM EGTA , 2mM DTT, 1µM okadaic acid (Sigma) supplemented with protease inhibitor cocktail. Ultra-centrifugation was next performed at 100,000g for 1 hour. The phosphorylation reaction of 10 µM ^{15}N-Tau protein (4) was performed at 37°C for 24h with 500 µl of rat brain extract in 10 mL of phosphorylation buffer (2 mM ATP, 40mM Hepes.KOH pH 7.3, 2mM MgCl2, 5mM EGTA, 2mM DTT complemented with a protease inhibitor cocktail and 1 µM okadaic acid (Sigma).

Enzymatic incubations were terminated by heating at 75°C fro 15 min and followed by centrifugation. The phosphorylation mixture was buffer-exchanged using desalting centrifugal devices (0.5ml bed of G25 resin, cut-off of 7KDa, Thermo Scientific Zeba Desalting Columns) against NMR buffer.

Co-localization measurement

Neurons were imaged with a Zeiss LSM 710 confocal imaging system using a 40x or 63x oil-immersion objectives. Z-stacks were 0.36 µm per step with a 1 AU pinhole. The co-localization coefficients were measured for each stack using ZEN 2012 software following the method already published by Manders et al (5).

Supplemental References

1. Welburn J, Endicott J (2005) Methods for preparation of proteins and protein complexes that regulate the eukaryotic cell cycle for structural studies. *Methods Mol Biol* 296:219–35.

2. Amniai L, et al. (2009) Alzheimer disease specific phosphoepitopes of Tau interfere with assembly of tubulin but not binding to microtubules. *FASEB J* 23(4):1146–1152.

3. Prabakaran S, et al. (2011) Comparative analysis of Erk phosphorylation suggests a mixed strategy for measuring phospho-form distributions. *Mol Syst Biol* 7:482.

4. Goedert M, et al. (1993) The abnormal phosphorylation of tau protein at Ser-202 in Alzheimer disease recapitulates phosphorylation during development. *Proc Natl Acad Sci U S A* 90(11):5066–70.

5. Manders EMM, Verbeek FJ, Aten JA (1993) Measurement of co-localization of objects in dual-colour confocal images. *J Microsc* 169(3):375–382.

BIN1 recovers tauopathy-induced long-term memory deficits in mice and interacts with Tau through Thr348 phosphorylation

In our previous work on BIN1-Tau interaction, we employed cellular and biochemical approaches to (i) identify the BIN1-SH3 domain and Tau-PRD as the domains involved on BIN1-Tau interaction, (ii) demonstrate that this interaction is regulated by (at least) phosphorylation of Tau at T231, and (iii) show that BIN1-Tau interaction occurs in the vicinity of actin cytoskeleton of cultured primary neurons (Sottejeau et al. 2015). Therefore, we decided to further characterize this interaction *in vivo* and *in vitro*.

Is has been previously shown that the Drosophila ortholog of BIN1 could modulate Tau neurotoxicity in vivo, however the impact of BIN1 expression levels on cognitive function has not yet been investigated. To address this point, we crossed a mouse model of tauopathy that overexpress human MAPT, but not the murine Mapt, with a mouse model that overexpressed the full human BIN1 gene. We observed that the overexpression of BIN1 induced short-term memory deficits earlier than the hTau mouse model but rescued this model long-term memory deficit. Similarly, the hBIN1 mouse model showed no deficit on long-term memory test. Although both short-term and long-term memory processes require the hippocampus, they take part in different cortical regions, i.e. lateral entorhinal and medial entorhinal cortex respectively (Van Cauter et al. 2013), indicating that BIN1 and Tau levels may differ in spatial and temporal dimensions, which could explain the opposite effects induced by BIN1 overexpression. Interestingly, BIN1 rescue of long-term memory deficits induced by hTau was associated with a strong decrease of phosphorylated Tau inclusions and a strong increase in BIN1-Tau interaction, in the hippocampus, suggesting that BIN1-Tau interaction may be protective against the formation of PHF, by blocking the re-localization and accumulation of phosphorylated Tau.

In addition, Tau overexpression was associated with myelin abnormalities at 18 months and BIN1 overexpression rescued Tau phenotype. Tau had already been associated with potential myelin dysfunction (Sotiropoulos et al. 2014; Krämer-Albers and White 2011), and recently BIN1 has been described to be expressed in oligodendrocytes, but dysregulated in AD (De Rossi et al. 2016; McKenzie et al. 2017).

Taking this information together with the latest reports showing that the protein levels of the neuronal isoform of BIN1 are decreased in AD (Glennon et al. 2013; Holler et al. 2014; De Rossi et al. 2016), we hypothesise that higher levels of BIN1 protein would be protective in AD, either through the regulation of BIN1-Tau interaction or through the rescue of myelin abnormalities induced by Tau.

Focusing on the regulation of BIN1-Tau interaction, we proceeded to investigate the dynamics of this interaction during neuronal development, and observed a clear increase of neuronal isoform of BIN1 and Tau protein levels, a concomitant decrease of Tau phosphorylation levels, particularly in epitopes associated with T231 (which we had already described to negatively impact the interaction between BIN1-SH3 and Tau-PRD), and a decrease of BIN1-Tau interaction, but not in the same proportion of the total protein or Tau phosphorylation levels. Then we confirmed that the expression level of BIN1 is a modulator of BIN1-Tau interaction through the silencing or overexpression BIN1 neuronal isoform (BIN1iso1) and observed a decrease of BIN1-Tau interaction upon underexpression and an increase upon overexpression of BIN1iso1. This data suggests that, even if BIN1-Tau interaction is restricted to certain loci in neurons, such as the actin tips (as described before), and dependent of Tau phosphorylation levels, variation in BIN1iso1 levels definitely affect the dynamics of BIN1-Tau interaction (supporting the data obtained with the transgenic mice) and its subsequent physiological or pathophysiological functions.

The fact that phosphorylation of Tau PRD (mainly at T231) inhibits its interaction with the BIN1 SH3 domain lead us to hypothesize that BIN1-Tau interaction dynamics is likely dependent on specific signaling pathways that regulate Tau phosphorylation.

In order to identify the molecular pathways involved in the regulation of BIN1-Tau interaction we developed a novel, semi-automated HCS approached, based on PNC as cellular model and PLA as readout of BIN1-Tau interaction. For this work, we chose to challenge our cellular model with the compound library Tocriscreen™ Mini (#2890; Tocris Biosciences; Bristol, UK), a library of well-characterized biologically active compounds, suitable for HTS/HCS and chemical biology applications, with proven solubility, purity and stability. This library provides compounds that target enzyme coupled receptors, GPRs, ion channels, transporters, cytosolic and nuclear receptors, enzymes and enzymatic complexes

(between others); allowing the screening of a wide-range of cellular processes, such as inflammation, apoptosis, cell differentiation, signal transduction, intracellular transport; and the possibility to be used in different fields like neuroscience, cancer, endocrinology, epigenetics, stem cell and cardiovascular research. In addition to the compounds of this library we also tested 6 Sanofi proprietary compounds that targeted well characterized enzymes, suspected to be deregulated in AD, in a blind manner.

Out of the 1126 tested compounds, 79 were excluded due to poor network quality. From the 1047, the strongest modulators of BIN1-Tau interaction were selected for the validation experiment. After dose-response curve (DRC) experiment, we retained 12 compounds that consistently exhibited the strongest modulation of BIN1-Tau interaction throughout all the screening and validation steps, which corresponds to about 1 % of all the tested compounds. This hit rate is very interesting, due to the fact that not very HCS studies are performed using physiological conditions and endogenous protein levels, even less are performed with PNC (especially post-natal) which have much more heterogeneous responses than cell lines, and to our knowledge this is only the second study to employ PLA as a readout, and the first to do it in 384-well plate format.

The 12 compounds selected from DRC experiments could be grouped into 5 categories, according to their targets: we identified compounds that were associated with the (i) regulation of phosphorylation, such as Cyclosporin A (CsA), an inhibitor of Calcineurin phosphatase activity that increased the interaction levels, and U0126, a MEK1/2 inhibitor that decreased BIN1-Tau interaction levels; in the category of (ii) NO-synthase (NOS) targeting compounds we identified TRIM, a potent inhibitor of neuronal and inducible NOS, and Diphenyleneiodonium chloride, a GPR3 agonist that also inhibits NADPH oxidase and NOS, and both increased the interaction; as (iii) Ca^{2+} homeostasis targeting compounds we identified (±)-Bay K 8644, a L-type Ca^{2+} channel activator, and DHBP dibromide, an inhibitor of endoplasmic reticulum Ca^{2+} release, and both also increased the interaction; in the (iv) receptor targeting compounds we identified that BRL37344 sodium salt, a β3 agonist, and BU 226 hydrochloride, a potent and highly selective I2 ligand, increased the interaction, while SB 258585 hydrochloride, a potent and selective 5-HT6 antagonist, increased BIN1-Tau interaction at very low concentration followed by a decrease of this effect in a concentration manner, in agreement with the provided K_i for this compound; as compounds with (v) other

targets we identified that JLK6, an inhibitor of γ-secretase-mediated βAPP processing, and MNITMT, a non-toxic immunosuppressive agent, also increased the interaction, while Doxorubicin hydrochloride, a tumour suppressor drug shown to inhibit DNA topoisomerase II and reduce Tau cellular levels was able to decrease BIN1-Tau interaction.

Knowing that BIN1-Tau interaction is modulated by Tau phosphorylation, we decided to further investigate the effect of CsA and U0126 on the modulation of BIN1-Tau interaction. We took especial interest on Calcineurin because it had not only been associated with AD and Tau dephosphorylation but also has been described to dephosphorylate Amphiphysin1, the homolog of BIN1 (Bauerfeind, Takei, and De Camilli 1997). Therefore, we postulated that Calcineurin could also target BIN1, and modulate BIN1-Tau interaction through its phosphorylation, but we had no simple way to address this suggestion.

It had been previously reported that BIN1iso1 was involved in intramolecular interaction between its own PRD and SH3 domain (Malki et al. 2017), and we reported that phosphorylation on PRD lead to a decrease of PRD-SH3 interaction (Sottejeau et al. 2015). Furthermore, when comparing Amphiphysin 1 and BIN1 sequences we observed that their PRD in the CLAP domains appears to be highly conserved. Interestingly, a Threonine of Amphiphysin1, in this sequence, that had been shown to be target of Cdk5 (Liang et al. 2007) has a corresponding Threonine in BIN1 sequence (T348). Thus, we hypothesized that T348 of BIN1 might be able to regulate the intramolecular interaction between PRD and SH3 domain of BIN1, similarly to how T231 of Tau regulates its interaction with BIN1.

To validate these two hypotheses, we developed and validated an antibody against BIN1 phosphorylated at T348, by assessing its sensitivity to Lambda protein phosphatase activity on crude protein extracts of PNC, and to cyclin-dependent kinases (Cdks) activity on purified recombinant protein. Then we used this antibody to assess the effect of CsA and U0126 on BIN1 phosphorylation, and observed a strong increase of BIN1 phosphorylated at T348 when incubating our PNC with CsA, and almost no effect when incubating with U0126. Conversely, Tau phosphorylation at T231 was strongly increased upon incubation of U0126, and was slightly affected upon incubation with CsA. Interestingly, T231 is not a target dephosphorylation site of Calcineurin (J. Z. Wang et al. 2012) and the modulation observed in the phosphorylation status of this epitope could be an off-target effect. Taken together

with the results from HCS, this data suggests that (i) the increase of BIN1-Tau interaction observed after inhibition of Calcineurin is due to an increase of BIN1 T348 phosphorylation, and (ii) the decrease of BIN1-Tau interaction upon inhibition of MEK1/2 was associated to an increase of Tau T231 phosphorylation.

Therefore, the regulation of BIN1-Tau interaction might also be associated with Calcineurin/Cdk5 signalling and MAPK signalling pathway: Calcineurin and Cdk5 have been proposed as a phosphatase/kinase duplet, responsible for the regulation of phosphorylated and dephosphorylated states of proteins involved in synaptic vesicle endocytosis, notably Amphiphysin1, during neurotransmission (Bauerfeind, Takei, and De Camilli 1997; Tomizawa et al. 2003), and might have a similar role on BIN1; and, on the other hand, Tau T231 is phosphorylated by ERK2, which is downstream of MEK1/2 in the MAPK signalling pathway (Qi et al. 2016).

We decided to further determine if the phosphorylation status of BIN1 at T348 could control the conformational dynamics of BIN1. Through nuclear magnetic resonance (NMR), we observed that (i) the SH3 domain of non-phosphorylated BIN1 is involved in intramolecular interaction with BIN1-CLAP-PRD, while the SH3 domain of BIN1 phosphorylated by Cdk2 (hole protein phosphorylated) and of BIN1iso1 with Threonine 348 mutated to glutamate (a phospho-mimetic mutation, BIN1 T348E) was free; and that (ii) BIN1-SH3 domain had much less affinity for BIN1-CLAP domain phosphorylated at T348 than for non-phosphorylated BIN1-CLAP domain. Interestingly it had been previously reported that BIN1-SH3 domain had much less affinity for non-phosphorylated BIN1-CLAP domain than for Tau-PRD (Malki et al. 2017). In addition, we confirmed the regulatory role of BIN1 phosphorylation at T348 by overexpressing BIN1iso1 and BIN1 T348E in PNC, and we observed a strong increase on BIN1-Tau interaction upon overexpression of BIN1 phospho-mimetic construct, as observed by the increase of BIN1-Tau PLA levels. This data show that phosphorylation of T348 is enough to induce the opened form of BIN1, leaving the SH3 domain available for interaction with the PRD of other proteins, including Tau, playing a central role in the regulation of BIN1-Tau interaction.

The interaction between BIN1 and Tau is strongly regulated by phosphorylation: phosphorylation of Tau at T231 reduces the interaction, while phosphorylation of BIN1 at

T348 increases the interaction. We know that there is an imbalance in the regulation of kinase/phosphatase activity during AD and this leads to an increase of Tau phosphorylated at T231, since the earlier stages of AD pathophysiological process. Conversely, nothing is known about the phosphorylation levels of BIN1 T348 in the brains of AD patients. Here, we confirmed that BIN1iso1 protein levels are decreased in the brains of AD patients and, for the first reported time, we observed an increase of the BIN1 phosphorylation levels at T348, relatively to BIN1iso1. We propose that this relative increase of T348 phosphorylation levels might be a compensatory mechanism to increase BIN1 function and/or BIN1-Tau interaction levels, and protect against the reduction of the neuronal isoform of BIN1.

In conclusion, our data supports the idea that BIN1 modulates the AD risk through an intricate regulation of its interaction with Tau, and that any modulation in BIN1 expression or activity may disrupt this regulatory balance with direct effects on learning and memory.

This work has been communicated to the scientific community through submission to bioRxiv, being presented here in its submitted form, main manuscript and supplementary data.

BIN1 recovers tauopathy-induced long-term memory deficits in mice and interacts with Tau through Thr^{348} phosphorylation

Maxime Sartori[1,2,3,4,*], Tiago Mendes[5,6,7,8,*], Shruti Desai[5,6,7,*], Alessia Lasorsa[7,9], Adrien Herledan[6,10,11], Nicolas Malmanche[5,6,7], Petra Mäkinen[12], Mikael Marttinen[12], Idir Malki[7,9], Julien Chapuis[5,6,7], Amandine Flaig[5,6,7], Anaïs-Camille Vreulx[5,6,7], Philippe Amouyel[5,6,7], Florence Leroux[6,10,11], Benoit Déprez[6,10,11], François-Xavier Cantrelle[7,9], Damien Maréchal[1,2,3,4], Laurent Pradier[8], Mikko Hiltunen[12], Isabelle Landrieu[7,9], Devrim Kilinc[5,6,7,#], Yann Herault[1,2,3,4,#], Jocelyn Laporte[1,2,3,4,#], Jean-Charles Lambert[5,6,7,#]

* Maxime Sartori, Tiago Mendes, and Shruti Desai contributed equally to this work.

# Devrim Kilinc, Yann Herault, Jocelyn Laporte and Jean-Charles Lambert contributed equally to this work.

[1] Institut de Génétique et de Biologie Moléculaire et Cellulaire (IGBMC), Illkirch, France

[2] INSERM U1258, Illkirch, France

[3] CNRS UMR7104, Illkirch, France

[4] Strasbourg University, Illkirch, France

[5] INSERM U1167, RID-AGE: Risk Factors and Molecular Determinants of Aging-Related Diseases, Lille, France

[6] Institut Pasteur de Lille, Lille, France

[7] University of Lille, DISTALZ Laboratory of Excellence (LabEx), Lille, France

[8] SANOFI Neuroscience Therapeutic Area, Chilly-Mazarin, France

[9] CNRS UMR8576, Lille, France

[10] University of Lille, EGID, Lille, France

[11] INSERM U1177, Drugs and Molecules for Living Systems, Lille, France

[12] Institute of Biomedicine, University of Eastern Finland, Kuopio, Finland

Correspondence to:

Yann Herault, PhD

IGBMC, 1 rue Laurent Fries, 67404 Illkirch, France.

Tel.: +33 3 88 65 57 15

Fax: +33 3 88 65 32 01

E-mail: herault@igbmc.fr

Jocelyn Laporte, PhD

IGBMC, 1 rue Laurent Fries, 67404 Illkirch, France.

Tel.: +33 3 88 65 34 12

Fax: +33 3 88 65 32 01

E-mail: jocelyn@igbmc.fr

Jean-Charles Lambert, PhD

Inserm UMR1167, Institut Pasteur de Lille, 1 rue du Pr. Calmette 59019 Lille cédex

Tel: + 33 3 20 87 73 91

Fax: + 33 3 20 87 78 94

E-mail: jean-charles.lambert@pasteur-lille.fr

Keywords: Alzheimer's disease, BIN1, Tau, tauopathy, long-term memory, neurodegeneration, high-content screening, proximity ligation assay, nuclear magnetic resonance, Cdk, calcineurin

Abstract

The bridging integrator 1 gene (*BIN1*) is a major genetic risk factor for Alzheimer's disease (AD). In this report, we investigated how BIN1-dependent pathophysiological processes might be associated with Tau. We first generated a cohort of control and transgenic mice either overexpressing human MAPT (Tg*MAPT*) or both human MAPT and BIN1 (Tg*MAPT*;Tg*BIN1*), which we followed-up from 3 to 15 months. In Tg*MAPT*;Tg*BIN1* mice short-term memory deficits appeared earlier than in Tg*MAPT* mice; however – unlike Tg*MAPT* mice – Tg*MAPT*;Tg*BIN1* mice did not exhibit any long-term or spatial memory deficits for at least 15 months. After sacrifice of the cohort at 18 months, immunohistochemistry revealed that BIN1 overexpression prevents both Tau mislocalization and somatic inclusion in the hippocampus, where an increase in BIN1-Tau interaction was also observed. We then sought mechanisms controlling the BIN1-Tau interaction. We developed a high-content screening approach to characterize modulators of the BIN1-Tau interaction in an agnostic way (1,126 compounds targeting multiple pathways), and we identified – among others – an inhibitor of Calcineurin, a Ser/Thr phosphatase. We determined that Calcineurin dephosphorylates BIN1 on a Cyclin-dependent kinase phosphorylation site at T348, promoting the open conformation of the neuronal BIN1 isoform. Phosphorylation of this site increases the availability of the BIN1 SH3 domain for Tau interaction, as demonstrated by nuclear magnetic resonance experiments and in primary neurons. Finally, we observed that the levels of the neuronal BIN1 isoform were decreased in AD brains, whereas phospho-BIN1(T348):BIN1 ratio was increased, suggesting a compensatory mechanism. In conclusion, our data support the idea that BIN1 modulates the AD risk through an intricate regulation of its interaction with Tau. Alteration in BIN1 expression or activity may disrupt this regulatory balance with Tau and have direct effects on learning and memory.

Introduction

Alzheimer's disease (AD) is the most common neurodegenerative disorder and is clinically characterized among others by memory deficits affecting first short term and then long term and spatial memory. AD constitutes a major public, medical, societal, and economic issue worldwide, with 35.6 million people suffering from the disease and a forecast of 106 million in 2050 [41]. Responding effectively to this AD crisis necessitates a better understanding of this disease in order to improve diagnosis and therapy.

AD is characterized by two main types of brain lesions: (i) amyloid plaques, resulting from the extracellular accumulation of amyloid beta (Aβ) peptides; (ii) neurofibrillar degeneration, due to the intracellular aggregation of abnormally hyperphosphorylated Tau proteins. This latter aggregation is associated with an ectopic localization of Tau from the axonal compartment to the somato-dendritic compartment [53].

The discovery of mutations in the *APP*, *PS1* and *PS2* genes (coding for amyloid precursor protein, APP, and presenilins 1 and 2), responsible for early-onset, autosomal-dominant forms of AD, has placed Aβ oligomer production at the center of the pathophysiological process [25]. A better understanding of the genetic component of the common, complex forms of AD, which is exceptionally high among multifactorial aging-related diseases [22], is required to decipher the pathophysiological processes of AD. Genome-wide association studies (GWAS) allowed for the identification of more than 30 loci associated with the late-onset forms of AD [27,31,32,47], including the bridging integrator 1 gene (*BIN1*). A part of these genes pointed out a potential failure in Aβ clearance, leading to more insidious Aβ accumulation in the brain [30,47]. On the other hand, it is only recently that AD genetic risk factors have been also associated with Tau pathology, following the development of systematic screenings in *Drosophila* which allowed for the identification of genetic modifiers by assessing eye roughness and eye size as readouts of Tau neurotoxicity [19,45,46] and their associations with endophenotypes related to Tau [6,16,19]. Such observations are of high importance since, contrary to amyloid plaques, neurofibrillary tangles (NFTs) are well correlated with cognitive impairment both in humans [39] and in animal models [28].

Among the genes described to genetically interact with human Tau transgene in *Drosophila*, BIN1 was further described to directly interact with the Tau protein by NMR spectroscopy using recombinant proteins, *in vitro* glutathion *S*-transferase (GST) pull-down from HEK293 lysates, as well as reciprocal co-immunoprecipitation from mouse brain synaptosome homogenates [14]. In addition, a genome-wide significant functional risk variant in the vicinity of *BIN1* locus has been associated with Tau loads (but not with Aβ loads) in AD brains [19].

The *BIN1* gene codes for Amphiphysin 2, also called BIN1, a ubiquitously expressed protein involved in membrane remodeling. BIN1 comprises a N-BAR domain involved in membrane curvature sensing, an SH3 domain that binds to proline-rich motifs present in a number of proteins including itself, and a clathrin- and AP2-binding domain (CLAP) specific of the neuronal isoform 1 [42]. In the central nervous system (CNS), BIN1 is mostly found in the axon initial segment, at the nodes of Ranvier [11], and at the synapse [44,17], and was also associated with myelinated axons and oligodendrocytes in the white and grey matter [18]. However, little is known about its function in the CNS. We recently described the consequences of increased human BIN1 expression in the mouse brain, which exhibits early alterations in the neuronal tract between the entorhinal cortex and the dentate gyrus of the hippocampus, leading to impaired novel object recognition and aging-related changes [17]. Altogether, BIN1 overexpression affects the aging brain and induces neurodegeneration [17].

Little is also known about BIN1 in the context of AD. Several teams evaluated potential links between AD and BIN1 and determined: (i) BIN1 may regulate BACE1 intracellular trafficking through multiple mechanisms and subsequently alter Aβ peptide production [37]; (ii) BIN1 may have a role in plasma membrane remodeling during myelination, which is known to be affected in AD [18,36]; (iii) BIN1 may participate in the neuron-to-neuron propagation of Tau prion strains [12]; and (iv) BIN1 may directly interact with Tau and interfere with Tau neurotoxicity *via* unknown mechanisms [19,35]. In this study, we developed a multidisciplinary approach encompassing molecular, cellular, and behavioral experiments to determine how BIN1 is involved in the pathophysiological processes of AD. To this end we assessed for the first time the impact of human *BIN1* overexpression in a mouse model of tauopathy and further dissected the interaction between Tau and BIN1 at the molecular and cellular levels.

Materials and Methods

Animal ethics

Animal experiments were approved by the Com'Eth (project file: 2014-056) and accredited by the French Ministry for Superior Education and Research in accordance with the Directive of the European Parliament: 2010/63/EU. For all tests described, mice were kept in specific pathogen free conditions with free access to food and water, and were bred with littermates. The light cycle was controlled as 12 h light and 12 h dark (lights on at 7AM). Before all behavioral experiments, handling was done every day for one week before the beginning of the experiment.

Mouse lines and genotyping

We used several mouse lines carrying the inactivation of *Mapt*: B6.Cg *Mapt*$^{tm1(EGFP)Klt/+}$, noted here *Mapt*$^{+/-}$ [50], a line overexpressing human Tau: B6.Cg *Mapt*$^{tm1(EGFP)Klt/tm1(EGFP)Klt}$ *Tg(MAPT)8cPdav/J*, named here hTau [2], and another line overexpressing human BIN1: B6 *Tg(Bin1)U154.16.16Yah*, named here TgBIN1/0 [17]. In order to generate cohorts of animals carrying hTau alone, hTau;Tg*BIN1*, and *Mapt*$^{+/-}$ as control littermates, we crossed *Mapt*$^{+/-}$;*Tg(MAPT)8cPdav/J* with *Mapt*$^{+/-}$;TgBIN1. All animals were crossed on C57BL/6J background. Primer sequences are available in Table S1.

Design of behavioral experiments

Animals studied in behavioral tasks were both males and females. Same animals were longitudinally tested at 3, 6, 9, 12, and 15 months. All animals were killed at 18 months for histology and molecular biology experiments.

Open field paradigm

For the open field paradigm, mice were tested in a 55 cm-diameter white round box. Mouse activity was recorded with the Ethovision video tracking system (Noldus, Paris, France) during a single session of 30 min. The arena was placed in a room homogeneously illuminated at 50 lux. Each mouse was allowed to explore the apparatus freely for 30 min with the experimenter out of the animal's sight. The distance travelled and time spent in the central and peripheral regions were recorded over the test session.

Novel object recognition task

This task was performed in the same conditions as in the open field paradigm (see above). The objects to be discriminated were a glass marble (2.5 cm in diameter) and a plastic dice (2 cm). The animals were first habituated to the open field for 30 min. The next day, they were submitted to a 10 min acquisition trial during which they were placed in the open field in

the presence of two similar objects (object A; marble or dice). The time the animal took to explore the object A (when the animal's snout was directed towards the object at a distance ≤ 1 cm) was recorded manually. A 10 min retention trial was performed 1 h later. During this trial, one of the familiar objects in the open field was replaced with a new one (object B), and the time periods that the animal took to explore the two objects were recorded (t_A and t_B for objects A and B, respectively). Two exclusion criteria were applied to select those animals that had memorized the objects: (i) during the acquisition trial, mice exploration should be longer than 3 s, and (ii) during the retention trial, mice exploration should also be longer than 3 s. The exploration index for object B was defined as $(t_B / (t_A + t_B)) \times 100$. Memory was defined by the percentage of time animals spent investigating the novel object statistically different from the chance (50%). To control for odor cues, the open field arena and the objects were thoroughly cleaned with 50% ethanol, dried, and ventilated between sessions. All animals were tracked with the Ethovision software.

Morris water maze task

The Morris water maze was used to test spatial learning and memory. Each session was performed one week after NOR task and constituted the last behavioral experiment. The water maze is a circular pool (150 cm in diameter, 60 cm in height), filled with water up to 40 cm mark that is maintained at 20-22°C, and made opaque using a white aqueous emulsion (Acusol OP 301 opacifier). The surface was split into 4 quadrants: South-East (SE), North-West (NW), North-East (NE), and South-West (SW). The escape platform, made of rough plastic, was submerged 1 cm below the water's surface. Experiments were performed to study reference memory through a spatial search strategy that involved finding the hidden platform. The spatial memory session consisted of a 6-day (J1 to J6) learning phase with four 90 s trials per day. Each trial started with mice facing the interior wall of the pool and ended when they climbed onto the platform located on the SE quadrant, or after a maximum searching time of 90 s. The starting position was changed pseudo-randomly between trials. Mice were left undisturbed in their home cage for 90 min intertrial intervals. On the 7^{th} day, mice were given the 60 s probe test, in which the platform had been removed. The distances traveled in each quadrant (NW, NE, SW, and SE) were recorded, as well as the time spent in the target quadrant. At 6, 9 and 12 months of age, the platform was located in the NE quadrant, whereas at 15 months of age, the platform was located in the SW quadrant. All animals were tracked with the Ethovision software.

Brain protein extraction and Western blotting

Mice were killed by cervical dislocation and brains were quickly removed and dissected. Structures were immediately frozen in liquid nitrogen, and conserved at -80°C. For protein

extraction we used fresh extraction buffer with pH adjusted to 7.5 (20 mM Tris at pH = 7.5; 50 mM NaCl; 2 mM EGTA; 1% Triton X-100; 10 mM NaF; 1 mM Na_3VO_4; 2 mM β Glycerophosphate; cOmplete™ EDTA-free protease inhibitor cocktail). Tissues were lysed using Precellys apparatus and centrifuged at 33,000 ×g for 30 min. Protein quantification was performed using the BCA protein assay (Thermo Scientific; Waltham, MA). 10-20 µg of total protein from extracts were separated in SDS–polyacrylamide gels (10%) and transferred to nitrocellulose membranes. Depending on the target protein, we used bovine serum albumin or milk (5% in Tris-buffered saline with 0.1% Tween-20, TTBS; 1 h at RT) to block non-specific binding sites of phosphorylated and non-phosphorylated proteins, respectively. Immunoblotting was carried out with primary antibodies (Table S2) for 1 h at RT. Then membranes were washed 5 times in TTBS, followed by incubation with secondary antibodies conjugated with horseradish peroxidase (Table S2). Immunoreactivity was visualized using ECL chemiluminescence system (SuperSignal™, Thermo Scientific). Chemiluminescence was captured with Amersham Imager and signals were quantified with ImageJ (NIH; Bethesda, MD).

Immunofluorescence in brain slices

Mice were anesthetized with 5% ketamine and 10% xylazine and perfused first with PBS and then with 4% paraformaldehyde (PFA) in PBS. After removal, brains were immerged in 4% PFA overnight at 4°C, followed by multiple rinses with PBS, and put in 30% sucrose in PBS until they sink. Once they sink, they were embedded in O.C.T. tissue freezing compound (Scigen; Gardena, CA), and stored at -80°C until they were cut with a cryostat at 10 µm thickness. For immunofluorosence, slices were first permeabilized with 0.1% Triton in PBS, with 10% horse serum and 5% BSA for 30 min. The primary antibody (Table S2) was then applied overnight at 4°C in the permeabilization buffer. After multiple rinses with PBS, the secondary antibody (Table S2) in 0.1% Triton was applied for 1 h at RT. After multiple rinses, slices were stained with 1:1000 Hoechst (Sigma; St. Louis, MO). After multiple rinses, slices were mounted in Fluorsave (Merck Millipore; Darmstadt, Germany). Slices were imaged with NanoZoomer slice scanner (Hamamatsu Photonics; Massy, France).

Electron microscopy of brain slices

Mice were PFA-fixed as described. After removal, brains were immerged in 4% PFA and 4% glutaraldehyde in PBS overnight at 4°C. Coronal sections were obtained with Leica VT1000 vibratome (Leica Biosystems; Nanterre, France), and the tissue was cut to expose the dorsal fornix and the upper part of the hippocampus. The tissues were post-fixed in 1% osmium tetroxide, dehydrated through graded ethanol (50, 70, 90, and 100%) and propylene oxide for 30 min each, and embedded in Epon 812 (EMS; Hatfield, PA). Semithin sections were

cut at 2 µm on an ultra-microtome (Ultracut UCT; Leica) and ultrathin sections were cut at 70 nm, contrasted with uranyl acetate and lead citrate, and examined at 70 kV using a Morgagni 268D electron microscope (Thermo Scientific). Images were captured digitally by Mega View III camera (Soft Imaging System; Münster, Germany).

Primary neuronal culture

Culture media and supplements were from Thermo Scientific, unless mentioned otherwise. Primary hippocampal neurons were obtained from P0/P1 rats, according to previously described procedures with minor modifications [5,29]. Briefly, cortices and hippocampi were isolated from new-born rats, washed with ice-cold dissection medium (HBSS supplemented with HEPES, sodium pyruvate, and penicillin/streptomycin), and trypsinized (2.5%; 10 min; 37°C). Trypsin was inactivated with dissociation medium (MEM supplemented with inactivated FBS, Glutamax, D-glucose (Sigma), MEM vitamins, and penicillin/streptomycin), followed by DNase (5 mg/ml; Sigma) incubation for 1 min and wash with dissection medium. Media was replaced by dissociation medium and tissue was triturated with a fire-polished cotton-plugged Pasteur pipette to obtain a homogenous cell suspension, followed by centrifugation (200 ×*g* for 5 min) and wash with dissociation medium. Cells were resuspended in culture medium (Neurobasal A supplemented with Glutamax and B_{27} neural supplement with antioxidants), counted, and plated in 384-well plates (Greiner bio-one; Kremsmünster, Austria) at a density of 50,000 cells/cm^2 for HCS, on Ø13 mm coverslips in 24-well plates at a density of 25,000 cells/cm² for proximity ligation assay (PLA), or directly in 24-well plates without coverslips at density 100,000 cells/cm^2 for immunoblots. Coverslips and plates were pre-coated with poly-L-lysine (Alamanda Polymers; Huntsville, AL) overnight at 37°C and rinsed thoroughly with water. After 20-24 h, culture media was replaced with supplemented Neurobasal A medium and cultures were maintained in a tissue culture incubator (Panasonic; Osaka, Japan) at 37°C and 5% CO_2 for 7, 14, or 21 days.

Viral transductions

Primary neuronal cultures (PNC) were transduced on DIV8 with lentiviral constructs for silencing (MOI = 4) using Mission pLKO,1-puro-CMV-shRNA vectors (Sigma), non-targeting (05191520MN) and shBIN1 (TRCN0000380439). Overexpression constructs were obtained from Gene Art (Thermo Fisher) based on pLenti6/Ubc/v5-DEST vectors (Life Technologies, Carlsbad, CA): BIN1iso1 (NM_009668), BIN1iso1 phosphomimetic T348E (cDNA with Thr^{348}→Glu), BIN1 isoform 9 (NM_139349), and an overexpression control vector (mock). The transduction was performed according to a previously described procedure with minor modifications [34]: For PNC in 24-well plates, viral constructs at multiplicity of infection (MOI) 2 were added to pre-warmed supplemented Neurobasal A media with Polybrene (0.1% final

concentration; Sigma) at 10× concentration. Half of the culture media from multi-well plates were collected and stored. The transduction mixture was added to each well to reach 250 µl final volume and neurons were incubated for 6 h. At the end of this period, wells were topped with 250 µl collected media and neurons were maintained in the incubator until fixation or protein harvest. Transduced neurons were either fixed or harvested on DIV14.

Immunoblotting

PNC were harvested in minimum volume of 40 µl/well in ice-cold lysis buffer as described elsewhere [13]. Lysates were mixed with 4× LDS (Novex; Life Technologies) and 10× reducing agent (Novex) loaded on pre-cast NuPage 4-12% bis-Tris acrylamide 10 well gels (Novex) and transferred to nitrocellulose membranes using the BioRad Trans-blot transfer system kit (BioRad, Hercules, CA). Membranes were blocked in 5% non-fat milk in 1x TNT buffer. Primary antibodies were diluted in SuperBlock T20 (TBS) blocking buffer (Thermo Fisher) and kept at 4°C overnight: mouse BIN1-99D (clone 99D; 1:1,000; cat. no. 05-449, Merck Millipore), rabbit TauC (1:10,000), mouse beta-actin (1:10,000; Sigma), rabbit phospho-BIN1 Thr 348 (1:10,000; custom made by Biotem, Apprieu, France), mouse Tau 1 non-phospho Ser 195-Ser 202 (aa197-205) (1:10,000; Merck Millipore), mouse AT180 phospho Thr 231 (1:500, Thermo Fisher), mouse RZ3 Thr 231 (1:500), and mouse PHF1 phospho Ser396/404 (1:1000). The last two antibodies were kind gifts from Peter Davies. We further confirmed the specificity of this antibody for the neuronal isoform by silencing BIN1 and overexpressing BIN1iso1 or BIN1iso9 (Fig. S1). Detection was performed using horseradish peroxidase (HRP)-conjugated secondary antibodies (1:5000, Jackson) for 1-2 h at RT. The membrane was revealed through chemiluminescence (Luminata Crescendo™, EMD Merck Millipore) and imaged with Amersham Imager 600 (GE Healthcare, Mississauga, Canada). The images were quantified with ImageQuantTL Software (GE Healthcare).

Analysis of neuropathological human sample cohort

Assessment of AD-related neurofibrillary pathology (Braak stage) was performed for 14 individuals after death (Table S3) with immunostaining of paraffin sections with AT8 antibody, which detects hyperphosphorylated Tau [7]. Protein extractions from the frozen temporal lobe tissue samples were performed as previously described [38]. Protein quantification was performed using BCA protein assay. Total proteins (20 µg/lane) were separated on 4-12% Bis-Tris-polyacrylamide gel electrophoresis (PAGE; Invitrogen) under reducing conditions and subsequently blotted onto polyvinylidene difluoride membranes using iBlot 2 Dry Blotting System (Thermo Scientific). Primary antibodies against phospho-BIN1 Thr 348 (1:1,000), total BIN1 (1:1,000) and β-actin (1:1,000; cat. no. ab8226, Abcam)

were used for immunoblotting. After incubation with the appropriate HRP-conjugated secondary antibodies, the protein bands were detected using ImageJ.

Lambda protein phosphatase assay

Crude protein extracts were incubated with Lambda protein phosphatase (New England Biolabs; Ipswich, MA), following supplier's instructions with minor changes. DIV21 PNC were harvested on ice in 40 µl ice-cold lysis buffer per well without protein phosphatase inhibitors, lysates were sonicated, centrifuged for 10 min at 1,000× *g* and the supernatant was distributed into 2 new tubes; volumes were adjusted to 40 µl with MilliQ H_2O, and supplemented with 5 µl of 10× NEBuffer and 5 µl of 10 mM $MnCl_2$ (provided with the enzyme); 1 µl of lambda protein phosphatase (λ-PP) was added to one of the tubes and both tubes were incubated for 30 min at 30°C. 4× LDS and 10× reducing agent were added to the tubes, samples were boiled at 95°C for 10 min and immunoblotted as described before.

In vitro assay with recombinant proteins

BIN1 phosphorylation *in vitro* was assessed in kinase buffer containing 20 mM MOPS, pH 7.4, 5 mM $MgCl_2$, 100 µM ATP, and 1 mM DTT. Purified GST-BIN1 (500 ng) was incubated with recombinant GST-tagged Cdk5/p35 (100 ng) at RT for 1h. The reaction was terminated by the addition of boiled SDS sample buffer. After electrophoresis of the samples were run on SDS-PAGE. In addition, Cdk2/CycA3 kinase [52] was used to obtain Bin1iso1 phosphorylated on T348 residue. The capacity of the kinase to phosphorylate T348 was first verified using the CLAP (334-355) peptide as substrate and mass spectrometry to assess the addition of a phosphate group. In addition, the phosphorylated peptide was detected using the antibody directed against pT348 (Fig. S2a, inset). For NMR experiments, 100 µM ^{15}N-BIN1iso1 was incubated with recombinant Cdk2/CycA3 kinase (molar ratio 1/100), for 3 h at 37°C, in the presence of 2 mM ATP, 2.5 mM $MgCl_2$, 2 mM EGTA, 2 mM DTT, 30 mM NaCl and protease inhibitors in 50 mM HEPES, pH 8.0 (Fig. S2). Control experiment was performed in the absence of ATP. Phosphorylation of Bin1Iso1 at T348 was verified using western blot analysis with an antibody directed against pT348.

NMR spectroscopy

NMR experiments were recorded at 20°C on Bruker 900-MHz spectrometer. NMR measurements were performed in 50 mM sodium phosphate buffer, pH 7.3, 30 mM NaCl, 3 mM DTT and 10% D_2O. BIN1iso1, BIN1iso1-CLAP-T348E and Cdk2-phospho-BIN1iso1 ^{1}H-^{15}N HSQC spectra were all recorded with a TXI probe at a protein concentration of 100 µM. These 2D spectra were acquired with 3072 points in the direct and 180 points in indirect dimensions for spectral width of 13 ppm and 26 ppm, respectively, and with 512 scans. BIN1-SH3 domain ^{1}H-^{15}N HSQC spectrum was recorded with a cryogenic probe with 3072

points in the direct and 256 points in indirect dimensions for spectral width of 14 ppm and 26 ppm, respectively, and with 48 scans. Spectra were processed using TopSpin software (Bruker). BIN1-SH3 domain backbone assignments were previously reported [35]. The NMR titration data were obtained by adding aliquots of 4 mM stock solutions of unlabeled peptides Q L R K G P P V P P P P K H **T** P S K E V K Q CLAP (334-355) or phospho-T348 CLAP (334-355), phosphorylated residue in bold in the sequence, to 100 µM ^{15}N-labeled BIN1-SH3 domain, using HSQC spectra to monitor changes in amide and tryptophan indole chemical shift values. K_d were calculated based on these data (see Supplementary Information for details).

Semi-automated high-content screening for modulators of BIN1-Tau interaction

A compound screen was setup by combining a commercial library of 1,120 compounds (10 µM; #2890; Tocris Biosciences, Bristol, UK), 6 Sanofi proprietary compounds (0.1, 1, and 10 µM; Sanofi; Chilly-Mazarin, France), Okadaic acid (1 µM; Merck Millipore) as a control compound, and DMSO (0.1%; VWR; Radnor, PA). Tocriscreen™ Mini is a library of well-characterized biologically active compounds that allows the screening of a wide-range of cellular processes, such as inflammation, apoptosis, cell differentiation, signal transduction, intracellular transport. 1000× stock compounds were transferred into intermediate 384-well plates using Echo 550 liquid Handler (Labcyte; San Jose, CA), and plates were sealed and kept at -20°C. Neurons cultured in 384-well plates were maintained for 21 days and transferred to HCS platform incubator (Liconic instruments; Mauren, Liechtenstein) on the day of screening. Compounds in intermediate plates were resuspended in 30 µl Neurobasal A, to reach 5× concentration, followed by a 2 min-long centrifugation at 100 ×*g*. 10 µl of resuspended compounds were then added into respective wells in PNC plates using Bravo automated liquid handling platform (Agilent; Santa Clara, California, USA), containing 40 µl of culture media, and plates were returned to the incubator. To achieve equal treatment duration for all plates, the compounds were resuspended and transferred with 10 min intervals between plates. Neurons were incubated with compounds for 2.5 h and fixed with 4% paraformaldehyde (EMS; Hatfield, PA) in PBS (Dutscher; Brumath, France) for 20 min at RT, permeabilized with 0.3% Triton-X (Sigma) in PBS for 10 min at RT, and blocked with 5% normal donkey serum (Jackson ImmunoResearch, Ely, UK) and 0.1% Triton-X in PBS for 1 h at RT. Alternatively, neurons in 384-well plates were blocked with 2.5% BSA (Sigma) and 0.1% Triton-X in PBS, up to 14 days at 4°C. Neurons were washed with PBS at RT between each step.

Proximity ligation assay (PLA)

All components of PLA (Duolink PLA probes and *in situ* detection reagents) apart from the primary and secondary antibodies were from Sigma. PLA was performed following manufacturer's instructions with minor modifications [3,48]. After protein blocking, neurons were incubated with the following primary antibodies overnight at 4°C: BIN1-99D (mouse monoclonal IgG, 1:200; Merck Millipore), Tau (rabbit polyclonal IgG, 1:500; Dako-Agilent), MAP2 (chicken polyclonal IgG, 1:500; Synaptic Systems; Göttingen, Germany), and GFAP (chicken polyclonal IgG, 1:300; Synaptic Systems). Samples were washed with a solution of 0.15 M NaCl (Merck Millipore), 0.01 M Tris (Sigma), 0.05% Tween-20 (Sigma), at pH 7.4 (Buffer A), incubated with PLA probes Mouse-minus and Rabbit-plus (secondary antibodies labeled with complementary DNA strands) in Duolink antibody diluent for 1 h at 37°C, and washed with Buffer A. This was followed by the enzymatic ligation of the two DNA strands, provided that they were in close proximity (< 30 nm) [48], for 30 min at 37°C and another wash with Buffer A. This was followed by the enzymatic rolling-circle amplification of DNA and hybridization of Cy3-labelled oligonucleotides (PLA orange) for 100 min at 37°C. Samples were then washed with a solution of 0.1 M NaCl and 0.2 M Tris, at pH 7.5 (Buffer B). After the PLA process, samples were incubated with the following secondary antibodies for 1 h at RT: AlexaFlour488 donkey-anti-chicken, AlexaFlour488 donkey-anti-mouse, AlexaFlour647 donkey-anti-rabbit, and DyLight405 donkey-anti-chicken (1:500 for coverslips and 1:1000 for 384-well plates; Jackson ImmunoResearch; West Grove, PA). Coverslips were washed with PBS and mounted in glycerol. 384-well plates were washed with PBS and sealed.

PLA in brain slices was performed with additional modifications [24]. Slices were first permeabilized with 0.3% Triton in PBS for 30 min and blocked with Duolink blocking solution for 2 h at 37°C. Slices were next treated with the IgG blocking reagent overnight at 4°C and with the protein concentrate, according to manufacturer's instructions (M.O.M. Basic Kit; Vector Laboratories, Burlingame, CA). Primary antibodies BIN1-99D (1:80), Tau (1:200), and α-tubulin (mouse monoclonal, 1:200; clone DM1A; Sigma) were diluted in the Duolink antibody diluent and incubated overnight at 4°C. Samples were washed with Buffer A, incubated with PLA probes Mouse-minus and Rabbit-plus in Duolink antibody diluent for 1 h at 37°C, and washed with Buffer A. This was followed by DNA ligation for 30 min at 37°C and another wash with Buffer A. This was followed by the enzymatic amplification and PLA hybridization for 2 h at 37°C. Samples were then washed with Buffer B and 1:5000 Hoechst (H3569, Thermo Scientific). After the PLA process, samples were incubated with the secondary antibodies AlexaFlour488 donkey-anti-mouse and AlexaFlour647 donkey-anti-rabbit (1:200) for 2 h at RT, followed by several washes with Buffer B. To reduce

autofluorescence, the brain slices were treated with 0.1% Sudan Black B (Sigma) in 70% ethanol for 15 min. Samples were then washed with Buffer B and mounted in 90% glycerol.

Image acquisition and analysis

Coverslips were imaged with LSM 710 confocal microscope (Zeiss, Oberkochen, Germany) using a 40× 1.6 NA objective. Images were acquired at zoom 2 in z-stacks of 0.3 µm interval. 10-13 images per condition were acquired for each of the three independent experiments. Images were deconvoluted using AutoQuantX3 Software (Bitplane, Zurich, Switzerland) and analysed with Imaris Software (Bitplane), using the "surfaces" tool for defining PLA spots, Tau network, and BIN1 puncta in three dimensions. Imaris results were analyzed using a custom MATLAB (MathWorks; Natick, MA) code that removes outliers based on ±3 median absolute deviations (MAD).

384-well plates were imaged using IN Cell Analyzer 6000 Cell Imaging System (GE Healthcare; Little Chalfont, UK) equipped with a Nikon 60× 0.95 NA objective and a CMOS camera. 16 images (2,048 × 2,048 pixels) per well were acquired in four channels (DAPI, dsRed, FITC, and Cy5) using appropriate filter sets and with following acquisition parameters: 2×2 binning; bias = 96.9; gain = 1.0 (Fig. S3). Images were analyzed with Columbus image data storage and analysis system (Perkin Elmer; Waltham, MA) with analysis scripts optimized *via* a custom MATLAB code (Fig. S3B). Optimal analysis scripts were determined separately for each plate.

Brain slices were imaged with Axio Scan Z1 (Zeiss) using a 40× 0.95 NA objective. Images were acquired in 12 z-stacks of 1 µm interval. Regions of interest were marked around the hippocampus during acquisition in each of the 3 independent experiments. PLA spots were analyzed with Imaris using the "surfaces" tool. Imaris results were analyzed using MATLAB after removing outliers based on ±3 MAD.

HCS script optimization and plate validation

Before image transfer, IN Cell image registration and transfer files were manually edited to import images only from control wells to Columbus, thereby generating the so-called control plates for script optimization and plate validation. Analysis scripts consisted of a series of Columbus commands that determine (i) total Tau staining area and (ii) total area of PLA spots within the Tau network, for each well (Fig. S3A). Four optimization parameters were defined: (i) Tau area threshold in terms of standard deviation (SD) of Tau intensity; (ii) sensitivity parameter for PLA spot detection; (iii) background correction parameter for PLA spot detection; and (iv) minimum PLA spot contrast. Analysis scripts were created by assigning distinct values to each optimization parameter. For example, assigning three

distinct values per parameter resulted in 3^4 = 81 combinations; hence the optimization was performed by running Columbus with 81 separate analysis scripts.

Measured values were corrected for spatial bias (horizontal) using the slope of the line that fits the column averages in the control plate based on the least-squares method. Three values typically used in HCS analysis [8] were evaluated: (i) strictly standardized mean difference (β factor, $\beta = (\mu_n - \mu_p) \quad \overline{\sigma_n^2 + \sigma_p^2}$); (ii) Z factor ($Z' = 1 - 3(\sigma_p + \sigma_n) \ |\mu_p - \mu_n|$); and (iii) signal-to-background ratio (S/B = $\mu_p \ \mu_n$), where μ and σ are mean and standard deviation, and *p* and *n* indicate positive and negative controls. Optimal analysis script was determined as the one with the highest β factor (β ≥ 2), provided that it produced S/B of at least 10. Additional rounds of parameter optimization were performed as deemed necessary.

Plate analysis and hits selection

Full plates were analyzed with optimal analysis scripts after correcting for local bias in terms of total Tau area, total MAP2 area, and total area of PLA spots within Tau area (Fig. S3C): First the local median of 5x5 wells surrounding the target well calculated and normalized with the plate median excluding edge wells, *i.e.*, *corrected value = raw value* / (*local median* / *plate median)*. For each plate, compounds affecting network quality, defined as being outside median ± 3 median absolute deviations (MAD) in terms of Tau area or Tau:MAP2 area ratio (edge wells were excluded from these calculations), were excluded (Fig. S4). For each well, corrected PLA:Tau area ratio was normalized by plate mean, excluding edge wells and wells with compounds affecting network quality. After all screenings were performed, mean and SEM of normalized, corrected PLA:Tau area ratio were calculated for each compound, for compounds that did not affect network quality in at least 2 screenings. Compounds potentially affecting BIN1-Tau interaction were determined as those belonging to the top or bottom 5% tiers.

Validation of selected compounds

Hit validation was performed in a two-step procedure: first, dose-response curves were generated for selected compounds to identify specific effects; second, the impact of selected compounds on BIN1 phosphorylation was assessed through immunoblotting. Since several of the selected compounds had multiple protein targets at 10 µM concentration used in our screen, dose-response experiments were designed to validate the specific effects of the compounds and/or to identify relevant target proteins. Dose-response experiments were performed for 72 selected compounds that induced similar effect on PLA density in all three screens using the same protocol as for the compound screen. Selected compounds were diluted four log scales to obtain a dose-response curve (10nM, 100nM, 1µM and 10µM) and

each compound and concentration was tested in three separate plates. Script optimization, plate validation, plate analysis, and well correction and exclusion processes were performed as described above. For each well, corrected PLA:Tau area ratios were normalized by the mean obtained from DMSO-treated wells of the same plate. The means of each compound at 10 µM were compared with the results from screening (conducted at 10 µM), and compounds that had similar effects in both sets of experiments were retained for further analysis. For each compound, dose-response curves were fit with 4-parameter or 3-parameter (where Hill slope is 1) nonlinear regression models, based on the extra sum-of-squares F test using GraphPad Prism 7 (La Jolla, CA). PNC on DIV21 were incubated with selected compounds at 10 µM for 2.5 h and BIN1 and Tau phosphorylation was assessed through immunoblotting.

Statistical analysis

Statistical analyses were performed in GraphPad Prism 7 or in Matlab. When variables were normally distributed, parametric analyses were applied: one- or two-way analysis of variance (ANOVA), followed by Bonferroni-corrected post hoc tests, Student's t-test, or one sample t-test. When variables were non-normally distributed, we conducted non-parametric analysis: Kruskal-Wallis ANOVA, followed by Dunn's test or Wilcoxon signed rank test with Tukey-Kramer correction.

Results

BIN1 overexpression modulates hTau phenotypes in short- and long-term memory

Although a genetic interaction between Bin1 and *MAPT* has been shown in *Drosophila* and the corresponding proteins have been described to physically interact [14,35], the impact of BIN1 expression levels on cognitive function has not yet been investigated in a mammalian tauopathy model. For this purpose, we crossed the hTau mouse, a tauopathy model that overexpresses human *MAPT* (but does not express endogenous murine *Mapt* [40]) with the Tg*BIN1* mouse that overexpresses human *BIN1* under the control of its own promoter and recapitulates the tissue-specific expression of different BIN1 isoforms (Fig. S5) [17]. Briefly, generation of mice were obtained on C57BL/6J genetic background by crossing *Mapt*$^{+/-}$;Tg*MAPT/0* [2] and *Mapt*$^{+/-}$;Tg*BIN1/0* [17] to obtain *Mapt*$^{+/-}$ as control littermates, *Mapt*$^{-/-}$;Tg*MAPT/0* (noted here hTau) as the tauopathy model [40], and, finally, *Mapt*$^{-/-}$;Tg*MAPT*/0;Tg*BIN1/0* as the double transgenic model (noted here hTau;Tg*BIN1*). Notably, in the Tg*BIN1* mouse, brain *Mapt* expression is similar to that observed in the WT mouse (Fig. S5). Expression of human *BIN1* is able to rescue the perinatal lethality of Bin1$^{-/-}$ mice [15], and Bin1$^{-/-}$;Tg*BIN1* mice had normal locomotor activity at 4 months in the open field paradigm (Fig. S5).

To assess if *BIN1* overexpression affected the short-term, non-spatial memory deficit in the hTau mice, a novel object recognition (NOR) task was performed longitudinally at 3, 6, 9, 12, and 15 months. *MAPT* overexpression induced short-term memory deficits in males and females from 9 months on, characterized by their inability to discriminate between familiar and novel objects (Fig. 1a). Strikingly, hTau;Tg*BIN1* mice displayed short-term memory deficits earlier than hTau mice, by 3 months, both in males and females. Notably, *Mapt* heterozygous deletion alone had no impact on this task and Tg*BIN1* males present NOR deficits only starting from 6 months [17]. There was no place or object preference, regardless of genotype or sex (Fig. S6). In conclusion, hTau phenotypes in the NOR task appeared at an earlier age upon *BIN1* overexpression.

In parallel with the NOR test, we assessed in this mouse cohort (non-naïve animals) the effect of *BIN1* and *MAPT* overexpression on long-term spatial memory using Morris water maze (MWM) tasks at the same relative ages. All groups were able to achieve the same performance in reducing the distance needed to reach the hidden platform (Fig. 1b-e and S7). The hTau mice displayed a deficit in recalling the platform location 24 h after the last training session by 12 months (Fig. 1b-e and S8). However, hTau;Tg*BIN1* males were able to perform this task at all ages tested up to 15 months, indicating that *BIN1* overexpression rescued the long-term and spatial memory of the hTau mice (Fig. 1b-e). The hTau;Tg*BIN1*

females displayed a delayed deficit at 15 months compared to the hTau mice (Fig. S8). Notably, 15-month-old Tg*BIN1* mice did not have a deficit in this task (Fig. S9). To validate that the memory deficit observed for hTau mice were not due to a visual or locomotor deficit, we measured the distance and time required by the 15 month old mice to reach the visible platform. No difference was noted in the swimming velocities of different genotypes (Fig. S10). Overall, *BIN1* overexpression modulates hTau phenotypes by exacerbating short-term memory deficits and preventing long-term memory deficits.

Human BIN1 expression prevents Tau intracellular inclusions and increases BIN1-Tau complexes in the hippocampus

The hTau mice have been described to develop detectable Tau aggregation and intracellular inclusions in the hippocampus and entorhinal cortex by 9 months [1,40]. We therefore tested the hypothesis that the mechanism underlying the rescue of the long-term and spatial memory deficits in hTau males through *BIN1* overexpression may be linked to an alteration of this aggregation. We sacrificed our cohort at 18 months and performed immunolabeling with antibodies specifically targeting Tau phosphorylation at both Ser202 and Thr205 (AT8 antibody) and at Thr231 (AT180 antibody) in the hippocampus (Fig. 2). As expected, no staining was evident in control mice. In hTau mice, Tau was mislocalized to the somatic compartment and formed prominent intracellular inclusions in the hippocampus (dentate gyrus, CA3, CA2, and CA1) (Fig. 2a). However, in hTau;Tg*BIN1* mice the number of cells with intracellular inclusions decreased by 5.9-fold or by 4.3-fold in the hippocampus when labeled with AT8 or AT180 antibodies, respectively (Fig. 2a-c). Since it is known that hyperphosphorylation of soluble Tau precedes Tau somatic inclusion [10], we determined if reduction of Tau inclusions upon BIN1 overexpression is due to an alteration of Tau phosphorylation pattern or of soluble Tau levels. However, no difference in soluble phosphorylated Tau protein was observed between hTau and hTau;Tg*BIN1* mice in the hippocampus (Fig. S11), indicating that BIN1 does not potentially regulate the level of soluble phosphorylated Tau protein or its phosphorylation pattern.

It has been previously described that BIN1 is able to physically interact with Tau [14,49]. We assessed if BIN1 overexpression altered the amount and/or localization of BIN1-Tau complexes. For this purpose we used proximity ligation assay (PLA) in brain slices from sacrificed animals (Fig. 2d) and quantified the PLA density as a read-out of the BIN1-Tau interaction. We observed a strong increase in the PLA signal for the hTau;Tg*BIN1* mice when compared to both hTau mice and controls (2.7-fold and 6.2-fold in spot density, respectively) (Fig. 2d-f). As a positive control, we also used PLA to assess the interaction between α-tubulin and Tau and detected an increase in this interaction in hTau and hTau;Tg*BIN1* mice relative to controls (Fig. S12). Taken together, these data indicate that

BIN1 overexpression increases the amount of BIN1-Tau complexes in the hippocampus and prevents Tau mislocalization and somatic inclusion, notably in the brain regions involved in long-term and spatial memory.

BIN1 expression in neurons modulates the BIN1-Tau interaction

Our data in transgenic mice support the idea that the BIN1-Tau interaction is relevant for the pathophysiological functions of Tau in AD and potentially in neurons. To gain further insight into the regulation of BIN1-Tau interaction, we monitored its dynamics during neuronal maturation in hippocampal primary neuronal cultures (PNC) at 7, 14, and 21 days *in vitro* (DIV), using western blots and PLA (Fig. 3). We first observed an increase in BIN1 and Tau amounts with time (Fig. 3a-b), whereas Tau phosphorylation was lower at certain epitopes, in particular, at Thr231 (Fig. 3c). Of note, this phosphorylation site has been described to inhibit the interaction between Tau's proline-rich domain (PRD) and BIN1's SH3 domains [49]. The relative density of BIN1-Tau PLA in the neuronal network was highly variable at DIV7 due to the low network density and it decreased with neuronal maturation from DIV14 to DIV21 (Fig. 3d-e). The BIN1-Tau PLA signal was highly correlated with the Tau signal irrespective of DIV (Fig. 3f), suggesting a uniform distribution of PLA signals in the network. We then assessed the impact of BIN1 expression on the PLA signal at DIV14, by downregulating BIN1 or overexpressing BIN1 neuronal isoform 1 (BIN1iso1) at DIV8 *via* transduction of lentiviruses expressing shRNA against BIN1 or the corresponding cDNA, respectively (Fig. 3g-i and S13). BIN1 downregulation led to a decrease in PLA signal; conversely, BIN1iso1 overexpression led to an increase in PLA signal (Fig. 3g and 3i). These data indicate that even if the BIN1-Tau interaction occurred at restricted loci in neurons (*e.g.*, at microtubule tips, as previously described [49]), the BIN1-Tau complex formation depends on the global amount of BIN1 in neurons, as observed in the transgenic mice. Together, our data support the notion that variation in BIN1 expression affects the dynamics of BIN1-Tau complexes and their subsequent physiological and/or pathophysiological functions.

Identification of signaling pathways modulating the BIN1-Tau interaction in neurons

In addition to the BIN1 expression level as a modulator of the BIN1-Tau interaction, we had previously shown that phosphorylation of the Tau PRD domain (mainly at T231) inhibits its interaction with the BIN1 SH3 domain [49]. This suggested that BIN1-Tau interaction dynamics likely depends on specific signaling pathways that regulate Tau phosphorylation. However, the cell signaling pathways susceptible to modulate the dynamic BIN1-Tau interaction remained unknown. To answer this question, we developed an agnostic strategy

and set-up a semi-automated high-content screening (HCS) approach, using PNC as cellular model and PLA volume as readout for BIN1-Tau interaction (Fig. 4a).

We tested a library of 1,126 compounds (at 10 µM) known to mainly target key elements of canonical pathways (see the Materials and Methods section for a full description of the HCS design). In brief, HCS was made in triplicate (one well per compound in each screen) using independent cultures. 79 compounds showed potential toxicity, as assessed by Tau and MAP2 network densities (Fig. 4b), and were excluded. We then applied several selection criteria to identify most promising compounds: (i) only compounds showing an effect in the same direction in all three independent screens were retained for further investigation; (ii) we selected the 10% of compounds showing the strongest variations (5% increasing PLA and 5% decreasing PLA). This led to 72 compounds for validation in dose-response experiments (Fig. 4c). Following this validation step, we were able to retain 12 compounds (marked red in Fig. 4d) that consistently exhibited the strongest variations in PLA signals. We grouped the targets of these compounds into 5 categories: (i) phosphorylation; (ii) nitric oxide synthase; (iii) Ca^{2+} homeostasis; (iv) membrane receptors; and (v) others (see Fig. S14 for the dose-response curves). As BIN1-Tau interaction has been shown to be modulated by phosphorylation [49], we decided to focus on two compounds whose targets are regulators of phosphorylation: (i) the Calcineurin (CaN) inhibitor Cyclosporin A (CsA), which, at 10 nM, increased PLA:Tau ratio by 42.6%; and (ii) the MEK inhibitor U0126, which, at 10 µM, decreased PLA:Tau ratio by 36.2% (Fig. 4e). In conclusion, our results show that CaN and MEK-dependent signaling pathways – among others – are able to modulate the complex dynamics of the BIN1-Tau interaction in neurons.

The conformational change in BIN1 neuronal isoform 1 upon phosphorylation modulates BIN1-Tau interaction

Of particular interest, CaN is a Ser/Thr phosphatase which has been described to dephosphorylate Amphiphysin 1 (AMPH1), the homolog of BIN1 [4]. We thus postulated that CaN may also target BIN1 and sought potential phosphorylation sites within BIN1 explaining the increase in the PLA signal observed after CaN inhibition. Interestingly, we had previously characterized a conformational change in BIN1iso1 between open and closed forms. This involves an intramolecular interaction between the SH3 and CLAP PRD of BIN1iso1, making the SH3 domain unavailable for intermolecular interactions for instance with Tau [35]. Since phosphorylations in the PRD have already been described to inhibit PRD/SH3 domains [49], we postulated that phosphorylation in the CLAP PRD domains of BIN1iso1 may favor BIN1's open form and increase the BIN1-Tau interaction and consequently the PLA signal. When the protein sequences of AMPH1 and BIN1 are compared, their CLAP PRD domains appear to be highly conserved (Fig. 5a). Considering that AMPH1 T310 (corresponding to BIN1

T348) has been described to be phosphorylated by Cdks [21], we hypothesized that T348 (in the vicinity of the PRD sequence interacting with the BIN1-SH3 domain [35]) may be controlling the open/closed conformation of BIN1iso1.

We first developed an antibody against BIN1 phosphorylated at T348 to determine if the BIN1 T348 phosphorylation occurred in neurons. Treating neuronal protein extracts with a protein phosphatase pool decreased BIN1 T348 phosphorylation (Fig. 5b). As control, Tau T231 phosphorylation was also decreased (Fig. S15a). Next, since T348 is within a consensus sequence recognized for phosphorylation by cyclin-dependent kinases (Cdks), we tested if Cdks were able to phosphorylate BIN1 T348. By using recombinant Cdk2 or Cdk5 and BIN1iso1, we showed that both kinases are able to directly phosphorylate T348 (Fig. 5c), as well as Tau T231 *in vitro* (Fig. S15b) confirming previous results [49]. We finally tested CsA and U0126 in PNC for their effect on BIN1 T348 and Tau phosphorylation. We observed that CsA – but not U0126 – was able to significantly increase BIN1 T348 phosphorylation in PNC (85±26% vs. 4±26%, respectively) suggesting that CaN is indeed able to dephosphorylate BIN1 at T348 (Fig. 5d-e). Remarkably, CaN inhibition did not impact Tau T231 phosphorylation, which we had previously described as a major modulator of the BIN1-Tau interaction [49,33], suggesting that the BIN1 T348 phosphorylation alone drives the impact of CsA on PLA. Conversely, U0126 likely modifies the BIN1-Tau interaction through Tau T231 phosphorylation, without any impact on BIN1 T348 (Fig. 5d-e). Notably, we had previously characterized T231 as one of the 15 Ser/Thr sites where Tau gets phosphorylated by ERK2, downstream of MEK [43].

To determine if phospho-T348 may control the dynamics of the open/closed conformation of BIN1iso1, we used nuclear magnetic resonance (NMR). We first tested whether this phosphorylation could impact the intramolecular interactions of BIN1 SH3 in the context of full BIN1iso1 protein. Signal from the BIN1-SH3 domain was observed in the spectra of Cdk2-phosphorylated recombinant BIN1iso1, whereas these same signals were barely detectable in the spectra of non-phosphorylated BIN1iso1 under identical acquisition and processing conditions (Fig. S2). Detection of these signals in the context of the large BIN1iso1 protein showed that the BIN1-SH3 domain kept some mobility and that the equilibrium was less in favor of the intramolecular interaction once the BIN1-CLAP domain was phosphorylated compared to the non-phosphorylated BIN1iso1 protein. However, since we detected multiple phosphorylation sites in the Cdk2-BIN1iso1 by NMR (Fig. S2), we generated a recombinant BIN1iso1 with T348E (BIN1-CLAP-T348E) to mimic the single phosphorylation event. Signals from the BIN1-SH3 domain were also detected in the spectra of the mutated BIN1iso1 T348E (Fig. S16), suggesting that phosphorylation at T348 is sufficient to shift to the BIN1iso1 open form (Fig. 5f). Finally, to further validate this

observation, ^{15}N-labeled BIN1 SH3 domain was titrated with CLAP (334-355) or phospho-CLAP (334-355) peptides and the titration was monitored using ^{1}H-^{15}N heteronuclear single quantum coherence (HSQC) spectroscopy of ^{15}N-BIN1 SH3, one spectrum being recorded at each titration point (Fig. S17). The K_d values, obtained by fitting the chemical shift values measured in the spectra series to the saturation equation, were 71±13 µM for CLAP (334-355) peptide and 736±70 µM for phospho-CLAP (334-355) peptide, showing a 10-fold increase in K_d due to a single phosphorylation event in the peptide (Fig. 5g). Cumulatively, these results indicate that phosphorylation of T348 in the BIN1 CLAP domain is able to shift the dynamic equilibrium of the BIN1iso1 conformation towards the open form, thereby increasing the availability of the BIN1 SH3 domain for other interactions.

We next assessed whether the open/closed dynamics may impact the formation of the BIN1-Tau complex by controlling the availability of the BIN1iso1 SH3 domain in neurons and thus its ability to interact with Tau. For this purpose, we transduced at DIV8 hippocampal PNC with lentiviruses overexpressing wild-type BIN1iso1 and its mutated form, BIN1iso1-T348E, which, as previously demonstrated, leads to a systematically open form of BIN1iso1. We observed a 2.1-fold increase in PLA volume in PNC transduced with BIN1iso1-T348E when compared to BIN1iso1 (after normalization with respective BIN1 immunofluorescence) (Fig. 5h-i). This observation is in accordance with the increased availability of the BIN1iso1-T348E SH3 domain for Tau.

Finally, we quantified the amount of total and phospho-BIN1 (T348) neuronal isoforms in protein extracts from 14 brain samples with increasing neurofibrillary pathology (Braak stages 0 to 6). The relative amounts of total and phosphorylated BIN1 exhibited a trend to decrease with increasing Braak stage (Fig. 6a-c). Surprisingly, the phospho-Bin1:BIN1 ratio exhibited a trend to increase with increasing Braak stage (Fig. 6d). Among the 14 individuals, 4 were controls and 12 were diagnosed with AD. After stratification based on the AD status, we observed a statistically non-significant decrease in total BIN1 in AD cases compared to controls ($p = 0.05$), but not in phospho-BIN1 ($p = 0.71$) (Fig. 6d-e). Interestingly, phospho-BIN1:BIN1 ratio was significantly increased in the brains of AD cases ($p = 0.02$) (Fig. 6g). Altogether, these data indicate that, in pathological conditions, the global level of the neuronal isoform of BIN1 is decreased, but a higher fraction of this BIN1 population is phosphorylated.

Discussion

There is no longer any doubt that BIN1 is a major genetic risk factor for AD [32]. However, as for other GWAS-defined genes, it is often difficult to determine the implication of such genes in pathophysiological processes (or even in physiological ones in organs of interest). In this study, we aimed to determine if the BIN1-Tau interaction is involved in the neuropathological process of a mouse tauopathy model and to decipher the cellular processes and signaling pathways potentially regulating it.

To determine if BIN1 could interfere with Tau pathology *in vivo*, we first developed a mammalian tauopathy model overexpressing BIN1 isoforms including neuron-specific forms in the brain. We observed that *BIN1* overexpression in the hTau mice expedited the appearance of short-term memory deficits from 9 to 3 months, but prevented spatial and long-term memory deficits up to 15 months, the highest age tested. Remarkably, the rescue of spatial and long-term memory by *BIN1* overexpression was associated with a strong increase in the BIN1-Tau interaction in the neuronal network and a strong decrease in phosphorylated Tau inclusions within the neuronal somata in the hippocampus. Next, we analyzed the BIN1-Tau interaction in the physiological context. BIN1 expression level appeared to be a strong modulator of the BIN1-Tau interaction in PNC. To identify signaling pathways modulating the BIN1-Tau interaction in neurons, we developed an agnostic HCS approach and determined a number of potential targets; one of best hits being an inhibitor of CaN, a Ser/Thr phosphatase. This observation led us to identify BIN1 phosphorylation at T348 as both a CaN target and a major regulator of the BIN1-Tau interaction. We determined that BIN1 phosphorylation at T348 increased the availability of the BIN1-SH3 domain to interact with Tau and consequently led to an increase in this interaction in neurons. Finally, we determined that neuronal BIN1 isoforms (mainly isoform 1) decreased in the brains of postmortem AD patients compared to control cases, whereas – surprisingly – phospho-BIN1(T348):BIN1 ratio increased, suggesting that this site may also be involved in the AD process. Overall, we hypothesize that increased BIN1 expression and its phosphorylation on T348 protects hTau mice against spatial and long-term memory deficits (Fig. 7).

Altogether, our data support that a complex and dynamic regulation of the BIN1-Tau interaction is involved in the development of the AD pathophysiological process. However, the protective or deleterious effect of this interaction may vary depending on cognitive functions. Indeed, *BIN1* overexpression modulates *MAPT* phenotypes by exacerbating short-term memory deficits and by preventing long-term memory deficits. Both of these processes require the hippocampus, but the cortical regions involved are different, *i.e.*, lateral entorhinal cortex and medial entorhinal cortex, respectively [9,51]. The equilibrium between Tau and

BIN1 levels may be slightly different in these cortical brain regions and in temporality, potentially explaining the opposite effects observed. In addition, signaling pathways controlling the phosphorylation of BIN1 and Tau, and subsequently the BIN1-Tau interaction may also differ temporally and regionally. However, since we developed a cohort study, it was not possible to evaluate such temporal and regional variations at each time of behavioral tests. It is nevertheless worth noting that the rescue of spatial and long-term memory by BIN1 overexpression was associated with a strong decrease in phosphorylated Tau inclusions within the neuronal somata and a strong increase in the BIN1-Tau interaction in the hippocampus. Remarkably, in hTau mice, the BIN1-Tau interaction was lower than in both control and htau;Tg*BIN1* mice. These observations thus suggest that the BIN1-Tau interaction may be protective by blocking the relocalization and accumulation of phosphorylated Tau in the neuronal somata, a major hallmark of AD.

The hypothesis that a dynamic regulation of the BIN1-Tau interaction is involved in AD process also implies that a high level of BIN1 expression would be protective. However, we previously found that total BIN1 mRNA is over-represented in the brains of AD cases compared to controls [13], but did not evaluate at that time the isoform-dependency of the BIN1 expression. Subsequent publications reporting protein levels showed that unlike the overexpression of ubiquitous isoforms, the neuronal isoforms were specifically underexpressed in the AD brains [23,26]. We validated this observation in brain samples and showed that this decrease was dependent on the Braak stage (Fig 6). Since the neuronal isoforms are the main isoforms that are overexpressed in the brain of our transgenic mice model (Fig. S5), these data corroborate the idea that specific overexpression of the neuronal BIN1 isoforms may be protective. We may thus postulate that the overexpression of neuronal BIN1 isoforms in the Tg*BIN1* mouse reverses a neuropathological process that occurs in AD brains. This protective effect could be explained by the BIN1-Tau interaction in neurons. However, we cannot exclude other potential mechanisms. Indeed, we observed that at 18 months *MAPT* over-expression is associated with myelin abnormalities, and a significant rescue of this phenotype was observed in hTau;Tg*BIN1* mice (Fig. S18). Of note, the over-expression of BIN1 alone did not induce any myelin abnormalities (Fig. S19; also see supplementary results). Thus, the memory impairments observed in the behavioral analyses of the hTau mice may also be associated with myelin disorganization in the fornix, and be rescued upon BIN1 overexpression. Interesting, BIN1 has been described to be strongly expressed in oligodendrocytes [18] and Tau has been also previously linked with potential myelin dysfunction in tauopathies [20].

Identifying the signaling mechanisms controlling the BIN1-Tau interaction is of high interest to understand the pathophysiological processes in AD. These pathways could be either

protective or deleterious, by favoring or abrogating the BIN1-Tau interaction, respectively. In this report we characterized a key regulatory element, which is the phosphorylation of BIN1 at T348. Remarkably, we determined that the phospho-BIN1(T348):BIN1 ratio increased with increasing Braak stage in the brains of AD cases. These findings suggest that a higher fraction of brain BIN1 isoforms is phosphorylated at T348 in AD brains, where the global level of neuronal BIN1 isoforms is decreased. This may imply that the relative increase in BIN1 T348 phosphorylation occurs to compensate in part the decrease in the neuronal BIN1 isoforms in order to maintain the BIN1-Tau interaction. Altogether, these observations suggest that BIN1 T348 phosphorylation is involved in the development of AD.

Our data thus indicate that the BIN1-Tau interaction is complex and dynamic, potentially controlled by numerous actors modifying the level of phosphorylation of both BIN1 and Tau, including Cdks and CaN. Indeed, we had previously shown that the phosphorylation of Tau at T231 was a major regulator of the BIN1-Tau interaction, but in the opposite direction, *i.e.*, leading to a decrease in this interaction. Importantly, the increase in Tau phosphorylation at T231 is considered as an early marker of the development of AD [10]. This dual BIN1/Tau regulation is illustrated in our HCS screening, which revealed that inhibiting CaN favors the BIN1-Tau interaction by increasing BIN T348 phosphorylation, whereas inhibiting MEK hinders it by increasing Tau T231 phosphorylation. Cdks – particularly Cdk5 – highlight this complexity, since these kinases are able to phosphorylate both BIN1 T348 and Tau T231, but with opposite effects on the abilities of Tau and BIN1 to interact with each other: increased Cdk5 activity would increase BIN1's affinity for Tau through phosphorylation of BIN1 at T348, and, conversely, would decrease Tau's affinity for BIN1 through phosphorylating Tau at T231 (Fig. 7). This complex interplay between actors modulating BIN1 and Tau phosphorylation may be a limitation for developing drugs to favor or prevent the BIN1-Tau interaction. A better understanding of the mechanisms involved will thus be needed to identify potential cell signaling pathways and drug targets that would uncouple the BIN1-Tau phosphorylation crosstalk. In this context, CaN-dependent pathways may be of therapeutic interest, since we observed that only BIN1 T348 is modulated by CaN, but not Tau T231.

In conclusion, we reveal the impact of overexpression of BIN1, a major genetic risk factor of AD, in a tauopathy model. Our data also reinforce the hypothesis that a potential protective impact of this overexpression on the AD process may be linked to the direct interaction of BIN1 and Tau, and depends strongly on the phosphorylation statuses of both proteins.

Acknowledgements

We thank the imaging and animal platforms of the IGBMC and ICS for help, and Nadia Messaddeq, Coralie Spiegelhalter, and Alexia Menuet for technical assistance. We thank the BiCeL platform of the Institut Pasteur de Lille for technical support, and Meryem Tardivel and Antonino Bongiovanni for technical assistance. We thank Hamida Merzougui for technical assistance in recombinant protein preparation. We thank Fanny Eysert and Florie Demiautte for technical assistance in PNC. We thank Maxime Verschoore for technical assistance in PLA. We thank the Equipex ImagInEx HCS platform and Alexandre Vandeputte and Gaspard Deloison for technical assistance. We thank Nora L. Salaberry for technical assistance in preparing the summary cartoon. This study was funded by INSERM, CNRS, University of Strasbourg, ANR-10-LABX-0030-INR, a French state fund managed by the ANR under the framework program Investissements d'Avenir (10-IDEX-0002), TGE RMN THC (FR-3050, France), FRABio (University of Lille, CNRS, FR 3688), ANR-BIN-ALZ-15-CE16-0002, PHENOMIN (ANR-10-INBS-07 694), France Alzheimer, the Alzheimer's Association (BFG-14-318355), the EU Joint Programme – Neurodegenerative Diseases Research (JPND; 3DMiniBrain), Fondation Vaincre Alzheimer (2017 pilot grant), Institut Pasteur de Lille, and Nord-Pas-de-Calais Regional Council. This work was also funded by the Lille Métropole Communauté Urbaine, the French government's LABEX DISTALZ program (development of innovative strategies for a transdisciplinary approach to Alzheimer's disease) The NMR facilities were funded by the Nord Regional Council, CNRS, Institute Pasteur de Lille, European Community (FEDER), French Research Ministry and the University of Lille. This work was also funded by the Academy of Finland (307866), Sigrid Jusélius Foundation, and the Strategic Neuroscience Funding of the University of Eastern Finland. M.S. was a fellow of France Alzheimer and received a fellowship from the Fond Paul Mandel de l'Université de Strasbourg. T.M. was supported by a CIFRE fellowship (ANRT/Sanofi), by a Sanofi grant for laboratory supplies, and by the LABEX DISTALZ program.

Author contributions

I.L., D.K., Y.H., J.L., and J.-C.L. designed and/or supervised research. M.S. and D.M. performed the genotyping and first cohort selection and/or the behavioral experiments in animal model. M.S. performed Tau inclusion labeling and quantifications on mouse brains. S.D. performed PLA and quantification in mouse brains. T.M., S.D., N.M., J.C., A.F., and A.-C.V. performed the *in vitro* experiments. T.M., A.H., F.L., B.D., L.P., D.K., and J.-C.L. performed and/or analyzed the HCS experiments. P.M., M.M., and M.H. performed Western blots and/or analyzed the human sample cohort. A.L., I.M., F.-X.C., and I.L. performed

and/or analyzed the NMR experiments. M.S., T.M., P.A., L.P., I.L., D.K., Y.H., J.L., and J.-C.L. wrote and/or revised the paper.

Conflict of interest

L.P. is a full-time employee of Sanofi S.A. and T.M. was an employee of Sanofi S.A (2015–2017 period).

References

1. Andorfer C, Acker CM, Kress Y, Hof PR, Duff K, Davies P (2005) Cell-cycle reentry and cell death in transgenic mice expressing nonmutant human tau isoforms. J Neurosci 25:5446-5454. doi:10.1523/jneurosci.4637-04.2005
2. Andorfer C, Kress Y, Espinoza M, de Silva R, Tucker KL, Barde YA et al. (2003) Hyperphosphorylation and aggregation of tau in mice expressing normal human tau isoforms. J Neurochem 86:582-590
3. Bagchi S, Fredriksson R, Wallen-Mackenzie A (2015) In situ proximity ligation assay (PLA). Methods Mol Biol 1318:149-159. doi:10.1007/978-1-4939-2742-5_15
4. Bauerfeind R, Takei K, De Camilli P (1997) Amphiphysin I is associated with coated endocytic intermediates and undergoes stimulation-dependent dephosphorylation in nerve terminals. J Biol Chem 272:30984-30992
5. Beaudoin GM, 3rd, Lee SH, Singh D, Yuan Y, Ng YG, Reichardt LF et al. (2012) Culturing pyramidal neurons from the early postnatal mouse hippocampus and cortex. Nat Protoc 7:1741-1754. doi:10.1038/nprot.2012.099
6. Beecham GW, Hamilton K, Naj AC, Martin ER, Huentelman M, Myers AJ et al. (2014) Genome-wide association meta-analysis of neuropathologic features of Alzheimer's disease and related dementias. PLoS Genet 10:e1004606. doi:10.1371/journal.pgen.1004606
7. Braak H, Alafuzoff I, Arzberger T, Kretzschmar H, Del Tredici K (2006) Staging of Alzheimer disease-associated neurofibrillary pathology using paraffin sections and immunocytochemistry. Acta Neuropathol 112:389-404. doi:10.1007/s00401-006-0127-z
8. Bray MA, Carpenter A, Imaging Platform BIoMIT, Harvard (2004) Advanced assay development guidelines for image-based high content screening and analysis. In: Sittampalam GS, Coussens NP, Brimacombe K et al. (eds) Assay Guidance Manual. Eli Lilly & Company and the National Center for Advancing Translational Sciences, Bethesda (MD),
9. Broadbent NJ, Squire LR, Clark RE (2004) Spatial memory, recognition memory, and the hippocampus. Proc Natl Acad Sci U S A 101:14515-14520. doi:10.1073/pnas.0406344101
10. Buee L, Bussiere T, Buee-Scherrer V, Delacourte A, Hof PR (2000) Tau protein isoforms, phosphorylation and role in neurodegenerative disorders. Brain Res Brain Res Rev 33:95-130
11. Butler MH, David C, Ochoa GC, Freyberg Z, Daniell L, Grabs D et al. (1997) Amphiphysin II (SH3P9; BIN1), a member of the amphiphysin/Rvs family, is concentrated in the cortical cytomatrix of axon initial segments and nodes of ranvier in brain and around T tubules in skeletal muscle. J Cell Biol 137:1355-1367
12. Calafate S, Flavin W, Verstreken P, Moechars D (2016) Loss of Bin1 promotes the propagation of Tau pathology. Cell Rep 17:931-940. doi:10.1016/j.celrep.2016.09.063
13. Chapuis J, Flaig A, Grenier-Boley B, Eysert F, Pottiez V, Deloison G et al. (2017) Genome-wide, high-content siRNA screening identifies the Alzheimer's genetic risk factor FERMT2 as a major modulator of APP metabolism. Acta Neuropathol 133:955-966. doi:10.1007/s00401-016-1652-z
14. Chapuis J, Hansmannel F, Gistelinck M, Mounier A, Van Cauwenberghe C, Kolen KV et al. (2013) Increased expression of BIN1 mediates Alzheimer genetic risk by modulating tau pathology. Mol Psychiatry 18:1225-1234. doi:10.1038/mp.2013.1
15. Cowling BS, Prokic I, Tasfaout H, Rabai A, Humbert F, Rinaldi B et al. (2017) Amphiphysin (BIN1) negatively regulates dynamin 2 for normal muscle maturation. J Clin Invest 127:4477-4487. doi:10.1172/jci90542
16. Cruchaga C, Kauwe JS, Harari O, Jin SC, Cai Y, Karch CM et al. (2013) GWAS of cerebrospinal fluid tau levels identifies risk variants for Alzheimer's disease. Neuron 78:256-268. doi:10.1016/j.neuron.2013.02.026

17. Daudin R, Marechal D, Wang Q, Abe Y, Bourg N, Sartori M et al. (2018) BIN1 genetic risk factor for Alzheimer is sufficient to induce early structural tract alterations in entorhinal cortex-dentate gyrus pathway and related hippocampal multi-scale impairments. bioRxiv. doi:10.1101/437228
18. De Rossi P, Buggia-Prevot V, Clayton BL, Vasquez JB, van Sanford C, Andrew RJ et al. (2016) Predominant expression of Alzheimer's disease-associated BIN1 in mature oligodendrocytes and localization to white matter tracts. Mol Neurodegener 11:59. doi:10.1186/s13024-016-0124-1
19. Dourlen P, Fernandez-Gomez FJ, Dupont C, Grenier-Boley B, Bellenguez C, Obriot H et al. (2017) Functional screening of Alzheimer risk loci identifies PTK2B as an in vivo modulator and early marker of Tau pathology. Mol Psychiatry 22:874-883. doi:10.1038/mp.2016.59
20. Ferrer I (2018) Oligodendrogliopathy in neurodegenerative diseases with abnormal protein aggregates: The forgotten partner. Prog Neurobiol 169:24-54. doi:10.1016/j.pneurobio.2018.07.004
21. Floyd SR, Porro EB, Slepnev VI, Ochoa GC, Tsai LH, De Camilli P (2001) Amphiphysin 1 binds the cyclin-dependent kinase (cdk) 5 regulatory subunit p35 and is phosphorylated by cdk5 and cdc2. J Biol Chem 276:8104-8110. doi:10.1074/jbc.M008932200
22. Gatz M, Reynolds CA, Fratiglioni L, Johansson B, Mortimer JA, Berg S et al. (2006) Role of genes and environments for explaining Alzheimer disease. Arch Gen Psychiatry 63:168-174. doi:10.1001/archpsyc.63.2.168
23. Glennon EB, Whitehouse IJ, Miners JS, Kehoe PG, Love S, Kellett KA et al. (2013) BIN1 is decreased in sporadic but not familial Alzheimer's disease or in aging. PLoS One 8:e78806. doi:10.1371/journal.pone.0078806
24. Gomes I, Sierra S, Devi LA (2016) Detection of receptor heteromerization using in situ proximity lgation assay. Curr Protoc Pharmacol 75:2.16.11-12.16.31. doi:10.1002/cpph.15
25. Hardy J, Selkoe DJ (2002) The amyloid hypothesis of Alzheimer's disease: progress and problems on the road to therapeutics. Science 297:353-356. doi:10.1126/science.1072994
26. Holler CJ, Davis PR, Beckett TL, Platt TL, Webb RL, Head E et al. (2014) Bridging integrator 1 (BIN1) protein expression increases in the Alzheimer's disease brain and correlates with neurofibrillary tangle pathology. J Alzheimers Dis 42:1221-1227. doi:10.3233/jad-132450
27. Hollingworth P, Harold D, Sims R, Gerrish A, Lambert JC, Carrasquillo MM et al. (2011) Common variants at ABCA7, MS4A6A/MS4A4E, EPHA1, CD33 and CD2AP are associated with Alzheimer's disease. Nat Genet 43:429-435. doi:10.1038/ng.803
28. Huber CM, Yee C, May T, Dhanala A, Mitchell CS (2018) Cognitive decline in preclinical Alzheimer's disease: amyloid-beta versus tauopathy. J Alzheimers Dis 61:265-281. doi:10.3233/jad-170490
29. Kaech S, Banker G (2006) Culturing hippocampal neurons. Nat Protoc 1:2406-2415. doi:10.1038/nprot.2006.356
30. Lambert JC, Amouyel P (2010) Deciphering genetic susceptibility to frontotemporal lobar dementia. Nat Genet 42:189-190. doi:10.1038/ng0310-189
31. Lambert JC, Heath S, Even G, Campion D, Sleegers K, Hiltunen M et al. (2009) Genome-wide association study identifies variants at CLU and CR1 associated with Alzheimer's disease. Nat Genet 41:1094-1099. doi:10.1038/ng.439
32. Lambert JC, Ibrahim-Verbaas CA, Harold D, Naj AC, Sims R, Bellenguez C et al. (2013) Meta-analysis of 74,046 individuals identifies 11 new susceptibility loci for Alzheimer's disease. Nat Genet 45:1452-1458. doi:10.1038/ng.2802
33. Lasorsa A, Malki I, Cantrelle FX, Merzougui H, Boll E, Lambert JC et al. (2018) Structural basis of Tau interaction with BIN1 and regulation by Tau phosphorylation. Front Mol Neurosci 11:421. doi:10.3389/fnmol.2018.00421

34. Long K, Mohan C, Anderl J, Huryn-Selvar K, Liu H, Su K et al. (2015) Analysis of autophagosome formation using lentiviral biosensors for live fluorescent cellular imaging. Methods Mol Biol 1219:157-169. doi:10.1007/978-1-4939-1661-0_12
35. Malki I, Cantrelle FX, Sottejeau Y, Lippens G, Lambert JC, Landrieu I (2017) Regulation of the interaction between the neuronal BIN1 isoform 1 and Tau proteins - role of the SH3 domain. Febs j 284:3218-3229. doi:10.1111/febs.14185
36. McKenzie AT, Moyon S, Wang M, Katsyv I, Song WM, Zhou X et al. (2017) Multiscale network modeling of oligodendrocytes reveals molecular components of myelin dysregulation in Alzheimer's disease. Mol Neurodegener 12:82. doi:10.1186/s13024-017-0219-3
37. Miyagawa T, Ebinuma I, Morohashi Y, Hori Y, Young Chang M, Hattori H et al. (2016) BIN1 regulates BACE1 intracellular trafficking and amyloid-beta production. Hum Mol Genet 25:2948-2958. doi:10.1093/hmg/ddw146
38. Natunen T, Parrado AR, Helisalmi S, Pursiheimo JP, Sarajarvi T, Makinen P et al. (2013) Elucidation of the BACE1 regulating factor GGA3 in Alzheimer's disease. J Alzheimers Dis 37:217-232. doi:10.3233/jad-130104
39. Nelson PT, Alafuzoff I, Bigio EH, Bouras C, Braak H, Cairns NJ et al. (2012) Correlation of Alzheimer disease neuropathologic changes with cognitive status: a review of the literature. J Neuropathol Exp Neurol 71:362-381. doi:10.1097/NEN.0b013e31825018f7
40. Polydoro M, Acker CM, Duff K, Castillo PE, Davies P (2009) Age-dependent impairment of cognitive and synaptic function in the htau mouse model of tau pathology. J Neurosci 29:10741-10749. doi:10.1523/jneurosci.1065-09.2009
41. Prince M, Bryce R, Albanese E, Wimo A, Ribeiro W, Ferri CP (2013) The global prevalence of dementia: a systematic review and metaanalysis. Alzheimers Dement 9:63-75.e62. doi:10.1016/j.jalz.2012.11.007
42. Prokic I, Cowling BS, Laporte J (2014) Amphiphysin 2 (BIN1) in physiology and diseases. J Mol Med (Berl) 92:453-463. doi:10.1007/s00109-014-1138-1
43. Qi H, Prabakaran S, Cantrelle FX, Chambraud B, Gunawardena J, Lippens G et al. (2016) Characterization of neuronal Tau protein as a target of extracellular signal-regulated kinase. J Biol Chem 291:7742-7753. doi:10.1074/jbc.M115.700914
44. Ramjaun AR, Micheva KD, Bouchelet I, McPherson PS (1997) Identification and characterization of a nerve terminal-enriched amphiphysin isoform. J Biol Chem 272:16700-16706
45. Shulman JM, Chipendo P, Chibnik LB, Aubin C, Tran D, Keenan BT et al. (2011) Functional screening of Alzheimer pathology genome-wide association signals in Drosophila. Am J Hum Genet 88:232-238. doi:10.1016/j.ajhg.2011.01.006
46. Shulman JM, Imboywa S, Giagtzoglou N, Powers MP, Hu Y, Devenport D et al. (2014) Functional screening in Drosophila identifies Alzheimer's disease susceptibility genes and implicates Tau-mediated mechanisms. Hum Mol Genet 23:870-877. doi:10.1093/hmg/ddt478
47. Sims R, van der Lee SJ, Naj AC, Bellenguez C, Badarinarayan N, Jakobsdottir J et al. (2017) Rare coding variants in PLCG2, ABI3, and TREM2 implicate microglial-mediated innate immunity in Alzheimer's disease. Nat Genet 49:1373-1384. doi:10.1038/ng.3916
48. Soderberg O, Leuchowius KJ, Gullberg M, Jarvius M, Weibrecht I, Larsson LG et al. (2008) Characterizing proteins and their interactions in cells and tissues using the in situ proximity ligation assay. Methods 45:227-232. doi:10.1016/j.ymeth.2008.06.014
49. Sottejeau Y, Bretteville A, Cantrelle FX, Malmanche N, Demiaute F, Mendes T et al. (2015) Tau phosphorylation regulates the interaction between BIN1's SH3 domain and Tau's proline-rich domain. Acta Neuropathol Commun 3:58. doi:10.1186/s40478-015-0237-8
50. Tucker KL, Meyer M, Barde YA (2001) Neurotrophins are required for nerve growth during development. Nat Neurosci 4:29-37. doi:10.1038/82868

51. Van Cauter T, Camon J, Alvernhe A, Elduayen C, Sargolini F, Save E (2013) Distinct roles of medial and lateral entorhinal cortex in spatial cognition. Cereb Cortex 23:451-459. doi:10.1093/cercor/bhs033
52. Welburn J, Endicott J (2005) Methods for preparation of proteins and protein complexes that regulate the eukaryotic cell cycle for structural studies. Methods Mol Biol 296:219-235
53. Zempel H, Mandelkow E (2014) Lost after translation: missorting of Tau protein and consequences for Alzheimer disease. Trends Neurosci 37:721-732. doi:10.1016/j.tins.2014.08.004

Figure Captions

Fig. 1 *BIN1* overexpression worsens hTau phenotypes in short-term memory and rescues long-term memory deficit due to MAPT overexpression in hTau males. **a.** Discrimination indices for novel object recognition with one hour of retention at 3, 6, 9, 12, and 15 months are shown for control, hTau, and hTau;Tg*BIN1* mice. Dashed lines represent object preference by chance. Blue dots, males; pink dots, females. One-sample *t*-test compared to chance at 50%; *p<0.05, **p<0.01. **b.** Distance traveled to reach the platform of the Morris water maze for 12-month-old hTau and hTau;Tg*BIN1* males. Data represent mean ± SEM for consecutive days of acquisition (control, n=11; hTau, n=11; hTau;Tg*BIN1*, n=13). **c.** Probe test without platform at 12 months, performed 24 h after the last training session. Dashed line represents chance. Data represent mean ± SEM for each quadrant (control, n=11; hTau, n=11; hTau,Tg*BIN1*, n=13). Underlined quadrant marks original platform location. **d.** Distance traveled to reach the platform for 15-month-old hTau and hTau;Tg*BIN1* males. Data represent mean ± SEM for consecutive days of acquisition (control, n=11; hTau, n=10; hTau;Tg*BIN1*, n=13). **e.** Probe test without platform at 15 months, performed 24 h after the last training session. Dashed line represents chance. Data represent mean ± SEM for each quadrant (control, n=11; hTau, n=10; hTau,Tg*BIN1*, n=13). Underlined quadrant marks original platform location. One-sample *t*-test compared to chance at 25%; *p<0.05, **p<0.01.

Fig. 2 BIN1 overexpression prevents Tau inclusions and increases BIN1-Tau interaction in hTau hippocampi. **a.** Immunohistofluorescence of different phospho-Tau proteins in hippocampi of control, hTau and hTau;Tg*BIN1* males at 18 months. Antibodies used were detecting p-Ser202/p-Thr205 Tau (AT8) or p-Thr231 Tau (AT180). Insets show zooms of the hilus areas encompassing the neuronal cell bodies; intracellular inclusions are visible for hTau, but barely for hTau;Tg*BIN1*. Scale bars = 500 µm; insets, 50 µm. **b-c.** Quantification of the number of cells with intracellular Tau inclusions per mm^2 in control, hTau and hTau;Tg*BIN1* mice labeled with the two phospho-Tau antibodies (control, n=4; hTau, n=4; hTau;Tg*BIN1*, n=5). **d.** BIN1-Tau PLA (cyan), and BIN1 (yellow), Tau (magenta), and Hoechst (white) stainings in the hippocampi of the same mice. Zoomed areas show PLA and Tau channels only. See Fig. S12 for Tubulin-Tau PLA, conducted as technical control. **e-f.** Quantification of BIN1-Tau PLA density. Data expressed as PLA spot number per tissue area (E) or total PLA spot volume per tissue area (F), normalized with control mean (control, n=9; hTau, n=11; hTau;Tg*BIN1*, n=12 hemispheres for spot number; control, n=10; hTau, n=12; hTau;Tg*BIN1*, n=12 hemispheres for volume). Red bars and black squares indicate sample median and mean, respectively. Kruskal-Wallis ANOVA, followed by multiple

comparisons test with Tukey-Kramer correction; *** p < 0.0001; * p < 0.05. N/S, not significant. Scale bars = 500 µm; zooms, 50 µm.

Fig. 3 Characterization of BIN1-Tau interaction in primary neuron cultures (PNC). **a.** Representative immunoblots from neuronal extracts obtained at DIV7, DIV14, and DIV21 (in duplicate) showing BIN1 and total and phosphorylated forms of Tau (Tau1 for non-phospho Ser195/Ser198/Ser199/Ser202; PHF1 for p-Ser396/Ser404; RZ3 and AT180 for p-Thr231). **b-c.** Relative changes in BIN1 and Tau protein levels and in Tau phosphorylation during neuronal maturation. **d.** Representative images of PNC showing PLA spots and Tau immunolabeling during neuronal maturation. **e.** Change in PLA density during neuronal maturation. N = 3 independent experiments. **f.** Correlation between total PLA volume and total Tau volume in a representative experiment. Each dot represents a confocal image. **g.** Representative images of PNC under- and overexpressing BIN1, showing PLA and Tau and BIN1 immunolabeling. shNT: non-targeting shRNA. **h-i.** Total BIN1 volume and PLA density in PNC under- and overexpressing BIN1, normalized with respective controls (shBIN1 with shNT and BIN1iso1 with Mock). N = 3 independent experiments. In box plots, red bars and black squares indicate sample median and mean, respectively. Wilcoxon rank-sum test; * p < 0.05; ** p < 0.01; *** p < 0.001; N/S: not significant.

Fig. 4 High-content screening (HCS) with PLA:Tau volume ratio in the Tau network as readout identifies the regulators of the BIN1-Tau interaction. **a.** The HCS workflow consists of compound screen (DIV21; 10 µM; 2.5 h) in PNC cultured in 384-well plates, plate-by-plate image segmentation and analysis, hit selection, and hit validation *via* dose-response experiments. **b.** Exemplary images from the HCS showing U0126 and Cyclosporin A (CsA) that decreased and increased PLA density, respectively. Scale bars = 50 µm. **c.** PLA:Tau area ratio for 1,047 compounds that did not induce damage in the neuronal network. Mean ± SD from 3 independent screens. **d.** Top and bottom 5% modulators (72 compounds) were retained for dose-response experiments. 12 compounds were validated in dose-response experiments are shown in red. **e.** Dose-response curves of U0126 and CsA (see Fig. S14 for all validated compounds). Mean ± SD from 3 independent experiments.

Fig. 5 BIN1 phosphorylation at T348 regulates BIN1-Tau interaction by modulating open/closed conformation of BIN1. **a.** Alignment of Amphiphysin 1 and BIN1iso1; domains not to scale. The underlined sequence indicates the BIN1 PRD sequence interacting with the BIN1 SH3 domain. **b.** Lambda protein phosphatase (λ-PP) treatment dephosphorylates

BIN1; 2 lanes per condition. **c.** *In vitro* phosphorylation assays with recombinant proteins show that Cdk2 and Cdk5 phosphorylate BIN1 at T348. Also see Fig. S2. **d-e.** Immunoblots and quantification showing the effects of U0126 and CsA (10 µM; 2.5 h) on BIN1 and Tau phosphorylation. Inset shows the effect of 10 nM CsA on BIN1 phosphorylation. Mean ± SD from 3 independent experiments. One-way ANOVA and paired t-test; * $p < 0.05$; ** $p < 0.01$. **f.** Behavior of BIN1-SH3 domain in the whole BIN1 isoform 1 protein as a function of phosphorylation by Cdk2 or of a mutation at threonine (T) 348 to glutamate (E) as monitored by ^{1}H-^{15}N HSQC spectra of BIN1iso1 CLAP T348E protein (in blue), Cdk2-phospho-BIN1iso1 (superimposed in red), and BIN1iso1 protein (superimposed in green). Also see Fig. S16. **g.** Titration of BIN1-SH3 domain with concentration of CLAP (334-355) or phospho-T348 CLAP (334-355) peptides. Normalized saturation curves (shown for residue 559), built from the gradual chemical shift changes (normalized; 1 denotes the largest change), are shown as pink stars for CLAP (334-355) and red stars for phospho-CLAP (334-355). Saturation curves are in cyan and green for CLAP (334-355) and phospho-CLAP (334-355), respectively. Also see Fig. S17. **h.** Representative images of PNC overexpressing BIN1iso1 and the BIN1iso1 T348E, its systematically open form, showing PLA signals and Tau and BIN1 immunolabeling. **i.** PLA density after normalization with respective BIN1 immunofluorescence in PNC overexpressing BIN1iso1 and BIN1iso1 T348E (for clarity, datasets were further normalized with the mean of BIN1iso1). N = 3 independent experiments. Red bars and black squares indicate sample median and mean, respectively. Wilcoxon rank-sum test; *** $p < 0.001$.

Fig. 6 BIN1 amount and phosphorylation status in post-mortem AD brains. **a.** Western blots showing total BIN1 (99D antibody), BIN1 phosphorylated at T348 (p-T348), and β-actin in the temporal lobes of 14 individuals with increasing neurofibrillary pathology (Braak stage; see Table S3 for demographic details and pathological statuses). **b-d.** Quantification of the BIN1:β-actin, BIN1-p-T348:β-actin, and BIN1-p-T348:BIN1 signals, normalized with the mean of the control group (Braak stage = 0). Dashed red lines indicate exponential fits; *p*-values refer to the Kolmogorov-Smirnov test for the normal distribution of residuals. Data marked in green indicate non-AD cases according to neuropathological diagnosis. **e-g.** Comparison of BIN1:β-actin, BIN1-p-T348:β-actin, and BIN1-p-T348:BIN1 signals between non-AD and AD cases. Red bars and black squares indicate sample median and mean, respectively; *p*-values refer to the Wilcoxon rank-sum test.

Fig. 7 Complexity and dynamics of the BIN1-Tau interaction in neurons. **a.** At the molecular level, the open/closed conformation of BIN1 regulates the BIN1-Tau interaction in neurons under the control of the BIN1 T348 phosphorylation by CaN and Cdks. In addition, phosphorylation of Tau at T231 decreases the BIN1-Tau interaction. **b.** In healthy neurons, the BIN1-Tau interaction occurs at physiological levels. **c.** In AD pathology, a decrease in BIN1iso1 leads to a decrease in BIN1-Tau interaction, potentially favoring the formation of neurofibrillary tangles (NFT), in spite of potential compensation through BIN1 T348 phosphorylation. **d.** In tauopathy, overexpression of BIN1iso1 in neurons (as in the case for hTau;Tg*BIN1* mice) leads to an increase in the BIN1-Tau interaction and correlates with the disappearance of Tau somatic inclusions.

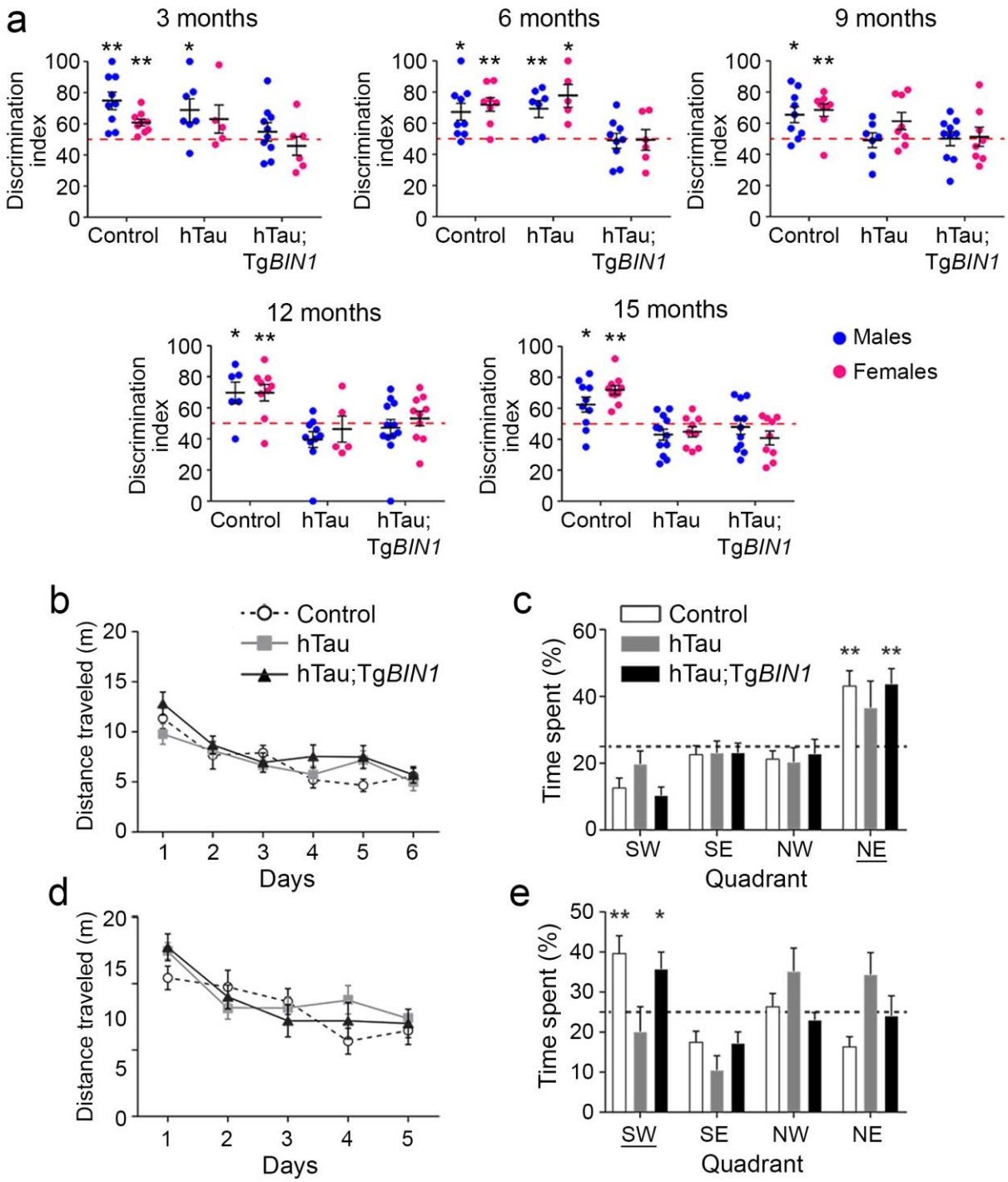
a
3 months
6 months
9 months
12 months
15 months
Discrimination index
Control
hTau
hTau; TgBIN1
Males
Females
b
Control
hTau
hTau;TgBIN1
Distance traveled (m)
Days
c
Time spent (%)
SW
SE
NW
NE
Quadrant
d
e

Fig. 1

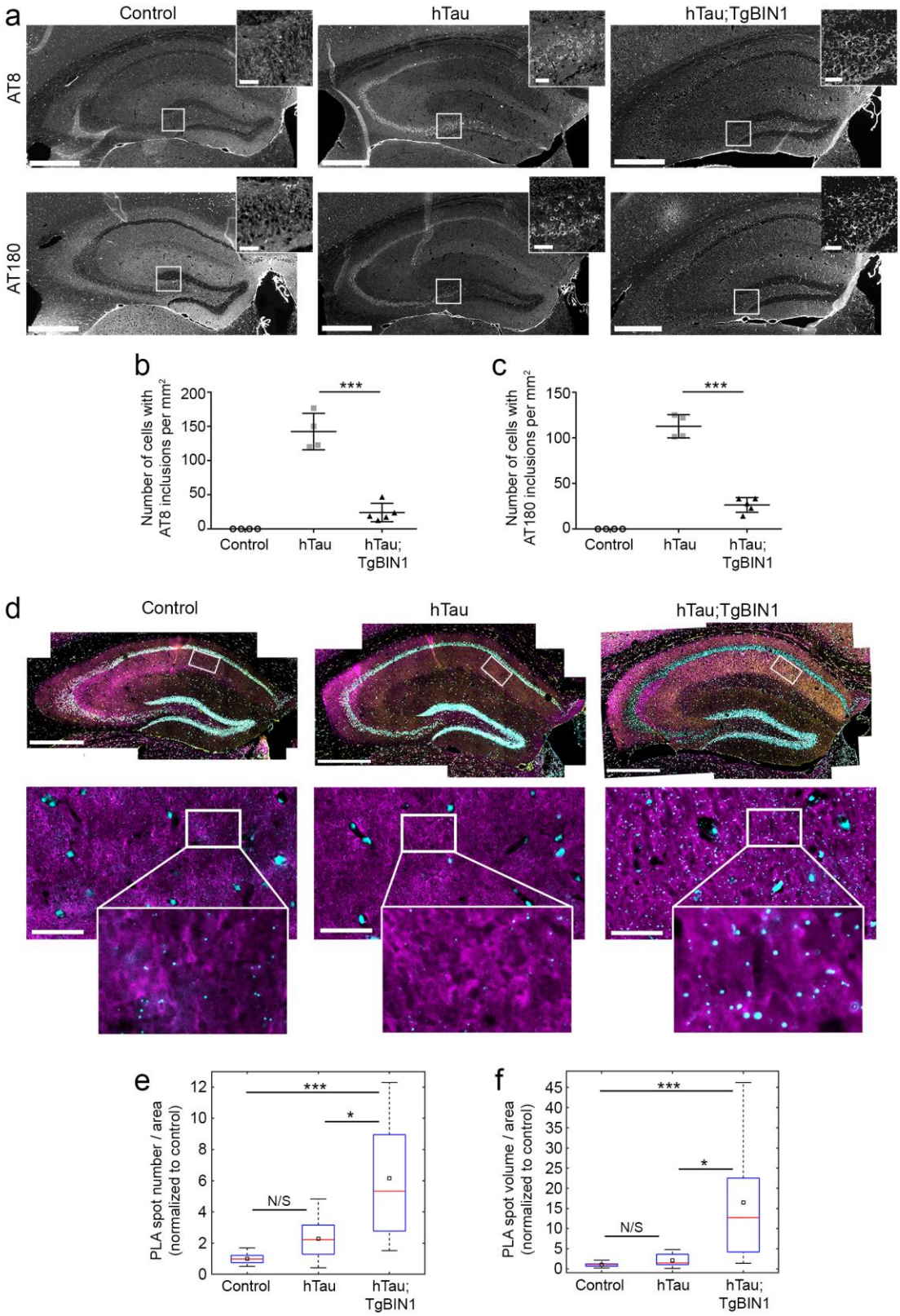
a
Control
hTau
hTau;TgBIN1
AT8
AT180
b
Number of cells with AT8 inclusions per mm²
***
Control
hTau
hTau; TgBIN1
c
Number of cells with AT180 inclusions per mm²
***
Control
hTau
hTau; TgBIN1
d
Control
hTau
hTau;TgBIN1
e
PLA spot number / area (normalized to control)
***
*
N/S
Control
hTau
hTau; TgBIN1
f
PLA spot volume / area (normalized to control)
***
*
N/S
Control
hTau
hTau; TgBIN1

Fig. 2

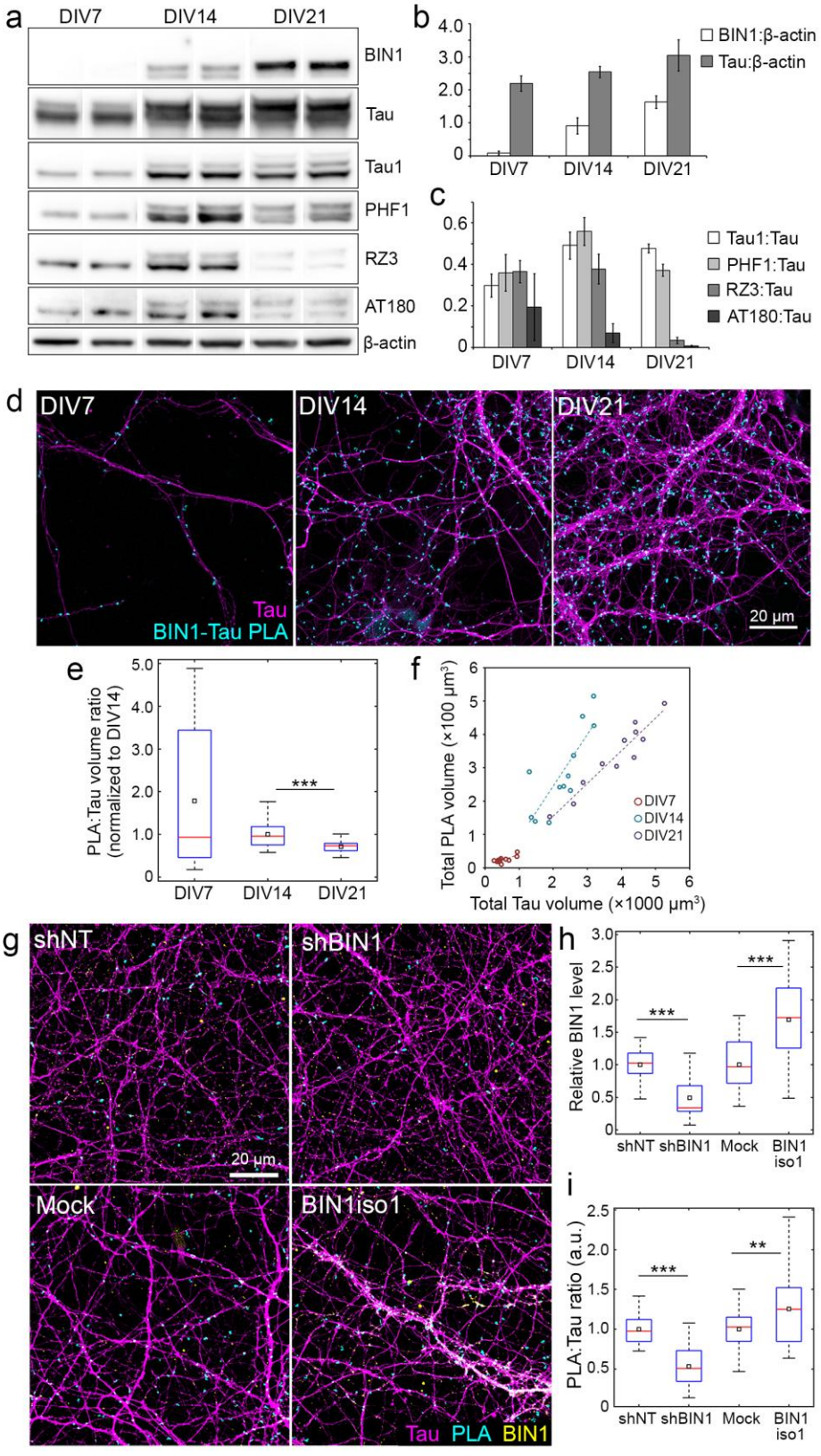
a
DIV7
DIV14
DIV21
BIN1
Tau
Tau1
PHF1
RZ3
AT180
β-actin
b
BIN1:β-actin
Tau:β-actin
c
Tau1:Tau
PHF1:Tau
RZ3:Tau
AT180:Tau
d
DIV7
DIV14
DIV21
Tau
BIN1-Tau PLA
20 μm
e
PLA:Tau volume ratio (normalized to DIV14)
***
f
Total PLA volume (×100 μm³)
Total Tau volume (×1000 μm³)
g
shNT
shBIN1
Mock
BIN1iso1
Tau PLA BIN1
h
Relative BIN1 level
shNT shBIN1 Mock BIN1 iso1
i
PLA:Tau ratio (a.u.)
**

Fig. 3

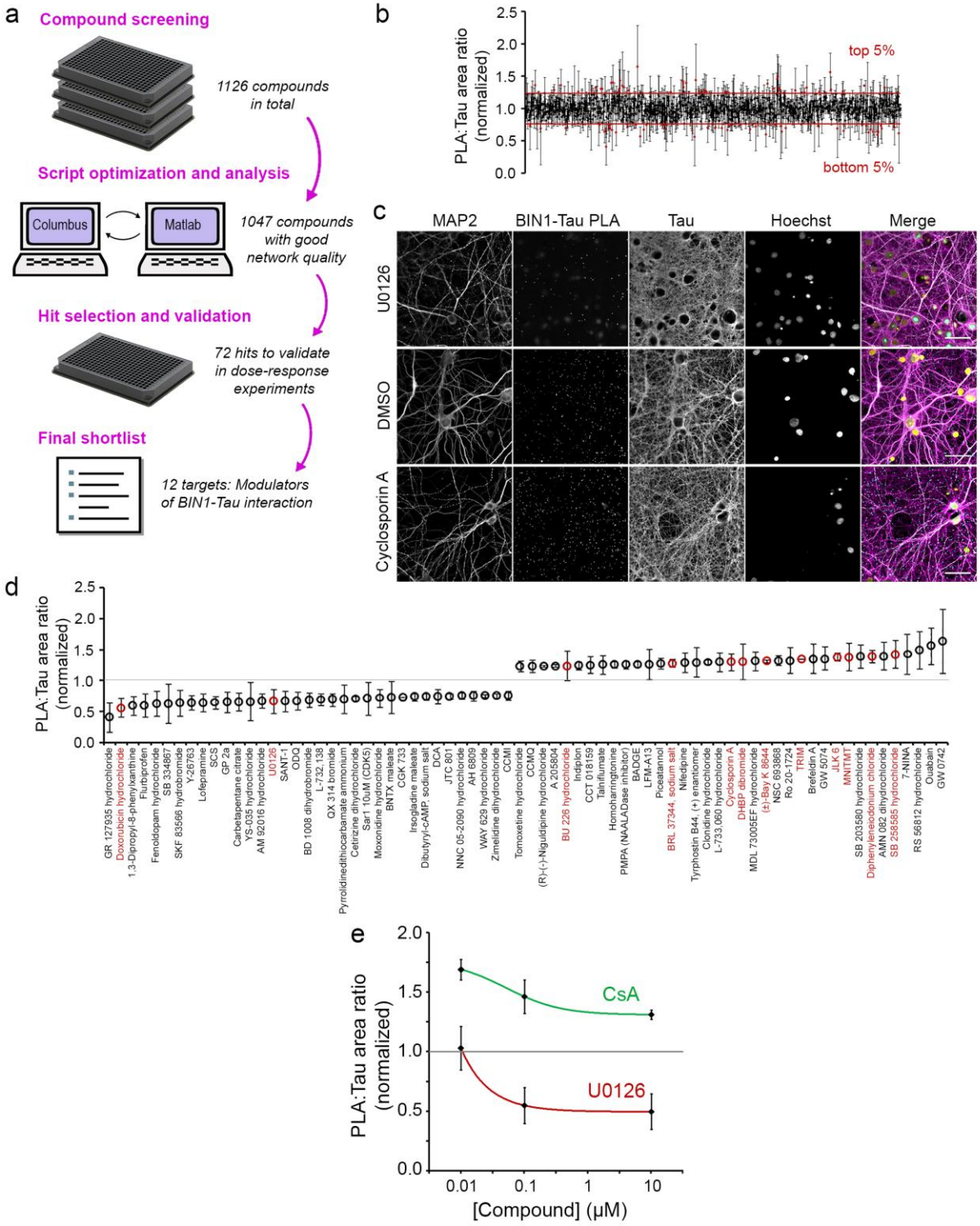
a
Compound screening
1126 compounds in total
Script optimization and analysis
Columbus
Matlab
1047 compounds with good network quality
Hit selection and validation
72 hits to validate in dose-response experiments
Final shortlist
12 targets: Modulators of BIN1-Tau interaction
b
PLA:Tau area ratio (normalized)
top 5%
bottom 5%
c
MAP2
BIN1-Tau PLA
Tau
Hoechst
Merge
U0126
DMSO
Cyclosporin A
d
PLA:Tau area ratio (normalized)
e
CsA
U0126
PLA:Tau area ratio (normalized)
[Compound] (μM)

Fig. 4

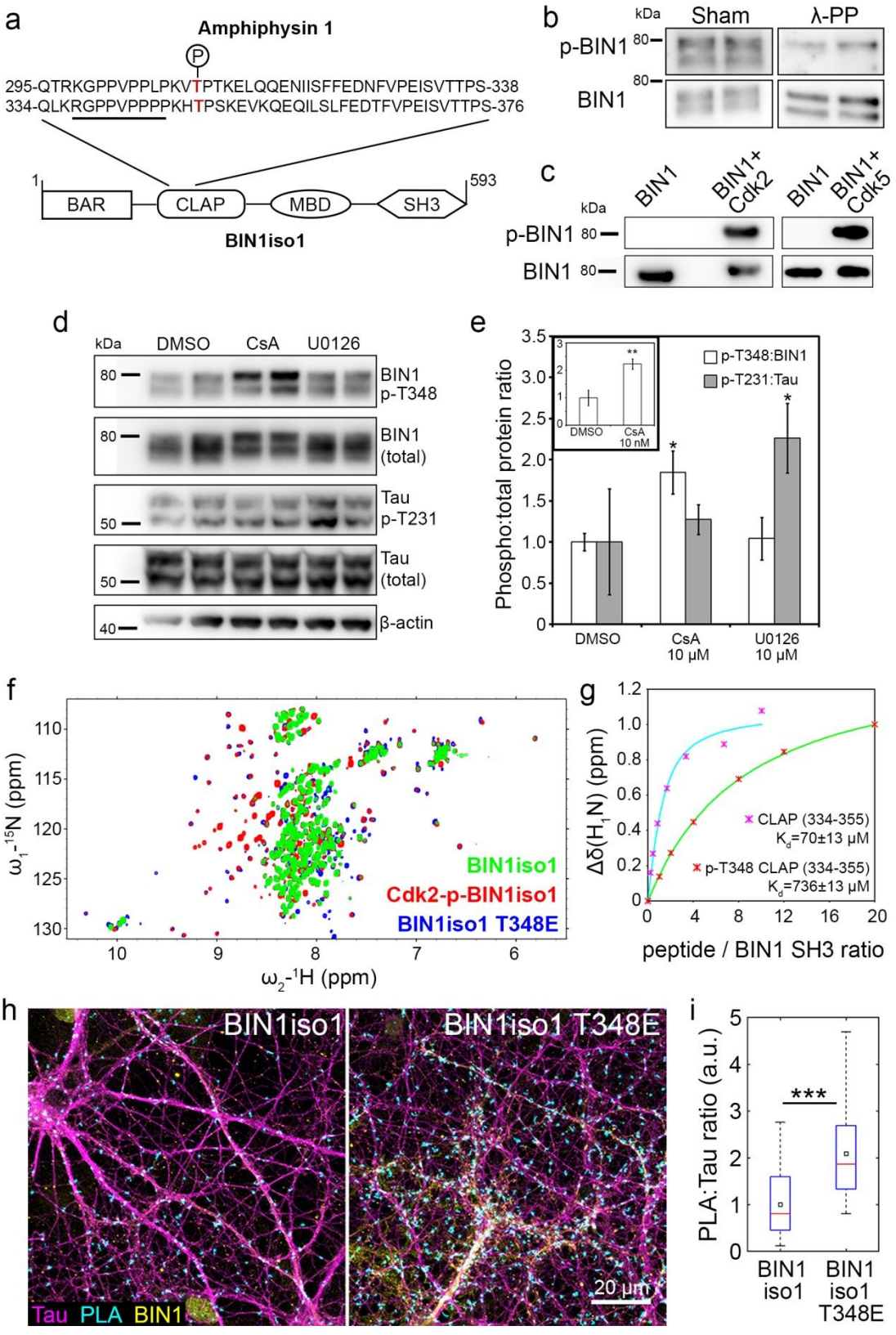
a
Amphiphysin 1
295-QTRKGPPVPPLPKVTPTKELQQENIISFFEDNFVPEISVTTPS-338
334-QLKRGPPVPPPPKHTPSKEVKQEQILSLFEDTFVPEISVTTPS-376
BAR
CLAP
MBD
SH3
BIN1iso1
b
kDa
Sham
λ-PP
p-BIN1
BIN1
c
BIN1
BIN1+ Cdk2
BIN1+ Cdk5
p-BIN1
BIN1
d
DMSO
CsA
U0126
BIN1 p-T348
BIN1 (total)
Tau p-T231
Tau (total)
β-actin
e
Phospho:total protein ratio
p-T348:BIN1
p-T231:Tau
DMSO
CsA 10 μM
U0126 10 μM
f
BIN1iso1
Cdk2-p-BIN1iso1
BIN1iso1 T348E
g
CLAP (334-355) Kd=70±13 μM
p-T348 CLAP (334-355) Kd=736±13 μM
peptide / BIN1 SH3 ratio
h
BIN1iso1
BIN1iso1 T348E
Tau PLA BIN1
20 μm
i
PLA:Tau ratio (a.u.)
BIN1 iso1
BIN1 iso1 T348E

Fig. 5

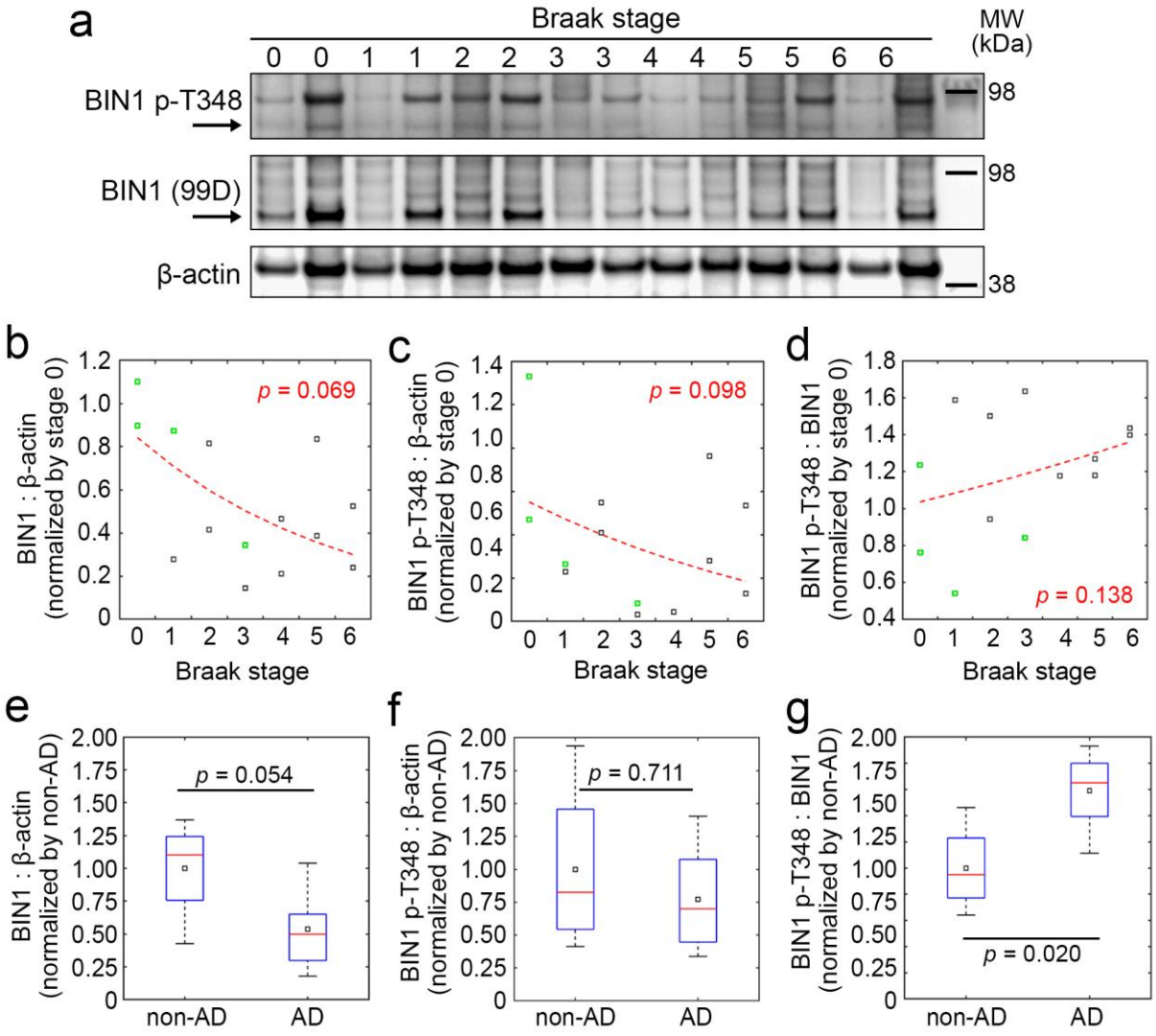
a
Braak stage
0 0 1 1 2 2 3 3 4 4 5 5 6 6
MW (kDa)
BIN1 p-T348
BIN1 (99D)
β-actin
98
98
38
b
BIN1 : β-actin (normalized by stage 0)
p = 0.069
Braak stage
c
BIN1 p-T348 : β-actin (normalized by stage 0)
p = 0.098
Braak stage
d
BIN1 p-T348 : BIN1 (normalized by stage 0)
p = 0.138
Braak stage
e
BIN1 : β-actin (normalized by non-AD)
p = 0.054
non-AD
AD
f
BIN1 p-T348 : β-actin (normalized by non-AD)
p = 0.711
non-AD
AD
g
BIN1 p-T348 : BIN1 (normalized by non-AD)
p = 0.020
non-AD
AD

Fig. 6

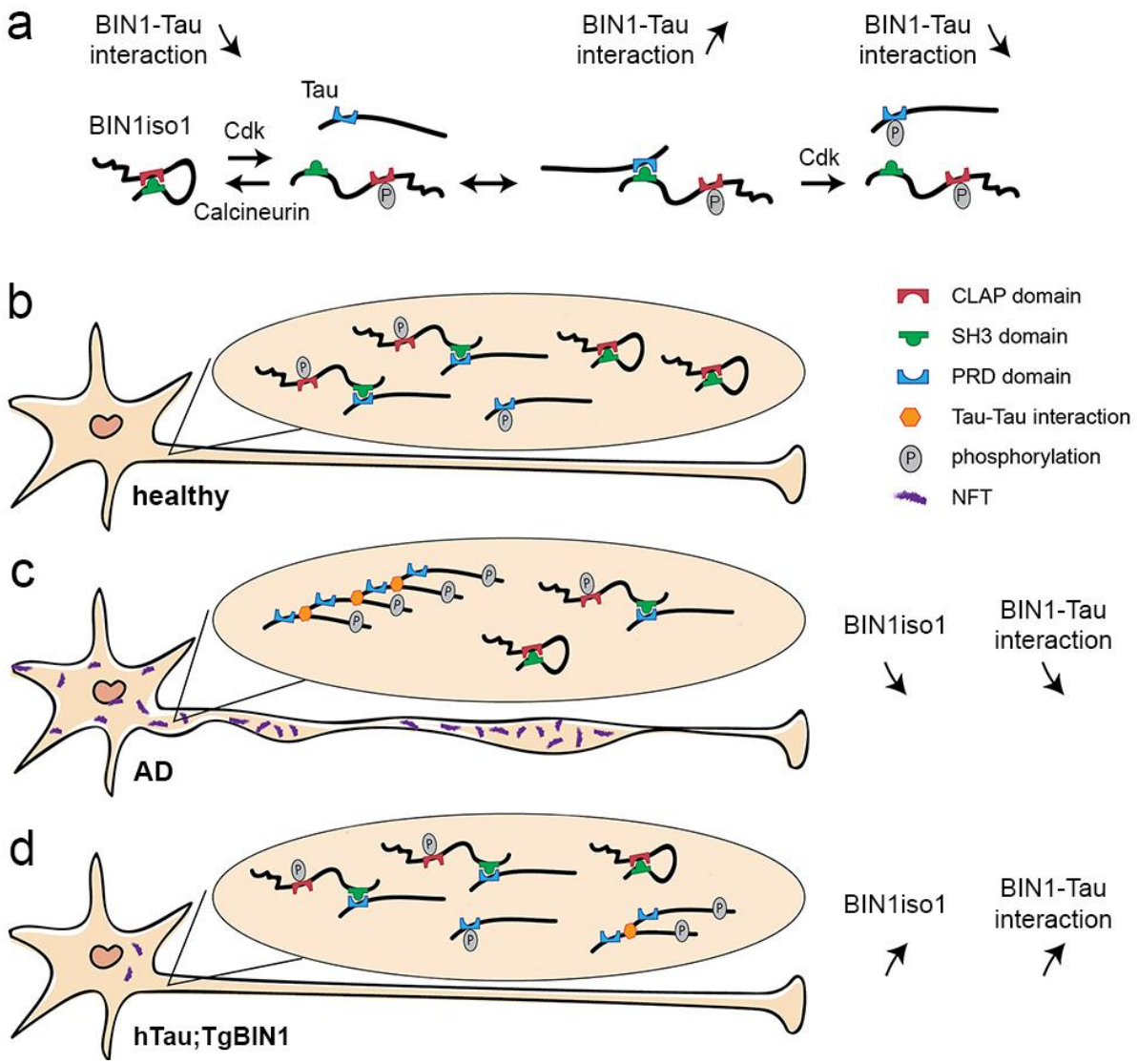
a
BIN1-Tau interaction
BIN1-Tau interaction
BIN1-Tau interaction
BIN1iso1
Cdk
Tau
Calcineurin
Cdk
b
CLAP domain
SH3 domain
PRD domain
Tau-Tau interaction
phosphorylation
NFT
healthy
c
BIN1iso1
BIN1-Tau interaction
AD
d
BIN1iso1
BIN1-Tau interaction
hTau;TgBIN1

Fig. 7

BIN1 recovers tauopathy-induced long-term memory deficits in mice and interacts with Tau through Thr^{348} phosphorylation

Maxime Sartori[1,2,3,4,*], Tiago Mendes[5,6,7,8,*], Shruti Desai[5,6,7,*], Alessia Lasorsa[7,9], Adrien Herledan[6,10,11], Nicolas Malmanche[5,6,7], Petra Mäkinen[12], Mikael Marttinen[12], Idir Malki[7,9], Julien Chapuis[5,6,7], Amandine Flaig[5,6,7], Anaïs-Camille Vreulx[5,6,7], Philippe Amouyel[5,6,7], Florence Leroux[6,10,11], Benoit Déprez[6,10,11], François-Xavier Cantrelle[7,9], Damien Maréchal[1,2,3,4], Laurent Pradier[8], Mikko Hiltunen[12], Isabelle Landrieu[7,9], Devrim Kilinc[5,6,7,#], Yann Herault[1,2,3,4,#], Jocelyn Laporte[1,2,3,4,#], Jean-Charles Lambert[5,6,7,#]

Supplementary Information

* Maxime Sartori, Tiago Mendes, and Shruti Desai contributed equally to this work.

# Devrim Kilinc, Yann Herault, Jocelyn Laporte and Jean-Charles Lambert contributed equally to this work.

[1] Institut de Génétique et de Biologie Moléculaire et Cellulaire (IGBMC), Illkirch, France

[2] INSERM U1258, Illkirch, France

[3] CNRS UMR7104, Illkirch, France

[4] Strasbourg University, Illkirch, France

[5] INSERM, U1167, RID-AGE-Risk Factors and Molecular Determinants of Aging-Related Diseases, Lille, France

[6] Institut Pasteur de Lille, Lille, France

[7] University of Lille, DISTALZ Laboratory of Excellence (LabEx), Lille, France

[8] SANOFI Neurosciences, Chilly-Mazarin, France

[9] CNRS UMR8576, Lille, France

[10] University of Lille, EGID, Lille, France

[11] Inserm, U1177, Lille, France

[12] Institute of Biomedicine, University of Eastern Finland, Kuopio, Finland

Supplementary Materials and Methods

HCS image segmentation in Columbus

HCS was performed in the IN Cell platform. IN Cell image registration and transfer files (.xdce files) were manually edited to import images to Columbus only from control wells, thereby generating the so-called "control plates" for script optimization and plate validation. HCS image analysis was performed using Columbus software (Fig. S3). In order to improve the detection of Tau and MAP2 areas, somatic regions were excluded from the Tau (Cy5 channel) and MAP2 (FITC channel) images by removing the Hoechst signal (DAPI channel), using the formula $A \times \ if\ B_{median} + 0.1 \times B_{stddev}\ , 1,0\ )$, where *A* is the Cy5 or the FITC channel and *B* is the DAPI channel. Tau and MAP2 areas were calculated after thresholding using the formula $(if(A > \ A_{mean} - q_1 \times A_{stddev}), 1, 0\ )$, where *A* is the somata-excluded Cy5 or FITC channels and q_1 is area threshold coefficient in terms of SD. For the FITC channel (MAP2), the parameter q_1 had a constant value of 0.1. For the Cy5 channel (Tau), q_1 was one of the optimization parameters determined through an iterative process, *i.e.*, script optimization. PLA spots (dsRed channel) in the thresholded Tau area using the *Find Spots* and *Select Population* building blocks of Columbus following *Method D*. Here, the *Splitting Coefficient* was kept constant at 0.9, *Spot Area* was restrained between 15 and 60 px^2, and the upper threshold of *Spot Contrast* was kept constant at 0.9. In addition, three parameters of this building block were determined through script optimization: q_2, threshold of *Detection Sensitivity*; q_3, threshold of *Background Correction*; and q_4, lower threshold of *Spot Contrast*.

Iterative process to determine optimum parameters for image segmentation script

Each control plate was used to optimize the image segmentation parameters to be used to analyze the corresponding full plate. Multiple Columbus analysis scripts were created by assigning distinct values combinatorially to each of the optimization parameter (q_1-q_4). For example, assigning three distinct values per parameter results in 3^4 = 81 combinations; hence the optimization was performed by running Columbus in the *Batch Analysis* mode, using 81 analysis scripts. This resulted in 81 result files per control plate, which were then analyzed in MATLAB. Data obtained for each well of the control plate were corrected for spatial bias (horizontal), using the slope of the line that fits the column averages based on the least-squares method. For each control plate, three values typically used in HCS analysis (Bray and Carpenter, 2013) were calculated: (i) strictly standardized mean difference, β factor, $\beta = (\mu_n - \mu_p)\ \overline{\sigma_n^2 + \sigma_p^2}$; (ii) Z prime factor $Z^{'} = 1 - 3(\sigma_p + \sigma_n)\ |\mu_p - \mu_n|$; and (iii) signal-to-background ratio (S/B = $\mu_p\ \mu_n$), where μ and σ are mean and standard deviation, and *p* and *n* indicate positive and negative controls

(PLA conducted without the BIN1 primary antibody or without the Mouse-minus probe). The optimal parameter set for analysis script was determined to be the one with the highest β factor (β ≥ 2), provided that it produced S/B of at least 10. Additional rounds of parameter optimization were performed when necessary.

Full plate analysis and identification of hits

Full plates were analyzed in Columbus with the corresponding optimal analysis script. For each well, Tau area, MAP2 area, and PLA spot area within Tau area were corrected for local bias by normalizing the raw values by the ratio of the local median (median of the surrounding wells in the 5×5 neighborhood) to the plate median (excluding edge wells), *i.e.*, $corrected\ value = raw\ value\ \frac{local\ median}{plate\ median}$. For each plate, compounds affecting network quality, defined as not having Tau area or Tau:MAP2 area ratio within median ± 3 median absolute deviations (MAD), were excluded (Fig. S4). Edge wells were not taken into account when calculating median and MAD. Corrected PLA:Tau area ratio for each well was then normalized by the mean of non-excluded wells. Finally, normalized, corrected PLA:Tau area ratio obtained from 3 screens were pooled to calculate mean and SEM for each compound that were not excluded from at least 2 screenings. Compounds potentially affecting BIN1-Tau interaction were determined as those belonging to the top or bottom 5% tiers.

Validation of selected compounds

Hit validation was performed by generating dose-response curves for selected compounds to identify specific effects on BIN1-Tau interaction. Since several of the selected compounds had multiple protein targets at 10 µM concentration (as used in the HCS) dose-response experiments were designed to determine if the effects were specific and/or to identify relevant targets. Dose-response experiments were performed for 72 compounds from the top and bottom 5%, which gave similar results in all 3 screens. Compounds were diluted four log scales to obtain a dose-response curve (10 nM, 100 nM, 1 µM and 10 µM) and each compound and concentration was tested in three separate plates under identical conditions as in HCS. Script optimization, plate validation, plate analysis, and well correction and exclusion steps were executed as described above. The DMSO-normalized mean of each compound at 10 µM was compared with the screen result (also at 10 µM), and compounds that had similar effects in both sets of experiments were retained for further analysis. For each compound, dose-response curves were fit with 4-parameter or 3-parameter (where Hill slope is 1) nonlinear regression models, based on the extra sum-of-squares F test using GraphPad Prism 7 (La Jolla, CA).

K_d determination using NMR data

The $^{1}H,^{15}N$ combined chemical shift changes, $\Delta\delta(^{1}H,^{15}N)$, were calculated using the following equation: $\Delta\delta(H,N) = (\Delta\delta^{2}_{H} + \Delta\delta^{2}_{N} \times 0.159)^{1/2}$, where $\Delta\delta_{H}$ and $\Delta\delta_{N}$ are the chemical shift (δ) changes for ^{1}H and ^{15}N, respectively. Dissociation constants were obtained by fitting the chemical shift perturbation data to the following equation: $\delta_{obs} = \Delta\delta_{max} (a + b + K_d – ((a + b + K_d)^2 – 4ab)^{1/2}) / 2a$, where $\Delta\delta_{obs}$ is the weighted average of the chemical shifts in the free and bound states and $\Delta\delta_{max}$ is the maximal signal change upon saturation (bound state). K_d is the dissociation constant, *a* and *b* are the total peptide and BIN1 SH3 concentrations, respectively. K_d was calculated based on chemical shift perturbations of each resonance with $\Delta\delta(H,N) > 0.01$ ppm when comparing the bound and free states, and averaged.

Supplementary Results

Myelin alterations in the fornix

The degree of fornix alteration is correlated with memory impairments. Coronal visualization of the fornix at 18 months in hTau and hTau;Tg*BIN1* mice was performed using electron microscopy. *MAPT* overexpression is associated with myelin abnormalities. Indeed, most nerve fibers in the hTau mice presented multiple myelin rings (Fig. S18, arrowheads); however, a significant rescue of this phenotype was observed in hTau;Tg*BIN1* mice. The overexpression of BIN1 alone did not induce any myelin abnormalities (Fig. S19). Thus, the memory impairments observed in the behavioral analyses of the hTau mice may be also associated with myelin disorganization in the fornix, and were rescued upon BIN1 overexpression. Finally, as spatial memory was perturbed in hTau mice, ultrastructural analysis of proximal axons projecting from the CA3 was also conducted *via* electron microscopy. No obvious ultrastructural defects were observed and, notably, the microtubule network appeared well aligned and distributed inside the nerve fibers in hTau, Tg*BIN1*, and hTau;Tg*BIN1* mice (Fig. S20).

Supplementary Tables

Table S1. Primer sequences

Primer	***5'→ 3'***
Mapt KI WT UP	CTCAGCATCCCACCTGTAAC
Mapt KI WT DW	CCAGTTGTGTATGTCCACCC
Mapt KI Tg UP	AAGTTCATCTGCACCACCG
Mapt KI Tg DW	TGCTCAGGTAGTGGTTGTCG
TgMAPT (mut) UP	ACTTTGAACAGGATGGCTGAGCCC
TgMAPT (mut) DW	CTGTGCATGGCTGTCCACTAACCTT
TgMAPT (WT) UP	CTAGGCCACAGAATTGAAAGATCT
TgMAPT (WT) DW	GTAGGTGGAAATTCTAGCATCATCC
TgBIN1 UP	CGAGGCCTGCGCCGCGATGGC
TgBIN1 DW	CGCAGCCTGGGGACCTCGAAG

Table S2. Antibodies used in brain slices

Antibody	***Reference***
Tau [E178]	Abcam, ab32057
BIN1 [C99D]	Sigma, B9428
Phospho Tau Thr231 [AT180]	Thermo Scientific, MN1040
Phospho Tau Ser202 [AT8]	Thermo Scientific, MN1020

Table S3. Demographic details of the neuropathological cohort.

Individual	*Braak stage*	*Gender*	*Age at death*	*Post-mortem delay (h)*	*Brain weight (g)*	*Neuropathological diagnosis*
1	0	M	61	7	900	Non-AD
2	0	F	52	8	1190	Non-AD
3	1	F	82	7	950	AD
4	1	M	84	7	1130	Non-AD
5	2	F	84	5	1100	AD
6	2	F	82	4	1110	AD
7	3	F	76	4	990	AD
8	3	F	92	18	1060	Non-AD
9	4	F	76	24	1165	AD
10	4	F	85	4	1070	AD
11	5	F	85	4	800	AD
12	5	M	80	5	1000	AD
13	6	F	78	5	995	AD
14	6	F	85	4	1035	AD

Supplementary Figures:

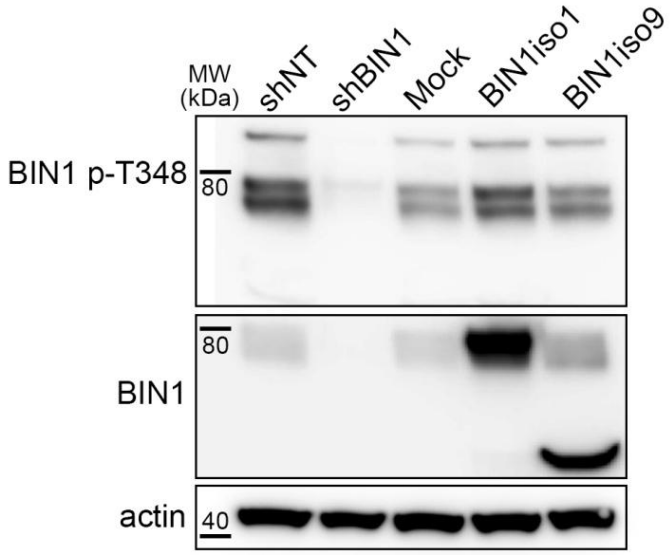

Fig. S1 Specificity of BIN1 p-T348 antibody to the neuronal isoforms of BIN1 in PNC. Western blot of neurons transduced with shNT, shBIN1, Mock, BIN1iso1 (containing T348), and BIN1iso9 (without the CLAP domain or T348) constructs. BIN1 p-T348 signal is modulated as a function of BIN1iso1 under- and overexpression. No BIN1 p-T348 signal was detected at the molecular weight of BIN1iso9, while endogenous BIN1iso1 was seen in all but the shBIN1-expressing neurons.

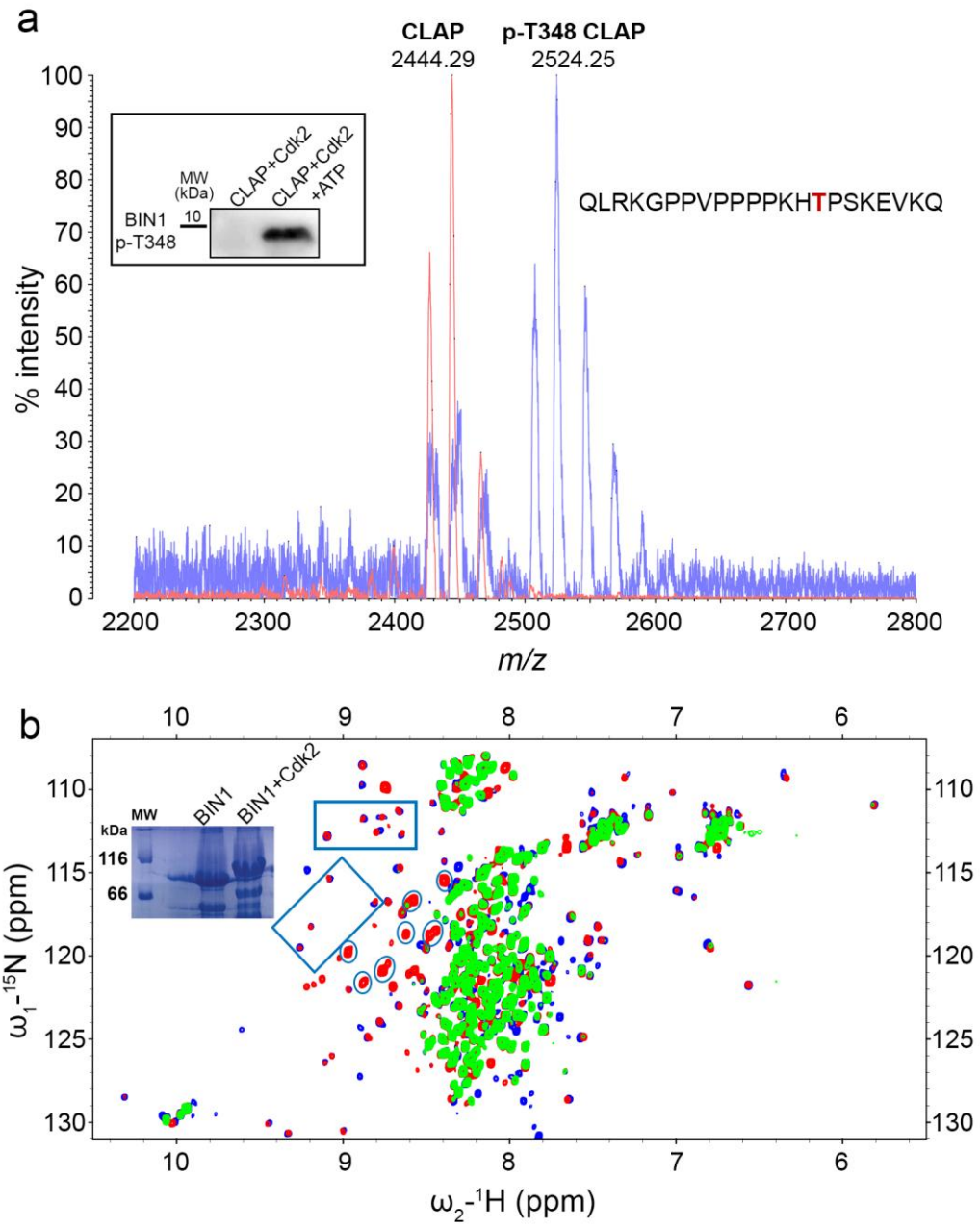

Fig. S2 NMR measurements confirm that Cdk2 phosphorylates BIN1 CLAP at T348. **a.** Maldi-TOF analysis of CLAP (334-355) peptide before (red) and after (blue) incubation with Cdk2/CycA3 kinase. Incubation of the peptide with the kinase (molar ratio 1/100) at 37°C for 3 h, in the presence of 2 mM ATP, 2.5 mM $MgCl_2$, 2 mM EGTA, 2 mM DTT, 30 mM NaCl and protease inhibitors in 50 mM HEPES, pH 8.0, resulted in a mass increase compatible with the incorporation of one phosphate group. T238 is the only Pro-directed site compatible with the kinase specificity in the peptide. Inset: BIN1 p-T348 antibody recognizes the BIN1 CLAP (334-355) peptide upon Cdk2 phosphorylation. **b.** ^{1}H-^{15}N HSQC spectra of BIN1Iso1-CLAP-T348E protein (blue), Cdk2-phospho-BIN1Iso1 (superimposed in red) and BIN1Iso1 protein (superimposed in green). Boxed resonances, superimposed in the blue and red

spectra, correspond to some of the resonances of the BIN1-SH3 domain, and are only detected in the presence of T348 phosphorylation or the T348E mutation of the CLAP domain (see also Fig. S16). Circled resonances, only detected in the red spectrum (or Cdk2-phospho-BIN1) correspond to resonances with typical H-N chemical shift values for pS/pT residues. Inset: Multiple sites of Cdk2-BIN1 were thus modified in the conditions of this assay, as also shown by the characteristic gel-shift observed by SDS-PAGE.

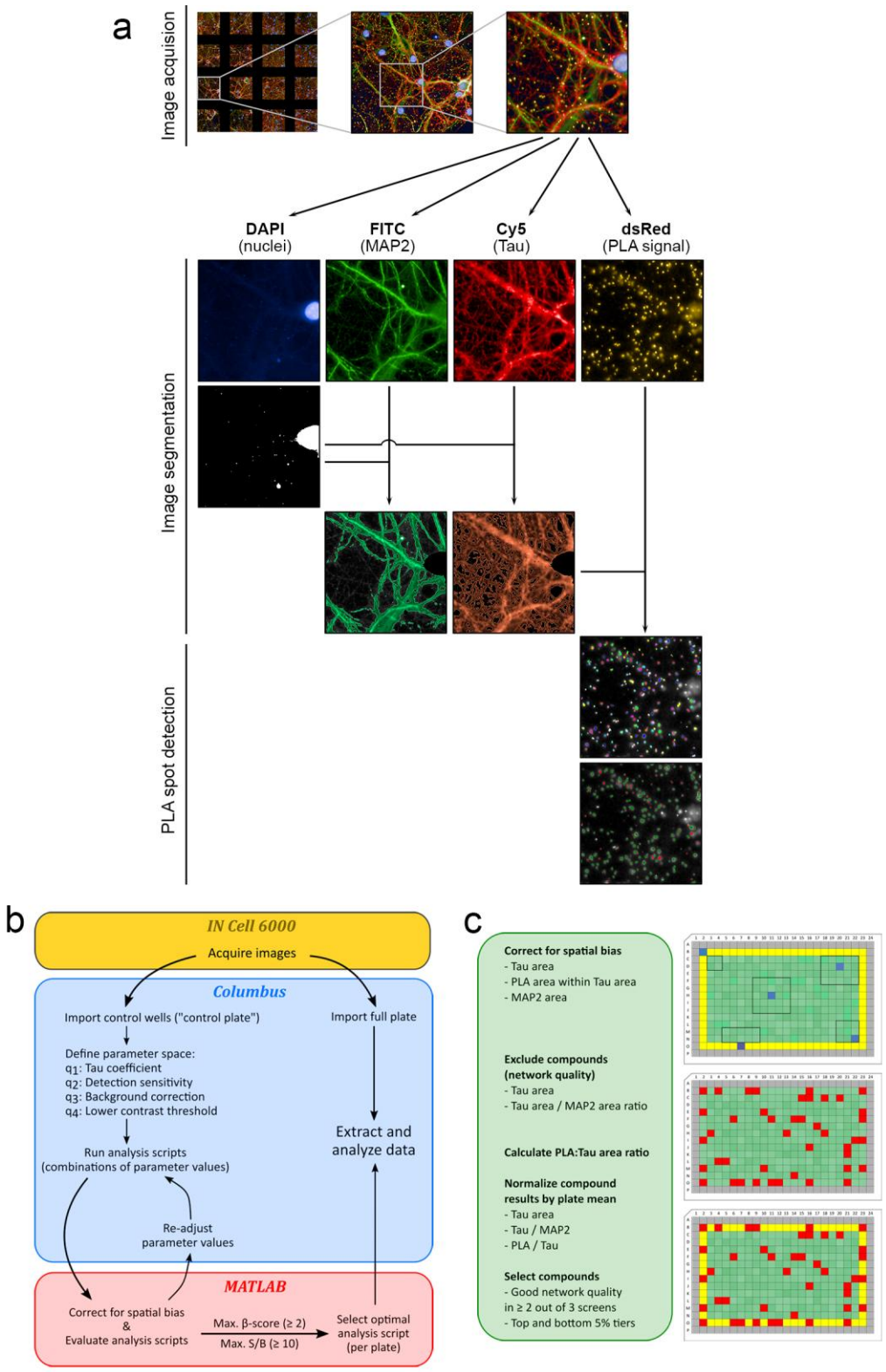

Fig. S3 HCS image analysis and quantification procedures. **a.** Details of image acquisition, segmentation and PLA detection processes: Acquisition of 16 fields per well in four wavelengths using IN Cell Analyzer 6000; exclusion of somatic regions from FITC and Cy5 channels and delimitation of MAP2 and Tau areas in the Columbus software; detection of PLA spots in non-somatic Tau areas and their filtering based on area and contrast (green

spots in the last image). **b.** Schematic showing the iterative process for selecting the optimum analysis script separately for each plate. **c.** Demonstration of data analysis in a representative plate layout. Yellow wells are used to correct for spatial bias. Blue wells and the corresponding 5×5 neighborhood (black outlines) illustrate the correction for local bias. Red wells were excluded based on network quality and the remaining (green) wells were used to calculate plate means for normalization.

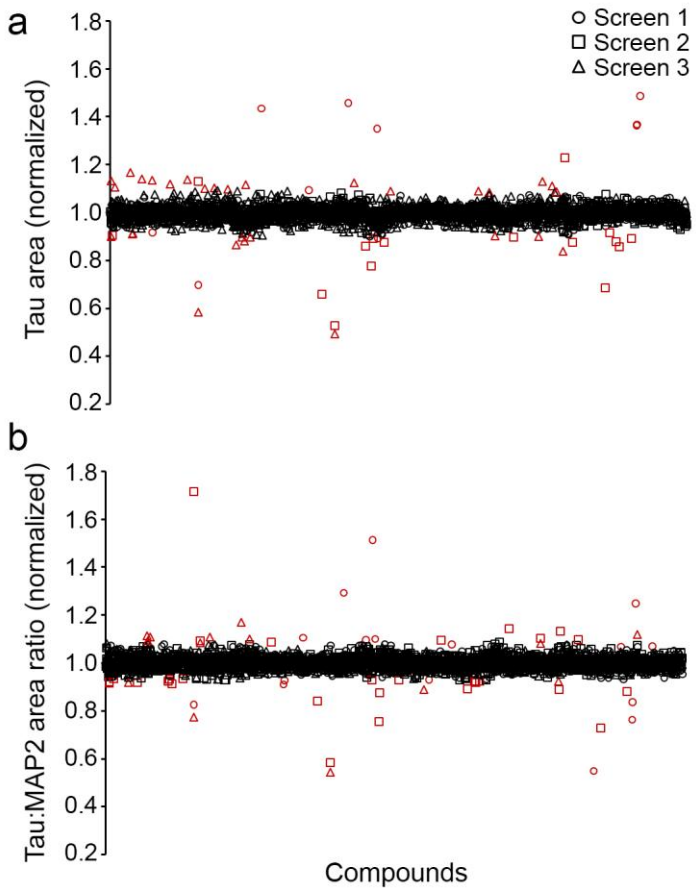

Fig. S4 Distribution of Tau area (**a**) and Tau:MAP2 area ratio (**b**) of all 1,126 compounds in the three screenings, after plate-by-plate normalization (excluded data points shown in red).

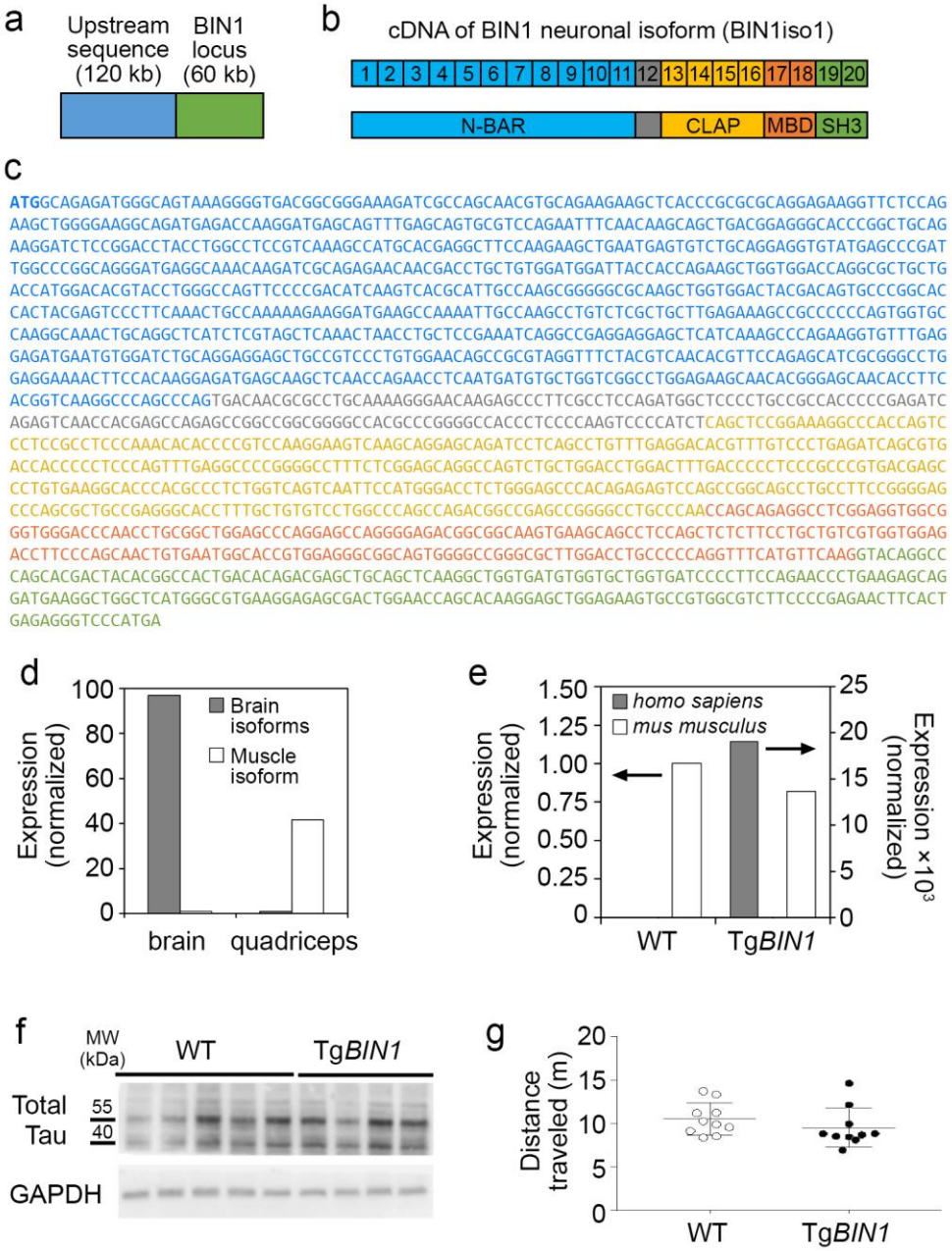

Fig. S5 MAPT and BIN1 expression in the Tg*BIN1* mouse. **a.** Drawing of the BAC RP11-437K23 encompassing the *BIN1* locus and upstream sequences. **b.** RNA was extracted from hippocampus of Tg*BIN1* mice, reverse-transcribed, cloned and sequenced. Human exons present in hippocampus and corresponding protein domains are displayed with corresponding colors. BAR, BIN-Amphiphysin-Rvs; CLAP, Clathrin and AP2 binding domain; MBD, Myc binding domain; SH3, Src homology domain. **c.** Isoform 1 was the main human BIN1 isoform detected, whose sequence is shown. **d.** Quantification of neuronal and muscular BIN1 isoforms by RT-qPCR from brain and quadriceps of Tg*BIN1* mouse. **e.** Quantification of total murine Bin1 and human BIN1 RNA by RT-qPCR from brain of WT and Tg*BIN1* mice. **f.** Western blots of total Tau in the brains of WT and Tg*BIN1* mice. **g.** Distance traveled by WT and Tg*BIN1* mice in the open field test.

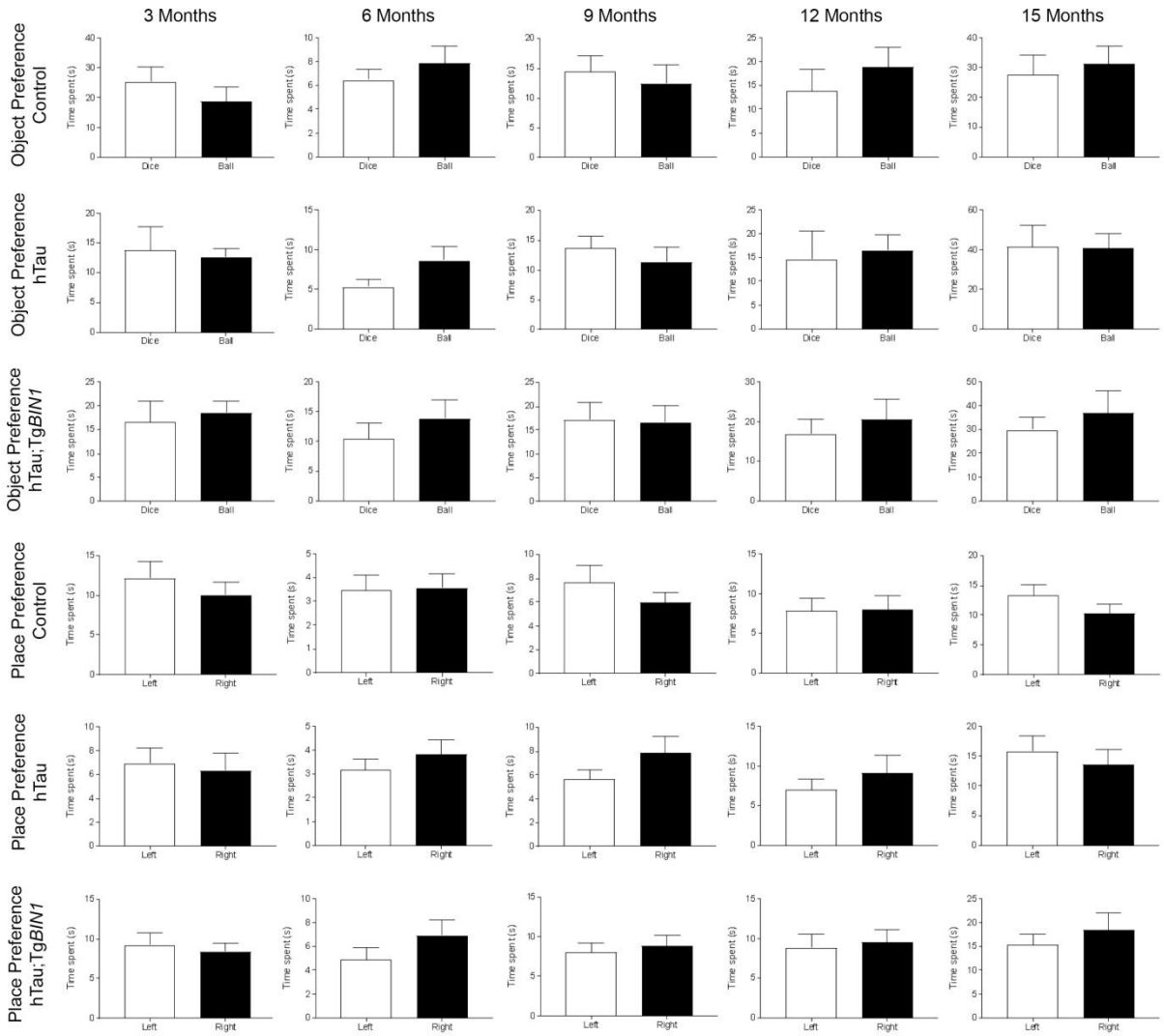

Fig. S6 Validation of lack of object preference. Percentage of time spent by the 3-, 6-, 9-, 12-, or 15-month-old control, hTau and hTau;Tg*BIN1* mice with objects located in the right or left positions, during the acquisition phase.

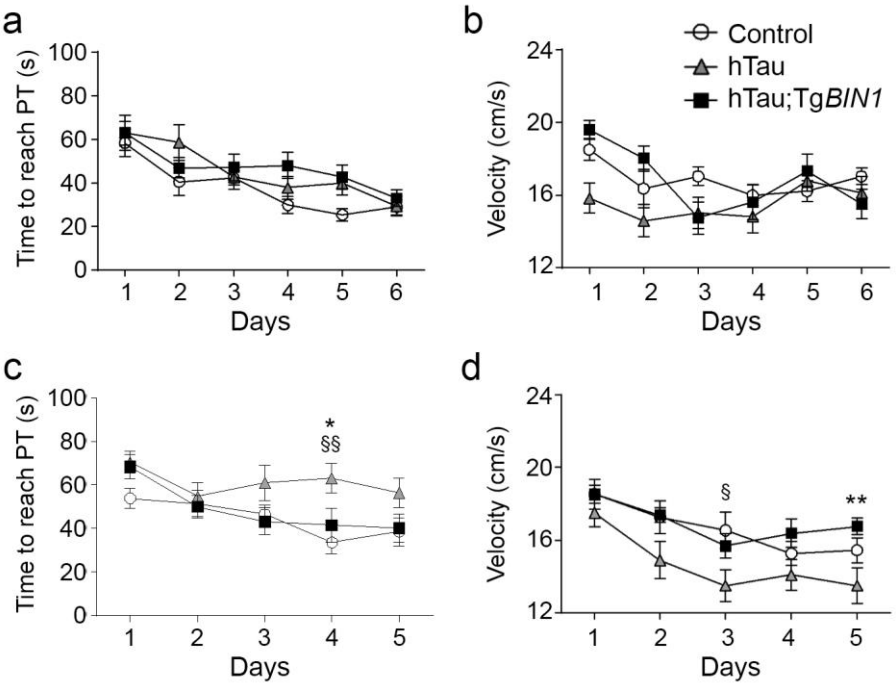

Fig. S7 Spatial and long-term memory in 12- and 15-month-old Tg*BIN1* males assessed with Morris water maze. **a.** Time to reach the platform (PT) at 12 months. **b.** Velocity during task acquisition. **c.** Time to reach the platform (PT) at 15 months. **d.** Velocity during task acquisition. Data represent mean ± SEM for consecutive days of acquisition (control n=11; hTau n=11; hTau;Tg*BIN1* n=13). Two-way ANOVA followed by Bonferroni *post hoc* test at each day of acquisition. § $p < 0.05$, §§ $p < 0.01$ for control vs hTau. * $p < 0.05$, ** $p < 0.01$ for hTau vs hTau;Tg*BIN1*.

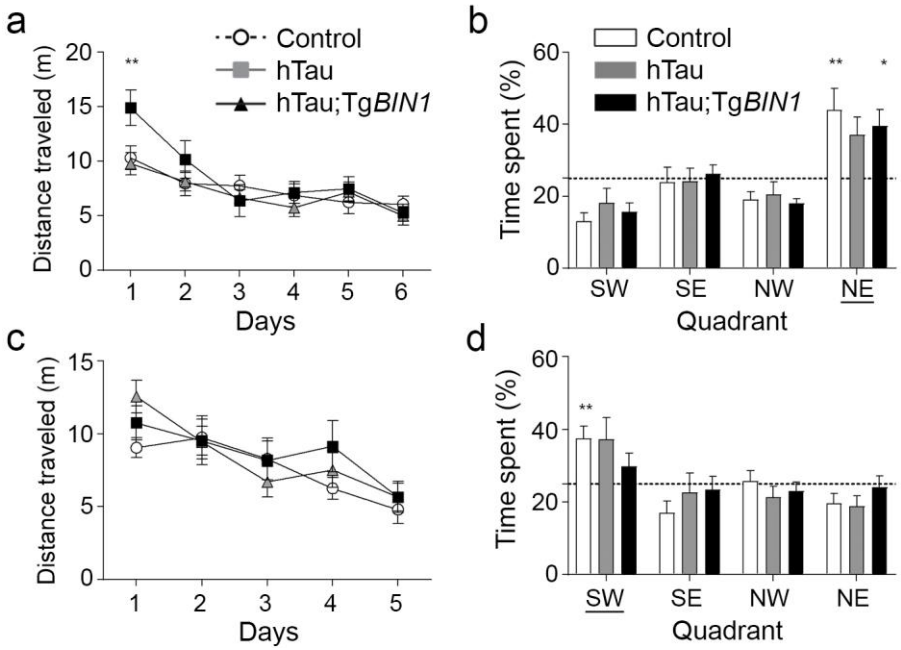

Fig. S8 Long-term memory deficits due to *MAPT* overexpression in hTau females is rescued by BIN1 overexpression at 12 but not 15 months. Spatial and long-term memory in 12- and 15-month-old control, hTau and hTau;Tg*BIN1* mice assessed with Morris water maze. **a.** Distance traveled to reach the platform at 12 months. Data represent mean ± SEM for consecutive days of acquisition (control, n=11; hTau, n=9; hTau;Tg*BIN1*, n=11). **b.** Probe test without platform at 12 months, performed 24 h after the last training session. Dashed line represents chance. Data represent mean ± SEM for each quadrant (control, n=11; hTau, n=9; hTau;Tg*BIN1*, n=11). Underlined quadrant marks original platform location. **c.** Distance traveled to reach the platform at 15 months. Data represent mean ± SEM for consecutive days of acquisition (control, n=11; hTau, n=9; hTau;Tg*BIN1*, n=11). **d.** Probe test without platform at 15 months, performed 24 h after the last training session. Dashed line represents chance. Data represent mean ± SEM for each quadrant (control, n=11; hTau, n=9; hTau;Tg*BIN1*, n=11). Underlined quadrant marks original platform location. One sample t-test compared to chance at 25% for the time spent in quadrants, *p<0.05, **p<0.01. Two-way ANOVA for the distance travelled, **p<0.01.

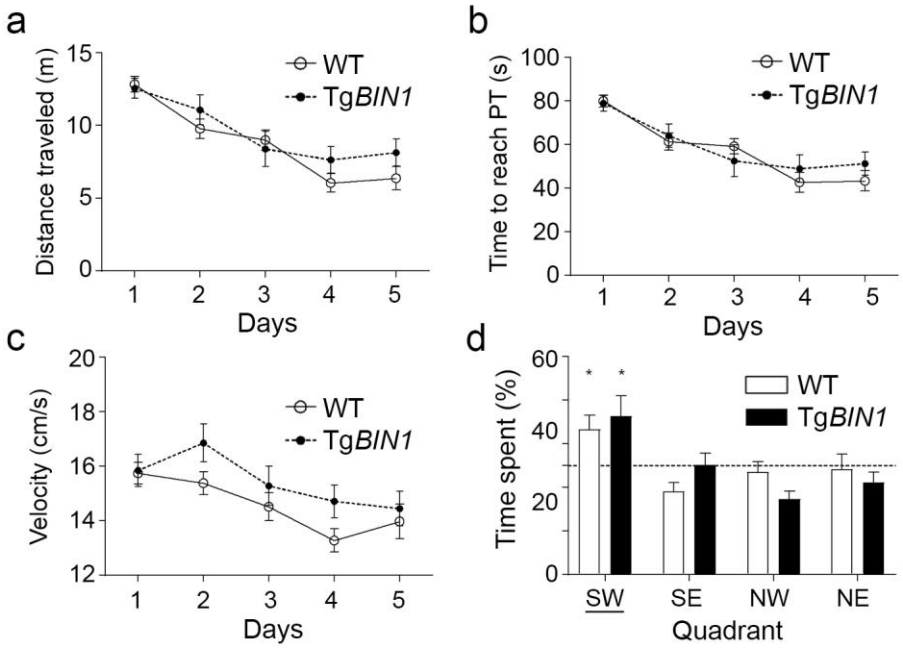

Fig. S9 *BIN1* overexpression does not affect long-term memory. Spatial and long-term memory in 15-month-old Tg*BIN1* males assessed with Morris water maze. **a.** Distance traveled to reach the platform. Data represent mean ± SEM for consecutive days of acquisition (WT, n=15; Tg*BIN1*, n=13). **b.** Time to reach the platform (PT). Data represent mean ± SEM for consecutive days of acquisition (WT, n=15; Tg*BIN1*, n=13). **c.** Velocity during task acquisition. Data represent mean ± SEM for consecutive days of acquisition (WT, n=15; Tg*BIN1*, n=13). **d.** Probe test without the platform, performed 24 h after the last training session. Dashed line represents chance. Data represent mean ± SEM for each quadrant (WT, n=15; Tg*BIN1*, n=13). Underlined quadrant marks original platform location. One sample t-test compared to chance at 25%; * $p < 0.05$.

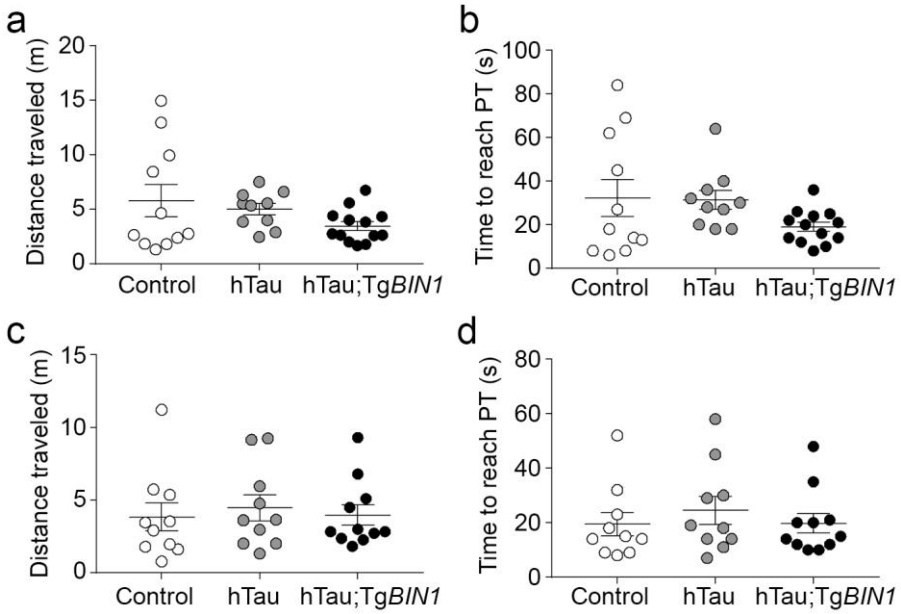

Fig. S10 Absence of visual or motor deficits in 15-month-old males and females for the Morris water maze. **a.** Distance traveled to reach the visible platform (PT) for males (control, n=11; hTau, n=11; hTau;Tg*BIN1*, n=13). **b.** Time to reach the visible platform for males (control, n=11; hTau, n=11; hTau;Tg*BIN1*, n=13). **c.** Distance traveled for females to reach the visible platform (PT; control, n=10; hTau, n=10; hTau;Tg*BIN1*, n=11). **d.** Time to reach the visible platform for females (control, n=10; hTau, n=10; hTau;Tg*BIN1*, n=11). Data represent mean ± SEM. One-way ANOVA followed by Bonferroni *post hoc* test.

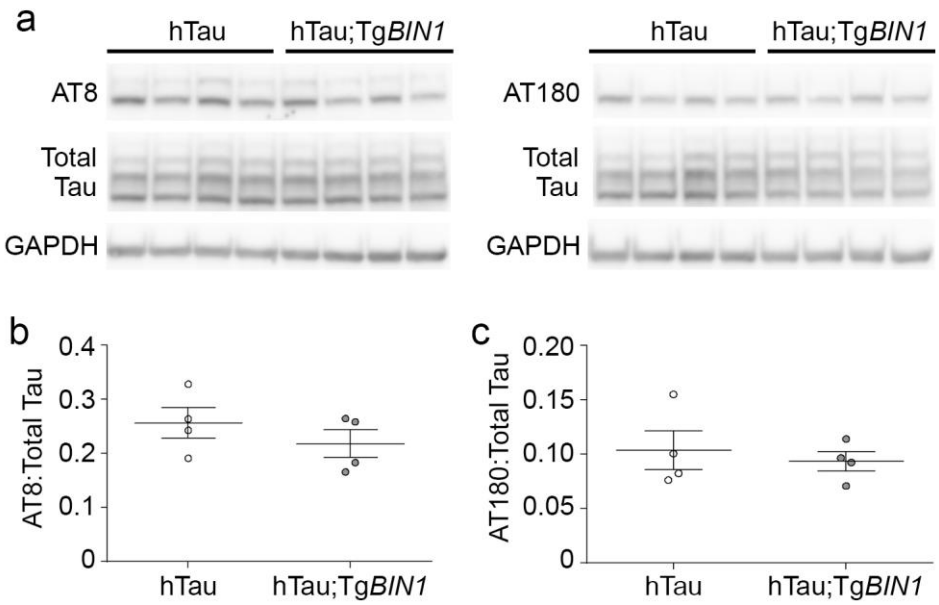

Fig. S11 BIN1 does not impact the levels of soluble phospho-Tau proteins. **a**. Western blots of hippocampal lysates from 18-month-old hTau and hTau;Tg*BIN1* male mice, labeled with antibodies detecting total Tau protein (total Tau), p-Ser202/p-Thr205 Tau (AT8) or p-Thr231 Tau (AT180), and GAPDH. Quantification of phospho-Tau over total Tau signal intensities for AT8 (**b**) and AT180 (**c**) antibodies.

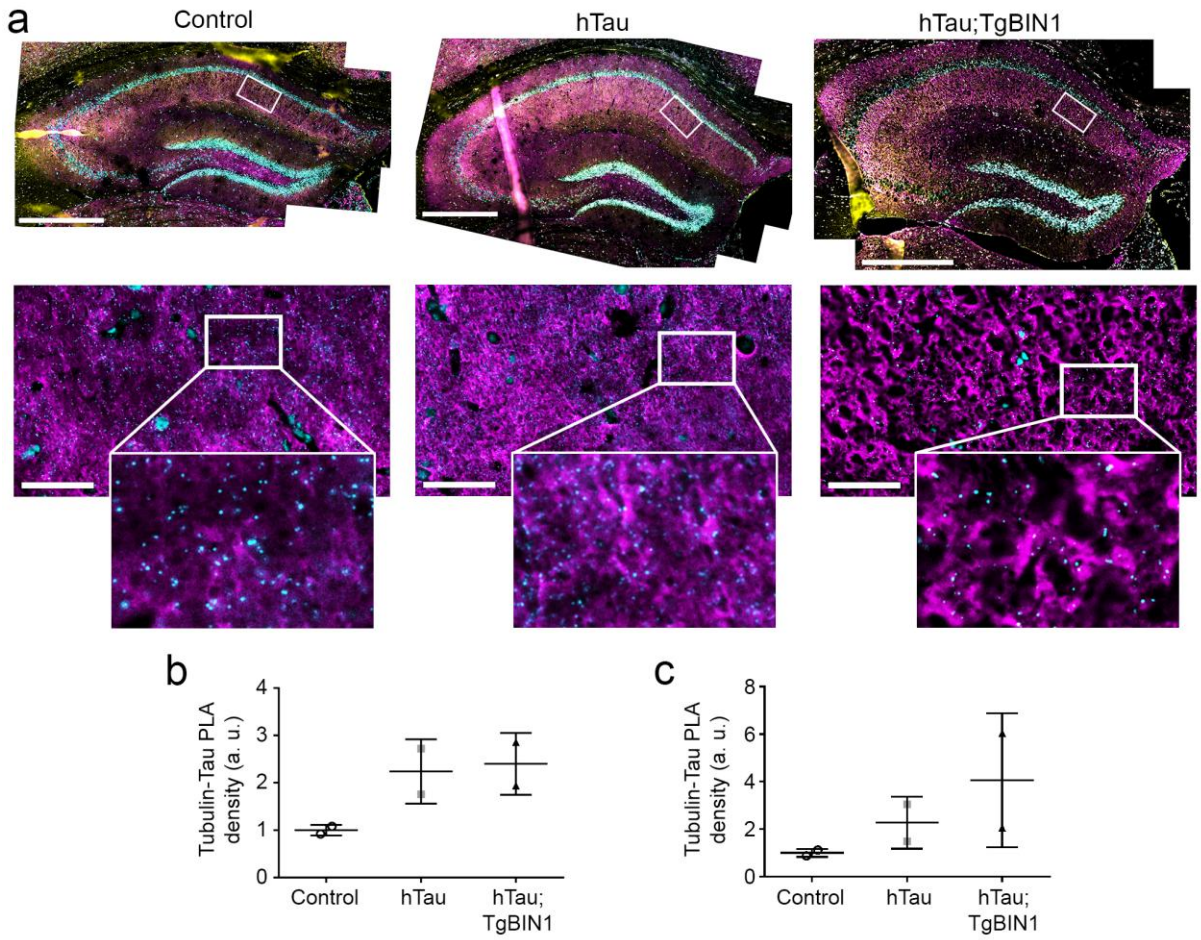

Fig. S12 Tubulin-Tau PLA in brain slices. **a.** Tubulin-Tau PLA (cyan), and Tubulin (yellow), Tau (magenta), and Hoechst (white) stainings in the hippocampi of control, hTau and hTau;Tg*BIN1* males at 18 months. Zoomed areas show PLA and Tau channels only. Scale bars = 500 µm; zooms, 50 µm. **b-c.** Quantification of the Tubulin-Tau PLA density. Data expressed as PLA spot number per tissue area (B) or total PLA spot volume per tissue area (C), normalized with control mean (control, n=2; hTau, n=2; hTau;Tg*BIN1*, n=2).

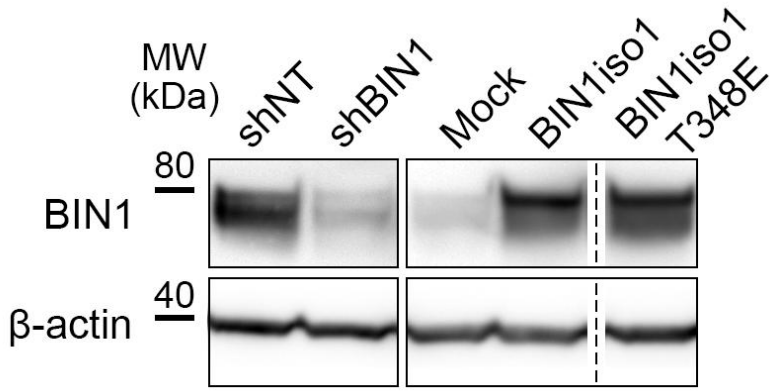

Fig. S13 Expression of BIN1 after transduction with BIN1 constructs. Representative Western blots showing BIN and β-actin protein levels in PNC at DIV14 after transduction at DIV8. Bands showing shNT and shBIN1 are from the same membrane as the other constructs, but with longer exposure to reveal the shBIN1 band.

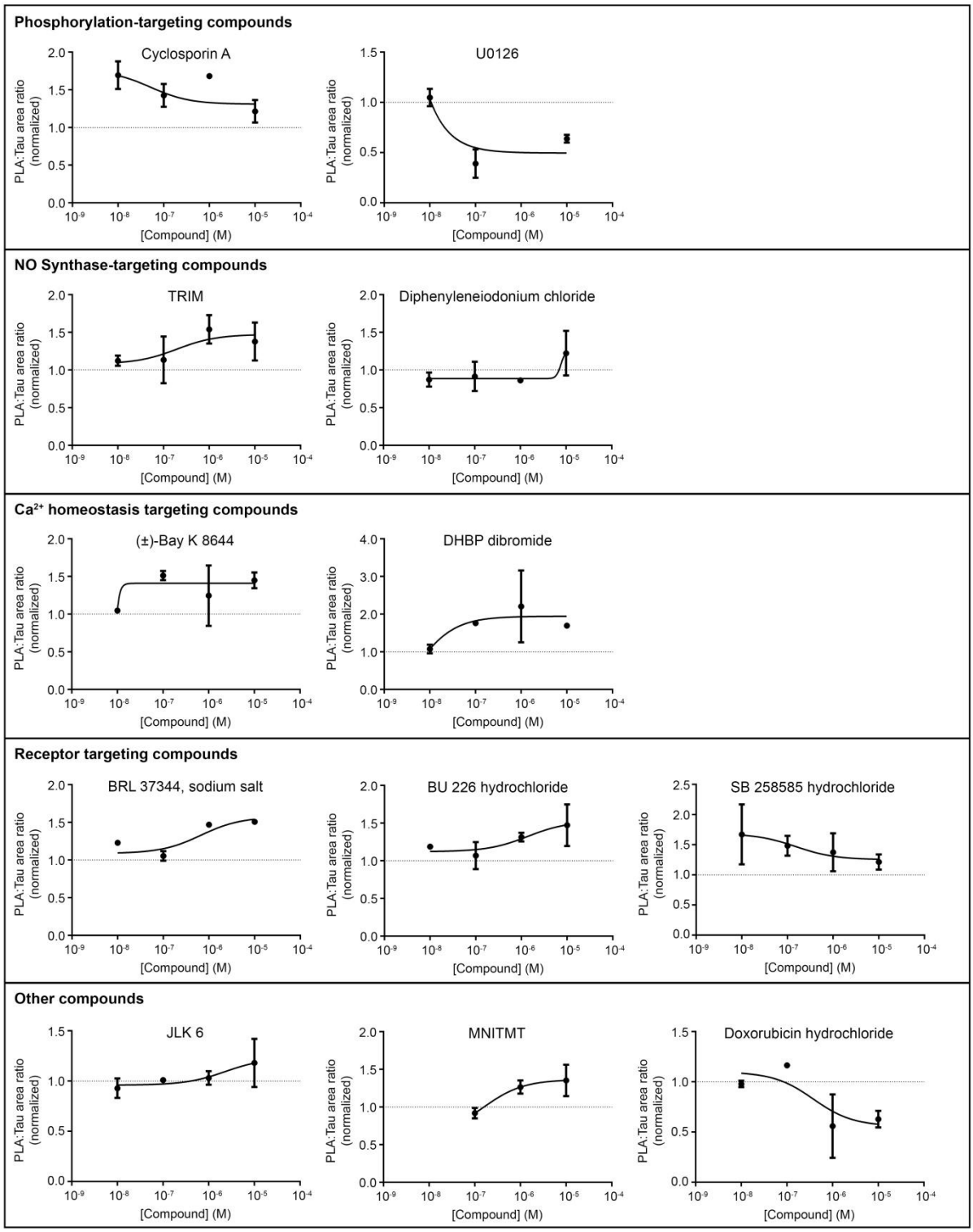

Fig. S14 Dose-response curves for the 12 shortlisted compounds grouped according to their targets. See Fig. 4 for details. Phosphorylation targeting compounds: Cyclosporin A, an inhibitor of Calcineurin (through forming a blocking complex with Cyclophilin); U0126, a potent MEK inhibitor. NO-synthase targeting compounds: TRIM, a potent inhibitor of neuronal and inducible NO-synthases; Diphenyleneiodonium chloride, a GPR3 agonist that also inhibits NO-synthase and NADPH oxidase. Ca^{2+} homeostasis targeting compounds: (±)-

Bay K 8644, a L-type Ca^{2+} channel activator; DHBP dibromide, an inhibitor of endoplasmic reticulum Ca^{2+} release. Receptor targeting compounds: BRL37344 sodium salt, a β3 agonist; BU 226 hydrochloride, a potent and highly selective I2 ligand; SB 258585 hydrochloride, a potent and selective 5-HT6 antagonist. Other compounds: JLK6, an inhibitor of γ-secretase-mediated βAPP processing; MNITMT, a non-toxic immunosuppressive agent; Doxorubicin hydrochloride, a tumor suppressor drug shown to inhibit DNA topoisomerase II and reduce Tau cellular levels.

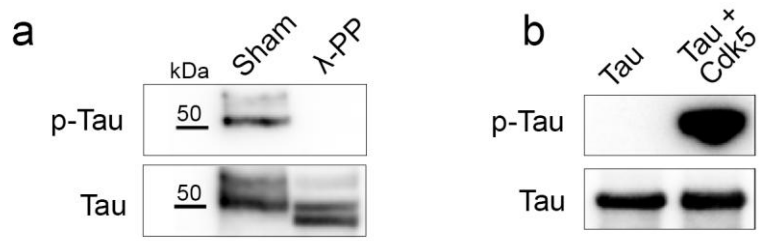

Fig. S15 Modulation of Tau phosphorylation *in vitro*. **a.** Reduction of Tau phosphorylation at Thr 231 after 30 min incubation of PNC crude extracts with lambda protein phosphatase (λ-PP). **b.** *In vitro* phosphorylated recombinant Tau at Thr 231 is observed after incubation with recombinant Cdk5 for 1 h. Cdk2 dependent phosphorylation of Tau at Thr 231 has been published previously (Ref. 49).

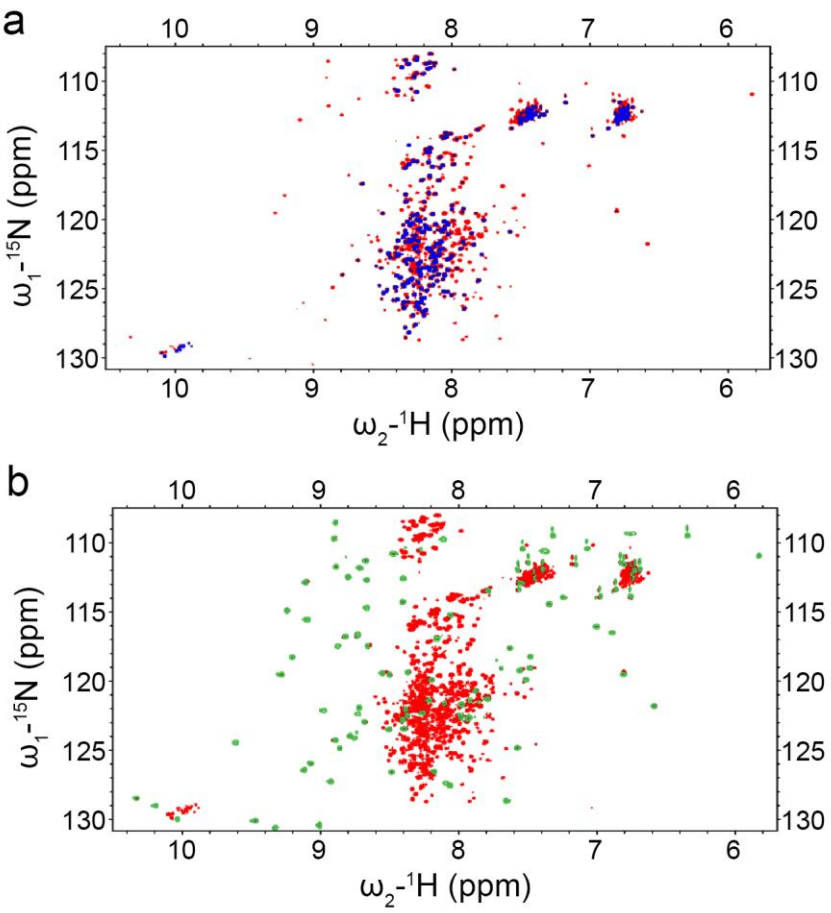

Fig. S16 Additional signals in BIN1iso1-CLAP-T348E matched signals from BIN1 SH3 domain. Overlays of ^{1}H-^{15}N HSQC spectra of (**a**) BIN1iso1-CLAP-T348E protein (in red) and BIN1iso1 protein (superimposed in blue) or of (**b**) BIN1iso1-CLAP-T348E protein (in red) and BIN1 SH3 domain (superimposed in green). In BIN1iso1 spectrum, in blue, due to the large size of the BIN1iso1 protein, only signals corresponding to mobile disordered regions are detected. These signals show a typical poor dispersion on the ^{1}H scale (ca. 7.5-8.5 ppm). Due to this intrinsic need of mobility to detect protein NMR signals, the SH3-BIN1 resonance are only detected when the domain behaves independently of the full protein, as is observed for BIN1iso1-CLAP-T348E (in red). Signals from the SH3-BIN1 domain show a good dispersion on the ^{1}H scale (ca. 6.5-9.5 ppm), as expected for globular domain signals. The additional signals observed in BIN1iso1-CLAP-T348E, in red, matched signals from the SH3-BIN1 domain, in green.

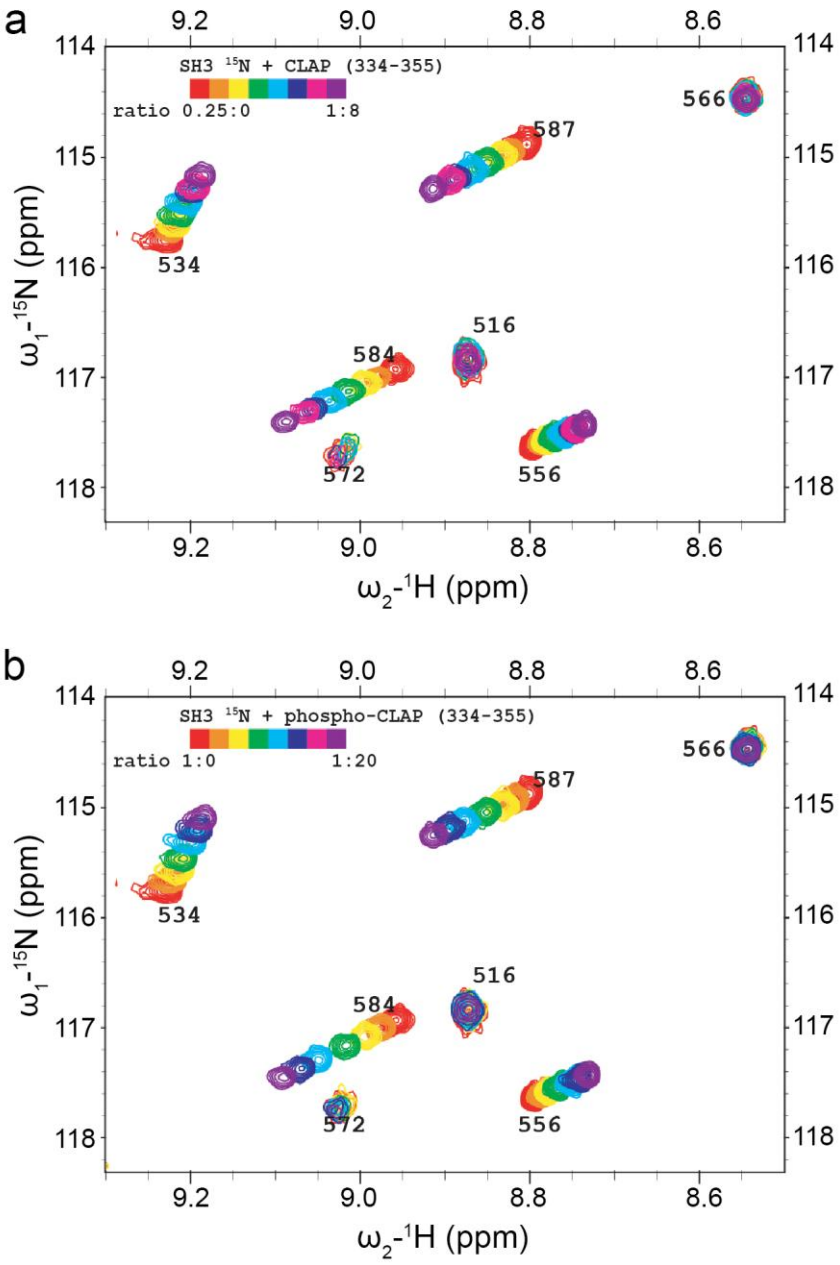

Fig. S17 Titration of ^{15}N-BIN1-SH3 with CLAP peptides. Detail of overlayed ^{1}H-^{15}N HSQC spectra of BIN1-SH3 domain, in the presence of increasing amount of (**a**) CLAP (334-355) peptide, molar ratios 0.25 to 8 (color scale, from red to violet), or of (**b**) phospho-CLAP (334-355) peptide, molar ratios 1 to 20 (color scale, from red to violet). One spectrum was recorded for each titration point. The gradual change of the chemical shift value for each resonance was then used to build a saturation curve (see Fig. 5g). Data were averaged to estimate the K_d values. Note that a larger excess of phospho-CLAP (334-355) peptide was needed to reach saturation, due to its lower affinity for BIN1-SH3 domain, compared to the non-phosphorylated peptide.

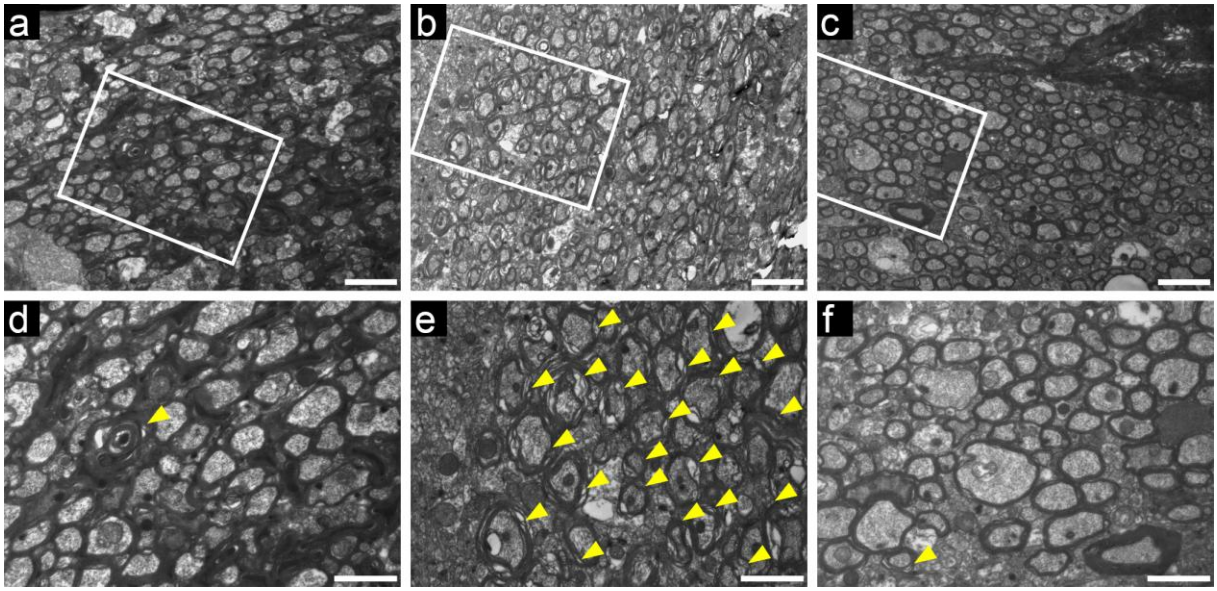

Fig. S18 Myelin alterations following hTau overexpression was prevented upon BIN1 overexpression. **a-c.** Electron microscopy analysis of the myelinated axons in the fornices of 18-month-old control (A), hTau (B), and hTau;Tg*BIN1* (C) males. **d-f.** Serial magnification of the marked areas. Arrowheads point to myelin abnormalities defined by multiple myelin rings. Micrographs are representative of 2 animals per genotype. Scale bars = 5 µm (a-c) and 2 µm (d-f).

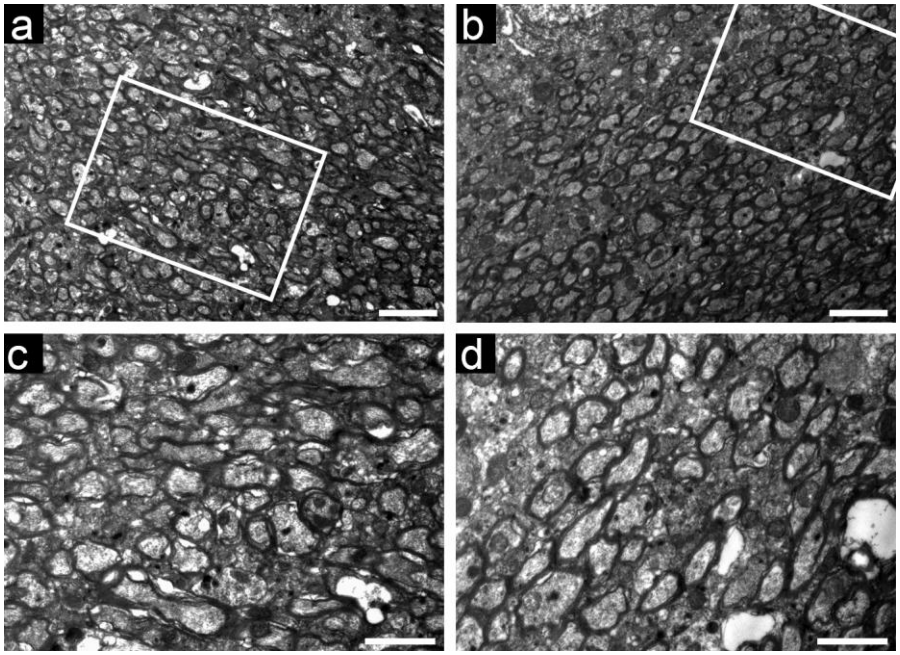

Fig. S19 Myelin structure is unaffected following BIN1 overexpression. **a-b.** Electron microscopy analysis of the myelinated axons in the fornices of 18-month-old *Mapt*$^{-/-}$;Tg*BIN1* (A) and *TgBIN1* (B) males. **c-d.** Serial magnification of the marked areas. Micrographs are representative of 2 animals per genotype. Scale bars = 5 µm (a-b) and 2 µm (c-d).

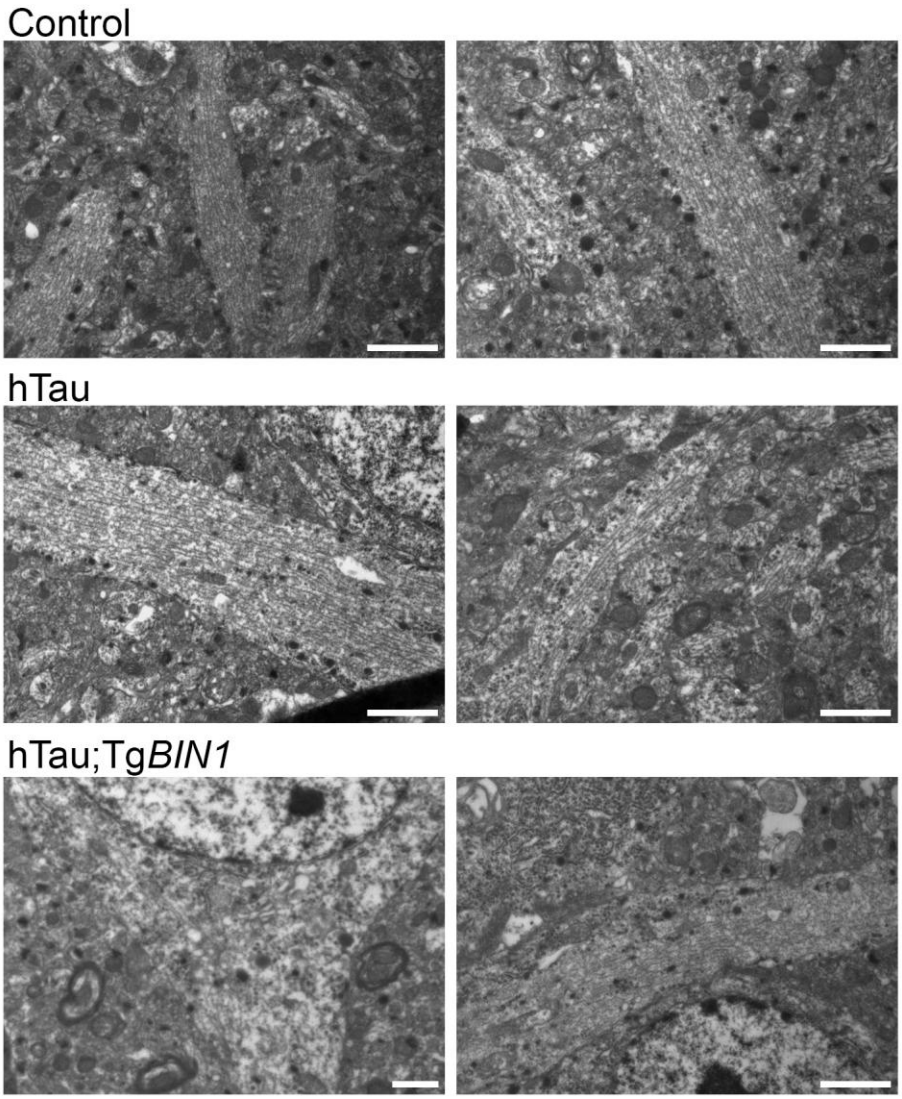

Fig. S20 Axonal ultrastructure is unaffected in transgenic mice. Electron microscopy analysis of axon fibers in the hippocampal CA1 region of 18-month-old control, hTau, and hTau;Tg*BIN1* males. Micrographs are representative of 2 animals per genotype. Scale bars = 2 µm.

Discussion and Conclusions

To better understand the interaction between BIN1 and Tau, we aimed to identify the interaction sites between BIN1 and Tau and how the interaction could be modulated, highlight the molecular pathways that could be involved in the modulation of BIN1-Tau interaction, and understand how BIN1-Tau interaction is involved in AD pathophysiological process.

Here, we reported that BIN1 and Tau interact through the binding of BIN1-SH3 domain and Tau-PRD, that this interaction is dependent of BIN1 and Tau phosphorylation levels and BIN1 protein levels and conformation, and that BIN1-Tau interaction occurs in the vicinity of actin cytoskeleton. We show that the previously reported conformational change observed in the neuronal isoform of BIN1 (Malki et al. 2017) is regulated by the phosphorylation of BIN1 at T348, a residue in the PRD of BIN1-CLAP domain: phosphorylation of BIN1 T348 releases BIN1-SH3 domain from its intramolecular interaction with BIN1-CLAP-PRD, leading to an open conformation of BIN1iso1 and subsequent availability to interact with other proteins, e.g. Tau. Similarly, phosphorylation of Tau at T231, in the PRD of Tau, abolishes the interaction between BIN1-SH3 and Tau-PRD. Interestingly, we observed that Cdk5, a kinase known to be deregulated in AD (Shukla, Skuntz, and Pant 2012), was able to phosphorylate both BIN1 T348 and Tau T231 *in vitro*, suggesting that the interaction between BIN1 and Tau is highly dynamic and probably subject to complex regulation.

In order to identify molecular pathway that could be involved in BIN1-Tau interaction, we developed a novel, semi-automated, HCS compound-based approach that used PNC as cellular model and PLA as the readout of BIN1-Tau interaction, and identified a few compounds that targeted molecular pathways such as NO-synthase activity, Ca^{2+} homeostasis, MAPK signalling pathway, and Calcineurin signalling. We decided to further validate the compounds Cyclosporin A (CsA), an inhibitor of Calcineurin phosphatase activity and U0126, an inhibitor of MEK1/2, and observed that while CsA increased the interaction by increasing BIN1 phosphorylation at T348, U0126 decreased BIN1-Tau interaction by increasing Tau phosphorylation levels at T231. Once again, the phosphorylation of BIN1 and Tau PRDs had opposite effect in regulation of BIN1-Tau interaction.

Using a mouse model of tauopathy, we observed that the overexpression of BIN1 neuronal isoforms, although exacerbated short-term memory deficits since young age, rescued the Tau induced behavioural phenotypes in long-term and spatial memory at the later age. This rescue was associated with a clear reduction of intracellular inclusions of Tau and with a drastic increase of BIN1-Tau interaction in the hippocampus. These results suggest a potential protective impact of the overexpression of BIN1 neuronal isoforms in the pathophysiological processes of AD, possibly linked with the increase of BIN1-Tau interaction. Finally, we showed that BIN1 neuronal isoform is decreased in brains of post-mortem AD patients, as previously reported (De Rossi et al. 2016; Holler et al. 2014; Glennon et al. 2013), and (surprisingly) the levels of BIN1 phosphorylated at T348, relative to BIN1iso1, were increased when compared to controls, suggesting that this site might also be involved in AD process.

Altogether, our data indicate that BIN1-Tau interaction is complex, dynamic, loci specific, and its regulation, especially through the phosphorylation of BIN1 and Tau, is somehow involved in the pathophysiological process of AD, but it is not yet clear if this interaction is protective or deleterious. The fact that BIN1 overexpression modulated Tau phenotype by increasing short-term memory deficits and rescuing long-term deficits suggest a potential equilibrium between BIN1 and Tau levels may differ in spatial and temporal dimensions. Indeed, both short- and long-term memory processes require the hippocampus, but they take part in different cortical regions, i.e. lateral entorhinal and medial entorhinal cortex respectively (Van Cauter et al. 2013). Interestingly, the rescue of long-term memory deficits by BIN1 overexpression was associated with the strong reduction of Tau inclusions and a strong increase of BIN1-Tau interaction. Since we developed a cohort study, it was only possible to evaluate the levels of Tau phosphorylation and BIN1-Tau interaction after the behavioural experiments (18 months). Although we observed that BIN1 overexpression had no impact on soluble phosphorylated Tau at this age of the mouse model, it has been previously shown that this hTau mouse model develop inclusions of phosphorylated Tau in the hippocampus as early as 4 months (Polydoro et al. 2009), and supplementary cytochemical and biochemical analysis, at earlier age of this mouse model, is necessary to fully understand the role of BIN1 expression on Tau phosphorylation, before tangle formation. Nonetheless these results suggest that the increase of BIN1 Tau

interaction levels may be protective against the re-localization and accumulation of phosphorylated Tau, a major hallmark of AD.

Although it had previously been demonstrated that BIN1 mRNA levels were increased in the brains of AD patients carrying the polymorphism rs59335482, when compared to controls (J Chapuis et al. 2013), that observation had not been associated with any specific isoform of BIN1, and posterior publications reported the underexpression of BIN1 neuronal isoform and the overexpression of the ubiquitous isoform of BIN1 in the post-mortem brains of AD patients (Glennon et al. 2013; Holler et al. 2014; De Rossi et al. 2016), which suggests that this increase in mRNA levels of BIN1 could lead to an increase of the ubiquitous and not the neuronal isoform. In line with those findings, we observed that the protein levels of BIN1 neuronal isoform were reduced in the brains of AD patients, when compared with controls. Since the main isoforms of BIN1 expressed in our mouse model are the neuronal isoforms, this data strengthens the idea that the specific overexpression of the neuronal isoforms of BIN1 might be protective, and we may thus postulate that the overexpression of brain isoforms in the Tg*BIN*1 mouse reverses, or at least arrests, a neuropathological process that occurs in AD brains. Unfortunately, neither this study nor previous publications assessed the presence of BIN1 polymorphisms in the samples used to assess BIN1 protein levels, so the association between BIN1 mRNA and protein isoforms levels cannot be confirmed.

Noteworthy, BIN1's protective effect could be partially explained by other mechanisms than BIN1-Tau interaction in neurons. In fact, we observed that BIN1 overexpression also rescued myelin abnormalities, present in the tauopathy mouse model, and had no effect on myelin when overexpressed alone. Thus, the memory deficits observed when overexpressing Tau may also be associated with these myelin abnormalities and rescued with BIN1 overexpression, in line with previous works linking Tau to potential myelin dysfunctions in tauopathies (Ferrer 2018) and reporting that BIN1 was strongly expressed in oligodendrocytes (De Rossi et al. 2016). In this last study, the authors used combinations of antibodies that do not recognise BIN1 neuronal isoform with antibodies that recognize almost all the isoforms of BIN1 and show, through IF and WB, that BIN1 iso9 is predominantly expressed in oligodendrocytes and is more expressed in AD cases than in control patients. Although they were not assessed in this study, we cannot exclude that the

mechanisms associated with the physiological roles of BIN1 in the regulation of endocytosis and recycling endosome pathway, shown to be associated with Tau propagation and Aβ production (Miyagawa et al. 2016; Ubelmann et al. 2017; Calafate et al. 2016), could also be deregulated in our animal models of tauopathy and be rescued by BIN1 overexpression, leading to the phenotypical and behavioural changes observed.

Moving forward from these possibilities, identifying the molecular mechanisms that regulate BIN1-Tau interaction might be highly important to understand the pathophysiological process of AD. In this regard, we defined the BIN1-SH3 domain and the Tau-PRD as the interaction sites of these proteins, and identified two major regulatory elements of BIN1-Tau interaction, the phosphorylation of BIN1 at T348 and the phosphorylation of Tau at T231, with opposite impacts on this interaction: while phosphorylation of Tau at T231 abrogates BIN1-Tau interaction, phosphorylation of BIN1 at T348 promotes its occurrence.

Tau T231 seems to play a central role in the regulation of Tau phosphorylation state: phosphorylation at S235 primes phosphorylation of T231 (Li et al. 2006); T231 is more easily phosphorylated when free than in association with microtubules and it is enough to dissociate Tau from the microtubules (Sengupta et al. 2006); phosphorylation at T231 inhibits dephosphorylation of S202/T205 (Landrieu et al. 2011); and phosphorylation of S202/T205 can induce Tau aggregation (Despres et al. 2017). Besides, enzymes that control this phosphorylation(s) (e.g. Cdk5, Gsk-3β, PP2A) are clearly deregulated during AD process (Iqbal, Liu, and Gong 2016).

On the other hand, the phosphorylation of BIN1 at T348 has never been described and its role is not known. However, it has recently been shown that the neuronal isoform of BIN1 is involved in intramolecular interaction between its SH3 domain and its CLAP domains, notably with a proline-rich region (Malki et al. 2017). In this work, we demonstrate that phosphorylation of BIN1 at T348 is enough to abolish that intramolecular interaction and promote the interaction of BIN1 with Tau. Moreover, we detected an increase of the relative levels of BIN1 phosphorylated at T348, in the brain samples of AD patients and increasing with Braak sage. Interestingly these findings indicate that while the global levels of BIN1 neuronal isoform is decreased, a higher fraction of this isoform is phosphorylated at

T348 in AD brains, thus suggesting that this increase in phosphorylation may occur as an attempt to compensate the decrease of BIN1 neuronal isoform and maintain the interaction between BIN1 and Tau. Independently of the mechanisms potentially involved, these observations suggest that phosphorylation of BIN1 at T348 may be involved in the pathophysiological process of AD.

Using an HCS approach, we identified several compounds that were able to modulate BIN1-Tau interaction in a concentration dependent manner, thus suggesting that these compounds were modulators of this interaction, either directly or through their target pathways. Noteworthy, several of the targets identified in our HCS approach are known to be deregulated in AD, such as NO-synthase (NOS) activity, Ca^{2+} homeostasis, Calcineurin, MEK1/2, Aβ production and Tau (L. Zhou and Zhu 2009; Norris 2018; O'Day, Eshak, and Myre 2015; Nisbet et al. 2015; Pei et al. 2002). Moreover, several of these targets seem to interact or at least share pathways, such as the case of the NOS regulation by Ca^{2+} levels via Calmodulin (Tricoire and Vitalis 2012), the β3-adrenergic receptor regulation of NOS activity in myocytes (Watts et al. 2013), and the Calcineurin association to dephosphorylation of Tau and NOS (Rameau, Chiu, and Ziff 2003; O'Day, Eshak, and Myre 2015). This data, together with the identification of Tau T231 and BIN1 T348 as key regulatory elements of BIN1-Tau interaction, corroborate the idea that this interaction is highly complex, both in its regulation and its function, in physiology and AD process, potentially controlled by numerous actors capable of modify the phosphorylation levels of both BIN1 and Tau. Thus, further investigation on the signalling mechanisms involved in BIN1-Tau interaction is warranted.

The divergent role of BIN1 and Tau phosphorylation in their interaction is highlighted in our HCS approach, which revealed that the inhibition of MEK1/2 leads to a decrease in BIN1-Tau interaction through the increase of Tau T231 phosphorylation levels, whereas the inhibition of Calcineurin phosphatase activity favours it by increasing the phosphorylation levels of BIN1 at T348. The complexity involved in the regulation of BIN1-Tau interaction can be further illustrated by the regulation of phosphorylation through cyclin-dependent kinases, especially Cdk5: Cdk5 is able to phosphorylate both BIN1 at T348 and Tau at T231 and we showed that he phosphorylation of these two epitopes had opposite effects on BIN1-Tau interaction. Thus, we proposed that Cdk5 phosphorylates BIN1 at T348, allowing

BIN1 to change its conformation and increase its affinity towards Tau, then Tau interacts with BIN1 and is subsequently phosphorylated by Cdk5 at T231, abolishing the interaction and releasing phosphorylated BIN1 and phosphorylated Tau.

This proposed pathway illustrates the challenge for the development or testing of drugs targeting the modulation of BIN1-Tau interaction: in this case, targeting the kinase alone could have very little or no effect in the modulation of the interaction. On the other hand, the inhibitor of Calcineurin phosphatase activity, CsA, is a compound of interest to study the modulation of BIN1-Tau interaction: upon inhibition of Calcineurin activity we observed a strong increase of the interaction associated with the increase of BIN1 T348 phosphorylation, but not so much of Tau T231. Therefore, a better understanding of the mechanisms involved in BIN1-Tau interaction is needed.

Of notice, Cdk5 is deregulated in AD (Shukla, Skuntz, and Pant 2012), and it has been shown that free Tau phosphorylated at T231 could initiate a cascade of phosphorylation, and/or inhibition of dephosphorylation, of other epitopes in Tau protein that would lead to Tau abnormal phosphorylation. Therefore, a thigh regulation of BIN1-Tau interaction levels, and of BIN1 T348 and Tau T231 phosphorylation levels, could be influential in avoiding the development of pathophysiological processes of AD.

In this regard, it has been shown that the neuronal isoforms of BIN1 exist in phosphorylated state in resting nerve terminals and, in order to interact with its endocytic partners, is rapidly dephosphorylated by Calcineurin upon membrane depolarization and/or stimulation of exo/endocytosis (Patrick Wigge and McMahon 1998; Marks and McMahon 1998; P Wigge et al. 1997), and this dephosphorylation is enhanced in a Ca^{2+}-dependent manner when a burst of endocytic activity is needed (Bauerfeind, Takei, and De Camilli 1997; Slepnev et al. 1998). Although the phosphorylation sites of BIN1 neuronal isoform involved in this process have never been identified, it was shown that the phosphorylation of Amphiphysin I by Cdk5, at T310 and other sites, was implicated in membrane binding and endocytosis (Tomizawa et al. 2003; Liang et al. 2007). Since the sequence surrounding T310 of Amphiphysin I is very similar to the sequence around T348 of the neuronal isoform of BIN1, we could postulate that this phosphorylation site could be involved not only in the regulation of BIN1-Tau interaction but also be involved in modulating BIN1's availability to

regulate endocytosis. Thus, it would be interesting to know if Calcineurin alone would be able to dephosphorylate BIN1 during its interaction with Tau or if it needed a disruption of BIN1-Tau interaction in order to dephosphorylate BIN1 and initiate its regulation of endocytic pathway.

These extrapolations, together with the partial co-localization of BIN1-Tau interaction with actin suggest that BIN1-Tau interaction may play a role in the interface between actin cytoskeleton and the recycle and endocytic machinery. The fact co-localization of BIN1-Tau interaction with endocytic and synaptic markers was not observed indicates that the interaction is not involved in the formation, or at least stabilization, of these structures. However, the participation of BIN1-Tau interaction in recycling and endocytic pathways cannot be completely excluded because the cells were not stimulated and the interaction might have not been required at that time. Interestingly it was shown that underexpression of BIN1 iso1 increased Clathrin-mediated endocytosis and promoted Tau pathology propagation (Calafate et al. 2016), but nothing was assessed regarding the development of Tau pathology. Moreover, it was also shown that underexpression of BIN1 iso1 increased the amounts of BACE1 and Aβ formation (Miyagawa et al. 2016) and that this effect was due to the accumulation of BACE1 on axonal early endosomes (Ubelmann et al. 2017), which could be a mechanism leading to the development of AD.

This work aimed to shed light onto the role of BIN1-Tau interaction through the identification of its modulators and molecular pathways involved in it.

Although it was not yet possible to unveil the role of BIN1-Tau interaction in physiology and/or in AD pathophysiological process, it is possible to clearly say that BIN1-Tau interaction and its regulation is somehow involved in the pathophysiological process of AD. We identified the protein domains involved in BIN1-Tau interaction and that the phosphorylation of both proteins modulated the interaction with opposite effects: phosphorylation of BIN1 at T348 leads to a conformational shift of the protein, increasing its affinity towards Tau and, increasing the interaction, whereas Tau phosphorylation at T231 reduces the affinity of BIN1-SH3 domain towards Tau PRD, decreasing the interaction.

This is the first time that the impact of the overexpression of BIN1, a major genetic risk factor of AD, is characterized in a model of tauopathy, and our data also suggests that the overexpression of BIN1 might have a protective impact on the AD process. However, whether this potential protective effect is linked with BIN1-Tau interaction or associated to a function of BIN1 (e.g. regulation of endocytosis and recycling endosome pathway) is still to be assessed; but it is definitely and strongly dependent on the phosphorylation statuses of both BIN1 and Tau proteins. Furthermore, it is recommended to perform immunohistochemical and biochemical analysis in younger animals of this model, to understand the role of BIN1 overexpression at earlier stages of AD development and to discriminate between causal and consequential events.

Although HCS approaches require extensive work and time dedicated to protocol and analysis optimization, they quickly provide large amounts of data that allow the simultaneous analysis of hundreds to thousands of experimental conditions, and minimize/optimize the number of hypotheses to be further tested, being one of the strongest tools currently available to study the role of AD-associated GWAS-defined genes. Thus, we developed a novel, semi-automated HCS approach, employing PNC as cellular model and PLA as readout of BIN1-Tau interaction (the first time these techniques are employed together with HCS), to identify molecular mechanisms that may be involved in BIN1-Tau interaction, such as NOS activity, Ca^{2+} homeostasis, Calcineurin and MEK1/2 signalling. Interestingly, all these molecular pathways are dysregulated in AD, and their involvement in BIN1-Tau interaction, in physiology or in the AD context, are worth of further investigation.

There is no more doubt that BIN1 is a major genetic risk factor of AD, but there is still much more to learn about its role and the role of BIN1-Tau interaction in the pathophysiological process of AD. Therefore, future work in the lab will involve the development of imaging strategies that will allow the identification of BIN1-Tau interaction relative position in the neurons, and the setting up of experiments to dissect molecular pathways, identified in our HCS approach, with possible involvement in BIN1-Tau interaction.

Bibliography

Adams, Stephanie L., Kathy Tilton, James A. Kozubek, Sudha Seshadri, and Ivana Delalle. 2016. “Subcellular Changes in Bridging Integrator 1 Protein Expression in the Cerebral Cortex During the Progression of Alzheimer Disease Pathology.” *Journal of Neuropathology & Experimental Neurology* 75 (8):779–90. https://doi.org/10.1093/jnen/nlw056.

Al-Bassam, Jawdat, Rachel S. Ozer, Daniel Safer, Shelley Halpain, and Ronald a. Milligan. 2002. “MAP2 and Tau Bind Longitudinally along the Outer Ridges of Microtubule Protofilaments.” *Journal of Cell Biology* 157 (7):1187–96. https://doi.org/10.1083/jcb.200201048.

Alzheimer’s Association. 2015. “2015 Alzheimer’s Disease Facts and Figures.” *Alzheimer’s & Dementia*. Vol. 11. Elsevier Ltd. https://doi.org/10.1016/j.jalz.2015.02.003.

Andorfer, Cathy, Yvonne Kress, Marisol Espinoza, Rohan De Silva, Kerry L. Tucker, Yves Alain Barde, Karen Duff, and Peter Davies. 2003. “Hyperphosphorylation and Aggregation of Tau in Mice Expressing Normal Human Tau Isoforms.” *Journal of Neurochemistry* 86 (3):582–90. https://doi.org/10.1046/j.1471-4159.2003.01879.x.

Armstrong, R a. 2011. “The Pathogenesis of Alzheimer’s Disease: A Reevaluation of the ‘Amyloid Cascade Hypothesis’.” *International Journal of Alzheimer’s Disease* 2011 (January). Hindawi Publishing Corporation:630865. https://doi.org/10.4061/2011/630865.

Augustinack, Jean C., Anja Schneider, Eva Maria Mandelkow, and Bradley T. Hyman. 2002. “Specific Tau Phosphorylation Sites Correlate with Severity of Neuronal Cytopathology in Alzheimer’s Disease.” *Acta Neuropathologica* 103 (1):26–35. https://doi.org/10.1007/s004010100423.

Bagchi, Sonchita, Robert Fredriksson, and Åsa Wallén-Mackenzie. 2015. “In Situ Proximity Ligation Assay (PLA).” *Methods in Molecular Biology* 1318 (January):149–59. https://doi.org/10.1007/978-1-4939-2742-5_15.

Baker, Matt, Irene Litvan, Henry Houlden, Jennifer Adamson, Dennis Dickson, Jordi Perez-Tur, John Hardy, Timothy Lynch, Eileen Bigio, and Mike Hutton. 1999. “Association of an Extended Haplotype in the Tau Gene with Progressive Supranuclear Palsy.” *Human Molecular Genetics* 8 (4):711–15. https://doi.org/10.1093/hmg/8.4.711.

Ballatore, Carlo, Virginia M.Y. Lee, and John Q. Trojanowski. 2007. “Tau-Mediated Neurodegeneration in Alzheimer’s Disease and Related Disorders.” *Nature Reviews Neuroscience* 8 (9):663–72. https://doi.org/10.1038/nrn2194.

Bauerfeind, Rudolf, Kohji Takei, and Pietro De Camilli. 1997. “Amphiphysin I Is Associated with Coated Endocytic Intermediates and Undergoes Stimulation-Dependent

Dephosphorylation in Nerve Terminals." *Journal of Biological Chemistry* 272 (49):30984–92. https://doi.org/10.1074/jbc.272.49.30984.

Benilova, Iryna, Eric Karran, and Bart De Strooper. 2012. "The Toxic Aβ Oligomer and Alzheimer's Disease: An Emperor in Need of Clothes." *Nature Neuroscience* 15 (3). Nature Publishing Group:349–57. https://doi.org/10.1038/nn.3028.

Benitez, Bruno a., Sheng Chih Jin, Rita Guerreiro, Rob Graham, Jenny Lord, Denise Harold, Rebecca Sims, et al. 2014. "Missense Variant in TREML2 Protects against Alzheimer's Disease." *Neurobiology of Aging* 35 (6). https://doi.org/10.1016/j.neurobiolaging.2013.12.010.

Bennett, Rachel E., Sarah L. DeVos, Simon Dujardin, Bianca Corjuc, Rucha Gor, Jose Gonzalez, Allyson D. Roe, et al. 2017. "Enhanced Tau Aggregation in the Presence of Amyloid B." *The American Journal of Pathology* 187 (7):1601–12. https://doi.org/10.1016/j.ajpath.2017.03.011.

Bettens, Karolien, Nathalie Brouwers, Sebastiaan Engelborghs, Jean Charles Lambert, Ekaterina Rogaeva, Rik Vandenberghe, Nathalie Le Bastard, et al. 2012. "Both Common Variations and Rare Non-Synonymous Substitutions and Small Insertion/deletions in CLU Are Associated with Increased Alzheimer Risk." *Molecular Neurodegeneration* 7 (1):1–12. https://doi.org/10.1186/1750-1326-7-322248099.

Bhaskar, Kiran, Shu Hui Yen, and Gloria Lee. 2005. "Disease-Related Modifications in Tau Affect the Interaction between Fyn and Tau." *Journal of Biological Chemistry* 280 (42):35119–25. https://doi.org/10.1074/jbc.M505895200.

Biswas, Sayantanee, and Katherine Kalil. 2017. "The Microtubule Associated Protein Tau Mediates the Organization of Microtubules and Their Dynamic Exploration of Actin-Rich Lamellipodia and Filopodia of Cortical Growth Cones." *The Journal of Neuroscience* 38 (2):2281–17. https://doi.org/10.1523/JNEUROSCI.2281-17.2017.

Blokzijl, A., R. Nong, S. Darmanis, E. Hertz, U. Landegren, and M. Kamali-Moghaddam. 2014. "Protein Biomarker Validation via Proximity Ligation Assays." *Biochimica et Biophysica Acta - Proteins and Proteomics* 1844 (5). Elsevier B.V.:933–39. https://doi.org/10.1016/j.bbapap.2013.07.016.

Böhm, Johann, Nasim Vasli, Marie Maurer, Belinda Cowling, G. Diane Shelton, Wolfram Kress, Anne Toussaint, et al. 2013. "Altered Splicing of the BIN1 Muscle-Specific Exon in Humans and Dogs with Highly Progressive Centronuclear Myopathy." *PLoS Genetics* 9 (6). https://doi.org/10.1371/journal.pgen.1003430.

Braak, H., and E. Braak. 1991. "Neuropathological Stageing of Alzheimer-Related Changes." *Acta Neuropathologica* 82 (4):239–59. https://doi.org/10.1007/BF00308809.

Braak, Heiko, and Kelly Del Tredici. 2012. "Where, When, and in What Form Does Sporadic Alzheimer's Disease Begin?" *Current Opinion in Neurology* 25 (6):708–14. https://doi.org/10.1097/WCO.0b013e32835a3432.

Bradshaw, Elizabeth M., Lori B. Chibnik, Brendan T. Keenan, Linda Ottoboni, Towfique Raj, Anna Tang, Laura L. Rosenkrantz, et al. 2013. "CD33 Alzheimer's Disease Locus: Altered Monocyte Function and Amyloid Biology." *Nature Neuroscience* 16 (7). Nature Publishing Group:848–50. https://doi.org/10.1038/nn.3435.

Bray, Mark-anthony, and Anne Carpenter. 2013. *Advanced Assay Development Guidelines for Image-Based High Content Screening and Analysis*. *Assay Guidance Manual*. Eli Lilly & Company and the National Center for Advancing Translational Sciences. https://doi.org/NBK126174 [bookaccession].

Brettschneider, Johannes, Kelly Del Tredici, Virginia M.-Y. Lee, and John Q. Trojanowski. 2015. "Spreading of Pathology in Neurodegenerative Diseases: A Focus on Human Studies." *Nature Reviews Neuroscience* 16 (2). NIH Public Access:109–20. https://doi.org/10.1038/nrn3887.

Brouwers, N., C. Van Cauwenberghe, S. Engelborghs, J. C. Lambert, K. Bettens, N. Le Bastard, F. Pasquier, et al. 2012. "Alzheimer Risk Associated with a Copy Number Variation in the Complement Receptor 1 Increasing C3b/C4b Binding Sites." *Molecular Psychiatry* 17 (2). Nature Publishing Group:223–33. https://doi.org/10.1039/c3ee42799d.

Buée, Luc, Thierry Bussière, Valérie Buée-Scherrer, André Delacourte, and Patrick R. Hof. 2000. "Tau Protein Isoforms, Phosphorylation and Role in Neurodegenerative Disorders." *Brain Research Reviews* 33 (1):95–130. https://doi.org/10.1016/S0165-0173(00)00019-9.

Butler, Margaret Husta, Carol David, Gian Carlo Ochoa, Zachary Freyberg, Laurie Daniell, Detlev Grabs, Ottavio Cremona, and Pietro De Camilli. 1997. "Amphiphysin II (SH3p9; BIN1), a Member of the amphiphysin/Rvs Family, Is Concentrated in the Cortical Cytomatrix of Axon Initial Segments and Nodes of Ranvier in Brain and around T Tubules in Skeletal Muscle." *Journal of Cell Biology* 137 (6). Rockefeller University Press:1355–67. https://doi.org/10.1083/jcb.137.6.1355.

Calafate, Sara, William Flavin, Patrik Verstreken, and Diederik Moechars. 2016. "Loss of Bin1 Promotes the Propagation of Tau Pathology." *Cell Reports* 17 (4). ElsevierCompany.:931–40. https://doi.org/10.1016/j.celrep.2016.09.063.

Camargo, Luiz Miguel, Xiaohua Douglas Zhang, Patrick Loerch, Ramon Miguel Caceres, Shane D. Marine, Paolo Uva, Marc Ferrer, et al. 2015. "Pathway-Based Analysis of Genome-Wide siRNA Screens Reveals the Regulatory Landscape of App Processing." *PLoS ONE* 10 (2):1–21. https://doi.org/10.1371/journal.pone.0115369.

Cauter, Tiffany Van, Jeremy Camon, Alice Alvernhe, Coralie Elduayen, Francesca Sargolini, and Etienne Save. 2013. "Distinct Roles of Medial and Lateral Entorhinal Cortex in Spatial Cognition." *Cerebral Cortex* 23 (2):451–59. https://doi.org/10.1093/cercor/bhs033.

Chapuis, J, F Hansmannel, M Gistelinck, a Mounier, C Van Cauwenberghe, K V Kolen, F Geller, et al. 2013. "Increased Expression of BIN1 Mediates Alzheimer Genetic Risk by

Modulating Tau Pathology." *Molecular Psychiatry* 18 (February):1225–34. https://doi.org/10.1038/mp.2013.1.

Chapuis, Julien, Amandine Flaig, Benjamin Grenier-Boley, Fanny Eysert, Virginie Pottiez, Gaspard Deloison, Alexandre Vandeputte, et al. 2017. "Genome-Wide, High-Content siRNA Screening Identifies the Alzheimer's Genetic Risk Factor FERMT2 as a Major Modulator of APP Metabolism." *Acta Neuropathologica* 133 (6). Springer Berlin Heidelberg:955–66. https://doi.org/10.1007/s00401-016-1652-z.

Charoenkwan, Phasit, Eric Hwang, Robert W Cutler, Hua-Chin Lee, Li-Wei Ko, Hui-Ling Huang, and Shinn-Ying Ho. 2013. "HCS-Neurons: Identifying Phenotypic Changes in Multi-Neuron Images upon Drug Treatments of High-Content Screening." *BMC Bioinformatics* 14 (Suppl 16):S12. https://doi.org/10.1186/1471-2105-14-S16-S12.

Cline, Erika N., Maria Assunção Bicca, Kirsten L. Viola, and William L. Klein. 2018. "The Aβ Oligomer Hypothesis – Beginning of the Third Decade." *Journal of Alzheimer's Disease*, 1–87. https://doi.org/10.3233/JAD-179941.

Cochran, J. Nicholas, Travis Rush, Susan C. Buckingham, and Erik D. Roberson. 2015. "The Alzheimer's Disease Risk Factor CD2AP Maintains Blood-Brain Barrier Integrity." *Human Molecular Genetics* 24 (23):6667–74. https://doi.org/10.1093/hmg/ddv371.

Coon, Keith D., Amanda J. Myers, David W. Craig, Jennifer A. Webster, John V. Pearson, Diane Hu Lince, Victoria L. Zismann, et al. 2007. "A High-Density Whole-Genome Association Study Reveals That APOE Is the Major Susceptibility Gene for Sporadic Late-Onset Alzheimer's Disease." *Journal of Clinical Psychiatry* 68 (4). [Physicians Postgraduate Press]:613–18. https://doi.org/10.4088/JCP.v68n0419.

Cooper, Daniel J., Giulia Zunino, John L. Bixby, and Vance P. Lemmon. 2017. "Phenotypic Screening with Primary Neurons to Identify Drug Targets for Regeneration and Degeneration." *Molecular and Cellular Neuroscience* 80 (April):161–69. https://doi.org/10.1016/j.mcn.2016.07.001.

Corder, Eh, Am Saunders, Wj Strittmatter, De Schmechel, Pc Gaskell, Gw Small, Ad Roses, Jl Haines, and Ma Pericak-Vance. 1993. "E Type 4 Allele Gene Dose of Apolipoprotein and the Risk of Alzheimer ' S Disease in Late Onset Families." *Science* 261 (5123):921–23.

Crehan, Helen, John Hardy, and Jennifer Pocock. 2013. "Blockage of CR1 Prevents Activation of Rodent Microglia." *Neurobiology of Disease* 54 (5). Elsevier Inc.:139–49. https://doi.org/10.1016/j.nbd.2013.02.003.

Creixell, Pau, Syed Haider, Guanming Wu, Tatsuhiro Shibata, Miguel Vazquez, Ville Mustonen, Abel Gonzalez-perez, et al. 2015. "Pathway and Network Analysis of Cancer Genomes." *Nature Methods* 12 (7):615–21. https://doi.org/10.1038/nmeth.3440.

Cruchaga, Carlos, Celeste M. Karch, Sheng Chih Jin, Bruno a. Benitez, Yefei Cai, Rita Guerreiro, Oscar Harari, et al. 2014. "Rare Coding Variants in the Phospholipase D3

Gene Confer Risk for Alzheimer's Disease." *Nature* 505 (7484). Nature Publishing Group:550–54. https://doi.org/10.1038/nature12825.

Dahlgren, Karie N., Arlene M. Manelli, W. Blaine Stine, Lorinda K. Baker, Grant A. Krafft, and Mary Jo LaDu. 2002. "Oligomeric and Fibrillar Species of Amyloid-B Peptides Differentially Affect Neuronal Viability." *Journal of Biological Chemistry* 277 (35):32046–53. https://doi.org/10.1074/jbc.M201750200.

Dammers, C., M. Schwarten, a. K. Buell, and D. Willbold. 2017. "Pyroglutamate-Modified Aβ(3-42) Affects Aggregation Kinetics of Aβ(1-42) by Accelerating Primary and Secondary Pathways." *Chemical Science* 8 (7):4996–5004. https://doi.org/10.1039/c6sc04797a.

Daub, Aaron, Punita Sharma, and Steven Finkbeiner. 2009. "High-Content Screening of Primary Neurons: Ready for Prime Time." *Curr Opin Neurobiol.* 29 (6):997–1003. https://doi.org/10.1016/j.biotechadv.2011.08.021.Secreted.

Daudin, Rachel, Damien Marechal, Qian Wang, Yoshihumi Abe, Nicolas Bourg, Maxime Sartori, Yann Loe-Mie, et al. 2018. "BIN1 Genetic Risk Factor for Alzheimer Is Sufficient to Induce Early Structural Tract Alterations in Entorhinal Cortex-Dentate Gyrus Pathway and Related Hippocampal Multi-Scale Impairments." *bioRxiv*, January, 1–40. https://doi.org/10.1101/437228.

Decker, Jochen Martin, Lars Krüger, Astrid Sydow, Shanting Zhao, Michael Frotscher, Eckhard Mandelkow, and Eva Maria Mandelkow. 2015. "Pro-Aggregant Tau Impairs Mossy Fiber Plasticity due to Structural Changes and Ca(++) Dysregulation." *Acta Neuropathologica Communications* 3:23. https://doi.org/10.1186/s40478-015-0193-3.

Deijk, Anne-Lieke F. van, Laus M. Broersen, J. Martin Verkuyl, August B. Smit, and Mark H. G. Verheijen. 2017. "High Content Analysis of Hippocampal Neuron-Astrocyte Co-Cultures Shows a Positive Effect of Fortasyn Connect on Neuronal Survival and Postsynaptic Maturation." *Frontiers in Neuroscience* 11 (AUG):1–14. https://doi.org/10.3389/fnins.2017.00440.

Deshpande, Atul, Erene Mina, Charles Glabe, and Jorge Busciglio. 2006. "Different Conformations of Amyloid Beta Induce Neurotoxicity by Distinct Mechanisms in Human Cortical Neurons." *Journal of Neuroscience* 26 (22):6011–18. https://doi.org/10.1523/JNEUROSCI.1189-06.2006.

Despres, Clément, Cillian Byrne, Haoling Qi, François-Xavier Cantrelle, Isabelle Huvent, Béatrice Chambraud, Etienne-Emile Baulieu, et al. 2017. "Identification of the Tau Phosphorylation Pattern That Drives Its Aggregation." *Proceedings of the National Academy of Sciences* 114 (34):201708448. https://doi.org/10.1073/pnas.1708448114.

Dourlen, P., F. J. Fernandez-Gomez, C. Dupont, B. Grenier-Boley, C. Bellenguez, H. Obriot, R. Caillierez, et al. 2017. "Functional Screening of Alzheimer Risk Loci Identifies PTK2B as an in Vivo Modulator and Early Marker of Tau Pathology." *Molecular Psychiatry* 22 (6). Nature Publishing Group:874–83. https://doi.org/10.1038/mp.2016.59.

Dourlen, Pierre, Julien Chapuis, and Jean-Charles Lambert. 2018. “Using High-Throughput Animal or Cell-Based Models to Functionally Characterize GWAS Signals.” *Current Genetic Medicine Reports*. Current Genetic Medicine Reports, 107–15. https://doi.org/doi/10.1007/s40142-018-0141-1.

Dräger, Nina M, Eliana Nachman, Moritz Winterhoff, Stefan Brühmann, Pranav Shah, Taxiarchis Katsinelos, Steeve Boulant, Aurelio A Teleman, Jan Faix, and Thomas R Jahn. 2017. “Bin1 Directly Remodels Actin Dynamics through Its BAR Domain.” *EMBO Reports*, September, e201744137. https://doi.org/10.15252/embr.201744137.

Dunys, Julie, Audrey Valverde, and Frédéric Checler. 2018. “Are N- and C-Terminally Truncated Aβ Species Key Pathological Triggers in Alzheimer’s Disease?” *Journal of Biological Chemistry* 293:jbc.R118.003999. https://doi.org/10.1074/jbc.R118.003999.

Eckermann, Katrin, Maria Magdalena Mocanu, Inna Khlistunova, Jacek Biernat, Astrid Nissen, Anne Hofmann, Kai Schönig, et al. 2007. “The B-Propensity of Tau Determines Aggregation and Synaptic Loss in Inducible Mouse Models of Tauopathy.” *Journal of Biological Chemistry* 282 (43):31755–65. https://doi.org/10.1074/jbc.M705282200.

Elie, Auréliane, Elea Prezel, Christophe Guérin, Eric Denarier, Sacnicte Ramirez-Rios, Laurence Serre, Annie Andrieux, et al. 2015. “Tau Co-Organizes Dynamic Microtubule and Actin Networks.” *Scientific Reports* 5 (1):9964. https://doi.org/10.1038/srep09964.

Evans, Nicholas A., Laura Facci, Davina E. Owen, Peter E. Soden, Stephen A. Burbidge, Rab K. Prinjha, Jill C. Richardson, and Stephen D. Skaper. 2008. “AB1-42 Reduces Synapse Number and Inhibits Neurite Outgrowth in Primary Cortical and Hippocampal Neurons: A Quantitative Analysis.” *Journal of Neuroscience Methods* 175 (1):96–103. https://doi.org/10.1016/j.jneumeth.2008.08.001.

Farrer, Lindsay A., L. Adrienne Cupples, Jonathan L. Haines, Bradley Hyman, Walter A. Kukull, Richard Mayeux, Richard H. Myers, Margaret A. Pericak-Vance, Neil Risch, and Cornelia M. van Duijn. 1997. “Effects of Age, Sex, and Ethnicity on the Association Between Apolipoprotein E Genotype and Alzheimer Disease.” *JAMA* 278 (16):1349. https://doi.org/10.1001/jama.1997.03550160069041.

Felice, Fernanda G. De, and Douglas P. Munoz. 2016. “Opportunities and Challenges in Developing Relevant Animal Models for Alzheimer’s Disease.” *Ageing Research Reviews* 26. Elsevier B.V.:112–14. https://doi.org/10.1016/j.arr.2016.01.006.

Fernandez, Marty A., Kelly M. Biette, Georgia Dolios, Divya Seth, Rong Wang, and Michael S. Wolfe. 2016. “Transmembrane Substrate Determinants for Γ-Secretase Processing of APP CTFβ.” *Biochemistry* 55 (40):5675–88. https://doi.org/10.1021/acs.biochem.6b00718.

Ferreira, I. L., L. M. Bajouco, S. I. Mota, Y. P. Auberson, C. R. Oliveira, and A. C. Rego. 2012. “Amyloid Beta Peptide 1-42 Disturbs Intracellular Calcium Homeostasis through Activation of GluN2B-Containing N-Methyl-D-Aspartate Receptors in Cortical Cultures.” *Cell Calcium* 51 (2). Elsevier Ltd:95–106. https://doi.org/10.1016/j.ceca.2011.11.008.

Ferrer, Isidro. 2018. “Oligodendrogliopathy in Neurodegenerative Diseases with Abnormal Protein Aggregates: The Forgotten Partner.” *Progress in Neurobiology* 169 (March). Elsevier:24–54. https://doi.org/10.1016/j.pneurobio.2018.07.004.

Frandemiche, M L, S De Seranno, T Rush, E Borel, a Elie, I Arnal, F Lante, and a Buisson. 2014. “Activity-Dependent Tau Protein Translocation to Excitatory Synapse Is Disrupted by Exposure to Amyloid-Beta Oligomers.” *J Neurosci* 34 (17):6084–97. https://doi.org/10.1523/JNEUROSCI.4261-13.2014.

Freitas, a. de, S. Banerjee, N. Xie, H. Cui, K. I. Davis, a. Friggeri, M. Fu, E. Abraham, and G. Liu. 2012. “Identification of TLT2 as an Engulfment Receptor for Apoptotic Cells.” *The Journal of Immunology* 188 (12):6381–88. https://doi.org/10.4049/jimmunol.1200020.

Fugier, Charlotte, Arnaud F Klein, Caroline Hammer, Stéphane Vassilopoulos, Ylva Ivarsson, Anne Toussaint, Valérie Tosch, et al. 2011. “Misregulated Alternative Splicing of BIN1 Is Associated with T Tubule Alterations and Muscle Weakness in Myotonic Dystrophy.” *Nature Medicine* 17 (6):720–25. https://doi.org/10.1038/nm.2374.

Fulga, Tudor a., Ilan Elson-Schwab, Vikram Khurana, Michelle L. Steinhilb, Tara L. Spires, Bradley T. Hyman, and Mel B. Feany. 2007. “Abnormal Bundling and Accumulation of F-Actin Mediates Tau-Induced Neuronal Degeneration in Vivo.” *Nature Cell Biology* 9 (2):139–48. https://doi.org/10.1038/ncb1528.

García-Campos, Miguel A., Jesús Espinal-Enríquez, and Enrique Hernández-Lemus. 2015. “Pathway Analysis: State of the Art.” *Frontiers in Physiology* 6 (DEC):1–16. https://doi.org/10.3389/fphys.2015.00383.

Gatz, Margaret, Chandra A. Reynolds, Laura Fratiglioni, Boo Johansson, James A. Mortimer, Stig Berg, Amy Fiske, and Nancy L. Pedersen. 2006. “Role of Genes and Environments for Explaining Alzheimer Disease.” *Archives of General Psychiatry* 63 (2):168. https://doi.org/10.1001/archpsyc.63.2.168.

Ge, K., J. DuHadaway, W. Du, M. Herlyn, U. Rodeck, and G. C. Prendergast. 1999. “Mechanism for Elimination of a Tumor Suppressor: Aberrant Splicing of a Brain-Specific Exon Causes Loss of Function of Bin1 in Melanoma.” *Proceedings of the National Academy of Sciences* 96 (17):9689–94. https://doi.org/10.1073/pnas.96.17.9689.

Genin, E, D Hannequin, D Wallon, K Sleegers, M Hiltunen, O Combarros, M J Bullido, et al. 2011. “APOE and Alzheimer Disease: A Major Gene with Semi-Dominant Inheritance.” *Molecular Psychiatry* 16 (9). NIH Public Access:903–7. https://doi.org/10.1038/mp.2011.52.

Gentier, Romina J., and Fred W. van Leeuwen. 2015. “Misframed Ubiquitin and Impaired Protein Quality Control: An Early Event in Alzheimer’s Disease.” *Frontiers in Molecular Neuroscience* 8 (September):1–12. https://doi.org/10.1177/875512250802400304.

Glennon, Elizabeth B C, Isobel J Whitehouse, J Scott Miners, Patrick G Kehoe, Seth Love, Katherine A B Kellett, and Nigel M Hooper. 2013. "BIN1 Is Decreased in Sporadic but Not Familial Alzheimer's Disease or in Aging." *PloS One* 8 (10). Public Library of Science:e78806. https://doi.org/10.1371/journal.pone.0078806.

Götz, J., F. Chen, J. Van Dorpe, and R. M. Nitsch. 2001. "Formation of Neurofibrillary Tangles in P301L Tau Transgenic Mice Induced by Aβ42 Fibrils." *Science* 293 (5534):1491–95. https://doi.org/10.1126/science.1062097.

Götz, Jürgen, and Naeman N Götz. 2009. "Animal Models for Alzheimer's Disease and Frontotemporal Dementia: A Perspective." *ASN Neuro* 1 (4):AN20090042. https://doi.org/10.1042/AN20090042.

Götz, Jürgen, and Lars M Ittner. 2008. "Animal Models of Alzheimer's Disease and Frontotemporal Dementia." *Nature Reviews. Neuroscience* 9 (7):532–44. https://doi.org/10.1038/nrn2420.

Griciuc, Ana, Alberto Serrano-Pozo, Antonio R. Parrado, Andrea N. Lesinski, Caroline N. Asselin, Kristina Mullin, Basavaraj Hooli, Se Hoon Choi, Bradley T. Hyman, and Rudolph E. Tanzi. 2013. "Alzheimer's Disease Risk Gene cd33 Inhibits Microglial Uptake of Amyloid Beta." *Neuron* 78 (4). Elsevier Inc.:631–43. https://doi.org/10.1016/j.neuron.2013.04.014.

Grundke-Iqbal, I, K Iqbal, Y. C. Tung, M Quinlan, H. M. Wisniewski, and L. I. Binder. 1986. "Abnormal Phosphorylation of the Microtubule-Associated Protein Tau (tau) in Alzheimer Cytoskeletal Pathology." *Proceedings of the National Academy of Sciences* 83 (13):4913–17. https://doi.org/10.1073/pnas.83.13.4913.

Guennec, Kilan Le, Gaël Nicolas, Olivier Quenez, Camille Charbonnier, David Wallon, Céline Bellenguez, Benjamin Grenier-Boley, et al. 2016. "ABCA7 Rare Variants and Alzheimer Disease Risk." *Neurology* 86 (23):2134–37. https://doi.org/10.1212/WNL.0000000000002627.

Guerreiro, Rita, Aleksandra Wojtas, Jose Bras, Minerva Carrasquillo, Ekaterina Rogaeva, Elisa Majounie, Carlos Cruchaga, et al. 2013. "*TREM2* Variants in Alzheimer's Disease." *New England Journal of Medicine* 368 (2):117–27. https://doi.org/10.1056/NEJMoa1211851.

Gulisano, Walter, Daniele Maugeri, Marian a. Baltrons, Mauro Fà, Arianna Amato, Agostino Palmeri, Luciano D'Adamio, et al. 2018. "Role of Amyloid-B and Tau Proteins in Alzheimer's Disease: Confuting the Amyloid Cascade." *Journal of Alzheimer's Disease* 64 (s1):S611–31. https://doi.org/10.3233/JAD-179935.

Gunn, Adam P., Bruce X. Wong, Timothy Johanssen, James C. Griffith, Colin L. Masters, Ashley I. Bush, Kevin J. Barnham, James A. Duce, and Robert A. Cherny. 2016. "Amyloid-B Peptide Aβ3pE-42 Induces Lipid Peroxidation, Membrane Permeabilization, and Calcium Influx in Neurons." *Journal of Biological Chemistry* 291 (12):6134–45. https://doi.org/10.1074/jbc.M115.655183.

Guo, Tong, Wendy Noble, and Diane P. Hanger. 2017. “Roles of Tau Protein in Health and Disease.” *Acta Neuropathologica* 133 (5):665–704. https://doi.org/10.1007/s00401-017-1707-9.

Gustafsdottir, Sigrun M., Edith Schallmeiner, Simon Fredriksson, Mats Gullberg, Ola Söderberg, Malin Jarvius, Jonas Jarvius, Mathias Howell, and Ulf Landegren. 2005. “Proximity Ligation Assays for Sensitive and Specific Protein Analyses.” *Analytical Biochemistry* 345 (1):2–9. https://doi.org/10.1016/j.ab.2005.01.018.

Hardy, J., and G. Higgins. 1992. “Alzheimer’s Disease: The Amyloid Cascade Hypothesis.” *Science* 256 (5054):184–85. https://doi.org/10.1126/science.1566067.

Hardy, John, and Dennis J Selkoe. 2002. “The Amyloid Hypothesis of Alzheimer’s Disease: Progress and Problems on the Road to Therapeutics.” *Science (New York, N.Y.)* 297 (5580):353–56. https://doi.org/10.1126/science.1072994.

Harrington, Adam J., Aram Raissi, Kacey Rajkovich, Stefano Berto, Jaswinder Kumar, Gemma Molinaro, Jonathan Raduazzo, et al. 2016. “MEF2C Regulates Cortical Inhibitory and Excitatory Synapses and Behaviors Relevant to Neurodevelopmental Disorders.” *eLife* 5 (OCTOBER2016):1–27. https://doi.org/10.7554/eLife.20059.

Hattori, H., K. K. Subramanian, J. Sakai, Y. Jia, Y. Li, T. F. Porter, F. Loison, et al. 2010. “Small-Molecule Screen Identifies Reactive Oxygen Species as Key Regulators of Neutrophil Chemotaxis.” *Proceedings of the National Academy of Sciences* 107 (8):3546–51. https://doi.org/10.1073/pnas.0914351107.

Herrup, Karl. 2015. “The Case for Rejecting the Amyloid Cascade Hypothesis.” *Nature Neuroscience* 18 (6):794–99. https://doi.org/10.1038/nn.4017.

Hick, Meike, Ulrike Herrmann, Sascha W. Weyer, Jan Philipp Mallm, Jakob Andreas Tschäpe, Marianne Borgers, Marc Mercken, et al. 2015. “Acute Function of Secreted Amyloid Precursor Protein Fragment APPsα in Synaptic Plasticity.” *Acta Neuropathologica* 129 (1):21–37. https://doi.org/10.1007/s00401-014-1368-x.

Himmler, a, D Drechsel, M W Kirschner, and D W Martin. 1989. “Tau Consists of a Set of Proteins with Repeated C-Terminal Microtubule-Binding Domains and Variable N-Terminal Domains.” *Molecular and Cellular Biology* 9 (4):1381–88. https://doi.org/10.1128/MCB.9.4.1381.Updated.

Holler, Christopher J., Paulina R. Davis, Tina L. Beckett, Thomas L. Platt, Robin L. Webb, Elizabeth Head, and M. Paul Murphy. 2014. “Bridging Integrator 1 (BIN1) Protein Expression Increases in the Alzheimer’s Disease Brain and Correlates with Neurofibrillary Tangle Pathology.” *Journal of Alzheimer’s Disease : JAD* 42 (4):1221–27. https://doi.org/10.3233/JAD-132450.

Hong, S., V. F. Beja-Glasser, B. M. Nfonoyim, A. Frouin, S. Li, S. Ramakrishnan, K. M. Merry, et al. 2016. “Complement and Microglia Mediate Early Synapse Loss in Alzheimer Mouse Models.” *Science* 352 (6286):712–16. https://doi.org/10.1126/science.aad8373.

Hong, Tingting, Huanghe Yang, Shan Shan Zhang, Hee Cheol Cho, Mariya Kalashnikova, Baiming Sun, Hao Zhang, et al. 2014. “Cardiac BIN1 Folds T-Tubule Membrane, Controlling Ion Flux and Limiting Arrhythmia.” *Nature Medicine* 20 (6):624–32. https://doi.org/10.1038/nm.3543.

Hsin, H., M. J. Kim, C.-F. Wang, and M. Sheng. 2010. “Proline-Rich Tyrosine Kinase 2 Regulates Hippocampal Long-Term Depression.” *Journal of Neuroscience* 30 (36):11983–93. https://doi.org/10.1523/JNEUROSCI.1029-10.2010.

Hu, Yan Shi, Juncai Xin, Ying Hu, Lei Zhang, and Ju Wang. 2017. “Analyzing the Genes Related to Alzheimer’s Disease via a Network and Pathway-Based Approach.” *Alzheimer’s Research and Therapy* 9 (1). Alzheimer’s Research & Therapy:1–15. https://doi.org/10.1186/s13195-017-0252-z.

Hurtado, David E., Laura Molina-Porcel, Michiyo Iba, Awo K. Aboagye, Steven M. Paul, John Q. Trojanowski, and Virginia M.Y. Lee. 2010. “Aβ Accelerates the Spatiotemporal Progression of Tau Pathology and Augments Tau Amyloidosis in an Alzheimer Mouse Model.” *American Journal of Pathology* 177 (4). American Society for Investigative Pathology:1977–88. https://doi.org/10.2353/ajpath.2010.100346.

Hutton, M., C. L. Lendon, P. Rizzu, M. Baker, S. Froelich, H. H. Houlden, S. Pickering-Brown, et al. 1998. “Association of Missense and 5’-Splice-Site Mutations in Tau with the Inherited Dementia FTDP-17.” *Nature* 393 (6686):702–4. https://doi.org/10.1038/31508.

Iaccarino, Leonardo, Gautam Tammewar, Nagehan Ayakta, Suzanne L. Baker, Alexandre Bejanin, Adam L. Boxer, Maria Luisa Gorno-Tempini, et al. 2018. “Local and Distant Relationships between Amyloid, Tau and Neurodegeneration in Alzheimer’s Disease.” *NeuroImage: Clinical* 17 (February 2017). Elsevier:452–64. https://doi.org/10.1016/j.nicl.2017.09.016.

Iqbal, Khalid, Fei Liu, and Cheng-Xin Gong. 2016. “Tau and Neurodegenerative Disease: The Story so Far.” *Nature Reviews Neurology* 12 (1):15–27. https://doi.org/10.1038/nrneurol.2015.225.

Itoh, Toshiki, and Pietro De Camilli. 2006. “BAR, F-BAR (EFC) and ENTH/ANTH Domains in the Regulation of Membrane-Cytosol Interfaces and Membrane Curvature.” *Biochimica et Biophysica Acta - Molecular and Cell Biology of Lipids* 1761 (8):897–912. https://doi.org/10.1016/j.bbalip.2006.06.015.

Ittner, Lars M., Yazi D. Ke, Fabien Delerue, Mian Bi, Amadeus Gladbach, Janet van Eersel, Heidrun Wölfing, et al. 2010. “Dendritic Function of Tau Mediates Amyloid-B Toxicity in Alzheimer’s Disease Mouse Models.” *Cell* 142 (3):387–97. https://doi.org/10.1016/j.cell.2010.06.036.

Jack, Clifford R., David S. Knopman, William J. Jagust, Ronald C. Petersen, Michael W. Weiner, Paul S. Aisen, Leslie M. Shaw, et al. 2013. “Tracking Pathophysiological Processes in Alzheimer’s Disease: An Updated Hypothetical Model of Dynamic

Biomarkers." *The Lancet Neurology* 12 (2):207–16. https://doi.org/10.1016/S1474-4422(12)70291-0.

Jain, Shushant, and Peter Heutink. 2010. "From Single Genes to Gene Networks: High-Throughput-High-Content Screening for Neurological Disease." *Neuron* 68 (2). Elsevier Inc.:207–17. https://doi.org/10.1016/j.neuron.2010.10.010.

Jarvius, Malin, Janna Paulsson, Irene Weibrecht, Karl-Johan Leuchowius, Ann-Catrin Andersson, Carolina Wählby, Mats Gullberg, et al. 2007. "In Situ Detection of Phosphorylated Platelet-Derived Growth Factor Receptor B Using a Generalized Proximity Ligation Method." *Molecular & Cellular Proteomics* 6 (9):1500–1509. https://doi.org/10.1074/mcp.M700166-MCP200.

Jay, Taylor R., Anna M. Hirsch, Margaret L. Broihier, Crystal M. Miller, Lee E. Neilson, Richard M. Ransohoff, Bruce T. Lamb, and Gary E. Landreth. 2017. "Disease Progression-Dependent Effects of TREM2 Deficiency in a Mouse Model of Alzheimer's Disease." *The Journal of Neuroscience* 37 (3):637–47. https://doi.org/10.1523/JNEUROSCI.2110-16.2017.

Jonsson, Thorlakur, Jasvinder K. Atwal, Stacy Steinberg, Jon Snaedal, Palmi V. Jonsson, Sigurbjorn Bjornsson, Hreinn Stefansson, et al. 2012. "A Mutation in APP Protects against Alzheimer's Disease and Age-Related Cognitive Decline." *Nature* 488 (7409):96. https://doi.org/10.1038/nature11283.

Jonsson, Thorlakur, Hreinn Stefansson, Stacy Steinberg, Ingileif Jonsdottir, Palmi V. Jonsson, Jon Snaedal, Sigurbjorn Bjornsson, et al. 2013. "Variant of TREM2 Associated with the Risk of Alzheimer's Disease." *New England Journal of Medicine* 368 (2):107–16. https://doi.org/10.1056/NEJMoa1211103.

Jun, G., C. a. Ibrahim-Verbaas, M. Vronskaya, J. C. Lambert, J. Chung, a. C. Naj, B. W. Kunkle, et al. 2016. "A Novel Alzheimer Disease Locus Located near the Gene Encoding Tau Protein." *Molecular Psychiatry* 21 (1):108–17. https://doi.org/10.1038/mp.2015.23.

Kanatsu, Kunihiko, Yuichi Morohashi, Mai Suzuki, Hiromasa Kuroda, Toshio Watanabe, Taisuke Tomita, and Takeshi Iwatsubo. 2014. "Decreased CALM Expression Reduces Aβ42 to Total Aβ Ratio through Clathrin-Mediated Endocytosis of Γ-Secretase." *Nature Communications* 5. https://doi.org/10.1038/ncomms4386.

Kanatsu, Kunihiko, and Taisuke Tomita. 2017. "Molecular Mechanisms of the Genetic Risk Factors in Pathogenesis of Alzheimer Disease." *Frontiers in Bioscience* 22 (1):4480. https://doi.org/10.2741/4480.

Kant, Rik van der, and Lawrence S.B. Goldstein. 2015. "Cellular Functions of the Amyloid Precursor Protein from Development to Dementia." *Developmental Cell* 32 (4). Elsevier Inc.:502–15. https://doi.org/10.1016/j.devcel.2015.01.022.

Karch, Celeste M., Amanda T. Jeng, Petra Nowotny, Janet Cady, Carlos Cruchaga, and Alison M. Goate. 2012. "Expression of Novel Alzheimer's Disease Risk Genes in Control and

Alzheimer's Disease Brains." *PLoS ONE* 7 (11). https://doi.org/10.1371/journal.pone.0050976.

Kim, Minji, Jaehong Suh, Donna Romano, Mimy H. Truong, Kristina Mullin, Basavaraj Hooli, David Norton, et al. 2009. "Potential Late-Onset Alzheimer's Disease-Associated Mutations in the ADAM10 Gene Attenuate A-Secretase Activity." *Human Molecular Genetics* 18 (20):3987–96. https://doi.org/10.1093/hmg/ddp323.

Kitago, Yu, Masamichi Nagae, Zenzaburo Nakata, Maho Yagi-Utsumi, Shizuka Takagi-Niidome, Emiko Mihara, Terukazu Nogi, Koichi Kato, and Junichi Takagi. 2015. "Structural Basis for Amyloidogenic Peptide Recognition by sorLA." *Nature Structural and Molecular Biology* 22 (3):199–206. https://doi.org/10.1038/nsmb.2954.

Knouff, Christopher, Myron E. Hinsdale, Hafid Mezdour, Michael K. Altenburg, Masahiko Watanabe, Steven H. Quarfordt, Patrick M. Sullivan, and Nobuyo Maeda. 1999. "Apo E Structure Determines VLDL Clearance and Atherosclerosis Risk in Mice." *Journal of Clinical Investigation* 103 (11):1579–86. https://doi.org/10.1172/JCI6172.

Krämer-Albers, Eva Maria, and Robin White. 2011. "From Axon-Glial Signalling to Myelination: The Integrating Role of Oligodendroglial Fyn Kinase." *Cellular and Molecular Life Sciences* 68 (12):2003–12. https://doi.org/10.1007/s00018-010-0616-z.

Krasemann, Susanne, Charlotte Madore, Ron Cialic, Caroline Baufeld, Narghes Calcagno, Rachid El Fatimy, Lien Beckers, et al. 2017. "The TREM2-APOE Pathway Drives the Transcriptional Phenotype of Dysfunctional Microglia in Neurodegenerative Diseases." *Immunity* 47 (3). Elsevier Inc.:566–81.e9. https://doi.org/10.1016/j.immuni.2017.08.008.

Kuperstein, Inna, Kerensa Broersen, Iryna Benilova, Jef Rozenski, Wim Jonckheere, Maja Debulpaep, Annelies Vandersteen, et al. 2010. "Neurotoxicity of Alzheimer's Disease Aβ Peptides Is Induced by Small Changes in the Aβ42 to Aβ40 Ratio." *The EMBO Journal* 29 (19):3408–20. https://doi.org/10.1038/emboj.2010.211.

LaFerla, F. M., and K. N. Green. 2012. "Animal Models of Alzheimer Disease." *Cold Spring Harbor Perspectives in Medicine* 2 (11):a006320–a006320. https://doi.org/10.1101/cshperspect.a006320.

Lambert, Jean Charles, and Philippe Amouyel. 2011. "Genetics of Alzheimer's Disease: New Evidences for an Old Hypothesis?" *Current Opinion in Genetics and Development* 21 (3). Elsevier Ltd:295–301. https://doi.org/10.1016/j.gde.2011.02.002.

Lambert, Jean-Charles, Simon Heath, Gael Even, Dominique Campion, Kristel Sleegers, Mikko Hiltunen, Onofre Combarros, et al. 2009. "Genome-Wide Association Study Identifies Variants at CLU and CR1 Associated with Alzheimer's Disease." *Nature Genetics* 41 (10). Nature Publishing Group:1094–99. https://doi.org/10.1038/ng.439.

Lambert, Jean-Charles, C A Ibrahim-Verbaas, D Harold, A C Naj, R Sims, C Bellenguez, A L DeStafano, et al. 2013. "Meta-Analysis of 74,046 Individuals Identifies 11 New

Susceptibility Loci for Alzheimer's Disease." *Nature Genetics* 45 (12):1452–58. https://doi.org/10.1038/ng.2802.

Landrieu, Isabelle, Caroline Smet-Nocca, Laziza Amniai, Justin Vijay Louis, Jean Michel Wieruszeski, Jozef Goris, Veerle Janssens, and Guy Lippens. 2011. "Molecular Implication of PP2A and Pin1 in the Alzheimer's Disease Specific Hyperphosphorylation of Tau." *PLoS ONE* 6 (6). https://doi.org/10.1371/journal.pone.0021521.

Lee, Eunkyung, Melissa Marcucci, Laurie Daniell, Marc Pypaert, Ora a. Weisz, Gian Carlo Ochoa, Khashayar Farsad, Markus R. Wenk, and Pietro De Camilli. 2002. "Amphiphysin 2 (Bin1) and T-Tubule Biogenesis in Muscle." *Science* 297 (5584):1193–96. https://doi.org/10.1126/science.1071362.

Lee, Gloria, and Chad J. Leugers. 2012. "Tau and Tauopathies." *Progress in Molecular Biology and Translational Science* 107 (January). NIH Public Access:263–93. https://doi.org/10.1016/B978-0-12-385883-2.00004-7.

Leprince, Corinne, Francisco Romero, Didier Cussac, Beatrice Vayssiere, Roland Berger, Armand Tavitian, and Jacques H. Camonis. 1997. "A New Member of the Amphiphysin Family Connecting Endocytosis and Signal Transduction Pathways." *Journal of Biological Chemistry* 272 (24). American Society for Biochemistry and Molecular Biology:15101–5. https://doi.org/10.1074/jbc.272.24.15101.

Leuchowius, Karl Johan, Irene Weibrecht, and Ola Söderberg. 2011. "In Situ Proximity Ligation Assay for Microscopy and Flow Cytometry." *Current Protocols in Cytometry*, no. SUPPL. 56:1–15. https://doi.org/10.1002/0471142956.cy0936s56.

Leuchowius, Karl-Johan, Malin Jarvius, Malin Wickström, Linda Rickardson, Ulf Landegren, Rolf Larsson, Ola Söderberg, Mårten Fryknäs, and Jonas Jarvius. 2010. "High Content Screening for Inhibitors of Protein Interactions and Post-Translational Modifications in Primary Cells by Proximity Ligation." *Molecular & Cellular Proteomics : MCP* 9 (1):178–83. https://doi.org/10.1074/mcp.M900331-MCP200.

Li, Tong, Cheryl Hawkes, Hamid Y. Qureshi, Satyabrata Kar, and Hemant K. Paudel. 2006. "Cyclin-Dependent Protein Kinase 5 Primes Microtubule-Associated Protein Tau Site-Specifically for Glycogen Synthase Kinase 3β." *Biochemistry* 45 (10):3134–45. https://doi.org/10.1021/bi051635j.

Liang, Shuang, Fan Yan Wei, Yu Mei Wu, Kenji Tanabe, Tadashi Abe, Yoshiya Oda, Yumi Yoshida, et al. 2007. "Major Cdk5-Dependent Phosphorylation Sites of Amphiphysin 1 Are Implicated in the Regulation of the Membrane Binding and Endocytosis." *Journal of Neurochemistry* 102 (5):1466–76. https://doi.org/10.1111/j.1471-4159.2007.04507.x.

Logue, Mark W., Matthew Schu, Badri N. Vardarajan, John Farrell, David a. Bennett, Joseph D. Buxbaum, Goldie S. Byrd, et al. 2014. "Two Rare AKAP9 Variants Are Associated with Alzheimer's Disease in African Americans." *Alzheimer's and Dementia* 10 (6). Elsevier:609–18. https://doi.org/10.1016/j.jalz.2014.06.010.

Mairet-Coello, Georges, Julien Courchet, Simon Pieraut, Virginie Courchet, Anton Maximov, and Franck Polleux. 2013. “The CAMKK2-AMPK Kinase Pathway Mediates the Synaptotoxic Effects of Aβ Oligomers through Tau Phosphorylation.” *Neuron* 78 (1). Elsevier Inc.:94–108. https://doi.org/10.1016/j.neuron.2013.02.003.

Malik, M., J. F. Simpson, I. Parikh, B. R. Wilfred, D. W. Fardo, P. T. Nelson, and S. Estus. 2013. “CD33 Alzheimer’s Risk-Altering Polymorphism, CD33 Expression, and Exon 2 Splicing.” *Journal of Neuroscience* 33 (33):13320–25. https://doi.org/10.1523/JNEUROSCI.1224-13.2013.

Malki, Idir, François-Xavier Xavier Cantrelle, Yoann Sottejeau, Guy Lippens, Jean-Charles Charles Lambert, and Isabelle Landrieu. 2017. “Regulation of the Interaction between the Neuronal BIN1 Isoform 1 and Tau Proteins - Role of the SH3 Domain.” *The FEBS Journal* 284 (19):3218–29. https://doi.org/10.1111/febs.14185.

Marks, Bruno, and Harvey T. McMahon. 1998. “Calcium Triggers Calcineurin-Dependent Synaptic Vesicle Recycling in Mammalian Nerve Terminals.” *Current Biology* 8 (13):740–49. https://doi.org/10.1016/S0960-9822(98)70297-0.

Mattiazzi Usaj, Mojca, Erin B. Styles, Adrian J. Verster, Helena Friesen, Charles Boone, and Brenda J. Andrews. 2016. “High-Content Screening for Quantitative Cell Biology.” *Trends in Cell Biology* 26 (8). Elsevier Ltd:598–611. https://doi.org/10.1016/j.tcb.2016.03.008.

McDonough, Patrick M., Natalie L. Prigozhina, Ranor C.B. Basa, and Jeffrey H. Price. 2017. “Assay of Calcium Transients and Synapses in Rat Hippocampal Neurons by Kinetic Image Cytometry and High-Content Analysis: An In Vitro Model System for Postchemotherapy Cognitive Impairment.” *ASSAY and Drug Development Technologies* 15 (5):220–36. https://doi.org/10.1089/adt.2017.797.

McKenzie, Andrew T., Sarah Moyon, Minghui Wang, Igor Katsyv, Won Min Song, Xianxiao Zhou, Eric B. Dammer, et al. 2017. “Multiscale Network Modeling of Oligodendrocytes Reveals Molecular Components of Myelin Dysregulation in Alzheimer’s Disease.” *Molecular Neurodegeneration* 12 (1). Molecular Neurodegeneration:1–20. https://doi.org/10.1186/s13024-017-0219-3.

Meunier, Brigitte, Muriel Quaranta, Laurent Daviet, Anastassia Hatzoglou, and Corinne Leprince. 2009. “The Membrane-Tubulating Potential of Amphiphysin 2/BIN1 Is Dependent on the Microtubule-Binding Cytoplasmic Linker Protein 170 (CLIP-170).” *European Journal of Cell Biology* 88 (2):91–102. https://doi.org/10.1016/j.ejcb.2008.08.006.

Miyagawa, Toji, Ihori Ebinuma, Yuichi Morohashi, Yukiko Hori, Mee Young Chang, Haruhiko Hattori, Tomoaki Maehara, et al. 2016. “BIN1 Regulates BACE1 Intracellular Trafficking and Amyloid-B Production.” *Human Molecular Genetics* 25 (14):ddw146. https://doi.org/10.1093/hmg/ddw146.

Morris, Meaghan, Sumihiro Maeda, Keith Vossel, and Lennart Mucke. 2011. “The Many Faces of Tau.” *Neuron* 70 (3). Elsevier Inc.:410–26. https://doi.org/10.1016/j.neuron.2011.04.009.

Muller, Alexander J, Judith F Baker, James B Duhadaway, Kai Ge, George Farmer, P Scott Donover, Raymond Meade, et al. 2003. “Targeted Disruption of the Murine Bin1 / Amphiphysin II Gene Does Not Disable Endocytosis but Results in Embryonic Cardiomyopathy with Aberrant Myofibril Formation Targeted Disruption of the Murine Bin1 / Amphiphysin II Gene Does Not Disable Endocytosis B.” *Molecular and Cellular Biology* 23 (12):4295–4306. https://doi.org/10.1128/MCB.23.12.4295.

Nhan, Hoang S., Karen Chiang, and Edward H. Koo. 2015. “The Multifaceted Nature of Amyloid Precursor Protein and Its Proteolytic Fragments: Friends and Foes.” *Acta Neuropathologica* 129 (1):1–19. https://doi.org/10.1007/s00401-014-1347-2.

Nicolas, G., C. Charbonnier, D. Wallon, O. Quenez, C. Bellenguez, B. Grenier-Boley, S. Rousseau, et al. 2016. “SORL1 Rare Variants: A Major Risk Factor for Familial Early-Onset Alzheimer’s Disease.” *Molecular Psychiatry* 21 (6):831–36. https://doi.org/10.1038/mp.2015.121.

Nisbet, Rebecca M., Juan-Carlos Polanco, Lars M. Ittner, and Jürgen Götz. 2015. “Tau Aggregation and Its Interplay with Amyloid-B.” *Acta Neuropathologica* 129 (2). Springer:207–20. https://doi.org/10.1007/s00401-014-1371-2.

Noble, Wendy, Diane P. Hanger, Christopher C.J. Miller, and Simon Lovestone. 2013. “The Importance of Tau Phosphorylation for Neurodegenerative Diseases.” *Frontiers in Neurology* 4 JUL (July):1–11. https://doi.org/10.3389/fneur.2013.00083.

Norris, Christopher M. 2018. “Calcineurin: Directing the Damage in Alzheimer Disease: An Editorial for ‘Neuronal Calcineurin Transcriptional Targets Parallel Changes Observed in Alzheimer Disease Brain’ on Doi: 10.1111/jnc.14469.” *Journal of Neurochemistry*, 1–4. https://doi.org/10.1111/jnc.14475.

O’Brien, Richard J., and Philip C. Wong. 2011. “Amyloid Precursor Protein Processing and Alzheimer’s Disease.” *Annual Review of Neuroscience* 34 (1):185–204. https://doi.org/10.1146/annurev-neuro-061010-113613.

O’Day, Danton H., Kristeen Eshak, and Michael a. Myre. 2015. “Calmodulin Binding Proteins and Alzheimer’s Disease.” *Journal of Alzheimer’s Disease* 46 (3):553–69. https://doi.org/10.3233/JAD-142772.

Oddo, Salvatore, Antonella Caccamo, Jason D. Shepherd, M. Paul Murphy, Todd E. Golde, Rakez Kayed, Raju Metherate, Mark P. Mattson, Yama Akbari, and Frank M. LaFerla. 2003. “Triple-Transgenic Model of Alzheimer’s Disease with Plaques and Tangles: Intracellular Aβ and Synaptic Dysfunction.” *Neuron* 39 (3):409–21. https://doi.org/10.1016/S0896-6273(03)00434-3.

Pagano, Katiuscia, Denise Galante, Cristina D'Arrigo, Alessandro Corsaro, Mario Nizzari, Tullio Florio, Henriette Molinari, Simona Tomaselli, and Laura Ragona. 2018. "Effects of Prion Protein on Aβ42 and Pyroglutamate-Modified AβpE3-42 Oligomerization and Toxicity." *Molecular Neurobiology*, 1–15. https://doi.org/10.1007/s12035-018-1202-x.

Pant, Saumya, Mahak Sharma, Kruti Patel, Steve Caplan, Chavela M. Carr, and Barth D. Grant. 2009. "AMPH-1/Amphiphysin/Bin1 Functions with RME-1/Ehd1 in Endocytic Recycling." *Nature Cell Biology* 11 (12). Nature Publishing Group:1399–1410. https://doi.org/10.1038/ncb1986.

Pei, Jin Jing, Heiko Braak, Wen Lin An, Bengt Winblad, Richard F. Cowburn, Khalid Iqbal, and Inge Grundke-Iqbal. 2002. "Up-Regulation of Mitogen-Activated Protein Kinases ERK1/2 and MEK1/2 Is Associated with the Progression of Neurofibrillary Degeneration in Alzheimer's Disease." *Molecular Brain Research* 109 (1-2):45–55. https://doi.org/10.1016/S0169-328X(02)00488-6.

Perl, Daniel P. 2010. "Neuropathology of Alzheimer's Disease." *Mount Sinai Journal of Medicine: A Journal of Translational and Personalized Medicine* 77 (1):32–42. https://doi.org/10.1002/msj.20157.

Peter, Brian J., Helen M. Kent, Ian G. Mills, Yvonne Vallis, P. Jonathan G. Butler, Philip R. Evans, and Harvey T. McMahon. 2004. "BAR Domains as Sensors of Membrane Curvature: The Amphiphysin BAR Structure." *Science* 303 (5657):495–99. https://doi.org/10.1126/science.1092586.

Piaceri, Irene, Benedetta Nacmias, Sandro Sorbi, and Benedetta Naemias. 2013. "Genetics of Familial and Sporadic Alzheimer's Disease." *Frontiers in Bioscience (Elite Edition)* 5 (5):167–77. https://doi.org/10.2741/E605.

Pimenova, Anna a., Towfique Raj, and Alison M. Goate. 2018. "Untangling Genetic Risk for Alzheimer's Disease." *Biological Psychiatry* 83 (4):300–310. https://doi.org/10.1016/j.biopsych.2017.05.014.

Pineda-Lucena, Antonio, Cynthia S W Ho, Daniel Y L Mao, Yi Sheng, Rob C Laister, Ranjith Muhandiram, Ying Lu, et al. 2005. "A Structure-Based Model of the c-Myc/Bin1 Protein Interaction Shows Alternative Splicing of Bin1 and c-Myc Phosphorylation Are Key Binding Determinants." *Journal of Molecular Biology* 351 (1):182–94. https://doi.org/10.1016/j.jmb.2005.05.046.

Pol, L. a. Van De, a. Hensel, F. Barkhof, H. J. Gertz, P. Scheltens, and W. M. Van Der Flier. 2006. "Hippocampal Atrophy in Alzheimer Disease: Age Matters." *Neurology* 66 (2):236–38. https://doi.org/10.1212/01.wnl.0000194240.47892.4d.

Polydoro, M., C. M. Acker, K. Duff, P. E. Castillo, and P. Davies. 2009. "Age-Dependent Impairment of Cognitive and Synaptic Function in the Htau Mouse Model of Tau Pathology." *Journal of Neuroscience* 29 (34):10741–49. https://doi.org/10.1523/JNEUROSCI.1065-09.2009.

Prendergast, George C., Alexander J. Muller, Arivudanambi Ramalingam, and Mee Young Chang. 2009. “BAR the Door: Cancer Suppression by Amphiphysin-like Genes.” *Biochimica et Biophysica Acta - Reviews on Cancer* 1795 (1). Elsevier B.V.:25–36. https://doi.org/10.1016/j.bbcan.2008.09.001.

Prokic, Ivana, Belinda S. Cowling, and Jocelyn Laporte. 2014. “Amphiphysin 2 (BIN1) in Physiology and Diseases.” *Journal of Molecular Medicine* 2 (March):1–11. https://doi.org/10.1007/s00109-014-1138-1.

Pyndiah, Slovénie, Satoshi Tanida, Kazi M Ahmed, Erica K Cassimere, C. Choe, and D. Sakamuro. 2011. “C-MYC Suppresses BIN1 to Release Poly(ADP-Ribose) Polymerase 1: A Mechanism by Which Cancer Cells Acquire Cisplatin Resistance.” *Science Signaling* 4 (166):ra19–ra19. https://doi.org/10.1126/scisignal.2001556.

Qi, Haoling, Sudhakaran Prabakaran, François-Xavier Cantrelle, Béatrice Chambraud, Jeremy Gunawardena, Guy Lippens, and Isabelle Landrieu. 2016. “Characterization of Neuronal Tau Protein as a Target of Extracellular-Signal-Regulated Kinase.” *Journal of Biological Chemistry* 291 (6):jbc.M115.700914. https://doi.org/10.1074/jbc.M115.700914.

Raj, Towfique, Katie J. Ryan, Joseph M. Replogle, Lori B. Chibnik, Laura Rosenkrantz, Anna Tang, Katie Rothamel, et al. 2014. “CD33: Increased Inclusion of Exon 2 Implicates the Ig V-Set Domain in Alzheimer’s Disease Susceptibility.” *Human Molecular Genetics* 23 (10):2729–36. https://doi.org/10.1093/hmg/ddt666.

Rameau, Gerald a., Ling Yu Chiu, and Edward B. Ziff. 2003. “NMDA Receptor Regulation of nNOS Phosphorylation and Induction of Neuron Death.” *Neurobiology of Aging* 24 (8):1123–33. https://doi.org/10.1016/j.neurobiolaging.2003.07.002.

Ramjaun, A. R., K. D. Micheva, I. Bouchelet, and P. S. McPherson. 1997. “Identification and Characterization of a Nerve Terminal-Enriched Amphiphysin Isoform.” *Journal of Biological Chemistry* 272 (26). American Society for Biochemistry and Molecular Biology:16700–706. https://doi.org/10.1074/jbc.272.26.16700.

Ramjaun, Antoine R., and Peter S. McPherson. 2002. “Multiple Amphiphysin II Splice Variants Display Differential Clathrin Binding: Identification of Two Distinct Clathrin-Binding Sites.” *Journal of Neurochemistry* 70 (6):2369–76. https://doi.org/10.1046/j.1471-4159.1998.70062369.x.

Rapoport, M., H. N. Dawson, L. I. Binder, M. P. Vitek, and A. Ferreira. 2002. “Tau Is Essential to B-Amyloid-Induced Neurotoxicity.” *Proceedings of the National Academy of Sciences* 99 (9):6364–69. https://doi.org/10.1073/pnas.092136199.

Reinhard, Constanze, Sébastien S Hébert, and Bart De Strooper. 2005. “The Amyloid-B Precursor Protein: Integrating Structure with Biological Function.” *The EMBO Journal* 24 (23):3996–4006. https://doi.org/10.1038/sj.emboj.7600860.

Reitz, Christiane, and Richard Mayeux. 2014. “Alzheimer Disease: Epidemiology, Diagnostic Criteria, Risk Factors and Biomarkers.” *Biochemical Pharmacology* 88 (4). Elsevier Inc.:640–51. https://doi.org/10.1016/j.bcp.2013.12.024.

Resende, R., E. Ferreiro, C. Pereira, and C. Resende de Oliveira. 2008. “Neurotoxic Effect of Oligomeric and Fibrillar Species of Amyloid-Beta Peptide 1-42: Involvement of Endoplasmic Reticulum Calcium Release in Oligomer-Induced Cell Death.” *Neuroscience* 155 (3):725–37. https://doi.org/10.1016/j.neuroscience.2008.06.036.

Reynolds, C. Hugh, Claire J. Garwood, Selina Wray, Caroline Price, Stuart Kellie, Timothy Perera, Marketa Zvelebil, et al. 2008. “Phosphorylation Regulates Tau Interactions with Src Homology 3 Domains of Phosphatidylinositol 3-Kinase, Phospholipase Cγ1, Grb2, and Src Family Kinases.” *Journal of Biological Chemistry* 283 (26):18177–86. https://doi.org/10.1074/jbc.M709715200.

Rosenthal, Samantha L, and M Ilyas Kamboh. 2014. “Late-Onset Alzheimer’s Disease Genes and the Potentially Implicated Pathways.” *Current Genetic Medicine Reports* 2:85–101. https://doi.org/10.1007/s40142-014-0034-x.

Rossi, Pierre De, Virginie Buggia-Prevot, Robert Andrew, Sofia Krause, Elizabeth Woo, Peter Nelson, Peter Pytel, and Gopal Thinakaran. 2017. “BIN1 Localization Is Distinct from Tau Tangles in Alzheimer’s Disease.” *Matters*, January, 1–8. https://doi.org/10.19185/matters.201611000018.

Rossi, Pierre De, Virginie Buggia-Prévot, Benjamin L. L. Clayton, Jared B. Vasquez, Carson van Sanford, Robert J. Andrew, Ruben Lesnick, et al. 2016. “Predominant Expression of Alzheimer’s Disease-Associated BIN1 in Mature Oligodendrocytes and Localization to White Matter Tracts.” *Molecular Neurodegeneration* 11 (1). Molecular Neurodegeneration:59. https://doi.org/10.1186/s13024-016-0124-1.

Ryan, Kristen R., Oksana Sirenko, Fred Parham, Jui Hua Hsieh, Evan F. Cromwell, Raymond R. Tice, and Mamta Behl. 2016. “Neurite Outgrowth in Human Induced Pluripotent Stem Cell-Derived Neurons as a High-Throughput Screen for Developmental Neurotoxicity or Neurotoxicity.” *NeuroToxicology* 53. Elsevier B.V.:271–81. https://doi.org/10.1016/j.neuro.2016.02.003.

Saftig, Paul, and Stefan F. Lichtenthaler. 2015. “The Alpha Secretase ADAM10: A Metalloprotease with Multiple Functions in the Brain.” *Progress in Neurobiology* 135. Elsevier Ltd:1–20. https://doi.org/10.1016/j.pneurobio.2015.10.003.

Sakamuro, Daitoku, Katherine J. Elliott, Robert Wechsler-Reya, and George C. Prendergast. 1996. “BIN1 Is a Novel MYC-Interacting Protein with Features of a Tumour Suppressor.” *Nature Genetics* 14 (1):69–77. https://doi.org/10.1038/ng0996-69.

Satoh, Kanayo, Sumiko Abe-Dohmae, Shinji Yokoyama, Peter St. George-Hyslop, and Paul E. Fraser. 2015. “ATP-Binding Cassette Transporter A7 (ABCA7) Loss of Function Alters Alzheimer Amyloid Processing.” *Journal of Biological Chemistry* 290 (40):24152–65. https://doi.org/10.1074/jbc.M115.655076.

Schellenberg, Gerard D., and Thomas J. Montine. 2012. “The Genetics and Neuropathology of Alzheimer’s Disease.” *Acta Neuropathologica* 124 (3):305–23. https://doi.org/10.1007/s00401-012-0996-2.

Selkoe, Dennis J, and John Hardy. 2016. “The Amyloid Hypothesis of Alzheimer’s Disease at 25 Years.” *EMBO Molecular Medicine* 8 (6):595–608. https://doi.org/10.15252/emmm.201606210.

Sengupta, Amitabha, Michal Novak, Inge Grundke-Iqbal, and Khalid Iqbal. 2006. “Regulation of Phosphorylation of Tau by Cyclin-Dependent Kinase 5 and Glycogen Synthase Kinase-3 at Substrate Level.” *FEBS Letters* 580 (25):5925–33. https://doi.org/10.1016/j.febslet.2006.09.060.

Seshadri, S, A L Fitzpatrick, A Ikram, A L DeStafano, V Gudnason, M Boada, J C Bis, et al. 2010. “Genome-Wide Analysis of Genetic Loci Associated With Alzheimer Disease.” *The Journal of the American Medical Association* 303 (18):1832–40. https://doi.org/10.1001/jama.2010.574.

Sherman, Sean P, and Anne G Bang. 2018. “High-Throughput Screen for Compounds That Modulate Neurite Growth of Human Induced Pluripotent Stem Cell-Derived Neurons.” *Disease Models & Mechanisms* 11 (2):dmm031906. https://doi.org/10.1242/dmm.031906.

Shukla, Varsha, Susan Skuntz, and Harish C. Pant. 2012. “Deregulated Cdk5 Activity Is Involved in Inducing Alzheimer’s Disease.” *Archives of Medical Research* 43 (8). Elsevier Inc:655–62. https://doi.org/10.1016/j.arcmed.2012.10.015.

Shulman, Joshua M., Selina Imboywa, Nikolaos Giagtzoglou, Martin P. Powers, Yanhui Hu, Danelle Devenport, Portia Chipendo, et al. 2014. “Functional Screening in Drosophila Identifies Alzheimer’s Disease Susceptibility Genes and Implicates Tau-Mediated Mechanisms.” *Human Molecular Genetics* 23 (4):870–77. https://doi.org/10.1093/hmg/ddt478.

Sims, Rebecca, Sven J. Van Der Lee, Adam C. Naj, Céline Bellenguez, Nandini Badarinarayan, Johanna Jakobsdottir, Brian W. Kunkle, et al. 2017. “Rare Coding Variants in PLCG2, ABI3, and TREM2 Implicate Microglial-Mediated Innate Immunity in Alzheimer’s Disease.” *Nature Genetics* 49 (9):1373–84. https://doi.org/10.1038/ng.3916.

Singh, Shantanu, Anne E. Carpenter, and Auguste Genovesio. 2014. “Increasing the Content of High-Content Screening.” *Journal of Biomolecular Screening* 19 (5):640–50. https://doi.org/10.1177/1087057114528537.

Slepnev, Vladimir I., Gian Carlo Ochoa, Margaret H. Butler, Detlev Grabs, and Pietro De Camilli. 1998. “Role of Phosphorylation in Regulation of the Assembly of Endocytic Coat Complexes.” *Science* 281 (5378):821–24. https://doi.org/10.1126/science.281.5378.821.

Söderberg, Ola, Mats Gullberg, Malin Jarvius, Karin Ridderstråle, Karl-Johan Leuchowius, Jonas Jarvius, Kenneth Wester, et al. 2006. “Direct Observation of Individual Endogenous Protein Complexes in Situ by Proximity Ligation.” *Nature Methods* 3 (12):995–1000. https://doi.org/10.1038/nmeth947.

Sotiropoulos, Ioannis, André T. Lopes, Vitor Pinto, Sofia Lopes, Sara Carlos, Sara Duarte-Silva, Andreia Neves-Carvalho, et al. 2014. “Selective Impact of Tau Loss on Nociceptive Primary Afferents and Pain Sensation.” *Experimental Neurology* 261:486–93. https://doi.org/10.1016/j.expneurol.2014.07.008.

Sottejeau, Yoann, Alexis Bretteville, François-Xavier Cantrelle, Nicolas Malmanche, Florie Demiaute, Tiago Mendes, Charlotte Delay, et al. 2015. “Tau Phosphorylation Regulates the Interaction between BIN1’s SH3 Domain and Tau’s Proline-Rich Domain.” *Acta Neuropathologica Communications* 3 (1). Acta Neuropathologica Communications:58. https://doi.org/10.1186/s40478-015-0237-8.

Spires-Jones, Tara, and Shira Knafo. 2012. “Spines, Plasticity, and Cognition in Alzheimer’s Model Mice.” *Neural Plasticity* 2012. https://doi.org/10.1155/2012/319836.

Spires-Jones, Tara L., and BradleyT Hyman. 2014. “The Intersection of Amyloid Beta and Tau at Synapses in Alzheimer’s Disease.” *Neuron* 82 (4). Elsevier Inc.:756–71. https://doi.org/10.1016/j.neuron.2014.05.004.

Stadler, Charlotte, Elton Rexhepaj, Vasanth R Singan, Robert F Murphy, Rainer Pepperkok, Mathias Uhlén, Jeremy C Simpson, and Emma Lundberg. 2013. “Immunofluorescence and Fluorescent-Protein Tagging Show High Correlation for Protein Localization in Mammalian Cells.” *Nature Methods* 10 (4). Nature Publishing Group:315–23. https://doi.org/10.1038/nmeth.2377.

Steinberg, Stacy, Hreinn Stefansson, Thorlakur Jonsson, Hrefna Johannsdottir, Andres Ingason, Hannes Helgason, Patrick Sulem, et al. 2015. “Loss-of-Function Variants in ABCA7 Confer Risk of Alzheimer’s Disease.” *Nature Genetics* 47 (5). Nature Publishing Group:445–47. https://doi.org/10.1038/ng.3246.

Strittmatter, W. J., a. M. Saunders, D. Schmechel, M. Pericak-Vance, J. Enghild, G. S. Salvesen, and a. D. Roses. 1993. “Apolipoprotein E: High-Avidity Binding to Beta-Amyloid and Increased Frequency of Type 4 Allele in Late-Onset Familial Alzheimer Disease.” *Proceedings of the National Academy of Sciences* 90 (5):1977–81. https://doi.org/10.1073/pnas.90.5.1977.

Strittmatter, Warren J, Karl H Weisgraber, David Y Huang, Li-Ming Dong, Guy S Salvesen1, Margaret Pericak-Vance, Donald Schmechel, Ann M Saunders, Dmitry Goldgaberii, and Allen D Roses. 1993. “Binding of Human Apolipoprotein E to Synthetic Amyloid ,B Peptide: Isoform-Specific Effects and Implications for Late-Onset Alzheimer Disease.” *Medical Sciences* 90 (September):8098–8102. https://doi.org/10.1073/pnas.90.17.8098.

Strooper, B. De. 2010. “Proteases and Proteolysis in Alzheimer Disease: A Multifactorial View on the Disease Process.” *Physiological Reviews* 90 (2):465–94. https://doi.org/10.1152/physrev.00023.2009.

Sun, Y, S Wu, G Bu, M K Onifade, S N Patel, M J LaDu, A M Fagan, and D M Holtzman. 1998. “Glial Fibrillary Acidic Protein-Apolipoprotein E (apoE) Transgenic Mice: Astrocyte-Specific Expression and Differing Biological Effects of Astrocyte-Secreted apoE3 and apoE4 Lipoproteins.” *The Journal of Neuroscience : The Official Journal of the Society for Neuroscience* 18 (9):3261–72. https://doi.org/10.1523/JNEUROSCI.18-09-03261.1998.

Tackenberg, C., S. Grinschgl, a. Trutzel, a. C. Santuccione, M. C. Frey, U. Konietzko, J. Grimm, R. Brandt, and R. M. Nitsch. 2013. “NMDA Receptor Subunit Composition Determines Beta-Amyloid-Induced Neurodegeneration and Synaptic Loss.” *Cell Death and Disease* 4 (4). Nature Publishing Group:e608–10. https://doi.org/10.1038/cddis.2013.129.

Tan, Meng-Shan Shan, Jin-Tai Tai Yu, and Lan Tan. 2013. “Bridging Integrator 1 (BIN1): Form, Function, and Alzheimer’s Disease.” *Trends in Molecular Medicine* 19 (10). Elsevier Ltd:594–603. https://doi.org/10.1016/j.molmed.2013.06.004.

Tanzi, Rudolph E. 2012. “The Genetics of Alzheimer Disease.” *Cold Spring Harbor Perspectives in Medicine* 2 (10):a006296–a006296. https://doi.org/10.1101/cshperspect.a006296.

Teipel, Stefan J., Wilhelm H. Flatz, Helmut Heinsen, Arun L.W. Bokde, Stefan O. Schoenberg, Stephanie Stöckel, Olaf Dietrich, Maximilian F. Reiser, Hans Jürgen Möller, and Harald Hampel. 2005. “Measurement of Basal Forebrain Atrophy in Alzheimer’s Disease Using MRI.” *Brain* 128 (11):2626–44. https://doi.org/10.1093/brain/awh589.

Tian, Yuan, Jerry C Chang, Emily Y Fan, Marc Flajolet, and Paul Greengard. 2013. “Adaptor Complex AP2/PICALM, through Interaction with LC3, Targets Alzheimer’s APP-CTF for Terminal Degradation via Autophagy.” *Proceedings of the National Academy of Sciences of the United States of America* 110 (42):17071–76. https://doi.org/10.1073/pnas.1315110110.

Tomizawa, Kazuhito, Satoshi Sunada, Yun Fei Lu, Yoshiya Oda, Masahiro Kinuta, Toshio Ohshima, Taro Saito, et al. 2003. “Cophosphorylation of Amphiphysin I and Dynamin I by Cdk5 Regulates Clathrin-Mediated Endocytosis of Synaptic Vesicles.” *Journal of Cell Biology* 163 (4):813–24. https://doi.org/10.1083/jcb.200308110.

Toussaint, Anne, Belinda Simone Cowling, Karim Hnia, Michel Mohr, Anders Oldfors, Yannick Schwab, Uluc Yis, et al. 2011. “Defects in Amphiphysin 2 (BIN1) and Triads in Several Forms of Centronuclear Myopathies.” *Acta Neuropathologica* 121 (2):253–66. https://doi.org/10.1007/s00401-010-0754-2.

Tricoire, Ludovic, and Tania Vitalis. 2012. “Neuronal Nitric Oxide Synthase Expressing Neurons: A Journey from Birth to Neuronal Circuits.” *Frontiers in Neural Circuits* 6 (December):1–16. https://doi.org/10.3389/fncir.2012.00082.

Ubelmann, Florent, Tatiana Burrinha, Laura Salavessa, Ricardo Gomes, Cláudio Ferreira, Nuno Moreno, and Cláudia Guimas Almeida. 2017. "Bin1 and CD2AP Polarise the Endocytic Generation of Beta-amyloid." *EMBO Reports* 18 (1):102–22. https://doi.org/10.15252/embr.201642738.

Varma, Hemant, Donald C Lo, and Brent R Stockwell. 2011. *High-Throughput and High-Content Screening for Huntington's Disease Therapeutics*. *Neurobiology of Huntington's Disease: Applications to Drug Discovery*. https://doi.org/NBK55989.

Villemagne, Victor L., Samantha Burnham, Pierrick Bourgeat, Belinda Brown, Kathryn A. Ellis, Olivier Salvado, Cassandra Szoeke, et al. 2013. "Amyloid B Deposition, Neurodegeneration, and Cognitive Decline in Sporadic Alzheimer's Disease: A Prospective Cohort Study." *The Lancet Neurology* 12 (4). Elsevier Ltd:357–67. https://doi.org/10.1016/S1474-4422(13)70044-9.

Wang, Hui-Fu, Yu Wan, Xiao-Ke Hao, Lei Cao, Xi-Chen Zhu, Teng Jiang, Meng-Shan Tan, et al. 2016. "Bridging Integrator 1 (BIN1) Genotypes Mediate Alzheimer's Disease Risk by Altering Neuronal Degeneration." Edited by Daniela Galimberti. *Journal of Alzheimer's Disease* 52 (1):179–90. https://doi.org/10.3233/JAD-150972.

Wang, Jian Zhi, Yi Yuan Xia, Inge Grundke-Iqbal, and Khalid Iqbal. 2012. "Abnormal Hyperphosphorylation of Tau: Sites, Regulation, and Molecular Mechanism of Neurofibrillary Degeneration." *Advances in Alzheimer's Disease* 3:123–39. https://doi.org/10.3233/978-1-61499-154-0-123.

Wang, Xin, Xuan Zhou, Gongying Li, Yun Zhang, Yili Wu, and Weihong Song. 2017. "Modifications and Trafficking of APP in the Pathogenesis of Alzheimer's Disease." *Frontiers in Molecular Neuroscience* 10 (September):1–15. https://doi.org/10.3389/fnmol.2017.00294.

Wang, Yipeng, and Eckhard Mandelkow. 2016. "Tau in Physiology and Pathology." *Nature Reviews Neuroscience*. https://doi.org/10.1038/nrn.2015.1.

Watts, Vabren L., Fernando M. Sepulveda, Oscar H. Cingolani, Alice S. Ho, Xiaolin Niu, Rosa Kim, Karen L. Miller, et al. 2013. "Anti-Hypertrophic and Anti-Oxidant Effect of beta3-Adrenergic Stimulation in Myocytes Requires Differential Neuronal NOS Phosphorylation." *Journal of Molecular and Cellular Cardiology* 62. The Authors:8–17. https://doi.org/10.1016/j.yjmcc.2013.04.025.

Wechsler-Reya, Robert, Katherine Elliott, Meenhard Herlyn, and George C. Prendergast. 1997. "The Putative Tumor Suppressor BIN1 Is a Short-Lived Nuclear Phosphoprotein, the Localization of Which Is Altered in Malignant Cells." *Cancer Research* 57 (15):3258–63.

Wechsler-Reya, Robert, Daitoku Sakamuro, Jing Zhang, James Duhadaway, and George C. Prendergast. 1997. "Structural Analysis of the Human BIN1 Gene." *The Journal of Biological Chemistry* 272 (50):31453–58. https://doi.org/10.1074/jbc.272.50.31453.

Weibrecht, Irene, Karl-Johan Leuchowius, Carl-Magnus Clausson, Tim Conze, Malin Jarvius, W Mathias Howell, Masood Kamali-Moghaddam, and Ola Söderberg. 2010. "Proximity Ligation Assays: A Recent Addition to the Proteomics Toolbox." *Expert Review of Proteomics* 7 (3):401–9. https://doi.org/10.1586/epr.10.10.

Wenk, Gary L. 2003. "Neuropathologic Changes in Alzheimer's Disease." *Journal of Clinical Psychiatry*. [Physicians Postgraduate Press].

Wetzel-Smith, Monica K., Julie Hunkapiller, Tushar R. Bhangale, Karpagam Srinivasan, Janice a. Maloney, Jasvinder K. Atwal, Susan M. Sa, et al. 2014. "A Rare Mutation in UNC5C Predisposes to Late-Onset Alzheimer's Disease and Increases Neuronal Cell Death." *Nature Medicine* 20 (12). Nature Publishing Group:1452–57. https://doi.org/10.1038/nm.3736.

Wigge, P, K Köhler, Y Vallis, C A Doyle, D Owen, S P Hunt, and H T McMahon. 1997. "Amphiphysin Heterodimers: Potential Role in Clathrin-Mediated Endocytosis." *Molecular Biology of the Cell* 8 (10):2003–15. https://doi.org/10.1016/0040-6031(88)85258-4.

Wigge, Patrick, and Harvey T. McMahon. 1998. "The Amphiphysin Family of Proteins and Their Role in Endocytosis at the Synapse." *Trends in Neurosciences* 21 (8):339–44. https://doi.org/10.1016/S0166-2236(98)01264-8.

Winblad, B, A Cedazo-Minguez, C Graff, G Johansson, L Jönsson, M Kivipelto, T P Sakmar, et al. 2016. "The Lancet Neurology Commission Defeating Alzheimer's Disease and Other Dementias: A Priority for European Science and Society." *The Lancet Neurology Commision* 15 (15):455–532. https://doi.org/10.1016/S1474-4422(16)00062-4.

Xia, Xiaofeng, and Stephen T. Wong. 2012. "Concise Review: A High-Content Screening Approach to Stem Cell Research and Drug Discovery." *STEM CELLS* 30 (9):1800–1807. https://doi.org/10.1002/stem.1168.

Yeh, Felix L., Yuanyuan Wang, Irene Tom, Lino C. Gonzalez, and Morgan Sheng. 2016. "TREM2 Binds to Apolipoproteins, Including APOE and CLU/APOJ, and Thereby Facilitates Uptake of Amyloid-Beta by Microglia." *Neuron* 91 (2). Elsevier Inc.:328–40. https://doi.org/10.1016/j.neuron.2016.06.015.

Youmans, Katherine L., Leon M. Tai, Evelyn Nwabuisi-Heath, Lisa Jungbauer, Takahisa Kanekiyo, Ming Gan, Jungsu Kim, et al. 2012. "APOE4-Specific Changes in Aβ Accumulation in a New Transgenic Mouse Model of Alzheimer Disease." *Journal of Biological Chemistry* 287 (50):41774–86. https://doi.org/10.1074/jbc.M112.407957.

Yuan, Xiang Zhen, Sen Sun, Chen Chen Tan, Jin Tai Yu, and Lan Tan. 2017. "The Role of ADAM10 in Alzheimer's Disease." *Journal of Alzheimer's Disease* 58 (2):303–22. https://doi.org/10.3233/JAD-170061.

Zempel, Hans, Julia Luedtke, Yatender Kumar, Jacek Biernat, Hana Dawson, Eckhard Mandelkow, and Eva Maria Mandelkow. 2013. "Amyloid-B Oligomers Induce Synaptic

Damage via Tau-Dependent Microtubule Severing by TTLL6 and Spastin." *EMBO Journal* 32 (22). Nature Publishing Group:2920–37. https://doi.org/10.1038/emboj.2013.207.

Zhang, Xiaojie, and Weihong Song. 2013. "The Role of APP and BACE1 Trafficking in APP Processing and Amyloid-B Generation." *Alzheimer's Research and Therapy* 5 (5):1–8. https://doi.org/10.1186/alzrt211.

Zheng, Honghua, Chia Chen Liu, Yuka Atagi, Xiao Fen Chen, Lin Jia, Longyu Yang, Wencan He, et al. 2016. "Opposing Roles of the Triggering Receptor Expressed on Myeloid Cells 2 and Triggering Receptor Expressed on Myeloid Cells-like Transcript 2 in Microglia Activation." *Neurobiology of Aging* 42. Elsevier Inc:132–41. https://doi.org/10.1016/j.neurobiolaging.2016.03.004.

Zheng, Hui, and Edward H. Koo. 2011. "Biology and Pathophysiology of the Amyloid Precursor Protein." *Molecular Neurodegeneration* 6 (1):1–16. https://doi.org/10.1186/1750-1326-6-27.

Zhou, Kang, and Tingting Hong. 2017. "Cardiac BIN1 (cBIN1) Is a Regulator of Cardiac Contractile Function and an Emerging Biomarker of Heart Muscle Health." *Science China Life Sciences* 60 (3):257–63. https://doi.org/10.1007/s11427-016-0249-x.

Zhou, Li, and Dong Ya Zhu. 2009. "Neuronal Nitric Oxide Synthase: Structure, Subcellular Localization, Regulation, and Clinical Implications." *Nitric Oxide - Biology and Chemistry* 20 (4). Elsevier Inc.:223–30. https://doi.org/10.1016/j.niox.2009.03.001.

Zhou, Yuan, Ikuo Hayashi, Jacky Wong, Katherine Tugusheva, John J. Renger, and Celina Zerbinatti. 2014. "Intracellular Clusterin Interacts with Brain Isoforms of the Bridging Integrator 1 and with the Microtubule-Associated Protein Tau in Alzheimer's Disease." *PLoS ONE* 9 (7):e103187. https://doi.org/10.1371/journal.pone.0103187.